

Dissertation zur Erlangung des Doktorgrades der Naturwissenschaften
der Fakultät für Biologie
der Ludwig-Maximilians-Universität
München

Analysis of p53 and c-MYC,
two key transcription factors involved in
tumorigenesis

vorgelegt von

Peter Jung

am 16.10.2007

Diese Arbeit wurde in der selbstständigen Nachwuchsgruppe für Molekulare Onkologie
am Max-Planck Institut für Biochemie, Martinsried angefertigt.

First examiner: PD. Dr. Heiko Hermeking

Second examiner: Prof. Dr. Dirk Eick

Third examiner: Prof. Dr. Michael Boshart

Fourth examiner: Prof. Dr. Angelika Böttger

Additional examiners: Prof. Dr. Michael Ackmann
Prof. Dr. Jürgen Soll

Date of the oral examination: 07.02.2008

Erklärung

Hiermit erkläre ich, dass ich die vorliegende Dissertation selbstständig und nur unter Verwendung der angegebenen Quellen und Hilfsmittel verfasst habe. Sämtliche Experimente wurden von mir selbst durchgeführt, außer wenn explizit auf Dritte verwiesen wird. Weiter versichere ich, dass ich nicht anderweitig versucht habe, eine Dissertation oder Teile einer Dissertation einzureichen bzw. einer Prüfungskommission vorzulegen oder mich einer Doktorprüfung zu unterziehen.

München,

Peter Jung

During this thesis the following co-author papers have been published:

Tarasov, V., Jung, P.* , Verdoodt, B.* , Lodygin, D.* , Epanchintsev, A., Menssen, A., Meister, G. & Hermeking, H. (2007)

Differential regulation of microRNAs by p53 revealed by massively parallel sequencing: miR-34a is a p53 target that induces apoptosis and G₁-arrest

Cell cycle **6** (13), 1586-93

*these co-authors contributed equally to this work

Jung, P., Verdoodt, B., Bailey, A., Yates, JR 3rd, Menssen, A. & Hermeking, H. (2007)

Induction of Cullin 7 by DNA damage attenuates p53 function

Proc Natl Acad Sci U S A **104**, 11388-93

Menssen, A.* , Epanchintsev, A.* , Lodygin, D., Rezaei, N., Jung P., Verdoodt, B., Diebold, J. & Hermeking, H. (2007)

c-MYC Delays Prometaphase by Direct Transactivation of MAD2 and BubRI: Identification of Mechanisms Underlying c-MYC-Induced DNA damage and Chromosomal Instability

Cell cycle **6** (3), 339-352

*these authors contributed equally to this work

Epanchintsev, A.* , Jung, P.* , Menssen, A. & Hermeking, H. (2006)

Inducible microRNA expression by an all-in-one episomal vector

Nucleic Acids Research **34** (18):e119

*these authors contributed equally to this work

Jung, P., Menssen, A., Mayr, D. & Hermeking, H.

AP4 encodes a c-MYC-inducible repressor of p21 highly expressed in colonic progenitor and colorectal cancer cells

Genes & Development, under external review

Table of Content

1	Introduction	1
1.1	The origin of cancer	1
1.2	The tumor suppressor p53	1
1.2.1	Functional domains of the p53 protein	2
1.2.1.1	The N-terminal domain (NTD)	2
1.2.1.2	The DNA binding domain (DBD)	2
1.2.1.3	The C-terminal domain (CTD)	3
1.2.2	Regulation of p53 by E3-ligases	4
1.2.3	Neddylation and sumoylation of p53	7
1.2.4	MDMX: another key player in p53 regulation	7
1.2.5	Signaling to p53	8
1.2.5.1	Activation of p53 by DNA damage	8
1.2.5.2	Post-translational modifications modulate p53 activity	8
1.2.5.3	Relevance of p53 post-translational modifications	10
1.2.5.4	Activation of p53 by oncogenes	10
1.2.6	Relevance of p53 activation for tumor suppression	12
1.2.7	Pathways downstream of activated p53	12
1.2.7.1	Cell cycle arrest and senescence	13
1.2.7.2	Apoptosis	13
1.2.7.3	Cell cycle arrest or apoptosis ?	14
1.2.7.4	DNA repair	15
1.2.7.5	p53 as an anti-angiogenic factor	15
1.2.7.6	p53: more than meets the eye	16
1.3	The proto-oncogene <i>c-MYC</i>	18
1.3.1	<i>c-MYC</i> is activated in human neoplasia	18
1.3.2	Regulation of the <i>c-MYC</i> proto-oncogene	19
1.3.3	<i>c-MYC</i> acts as a transcription factor	21
1.3.4	Transactivation of <i>c-MYC</i> target genes	22
1.3.5	<i>c-MYC</i> -mediated target gene repression	23
1.3.6	The <i>c-MYC</i> target gene network	25
1.3.7	Biological consequences of <i>c-MYC</i> activation	25
1.3.7.1	<i>c-MYC</i> and cellular proliferation	26
1.3.7.2	<i>c-MYC</i> -mediated regulation of the cell cycle	26
1.3.7.3	<i>c-MYC</i> and differentiation	28
1.3.7.4	<i>c-MYC</i> and apoptosis	28
1.3.7.5	<i>c-MYC</i> influences cell growth and vascularization	29
1.3.8	<i>c-MYC</i> in tumor maintenance and progression	30
1.4	Aim of the study	32
2	Materials	33
2.1	Chemicals and Reagents	33
2.2	Enzymes	35

2.3	Antibodies	35
2.3.1	Primary antibodies	35
2.3.2	Secondary antibodies	36
2.4	Disposables and kits	37
2.5	Laboratory equipment	38
2.6	Oligonucleotides	39
2.6.1	Oligonucleotides for cloning	39
2.6.2	Oligonucleotides used for colony-PCR and sequencing	39
2.6.3	Oligonucleotides used for real-time quantitative PCR	40
2.6.4	Oligonucleotides for quantitative ChIP analyses	40
2.7	Expression plasmids	41
2.7.1	Standard expression vectors	41
2.7.2	Generated expression vectors	42
2.8	Bacteria strains	44
2.9	Eukaryotic cell lines	44
2.10	Stock solutions, buffers and culture media	46
3	Methods	51
3.1	Bacterial cell culture	51
3.1.1	Propagation and storage of <i>Escherichia coli</i> (<i>E.coli</i>) strains	51
3.1.2	Preparation of Calcium-competent <i>E.coli</i> XL1-blue cells	51
3.1.3	Transformation of competent bacteria	51
3.2	Molecular biological standard methods	52
3.2.1	Purification of plasmid DNA from <i>E.coli</i>	52
3.2.2	Enzymatic restriction-digestion and dephosphorylation of DNA	52
3.2.3	DNA ligation	53
3.2.4	Amplification of DNA by the polymerase chain reaction (PCR)	53
3.2.5	Analysis and purification of DNA fragments by agarose gel electrophoresis	54
3.2.6	DNA sequencing	55
3.3	Generation of microRNA-encoding DNA fragments	55
3.4	Real time quantitative PCR (RT-qPCR)	56
3.5	Site directed mutagenesis	57
3.6	Mammalian cell culture	57
3.6.1	Cultivation of human and rodent cell lines	57
3.6.2	Cryo-preservation of mammalian cells	58
3.6.3	Transient and stable transfection of eukaryotic cells	58
3.6.4	Retroviral infection	59
3.6.5	Generation of recombinant adenoviruses and infection of target cells	59
3.6.6	Proliferation assay	60
3.6.7	Transient reporter assays based on mammalian cells	61
3.7	Protein analysis and purification	61
3.7.1	Generation of goat polyclonal antibodies	61
3.7.1.1	Conjugation of peptides to carrier protein	62

Table of Content

3.7.1.2	Immunization of goats _____	62
3.7.1.3	Affinity purification of polyclonal antibodies _____	62
3.7.2	Preparation of whole cell lysates from mammalian cells _____	63
3.7.3	Polyacrylamide gel electrophoresis (PAGE), Western blotting and Immunodetection of proteins _____	64
3.7.4	Silver staining _____	65
3.7.5	Tandem affinity purification (TAP) _____	65
3.7.6	Multidimensional protein identification technology (MudPIT) _____	67
3.7.7	Indirect immunofluorescence labeling _____	68
3.7.8	Tissue sections and immunohistochemistry _____	68
3.7.9	Co-immunoprecipitation _____	69
3.7.10	Chromatin immunoprecipitation (ChIP) assay _____	70
3.8	DNA content analysis by FACS _____	71
3.9	BrdU labeling for detection of <i>de novo</i> DNA synthesis _____	71
3.10	Microscopy _____	72
4	Results I _____	73
4.1	Proteomic identification of p53-associated proteins _____	73
4.1.1	Generation of a p53-TAP fusion construct _____	73
4.1.2	Generation of a cellular system for identification of p53 interactors _____	75
4.1.3	iTAP/MudPIT analysis of p53-associated proteins _____	76
4.1.4	Putative p53 interactors identified by the iTAP/MudPIT approach _____	78
4.2	Cul7: a novel inhibitor of p53 activity _____	79
4.2.1	p53 interacts with Cul7 <i>in vivo</i> _____	79
4.2.2	Cul7 protein and mRNA accumulate after DNA damage _____	81
4.2.3	Cul7 induction upon DNA damage is caffeine-sensitive _____	84
4.2.4	Increased p53 activity and G ₁ arrest after knockdown of Cul7 _____	85
4.2.5	Ectopic expression of Cul7 inhibits p53 function _____	89
4.2.6	Cul7/Fbx29 does not exhibit E3-ligase activity towards p53 _____	92
5	Results II _____	94
5.1	AP4: a c-MYC inducible repressor of p21 _____	94
5.1.1	Episomal, conditional expression of ectopic c-MYC in MCF-7 breast cancer cells _____	94
5.1.2	Characterization of MCF-7-PJMMR1 cell line _____	95
5.1.3	AP4 mRNA and protein expression is induced by c-MYC _____	97
5.1.4	AP4 is an evolutionary conserved, direct c-MYC target gene _____	101
5.1.5	Induction of AP4 contributes to cell cycle progression _____	103
5.1.6	AP4 represses p21 mRNA and protein _____	105
5.1.7	AP4 occupies E-box sequences in the p21 promoter _____	107
5.1.8	AP4 interferes with the DNA damage/p53/p21 pathway _____	109
5.1.9	TGF- β -mediated induction of p21 is suppressed by AP4 _____	112
5.1.10	AP4 interferes with cell cycle arrest during differentiation _____	114
5.1.11	AP4 expression pattern in human colon and colorectal cancer specimen _____	116

6	Discussion	121
6.1	iTAP/MudPIT analysis of p53-associated proteins	121
6.1.1	Cul7: a component of modular E3-ligases	121
6.1.2	Cul7: a negative modulator of p53 activity	122
6.1.3	PARC: a close relative of Cul7	124
6.1.4	Role of Cul7 in normal proliferation and cell growth	125
6.1.5	Regulation of Cul7 level by genotoxic stress	127
6.1.6	Implication of the Cul7/p53 interaction for cancer therapy	127
6.2	AP4 is a c-MYC-responsive gene in human carcinoma	129
6.2.1	The transcription factor AP4	129
6.2.2	A c-MYC / AP4 / p21 cascade represses <i>p21</i>	130
6.2.3	Role of AP4 in c-MYC mediated anti-estrogen resistance during breast cancer therapy	133
6.2.4	Effect of AP4 on TGF- β signaling	134
6.2.5	Role of AP4 in the DNA damage response	136
6.2.6	Role of AP4 in differentiation	137
6.2.7	Role of c-MYC / AP4 / p21 in colonic differentiation and colorectal carcinoma	137
7	Summary	141
8	References	142
9	Abbreviations	168
10	Acknowledgments	172
11	Curriculum vitae	173

1 Introduction

1.1 The origin of cancer

The approximately 30 billion cells within a healthy human body exist in a complex organization based on mutual dependency and shared control mechanisms. Multiplication of cells is carefully regulated ensuring that each tissue maintains a size and architecture adapted to the needs of the organism. Cells in which these exquisite controls break down start to grow in an unleashed fashion and eventually form a cell mass called “tumor”. While some tumors do not cause serious health problems, those which spawn cells that metastasize throughout the body cause cancer disease ¹. Two key differences between cancer and other genetic diseases have been dogmatized: in the majority of cases, cancer disease is caused by somatic mutations while other genetic diseases are caused exclusively by mutations occurring in the germ-line ². In addition, an individual cancer does not result from a single mutation but rather follows the “multi-hit” concept where each mutation drives a new step towards malignant transformation ². Dependent on the type of cancer, 3-20 mutations appear to be required to complete this process ^{2,3}. Two sorts of genes turned out to be critical in the supervision of cellular proliferation and growth control: proto-oncogenes represent cell cycle accelerators while tumor suppressor genes can be considered as breaks which restrict cell growth ⁴. Their de-regulation plays an important role in the development and progression of cancer disease. Since the subject of this thesis is the regulation and function of two prominent transcription factors involved in tumorigenesis, p53 and c-MYC, they are introduced in the following chapters.

1.2 The tumor suppressor p53

The fame of the intensively studied protein p53 originates from its function as a tumor suppressor in human and other mammals ^{5,6}. First identified in 1979 as an associated protein of papovavirus SV40 large T antigen ^{7,8}, p53 was initially claimed to harbor oncogenic activity. Within the following ten years genetic and functional data provided compelling evidence that wild-type p53 functions as a tumor suppressor by inhibiting cell

proliferation and transformation⁹⁻¹². Mutations in evolutionary conserved codons of *p53* occur with a high frequency in diverse types of human cancer¹³. Baker et al. found that 75% of colorectal carcinoma harbor a mutated *p53* allele¹⁴ and show a concomitant deletion of the wild-type *p53* allele¹⁵. Furthermore, they demonstrated that wild-type *p53* is able to suppress the growth of human colorectal carcinoma cells¹⁵. The oncogenic features were caused by point-mutations in the *p53* expression vectors which were generated from sequences derived from cancer cells¹⁶. Of those tumors that retain wild-type *p53*, a large number inactivate *p53* function by other mechanisms, such as de-regulation of upstream or downstream signaling pathways¹⁷.

1.2.1 Functional domains of the p53 protein

1.2.1.1 The N-terminal domain (NTD)

The *p53* tumor suppressor gene encodes for a protein of 393 amino acids and is structurally organized in four functional domains (Figure 1). As a transcription factor, *p53* possesses a bipartite transactivation domain¹⁸ (TAD; amino acids 1-40 and 43-73) which, together with a proline-rich SH3 target-region (amino acids 60-97), forms the NTD¹⁹. This domain is devoid of tertiary structures and largely misses secondary structural elements^{20,21} which is a typical feature of most “acidic” TADs^{22,23}. Short patches of the *p53* TAD domain can form defined local sub-structures, such as “induced helices”, with their formation being dependent on the nature of the bound partner protein, as e.g. MDM2^{24,25}. A nuclear export sequence (NES) is located within the NTD (amino acids 11-27) and collaborates with the C-terminal NES (see section 1.2.1.3) to achieve nuclear export of *p53*²⁶. This export signal is inactivated by post-translational modifications of the NTD²⁶ which occur when *p53* is activated.

1.2.1.2 The DNA binding domain (DBD)

The central sequence-specific DNA binding domain (DBD) of *p53*, generally designated as “core domain” (amino acids 102-292), is critical for the DNA binding capacity of the *p53* transcription factor (Figure 1). The core domain specifically associates with DNA fragments consisting of two decameric “half-site”-recognition sequences 5`-Pu-Pu-Pu-C-(A/T)-(T/A)-G-Py-Py-Py-3` (Pu=A/G, Py=T/C) separated by a

spacer region spanning up to 13 bp²⁷. Binding of p53 to DNA occurs in a cooperative manner with four core domains occupying one DNA response element²⁸.

According to International databases^{29,30}, more than 90% of the tumorigenic mutations of p53 localize to the core domain. While a large subset of these p53 mutations occurs rather infrequent, eight of them, the so-called “hot-spot” mutations, account for approximately 30% of the documented p53 core domain mutations¹⁹ (see also Figure 1). These hot spot mutations either affect amino-acids directly contacting DNA or change the overall conformation of the DBD, indicating that the DNA-binding function of p53 is essential for tumor suppression.

1.2.1.3 The C-terminal domain (CTD)

The p53 C-terminal region harbors the tetramerization domain (TD, amino acids 326-355). The tetrameric form of p53, which consists of a dimer of dimers³¹⁻³³, represents its active state³⁴. A nuclear export sequence (NES, amino acids 340-351) is located within the TD and mediates nuclear-cytoplasmic shuttling³⁵. While this domain is exposed on the protein surface when p53 exists in its monomeric state, the NES is buried beneath the surface upon p53 oligomerization resulting in nuclear retention³⁵.

The negative auto-regulatory domain (RD) at the extreme C-terminus of p53 is connected to the TD through a basic linker region, which contains a bipartite nuclear localization signal (NLS) that mediates the nuclear import of p53³⁶. The RD (amino acids 369-393) has been implicated in auto-inhibition of p53 DNA-binding function^{37,38}. Since a direct binding of the RD to the DBD was so far not detectable³⁹, it remains enigmatic by which mechanism the RD exerts its inhibitory effect on the sequence-specific DNA-binding capacity of p53⁴⁰⁻⁴².

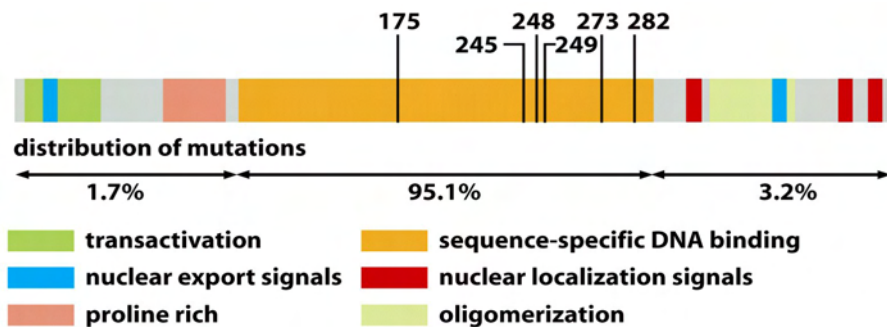


Figure 1. Functional domains of p53

The N-terminal transactivation domain (NTD) contacts the transcriptional machinery. The DNA binding domain (DBD or “core domain”) is affected by 95.1% of naturally occurring p53 mutations. The positions of “Hot-spot” mutations located in the DBD are indicated. The tetramerization domain (TD) and the regulatory region (RD) form the C-terminal domain (CTD) of p53 which also harbors sequence motifs that regulate p53 localization. (Adapted from Ref. 1)

1.2.2 Regulation of p53 by E3-ligases

In regularly proliferating cells, the function of the p53 tumor suppressor has to be kept in check to allow normal growth and development. A prerequisite for this regulation is the extremely short half-life of p53 (~6-20 min) which results in very low amounts of functional p53 protein⁴³. Under normal conditions, p53 is effectively degraded by the ubiquitin-dependent proteasomal pathway⁵. The oncoprotein MDM2 (**M**ouse **D**ouble **M**inute **2**, also termed HDM2 in humans) represents the best studied inhibitor of p53 function⁴⁴. The RING-finger domain of the MDM2 E3-ligase is necessary to promote ubiquitination and proteasomal degradation of p53 and also catalyzes self-ubiquitination of MDM2⁴⁵. The embryonic lethality caused by MDM2 knockout in mice is completely rescued by inactivation of p53^{46,47} illustrating the critical role for MDM2 in p53-regulation. Besides regulation of p53 protein-turnover, the mere physical association with MDM2 shields the N-terminal transactivation domain of p53 and decreases transactivation by p53⁴⁴. Since *MDM2* is a direct transcriptional target of p53, both genes constitute a negative feedback loop^{48,49}. Human tumors and tumor cell lines express excessive levels of oncogenic MDM2^{50,51} rendering activated p53 insufficient to fulfil its

tumor-suppressive task. A naturally occurring polymorphism in the *MDM2* promoter (SNP309) leads to an increased level of MDM2 and is associated with accelerated tumor formation in both sporadic and hereditary cancer ⁵².

MDM2 catalyzes the addition of single ubiquitin (Ub) moieties to a cluster of 6 lysine residues in the C-terminus of p53 ^{53,54}. Mono-ubiquitination of p53 by low levels of MDM2 leads to nuclear export and cytoplasmic degradation of p53, whereas increased MDM2 levels catalyze poly-ubiquitination and proteasomal degradation of p53 in the nucleus ⁵⁵. Furthermore, efficient poly-ubiquitination of p53 requires association with a so-called “E4-ligase” factor p300/CBP ⁵⁶. p300/CBP also plays a well established role in acetylation and transcriptional activation of p53 ⁵⁷. In addition, other MDM2-interacting proteins support p53 poly-ubiquitination or enhance the efficiency of its proteasomal degradation, as e.g. YY1 ^{58,59}, PACT ⁶⁰ and gankyrin ⁶¹. Gankyrin in turn is able to interact with the S6 proteasomal ATPase ⁶² and might therefore recruit p53 to its destruction machinery.

Recently performed mouse knock-in experiments provided evidence that MDM2 might not be the only non-viral mediator of p53 proteasomal degradation ^{63,64}. In support to this finding, further E3-ubiquitin ligases were shown to promote proteasomal degradation of p53, such as Pirh2 ⁶⁵, COP1 ⁶⁶, MULE/ARF-BP1 ⁶⁷, E6-AP ⁶⁸, CHIP ⁶⁹ and Synoviolin ⁷⁰. Pirh2 and COP1 represent direct p53 target genes ^{65,66} and consequently are components of negative feedback loops which limit p53 activity (see Figure 2).

Although the p53-binding protein PARC possesses E3-ligase activity, it does not inactivate p53 by ubiquitination but rather via sequestration in the cytoplasm ⁷¹. PARC was proposed to function as a cytoplasmic scaffold for mono-ubiquitinated p53 with poly-ubiquitination of p53 being catalyzed by a so far unidentified E4-ligase ⁷². CHIP is speculated to represent this cytoplasmic E4-ligase for p53 since it interacts with the RING-IBR-RING domain of Parkin ⁷³ and a similar motif can be found in PARC. As an atypical p53 E3-ligase, E4F1 oligo-ubiquitinates p53 at residues distinct from MDM2 target sites and exerts a positive effect on p53 activity ⁷⁴.

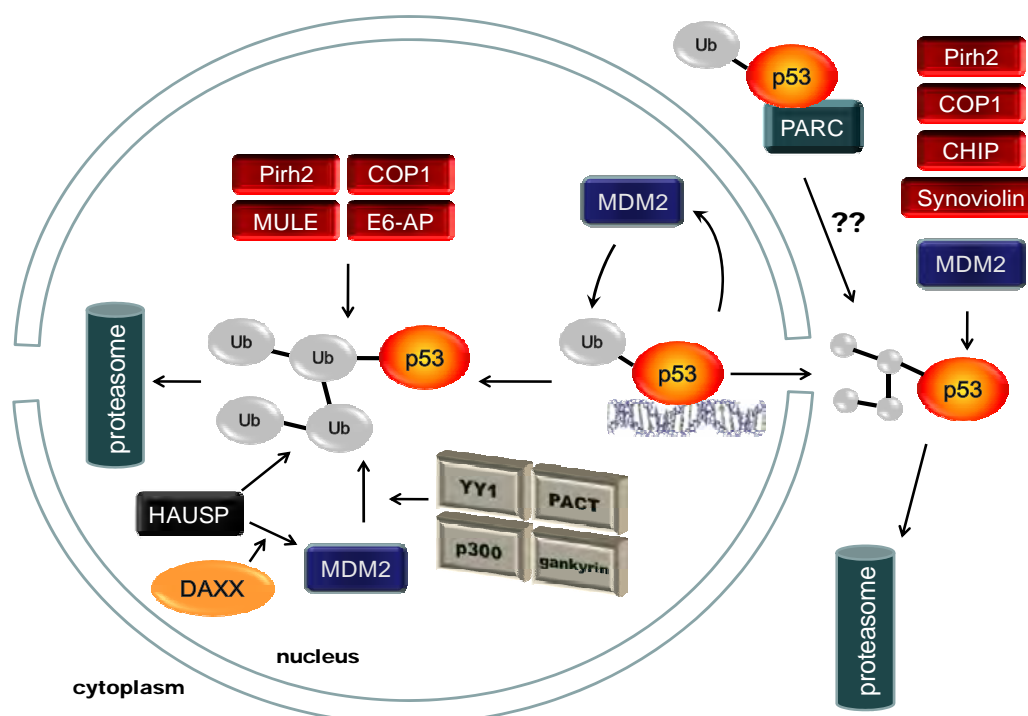


Figure 2. Regulation of p53 degradation by E3-ligases

MDM2 mono-ubiquitinates p53 in the nucleus and nuclear p53-Ub can undergo poly-ubiquitination by MDM2, COP1, Pirh2, E6-AP or MULE. Several factors (YY1, PACT, p300, gankyrin) support MDM2-mediated poly-ubiquitination of p53. The de-ubiquitinating enzyme (DUB) HAUSP acts on MDM2 thereby supporting degradation of p53 but can also, especially when in complex with DAXX, de-ubiquitinate and consequently activate p53. Alternatively, MDM2 can favor nuclear export of p53 and the cytoplasmic E3-ligases MDM2, Pirh2, COP1, CHIP or Synoviolin lead to further poly-ubiquitination of p53 and cytoplasmic degradation via the proteasome. PARC sequesters p53 in the cytoplasm and could serve as a molecular scaffold for p53-poly-ubiquitination presumably facilitated by one of the depicted cytoplasmic E3-ligases. Ub: ubiquitin.

An additional layer of complexity in the regulation of p53 by ubiquitination came with the identification of de-ubiquitinating (DUB) enzymes. HAUSP (Herpesvirus Associated Ubiquitin-Specific Protease) de-ubiquitinates MDM2 and this might be required to maintain sufficient amounts of MDM2 in a cell to keep the activity of p53 low in unstressed cells^{75,76}. The DAXX protein enforces the interaction between HAUSP and MDM2, thereby preventing auto-ubiquitination of MDM2 and, as a consequence, augmenting p53 degradation⁷⁷. However, HAUSP can also de-ubiquitinate p53 and MDMX^{78,79}. Another DUB enzyme, USP2a, de-ubiquitinates MDM2⁸⁰ but its role in regulating the p53 pathway in normal cells and cancer has not been determined.

1.2.3 Neddylaton and sumoylation of p53

Although ubiquitination represents the most intensively studied protein modification of p53, the ubiquitin-like proteins SUMO-1 and Nedd8 can also be conjugated to p53 which is catalyzed by specific E3-ligases. Initially, MDM2 was found to neddylate the CTD of p53 at 3 lysine residues (Lys^{370,372,373}), which can also be subject to MDM2-mediated ubiquitination⁸¹ and this leads to p53 inhibition. A component of a SCF complex, FBXO11, promotes neddylation of p53 at Lys³²⁰ and Lys³²¹ and thereby inhibits p53 function⁸².

Two initial studies demonstrated that sumoylation at K³⁸⁶ of p53 results in increased transcriptional activity of p53^{83,84}. Several factors have been described to participate in sumoylation of p53, including the PIAS family members PIAS1, PIAS α β and PIASy⁸⁵⁻⁸⁸ but data from these studies concerning the functional consequences of p53 sumoylation were rather conflicting^{89,90}. Recent reports provided evidence that sumoylation activates p53 function thereby promoting p53-mediated senescence and apoptosis^{91,92}. Interestingly, the SUMO-specific protease SUSP4 removes SUMO-1 from MDM2 thereby promoting self-ubiquitination of MDM2 and indirectly stabilization of p53⁹³.

1.2.4 MDMX: another key player in p53 regulation

Besides MDM2, MDMX (also known as MDM4) represents another key regulator of p53 and *MDMX*-amplification and/or over-expression has been reported for diverse tumors⁹⁴. Similar to MDM2, loss of *MDMX* results in embryonic lethality, which is rescued by knockout of p53⁹⁵⁻⁹⁷. As a structural relative to MDM2, MDMX harbors an N-terminal p53 binding domain and a C-terminal RING-finger domain⁹⁸ but lacks E3-ligase activity^{99,100}. In contrast to MDM2, MDMX does not represent a transcriptional target of p53⁹⁸ and functions mainly by direct inhibition of p53's transcriptional activity and independent of MDM2 function¹⁰¹⁻¹⁰³. However, a complex between C-terminal mutant MDM2, whose E3-ligase function was rendered inactive, and MDMX retains E3-ligase activity indicating that MDMX can directly contribute to E3-function despite harboring an inactive RING-finger domain^{104,105}.

1.2.5 Signaling to p53

Under circumstances, that make it necessary for cells to unleash the activity of p53, which has also been called the “Guardian of the genome”¹⁰⁶, the brakes on p53 must be released to liberate its tumor-suppressive power. For this purpose, cells possess a diverse battery of monitoring systems able to receive environmental and intracellular stress signals and several pathways exist which transmit these signals to p53⁵.

While there is a steadily growing list of these monitoring systems whose signals can be integrated by p53¹⁰⁷, the best studied alarm systems respond to DNA damage and the inappropriate activation of proto-oncogenes (see Figure 3).

1.2.5.1 Activation of p53 by DNA damage

The primary transducers during the response to damaged genomic DNA belong to the family of PI3-kinase-related proteins with ATM (Ataxia Telangiectasia Mutated) and ATR (ATM and Rad3-related) representing central mediators¹⁰⁸. The ATM protein kinase is primarily activated by DNA double strand breaks (DSBs), phosphorylates and thereby activates key effector proteins, as e.g. the kinase CHK2¹⁰⁹. Both, ATM and CHK2 phosphorylate p53¹¹⁰. ATR senses UV-light-induced DNA damage and DSBs but also responds to stalled replication forks¹¹¹. Once activated, ATR passes the signal to CHK1¹¹² leading to various modifications of the p53 protein¹¹³. Although ATM and ATR are generally thought to act independently of one another, there is strong experimental evidence that ATM is required for rapid activation of ATR after ionizing radiation-mediated DSBs^{114,115}.

1.2.5.2 Post-translational modifications modulate p53 activity

Once activated by DSBs, ATM/CHK2 and/or ATR/CHK1 lead to massive phosphorylation of p53 at its N- and C-terminal domains^{116,117}. Phosphorylation of Ser¹⁵ and Ser²⁰ of human p53 disrupts its interaction with MDM2^{118,119}. In addition, MDM2 phosphorylation by ATM impairs MDM2 activity¹²⁰. The combination of p53 and MDM2 phosphorylation causes activation of p53 transcriptional activity. Besides this, DNA damage-mediated activation of ATM reduces the binding affinity of HAUSP to MDM2¹²¹ and disrupts the MDM2/DAXX/HAUSP ternary complex⁷⁷ leading to

MDM2 auto-ubiquitination. Concomitantly, the p53-HAUSP interaction is enforced and the resulting de-ubiquitination increases the amount and activity of p53⁷⁷. ATM phosphorylates the E3-ligase COP1 which promotes self-degradation of COP1 and the disruption of this negative feedback loop contributes to stabilization of p53¹²². In contrast to MDM2 and COP1, the mechanism which might disrupt the Pirh2/p53 negative feedback loop after DNA damage is currently unknown. Regulation of Pirh2 was shown to occur in a cell cycle-dependent manner via its phosphorylation by Calmodulin-dependent kinase II (CaMKII) and phosphorylation of Pirh2 abrogates its E3-ligase activity towards p53¹²³.

Besides these examples, additional kinases are known to phosphorylate p53 and MDM2 upon genotoxic stress¹²⁴. The complexity is further increased by the interdependence of specific phosphorylation events¹²⁵. E.g. casein kinase I (CKI) requires prior phosphorylation of p53 Ser⁶ or Ser¹⁵ to accomplish phosphorylation of Ser⁹ or Thr¹⁸^{126,127}. Stress-activated PI-3 kinase members phosphorylate MDM2 and this supports its auto-ubiquitination¹²⁸. As a consequence, the half-life of MDM2 in stressed cells drops to ~5 min which represents another important contribution to activation of p53¹²⁸.

Acetylation of p53 has been implicated in an elevated specific DNA-binding capacity^{113,129,130}. The histone acetyltransferases (HATs) CREB binding protein (CBP)/p300 and p300/CBP-associated factor (PCAF), which interact with p53 through its N-terminus, acetylate the C-terminus of p53 at Lys³⁷², Lys³⁷³, Lys³⁸¹ and Lys³⁸² (p300/CBP) and Lys³²⁰ (PCAF)^{124,131,132}. Acetylation of p53 is also involved in its stabilization, since p300/CBP and MDM2 compete with each other in targeting the same lysine residues of p53 for acetylation and ubiquitination, respectively¹³³. Similarly, MDMX may block p300-mediated acetylation of p53^{96,134}. A complete activation of p53 after genotoxic stress is considered to occur by a phosphorylation-acetylation cascade¹³² since phosphorylation of several serine residues at the N-terminus of p53 was demonstrated to enhance the interaction of p53 with CBP/p300 and PCAF^{131,135}. Histone deacetylases (HDACs) are able to antagonize the activation of p53¹³⁶: e.g. HDAC1 deacetylates p53¹³⁷. Also the human Sir2 homolog, SIRT1, was shown to de-acetylate

p53^{138,139}, however, different functional consequences of p53 de-acetylation by the NAD⁺-dependent deacetylase SIRT1 have been reported^{138,140}.

In addition to phosphorylation and acetylation, many reports highlight the role of other post-translational modifications for the regulation of p53 activity, as methylation, glycosylation, ribosylation and O-GlcNAcylation^{124,141-144}.

1.2.5.3 Relevance of p53 post-translational modifications

A model which emphasizes the importance of post-translational modification events for p53 function is not supported by results obtained with mutant p53 knock-in mice¹⁴⁵. From these approaches it becomes more and more obvious that modification events of conserved p53 sites do not represent “on-off” - switches but rather serve to fine-tune p53 activity under different circumstances¹⁴⁵. Approaches using transgenic mice rather point to MDM2 and MDMX as major regulators of p53 and ongoing efforts aim to evaluate the importance of recently identified p53-associated proteins, such as the E3-ligases Pirh2 and COP1^{65,146}.

1.2.5.4 Activation of p53 by oncogenes

A second important pathway which leads to p53 activation is triggered by hyperproliferative signals emanating from oncogenic proteins such as c-MYC^{147,148}, Ras¹⁴⁹, E2F¹⁵⁰, E1A¹⁵¹, v-Abl¹⁵² and β -catenin¹⁵³. Activation of the p53 network in these scenarios may be mediated by p14^{ARF} (ARF)¹⁵⁴. ARF, which is encoded by an alternative reading frame of the *p16/INK4a* locus¹⁵⁵, interacts with MDM2 thereby alleviating the inhibitory p53-MDM2 interaction¹⁵⁶⁻¹⁵⁸. Interestingly, a similar mode of p53 activation involves the ribosomal L11 protein and this occurs after cellular stress caused by disordered ribosomal biogenesis¹⁵⁹. ARF further inhibits the ubiquitin-ligase activity of ARF-BP1/MULE towards p53 and this leads to stabilization of p53⁶⁷. ARF-deficient mice develop tumors¹⁶⁰⁻¹⁶², however, at a lower frequency than p53 knock-out mice^{163,164} demonstrating that abrogation of ARF-mediated oncogene-signaling to p53 contributes to cancer progression.

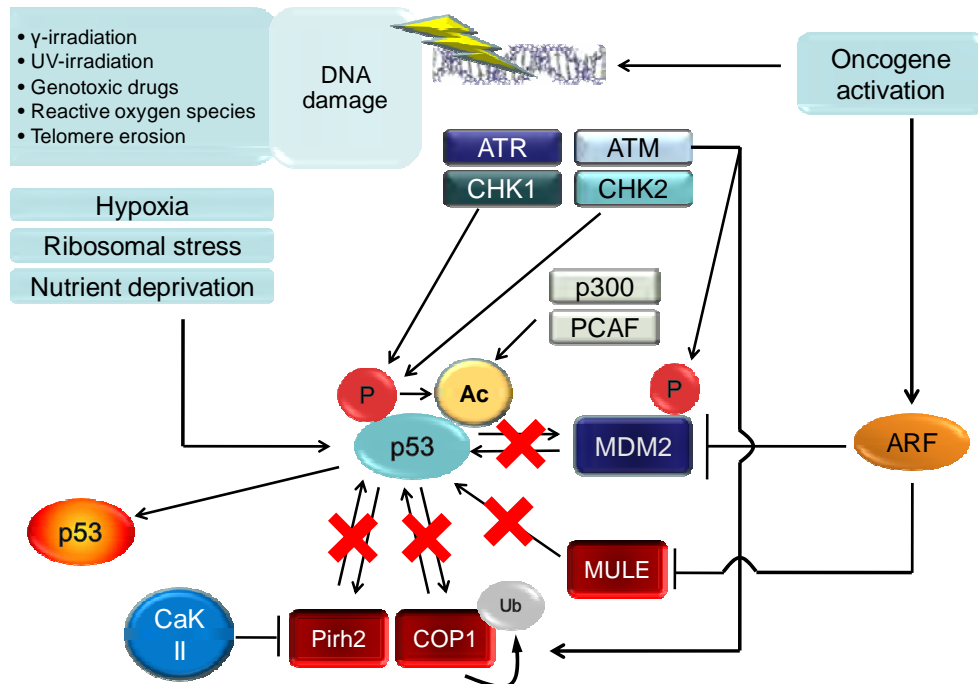


Figure 3. Activation of the p53 tumor suppressor protein

Multiple stress signals are integrated into the activity of the p53 protein. Especially after DNA damage, p53 is subjected to various post-translational modifications, such as phosphorylation (P) or acetylation (Ac) which disrupt the interaction with its major negative regulator MDM2 (indicated by a red cross). Activated ATM targets COP1 for self-ubiquitination and degradation and the cell cycle regulated kinase CaKII phosphorylates Pirh2 thereby disrupting the negative feed-back loops that control p53 (red crosses). After oncogenic stress, ARF not only interferes with the MDM2/p53 feedback loop but also abolishes the negative influence of the E3-ligase ARF-BP1/MULE (depicted as MULE) on p53. Upon ribosomal stress, L11 interacts with MDM2 thereby alleviating the inhibitory p53-MDM2 interaction. Taken together, these events are able to unleash the tumor-suppressive capacity of p53. Ub: ubiquitin-modification.

While the role of ARF in mediating activation of p53 after oncogenic stress is well established in mice, activation of oncogenes in human cells may result in activation of p53 via ARF-independent routes. For example, in human fibroblasts it was observed that activation of *c-MYC* does not increase *ARF* mRNA and protein levels and silencing of *ARF* by RNA interference (RNAi) has no effect on p53 activation due to de-regulated *c-MYC*¹⁶⁵. Others showed that inactivation of *ARF* by RNAi enhances cell growth in a p53-dependent manner but has a minor tumorigenic effect¹⁶⁶. In addition, human epithelial cells which are the origin of the most common type of human tumors, the carcinoma, do not show induction of *ARF* after activation of oncogenes^{167,168}. Oncogene

activation was recently shown to provoke the formation of reactive oxygen species (ROS) and inappropriate firing of replication origins, which ultimately results in DNA damage and activation of p53^{169,170,171-174}. Therefore, a more complex inter-connection between the DNA damage and oncogenic signaling pathways seems likely.

1.2.6 Relevance of p53 activation for tumor suppression

An important issue, which emerged from the observation that p53 can be activated by various stress signals, is the relative importance of these pathways for the tumor suppressive function of p53. A constitutive activation of 53BP1 and CHK2 has been observed in human cancer pointing to a permanent activation of the DNA damage signaling pathway¹⁷⁵. Since these factors act upstream of p53, their constitutive activation might be linked to the high frequency of p53 mutations in cancer. Activation of the ATM/ATR-regulated DNA damage network occurs early in tumorigenesis and the resulting activation of p53 in early hyperplastic and pre-cancerous lesions was shown to counteract tumor establishment^{176,177}. In striking contrast to these observations, two independent studies have shown that p53 is unable to prevent tumorigenesis in the absence of ARF, which responds to oncogene activation but not DNA damage^{178,179}. The data from Christophorou et al. indicate that only in a scenario when most cells have recovered from DNA damage, p53 might become beneficial by driving the elimination of the few cells that have acquired oncogene-activating mutations¹⁷⁹. However, since several recent reports revealed that activation of oncogenes leads to induction of DNA damage independent of ARF^{176,177}, the future will undoubtedly bring new answers to this important question.

1.2.7 Pathways downstream of activated p53

Once p53 has been activated by one of the stress signals described above, it specifically binds to DNA thereby inducing the expression of adjacent genes that are mainly involved in four processes: reversible and irreversible (senescence) cell cycle arrest, apoptosis, maintenance of genomic integrity and inhibition of vascularization⁵.

1.2.7.1 Cell cycle arrest and senescence

An early discovered consequence of p53 activation in almost all mammalian cell types is cell cycle arrest which is mediated by p53 target genes, such as *p21*¹⁸⁰, *14-3-3 σ* ¹⁸¹, *GADD-45*¹⁸² and *REPRIMO*¹⁸³. By engaging this set of target genes, p53 stops proliferation of damaged cells which provides time to repair DNA damage and prevents mutations from being transmitted to daughter cells. Senescence, an irreversible type of cell cycle arrest, permanently blocks proliferation¹⁸⁴. It may be caused by telomere erosion (so-called replicative senescence), but also by extrinsic forms of stress and is then referred to as “premature senescence”¹⁸⁴. p53-mediated senescence is considered as important as apoptosis for the tumor-suppressive function of p53, however, it is currently not fully understood, which p53 target genes contribute to the onset of senescence that may occur after activation of p53¹⁸⁵. pRb activation via the CDK inhibitor p21 might represent one route of p53-mediated senescence since disruption of *p21* by homologous recombination is able to bypass senescence in human diploid fibroblasts¹⁸⁶. However, disruption of p21 fails to bypass senescence in mouse cells¹⁸⁷. Furthermore, human cells can undergo senescence without activity of pRb or its family members which points to alternative, pRb-independent routes of p53-mediated senescence¹⁸⁸.

1.2.7.2 Apoptosis

When DNA damage exceeds the repair-capacity of a cell, p53 initiates a set of genes to promote programmed cell-death¹⁸⁹. The intrinsic apoptosis pathway involves a variety of p53 transcriptional targets. The Bax protein, a proapoptotic member of the Bcl-2 protein family, represents the prototypic mediator of p53-driven apoptosis¹⁹⁰. The proteins encoded by the more recently identified pro-apoptotic p53 target genes *NOXA*¹⁹¹, *PUMA*¹⁹² and *p53AIP1*¹⁹³ are also located at mitochondria and promote the release of cytochrome C by mitochondrial outer membrane permeabilization (MOMP). The relative contribution of these mediators to p53-mediated apoptosis seems to be cell type-dependent. Additional p53-induced genes have been implicated in the apoptotic response, e.g. *PERP*^{194,195} and *SCOTIN*¹⁹⁶. However, the exact mechanisms by which these factors promote apoptosis are currently unknown. Within the extrinsic apoptotic pathway, initiated outside of cells through pro-apoptotic cell surface receptors (also

called death receptors), p53 triggers the expression of the receptor ligand Fas/Apo-1¹⁹⁷ and the transmembrane trail receptor killer/DR5¹⁹⁸. Along with the p53 target gene *PIDD*¹⁹⁹, these proteins activate the initiator caspase 8 and the BH3-only protein Bid to drive the release of cytochrome C from mitochondria. Cytochrome C cooperates with APAF-1, which is encoded by another p53 target gene²⁰⁰, to form a structure designated as “apoptosome” and this causes activation of caspase 9 and subsequently caspase 3 leading to apoptosis¹⁸⁹.

1.2.7.3 Cell cycle arrest or apoptosis ?

The decision as to whether p53 mediates cell cycle arrest or apoptosis depends on the cellular background, external or internal survival factors, and the type and severity of cellular stress²⁰¹. Two main working hypothesis as to how p53 makes the choice between cell cycle arrest and apoptosis have been put forward: (1) the quantitative model suggests that growth arrest genes contain high-affinity binding sites for p53 while low-affinity binding sites might be located in promoters of apoptosis-promoting genes. While this model is supported by the observation that highly increased p53 activity favors apoptosis over cell cycle arrest²⁰², p53 binding regions located in pro-apoptotic target gene promoters do not in all cases display a low affinity towards p53²⁰³. Interestingly, differences in the composition of transcription-initiation complexes at the promoters of pro-apoptotic versus cell cycle arrest-mediating p53 target genes were detected²⁰⁴. While basal levels of p53 coordinate the assembly of a poised RNA polymerase II initiation complex at core promoters of growth arrest genes thereby lowering the threshold required for a p53 response, core promoters of pro-apoptotic genes show a lower degree of pre-bound initiation complexes under non-stressed conditions and require a higher and prolonged activation of p53 to allow their expression²⁰⁴. (2) Selective activation of p53 due to interaction with specific co-activators represents the basis for the qualitative model: for example, the product of the Wilms tumor suppressor gene, *WT1*, associates with p53 and interferes with its pro-apoptotic activity while p53-dependent cell cycle arrest remains unaffected²⁰⁵. A similar effect has been ascribed to the tumor suppressor protein BRCA1²⁰⁶. The proteins ASPP1 and ASPP2 (for Apoptosis Stimulating Protein of P53) shift the binding affinity of p53 towards promoters of pro-apoptotic genes²⁰⁷ and

this effect can be reverted by a highly conserved inhibitor of p53 mediated apoptosis, iASPP²⁰⁸. Similarly to the ASPP proteins, JMY interacts with p300 thereby enhancing the ability of p53 to drive the expression of apoptotic genes such as *BAX*²⁰⁹ and the co-activator STAT1 supports p53-mediated induction of *BAX*, *NOXA* and *FAS* expression²¹⁰. CHK2, in contrast to ATM, is dispensable for p53-mediated growth arrest upon DNA damage but is required for p53-mediated apoptosis²¹¹. p53 ubiquitinated by E4F1 triggers a transcriptional program that favors a p53-mediated cell cycle arrest versus p53-mediated apoptosis⁷⁴.

1.2.7.4 DNA repair

p53 preserves genomic integrity by regulating processes such as DNA repair and recombination as well as chromosomal segregation^{212,213}. For example, p53 enhances nucleotide excision repair by inducing the genes encoding for p48^{DDB2}²¹⁴ and xeroderma pigmentosum group c (XPC) protein²¹⁵ as well as the p53R2 subunit of ribonucleotide reductase²¹⁶. p53 has also been implicated in base excision repair²¹⁷⁻²¹⁹.

1.2.7.5 p53 as an anti-angiogenic factor

The ability to provoke neo-vascularization liberates tumors from proliferative constraints and the resulting change in tumor behaviour has been termed “angiogenic switch”²²⁰. p53 transactivates the anti-angiogenic thrombospondin gene *TSP1*²²¹ which encodes a secreted protein that remodels the cellular matrix²²². Loss of p53 function leads to a substantial decrease in Tsp-1 level within the extra-cellular matrix and increases the likelihood of new blood vessels being recruited to the tumor. In addition to *TSP1*, p53 transactivates the anti-angiogenic factors brain-specific angiogenesis inhibitor 1 (*BAIL*)²²³ and ephrin receptor A2^{224,225}. The pro-angiogenic factors VEGF²²⁶, bFGF²²⁷, and COX-2²²⁸ represent direct targets for p53-mediated transcriptional repression. Furthermore, p53 inhibits the hypoxia-sensing system by direct binding to HIF-1 α which is consequently targeted for degradation²²⁹ and thereby prevents the production of new blood vessels.

1.2.7.6 p53: more than meets the eye

Recently published data provide clear evidence for wider reaching effects of p53-mediated transactivation⁶. p53 was demonstrated to promote autophagy via interference with the survival promoting mTOR pathway²³⁰. In addition, the “Damage Regulated Autophagy Modulator” DRAM, a lysosomal protein and activator of macroautophagy, whose expression is reduced in human tumors, was recently identified as a transcriptional target of p53²³¹.

Interestingly, p53 was recently shown to regulate the expression of microRNAs *mi-R34a*, *mi-R34b* and *mi-R34c*, which contribute to p53-mediated apoptosis, senescence and cell cycle arrest.²³²⁻²³⁷

p53 may also have a role in the response to nutrient deprivation: low levels of glucose lead to activation of p53 by a pathway which engages AMP activated Kinase (AMPK) culminating in p53-phosphorylation and cell cycle arrest²³⁸. Loss of this checkpoint allows tumor cells to proliferate abnormally under nutrient-restricted conditions and thereby confers a critical growth advantage.

p53 induces the transcription of *SCO2* (Synthesis of Cytochrome C Oxidase II) which is required for assembly of the cytochrome C oxidase (COX) complex²³⁹. Restoration of *SCO2* expression in p53-deficient tumors is able to restore mitochondrial respiration²³⁹. Therefore, p53 inactivation might contribute to the metabolic change of tumor cells from oxidative phosphorylation to glycolysis-based energy production, also known as the “Warburg effect”²⁴⁰.

Furthermore, p53 induces *TIGAR*²⁴¹ (Tp53-Inducible Glycolysis and Apoptosis Regulator). The outcome of TIGAR activity is an elevated glutathion level which serves as a scavenger for reactive oxygen species (ROS). The protein products of additional p53 target genes, such as sestrins²⁴² and *ALDH4*²⁴³ act to lower intracellular ROS levels. This function of p53 seems to prevent DNA damage.

Skin melanocytes and keratinocytes use melanin for protection against UV-irradiation. The production of melanin is orchestrated by α -MSH (melanocyte stimulating hormone) and pro-opiomelanocortin (POMC), a multicomponent precursor unit from which MSH originates by proteolytic cleavage²⁴⁴. p53, activated by sun exposure, transactivates the *POMC* gene in keratinocytes thereby enhancing MSH production²⁴⁵. Decreased POMC

expression due to mutation of p53 may therefore explain the increase in skin cancer caused by inactivation of p53²⁴⁶.

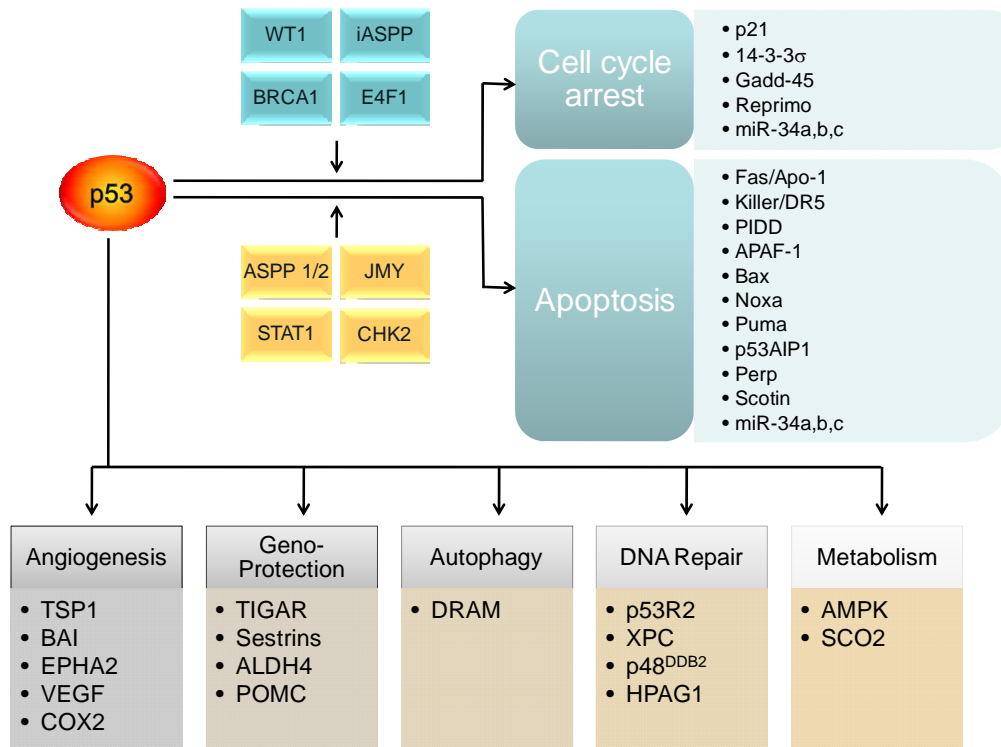


Figure 4. Downstream pathways activated by p53

After activation of p53, which is triggered by various incoming signals, p53 can elicit a multitude of cellular responses which involve different sets of target genes. Best characterized are p53-mediated cell cycle arrest and apoptosis with the decision between these two outcomes being dependent on the cellular background and the presence of different co-factors. p53 can also promote DNA repair after moderate DNA damage or enables cells to respond to nutrient deprivation by regulating genes of the metabolic pathway. p53 has a geno-protective role by mediating the removal to metabolically generated reactive oxygen species. p53 also protects against UV exposure by influencing the melanin production in skin.

Finally, there is an ongoing debate about the role of p53 in life span regulation. While constitutive, hyperactive p53 provokes a premature ageing phenotype in mice²⁴⁷, there is evidence that this is not the physiological function of p53 since mice containing an additional copy of *p53* (“p53-super mice”) display increased tumor protection without life-span reduction²⁴⁸. The same is true for mice expressing low levels of MDM2 or elevated ARF levels and consequently increased amounts of p53 protein^{249,250}. Interestingly, mice with elevated, but normally regulated ARF and p53 (“super ARF/p53

mice”) exhibit a strong resistance against cancer and a reduced level of ageing-related DNA damage ²⁵¹. Therefore, p53 may have a function in the protection against cellular ageing.

In conclusion, p53 may serve to protect cells from genomic damage but may also eliminate cells that were damaged to severely. For that reason, a model was proposed in which, dependent on the stress level, p53 is able to switch from a role as a cellular protector to an executioner ²⁵².

1.3 The proto-oncogene *c-MYC*

1.3.1 *c-MYC* is activated in human neoplasia

In 1979, the first *c-MYC* gene was discovered as the transforming gene (*v-MYC*) carried by the MC29 myelocytomatosis virus, a descendant of avian leukosis virus (ALV) ²⁵³. From this initial finding it took another 3 years until the cellular proto-oncogene *c-MYC* was implicated in human cancer due to its translocation in Burkitt`s lymphoma (BL) ^{254,255}. In BL, the *c-MYC* locus on 8q24.21 is constitutively activated by enhancer sequences of immunoglobulin genes due to a chromosomal translocation. As a consequence, *c-MYC* expression becomes independent from physiological signals ^{256,257}. Rearrangements of the *c-MYC* proto-oncogene are also common in other types of hematopoietic malignancies, such as acute lymphoblastic leukemia ²⁵⁸ (ALL), multiple myeloma ²⁵⁹ (MM) and primary plasma cell leukemia ²⁶⁰ (PCL). Further studies revealed *c-MYC* is also over-expressed in human tumors that have not undergone translocations of the *c-MYC* locus. In these cases, stabilization of *c-MYC* mRNA ^{261,262} or increased translation of *c-MYC* mRNA due to a mutated internal ribosomal entry site ²⁶³ can lead to increased protein levels of *c-MYC*. Phosphorylation sites located within the N-terminal domain of *c-MYC* modulate its transforming potential ^{264,265} and their mutation in cancer compromises degradation of *c-MYC* ²⁶⁶. *c-MYC* negatively auto-regulates its own expression and this mechanism is lost in transformed and tumor derived cell lines ^{267,268}. In most solid tumors, gene amplification accounts for aberrant expression of *c-MYC* ^{269,270}. E.g. amplification of *c-MYC* occurs in 20-30% of breast carcinomas and is related to poor prognosis ²⁷¹⁻²⁷⁴. Viral promoter insertion also accounts for increased

expression of *c-MYC* in human tumors²⁷⁵ and activating mutations in upstream regulators, such as PDGF^{276,277} or Notch1^{278,279} contribute to *c-MYC* activation. In colon carcinoma, mutations affecting the Wnt/APC/ β -catenin pathway activate the expression of *c-MYC*²⁸⁰⁻²⁸².

1.3.2 Regulation of the *c-MYC* proto-oncogene

Soon after *c-MYC* had been implicated in tumorigenesis, its expression in different cell types turned out to be strongly related to mitogenic signaling and proliferation^{283,284}. *c-MYC* levels are very low in quiescent cells²⁸⁵. However, a rapid increase of *c-MYC* mRNA and protein occurs when cells are exposed to mitogens^{285,286}. After this initial peak, *c-MYC* levels gradually decline to remain at a basal level in cycling cells^{287,288}. *c-MYC* levels rapidly increase in response to serum stimulation²⁸⁵ or mitogenic signals such as lipopolysaccharides²⁸³ and platelet-derived growth factor (PDGF)^{283,284}. Early findings pointed to a strict requirement of Src kinases for induction of *c-MYC* by PDGF²⁸⁹. It turned out that PDGF-stimulated, Src-dependent phosphorylation of Vav2, a guanine nucleotide exchange factor (GEF) and the consequent activation of a Rac-dependent pathway mediates induction of *c-MYC*²⁹⁰. In addition, the NOTCH1 and Wnt signaling pathways act as positive regulators of *c-MYC*²⁷⁹⁻²⁸¹. In contrast, transforming growth factor beta (TGF- β) leads to repression of *c-MYC* via Smad proteins in human skin keratinocytes and mammary epithelial cells^{291,292}. Another co-factor essential for TGF- β -mediated repression of *c-MYC* is C/EBP β which is commonly inactivated in human cancer due to activation of its inhibitor LIP²⁹³.

The short half-life of *c-MYC* protein (15-30 min)^{294,295} allows a stringent control of *c-MYC* activity. Degradation of *c-MYC* protein is ubiquitin-dependent and catalyzed by the 26S proteasome^{266,296}. Several E3-ligases have been implicated in targeting *c-MYC* for proteasomal degradation, such as SCF E3-ligase complexes containing the F-box proteins Skp2²⁹⁷ or Fbw7/hCDC4^{298,299}. The ubiquitin-specific protease USP28 associates with *c-MYC* indirectly via Fbw7 and USP28-mediated de-ubiquitination may cause stabilization of *c-MYC* in human tumors³⁰⁰.

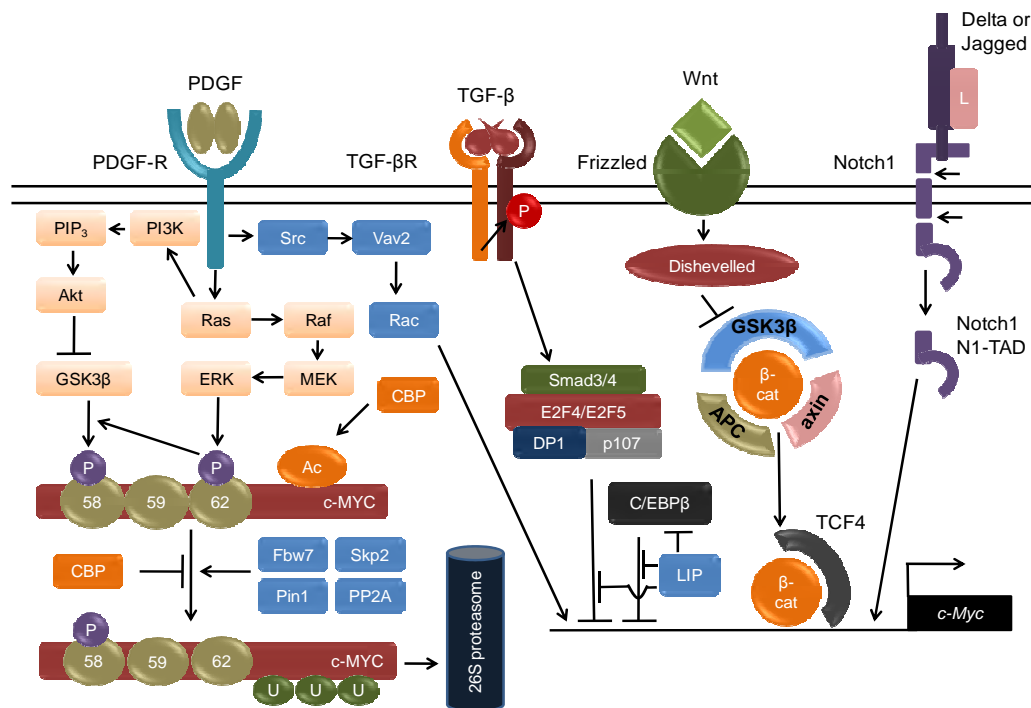


Figure 5: Regulation of c-MYC.

A multitude of upstream signaling pathways tightly control *c-MYC* mRNA and protein level. Stimulation of PDGF influences *c-MYC* protein turnover via two routes: In cycling cells, the Ras/Raf/MEK/ERK pathway stabilizes *c-MYC* via phosphorylation at Ser62, while PI3K/Akt signaling promotes phosphorylation of *c-MYC* at Ser58 through GSK3β culminating in *c-MYC* degradation. The E3-ligases Fbw7 and Skp2 ubiquitinate *c-MYC* thereby targeting it for proteasomal degradation. While the concerted action of Pin1/PP2A favors ubiquitination of *c-MYC* by Fbw7, CBP-mediated *c-MYC* acetylation counteracts its ubiquitination. PDGF-mediated Rac-signaling exerts a positive effect on *c-MYC* mRNA expression. Activation of the Frizzled receptor by Wnt triggers recruitment of Dishevelled leading to inhibition of GSK3β and as a result, unphosphorylated β-catenin (β-cat) is not longer degraded, accumulates in the cytosol, translocates to the nucleus and complexes with the transcription factor TCF4 to activate *c-MYC*. Activation of Notch1 by its ligands Delta or Jagged targets Notch1 for proteolytic cleavage and the released intracellular domain of Notch1 (N1-TAD) translocates to the nucleus, where it interacts with members of CSL transcription factors and induces *c-MYC* expression. Finally, TGF-β leads to repression of *c-MYC* via a complex containing Smad3/4, E2F4/5, DP1 and p107. An essential co-factor of TGF-β-mediated repression of *c-MYC*, C/EBPβ, is inactivated by LIP, which is commonly over-expressed in tumors and augments *c-MYC* expression. U: ubiquitin, P: phosphate group, Ac: acetyl group.

The Ras effector pathway controls *c-MYC* stability³⁰¹ via modification of two functionally opposing phosphorylation sites³⁰². Upon growth-factor stimulation, Ser-62 phosphorylation stabilizes *c-MYC* presumably via ERK³⁰². Ser-62 phosphorylation of *c-MYC* is a prerequisite for phosphorylation at Thr-58, which is catalyzed by glycogen synthase kinase 3 beta (GSK3β)³⁰². Phospho-Thr58 represents a binding site for the

E3-ligase Fbw7/hCDC4, which promotes ubiquitination and degradation of c-MYC^{298,299}. After mitogenic stimulation, the increased activity of the Ras-PI(3)K/Akt pathway leads to phosphorylation of GSK3 β which consequently gets inactivated and thereby facilitates stabilization of c-MYC³⁰³. Subsequently, Akt activity declines, which favors the degradation of c-MYC. Phosphorylation of c-MYC at Thr-58 generates a binding site for the prolyl isomerase PIN1 and modification of P59 by PIN1 allows recruitment of protein phosphatase 2A (PP2A) to c-MYC³⁰⁴. PP2A in turn catalyzes the de-phosphorylation of c-MYC at Ser-62 which promotes ubiquitination and proteasomal degradation of c-MYC³⁰⁴. Another example for regulation of c-MYC by post-translational modification is its acetylation by CREB binding protein (CBP) which interferes with ubiquitination and, as a consequence, stabilizes c-MYC³⁰⁵.

1.3.3 c-MYC acts as a transcription factor

The *c-MYC* gene consists of three discrete exons and encodes for a protein of 439 amino acids (64 kDa)³⁰⁶. Due to alternative translation-initiation from an upstream non-AUG (CUG) and a downstream AUG start site, two additional isoforms of c-MYC with distinct N-termini occur in cells^{307,308}. The C-terminal region of c-MYC contains a leucine zipper (LZ) and a helix-loop-helix motif (HLH) which are common to a class of related transcription factors^{309,310}. Via its HLH-LZ-dimerization motif c-MYC selectively heterodimerizes with the bHLH-LZ transcription factor MAX^{311,312}. The c-MYC/MAX heterodimer activates transcription via binding to the E-box consensus sequence CA(C/T)GTG in the vicinity of target gene promoters^{313,314}.

The N-terminus of c-MYC functions as a transactivation domain³¹⁵ and can be subdivided into smaller, evolutionary conserved regions: c-MYC homology boxes (MycBox) I and II have been implicated in c-MYC-mediated cellular transformation³¹⁶, apoptosis³¹⁷ and inhibition of differentiation³¹⁸. MycBox III and MycBox IV are also necessary for cellular transformation and MycBox III has been implicated in c-MYC-mediated apoptosis and transcriptional repression³¹⁹ whereas MycBox IV, besides affecting c-MYC-induced apoptosis and G₂ arrest, modulates DNA binding by c-MYC³²⁰. While the transactivation domain of c-MYC, which contains MycBox I and II, is critical for c-MYC-induced proliferation³²¹, the relative contribution of

MycBox III and IV motifs to cellular proliferation driven by c-MYC is a subject of ongoing research ³²². The observation that MycBox I is dispensable for transactivation but required for cellular transformation ³¹⁵ indicates that c-MYC may have transcription-independent functions.

1.3.4 Transactivation of c-MYC target genes

Transcriptional activation by c-MYC involves the association of the c-MYC/MAX heterodimer with co-factors and their recruitment to target gene promoters ^{322, 323}. c-MYC is able to recruit histone acetyltransferase (HAT) activity ³²⁴ to promoters of target genes via association with TRRAP (TRansformation/tRanscription domain-Associated Protein) ^{325,326}. c-MYC-mediated target gene activation is associated with an increase in histone H3 and histone H4 acetylation in the respective promoter region ^{327,328}. The evolutionary conserved TRRAP protein directly binds to MycBox II and association with TRRAP is essential for c-MYC-mediated transformation ³²⁴. TRRAP itself represents a component of the highly conserved protein complex SAGA (SPT/ADA/GCN5/Acetyltransferase), which is involved in transcriptional regulation and contains the histone acetyltransferase GCN5 ^{329,330}. In addition, TRRAP represents the core component of the H2A/H4 histone acetylase TIP60 complex which also contains the ATPases TIP48 and TIP49 ^{324,331}. c-MYC further recruits the SWI-SNF complex via direct association of MycBox II with the SNF5 homolog INI1/hSNF5 ³³². This multiprotein complex activates transcription by chromatin-remodelling in an ATP-dependent manner ³³³. However, MycBox II is not required for transactivation of all c-MYC target genes and further mechanisms exist by which c-MYC can achieve transactivation ³³⁴. The HATs CBP and p300 associate with the C-terminus of c-MYC and are recruited to promoters of c-MYC target genes ³⁰⁵. Altogether, the above mentioned co-factors promote transcription by chromatin-remodelling and histone acetylation which opens the DNA-nucleosome structure ³³⁵. Thereby, this modification of the so-called “histone code” facilitates the access of proteins to chromatin and the formation of transcriptional complexes at gene promoters ³³⁶.

Besides recruitment of HAT activity, c-MYC promotes efficient transcription elongation via the positive transcription elongation factor b (p-TEFb) ³³⁷. Recruitment of

p-TEFb by c-MYC/MAX leads to C-terminal phosphorylation of RNA-Polymerase II and promoter clearance³³⁷⁻³³⁹. The serine/threonine kinase PIM1 associates with the c-MYC/MAX dimer via MycBox II and catalyzes phosphorylation of histone H3 at Ser10 thereby enhancing the transcriptional capacity of c-MYC³⁴⁰. Finally, ubiquitination and protein turnover of c-MYC has been implicated in its transcriptional activity³⁴¹ and the SCF E3-ligase component Skp2 augments transactivation by c-MYC^{297,342}. Similarly, the HectH9 ubiquitin ligase, which ubiquitinates c-MYC at multiple sites, is able to augment the transcriptional activity of c-Myc³⁴³.

In contrast to c-MYC, the ubiquitously expressed MAX protein can form homo-dimers to directly contact DNA³¹² but MAX homodimers lack transactivation activity³⁴⁴. MAX heterodimerizes with other bHLH-LZ transcription factors, e.g. Mad1³⁴⁵, Mxi1(Mad2)³⁴⁶, Mad3³⁴⁷, Mad4³⁴⁷, Mnt (Rox)³⁴⁸ and Mga³⁴⁹. These MAX-containing heterodimers recruit histone-deacetylases (HDAC) to E-box promoters by direct association with the co-repressor SIN3^{350,351}. The HDAC-catalyzed removal of acetylated histone-tails closes the conformation of chromatin and results in gene repression³⁵². c-MYC, which is highly expressed in proliferating, non-differentiated cells, is down-regulated when cells undergo arrest or terminal differentiation whereas the expression of Mad/Mnt factors is being induced³⁵³. The process of terminal differentiation of human promyelocytic leukemia cells is accompanied by a switch from c-MYC/MAX to Mad/MAX heterodimers³⁵⁴.

1.3.5 c-MYC-mediated target gene repression

Initial studies revealed that c-MYC is able to repress the adenoviral late promoter (AdMLP)³⁵⁵. Also the differentiation-specific factors c/EBP α and serum albumine are repressed by c-MYC³⁵⁶. This effect is dependent on so-called initiator (Inr) elements, which are 17 bp pyrimidine-rich motifs^{356,357}. With the exception of the *p27^{KIP1}* promoter³⁵⁸, c-MYC does not directly contact the DNA of promoters in repressed target genes^{359,360}. Instead, c-MYC is recruited to these promoters by binding to other, promoter-associated proteins such as MIZ1³⁶¹, YY1³⁶², Sp1³⁶³, GTF2I (TFII-I)³⁵⁵ and NF-Y³⁶⁴ which transactivate gene expression. c-MYC interferes with the function of these transcription factors or blocks the access to essential co-factors. In case of MIZ1,

c-MYC competes with binding of the transcriptional co-activator p300 to MIZ1 at the Inr element³⁵⁹. Alternatively, TIP48 and TIP49 may be involved in the transcriptional repression through the c-MYC-MIZ1 complex³⁶⁵. Another study suggested that c-MYC recruits the co-repressor DNA methyltransferase Dnmt3a, which is required for *de novo* DNA methylation³⁶⁶, to promoters of target genes via association with MIZ1³⁶⁷.

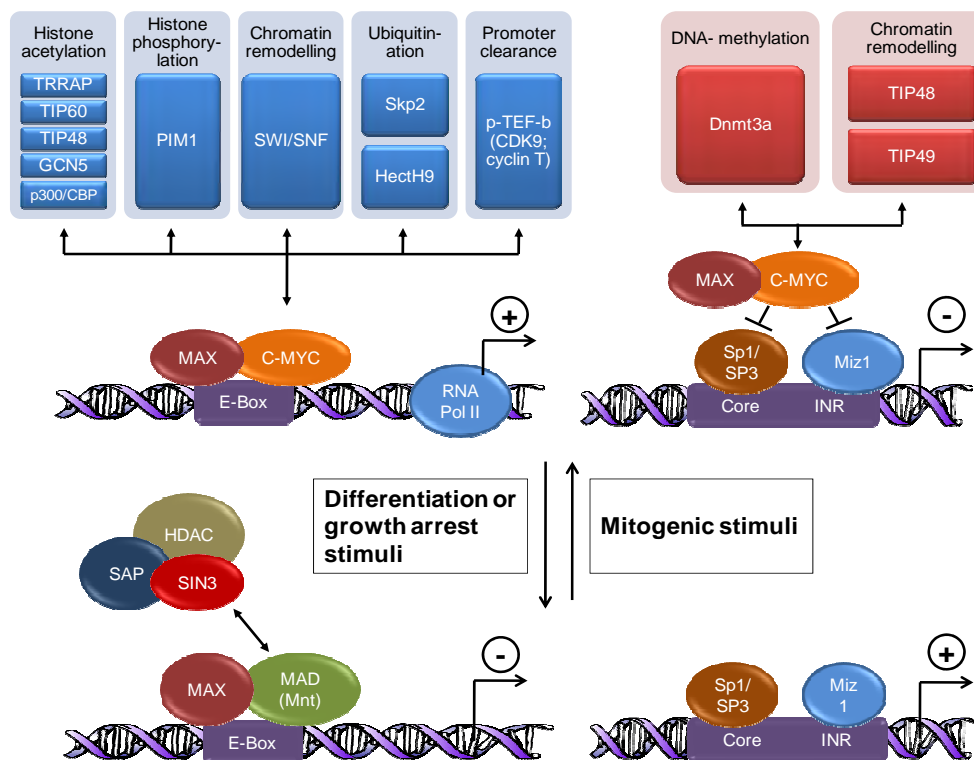


Figure 6: c-MYC target gene regulation.

c-MYC-MAX heterodimers transactivate target genes by binding to E-box elements and recruitment of several co-activators. These co-activators include the ATPases TIP48 and TIP49 (not shown), histone acetyltransferases such as GCN5, TIP60, CREB binding protein (CBP) and p300. GCN5 and TIP60 are indirectly associated with c-MYC through TRRAP which directly binds to MycBox II, a conserved element in the c-MYC transactivation domain. Other co-activators interacting with MycBox II are the serine/threonine kinase PIM1, positive transcription elongation factor b (p-TEFb) and the chromatin-remodelling complex SWI/SNF. Association with E3-ligases SCF-Skp2 or HectH9 are additional mediators of target gene activation by c-MYC. Mad/MAX or Mnt/MAX heterodimers antagonize transactivation by c-MYC through competing with c-MYC/MAX at target gene promoters and recruitment of histone deacetylases (HDAC) via SIN3. c-MYC/MAX heterodimers inhibit the activating transcription factor MIZ1 by blocking its access to p300 and recruitment of the DNA methyltransferase Dnmt3a. The ATPases TIP48 and TIP49 have also been implicated in c-MYC/MAX-mediated transcriptional repression. RNA Pol II: RNA polymerase II (adapted from Ref. 323)

1.3.6 The c-MYC target gene network

Multiple aspects of c-MYC biology are closely linked to its ability to transactivate and repress target genes³²². Expression array analyses, serial analysis of gene expression (SAGE) and analysis of c-MYC DNA binding sites revealed a large number of RNA Polymerase II (Pol II) regulated genes whose expression is influenced by c-MYC³⁶⁸⁻³⁷¹. However, recent reports have demonstrated that the profound effect of c-MYC on cellular growth and proliferation is due to its ability to influence transcription by all three nuclear RNA polymerases^{372,373}. In addition, c-MYC has been implicated in the regulation of microRNAs^{374,375}. A cluster of six microRNAs (= mir-17-92) located at chromosome 13 is directly induced by c-MYC and limits translation of E2F1³⁷⁴. Interestingly, the mir-17-92 polycistron has also been characterized as a human oncogene³⁷⁵, promotes tumor angiogenesis³⁷⁶ and blocks differentiation of lung progenitor cells³⁷⁷.

The genes regulated by c-MYC are involved in metabolic processes, cellular adhesion, organization of the cytoskeleton, cell cycle regulation, mitochondrial homeostasis, protein biosynthesis and DNA repair²⁵⁶. Altogether, c-MYC may regulate up to 15% of all genes present in the human genome²⁵⁶. However, only a fraction of these genes is responsive to c-MYC in all cell types analyzed³⁷⁸. Whether these genes are direct targets of c-MYC or respond indirectly to secondary events triggered by *c-MYC* activation is unknown in most cases. A direct c-MYC target gene is defined as a gene whose promoter is bound by c-MYC/MAX complexes which trigger its expression in the absence of *de novo* protein biosynthesis³⁷⁹. There is compelling evidence that the combined actions of multiple genes regulated by c-MYC contribute to the effects of *c-MYC* activation on cell cycle progression since a genome-wide screen revealed that the slow proliferation phenotype of c-MYC-deficient RAT1 cells can only be rescued by c-MYC or N-MYC, but not any other single cDNA³⁸⁰.

1.3.7 Biological consequences of c-MYC activation

Hanahan and Weinberg suggested that six essential alterations in cellular behaviour caused by distinct genetic alterations in cancer cells collectively account for malignant growth: self-sufficiency in growth signals, insensitivity to growth-inhibitory signals, evasion of programmed cell death, limitless replicative potential, sustained angiogenesis,

and tissue evasion and metastasis³⁸¹. Notably, oncogenic activation of *c-MYC* has been experimentally linked to all of these processes³⁸².

1.3.7.1 c-MYC and cellular proliferation

c-MYC activation is sufficient for induction of DNA synthesis and promotes cell cycle re-entry in quiescent fibroblasts^{383,384}. Targeted deletion of *c-MYC* in embryonic stem cells leads to retarded embryonic growth and development, which culminates in embryonic lethality³⁸⁵. This effect highlights the role of *c-MYC* in normal growth control and development. During development, *c-MYC* expression can be detected in a variety of tissues and correlates with proliferation, while downregulation of *c-MYC* leads to cell cycle arrest and onset of differentiation³⁸⁶⁻³⁸⁸. A critical role for *c-MYC* in cell cycle control became also obvious in *c-MYC*-deficient rat fibroblasts which show a reduced proliferation rate and cell cycle defects in the G₁ phase, as delayed phosphorylation of the retinoblastoma protein (pRb)³⁸⁹.

1.3.7.2 c-MYC-mediated regulation of the cell cycle

The decision between quiescence and proliferation is made in the G₁ phase of the cell cycle at the so-called “restriction point” (R)^{390,391}. This decision is governed by the phosphorylation state of the pRb protein: hypophosphorylated pRb obstructs passage through the R point while hyperphosphorylated pRb allows entry into S phase. *c-MYC* affects this important stage of the cell cycle at various levels: *CCND2* (*Cyclin D2*) and *CDK4* (*Cyclin dependent kinase 4*) are direct *c-MYC* target genes^{392,393}. As a consequence of *c-MYC* activation, the CDK inhibitors p21 and p27^{KIP1} are sequestered in Cyclin-D-CDK4 complexes^{392,394}, which augments Cyclin-E-CDK2 activity. Thr187 phosphorylation of p27^{KIP1} by Cyclin-E-CDK2 is a prerequisite for dissociation of p27^{KIP1} from Cyclin-E-CDK2³⁹⁵ and SCF-Skp2 E3-ligase-mediated ubiquitination and proteasomal degradation of p27^{KIP1}^{396,397}. The SCF-Skp2 components *CUL1* and *CKS* are directly induced by *c-MYC*^{368,398}. p27^{KIP1}-free Cyclin-E-CDK2 complexes are accessible to an activating phosphorylation by Cyclin-Activating Kinase (CAK)³⁹⁹, which is activated by *c-MYC* via a newly described post-transcriptional mechanism⁴⁰⁰.

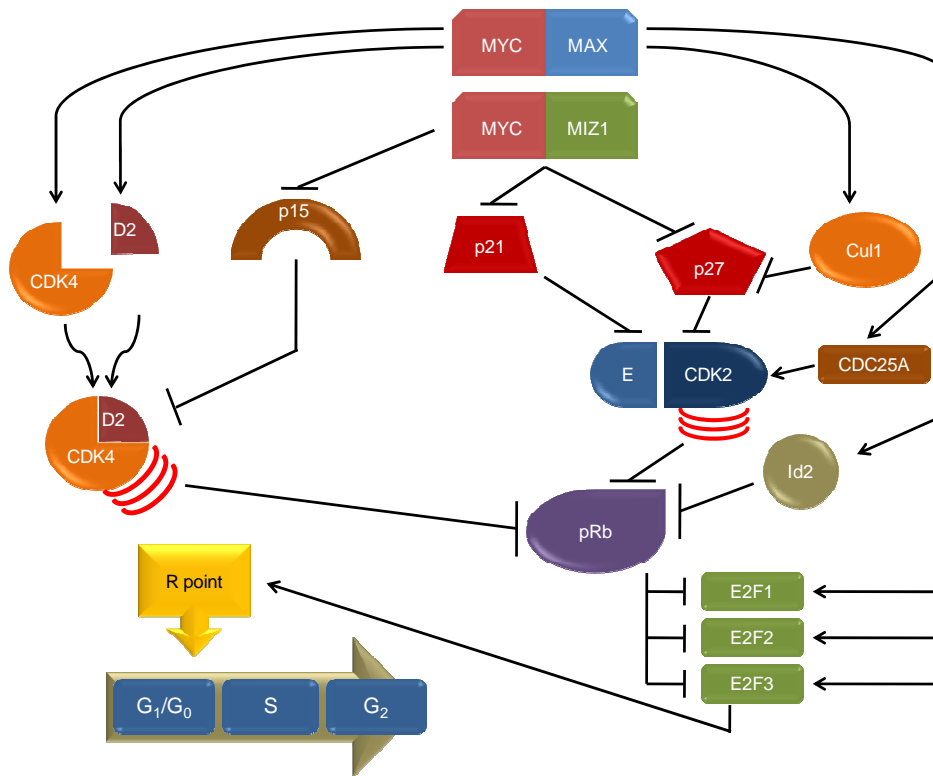


Figure 7: c-MYC and cell cycle entry at the G₁/S boundary.

c-MYC activates cyclin-dependent kinases (CDKs) mandatory for G₁/S progression by inducing *Cyclin D2* and *CDK4* and repression of CDK inhibitors p15^{Ink4b}, p21 and p27^{KIP1}. Increased CDK activity and the following hyperphosphorylation of the Retinoblastoma protein (pRb) liberates E2F which launches a transcriptional program that drives cell cycle progression through S phase. Besides direct transcriptional modulation of the CDK machinery, c-MYC activates CDK2 by promoting the degradation of p27^{KIP1} and via the CDC25A phosphatase which de-phosphorylates CDKs. Inactivation of pRb may also be achieved by c-MYC via activation of Id2, an inhibitor of pRb family members. Furthermore, *E2F1-3* represent direct targets of the c-MYC proto-oncogene. Adapted from Ref. 1.

In addition, c-MYC- and E2F-mediated transactivation of the CDC25A phosphatase stimulates CDK2 activity^{401,402}. c-MYC also leads to CDK activation via repression of the CDK inhibitors p21, p27^{KIP1}, p15^{INK4B}, and p16^{INK4A}^{403,404}. Once activated, Cyclin-E-CDK2 and Cyclin-D-CDK4 catalyze hyper-phosphorylation of the pocket proteins pRb⁴⁰⁵, p107 and p130⁴⁰⁶ and the released E2F transcription factors associate with DP1 leading to expression of various genes essential for cell cycle progression⁴⁰⁵. c-MYC furthermore activates a dominant-negative antagonist of Rb family members, Id2, and thereby increases E2F activity⁴⁰⁷. c-MYC is also able to directly induce expression of the genes encoding the transcription factors E2F1³⁶⁹, E2F2⁴⁰⁸ and E2F3⁴⁰⁹. Others provided

evidence that c-MYC drives G₁/S progression independent of E2F activity and via direct regulation of Cyclin-E-CDK2 function⁴¹⁰.

1.3.7.3 c-MYC and differentiation

Early findings revealed a role of c-MYC in blocking terminal differentiation in diverse cell types, as adipocytes or myoblasts^{411,412}. During differentiation, expression of c-MYC is down-regulated by SWI/SNF-complexes⁴¹³ and C/EBP α ⁴¹⁴ and, as a consequence, differentiation-promoting genes, which are repressed by c-MYC, are up-regulated, such as *p15^{Ink4b}*³⁵⁹, *p21*⁴¹⁵, *C/EBP α* ⁴¹⁶ and *H-ferritin*⁴¹⁷. The down-regulation of c-MYC is accompanied by a switch from c-MYC/MAX to Mad/MAX heterodimers bound to chromatin³⁵⁴ and, as a consequence, target genes, which have de-differentiating functions, are down-regulated. c-MYC plays an important role in the maintenance of undifferentiated, proliferative progenitor cells in the intestinal epithelium^{281,418}. Unexpectedly, enforced expression of c-MYC promotes differentiation of skin epidermal cells⁴¹⁹. The ability of c-MYC to reduce adhesive interactions between stem cells presumably causes this differentiation-promoting effect in skin epidermal cells⁴²⁰. Similarly, activation of *c-MYC* causes down-regulation of integrins and N-cadherin in hematopoietic stem cells (HSCs), which leads to premature exit of HSCs from the stem cell niche and differentiation⁴²¹. Furthermore, c-MYC represses E-cadherin via a post-transcriptional mechanism, which reduces cellular adherens and promotes transformation of mammary epithelial cells⁴²². Notably, the detachment of cell-cell contacts plays a critical role in tumor invasion and metastasis⁴²³.

1.3.7.4 c-MYC and apoptosis

Ectopic expression of c-MYC was found to promote apoptosis in murine hematopoietic cells⁴²⁴ and in mouse fibroblasts³¹⁷. Survival factors, like the serum cytokines insulin-like growth factor (IGF) or platelet-derived growth factor (PDGF), suppress c-MYC-induced apoptosis independently of their cell cycle promoting capacity⁴²⁵. c-MYC also sensitizes cells to apoptosis after treatment with genotoxic drugs³¹⁷ and enhances the cytotoxicity of TNF- α ^{426,427}, CD95⁴²⁸ and various other stimuli⁴²⁹. c-MYC-induced apoptosis is mediated by the tumor suppressor p53¹⁴⁷. This effect is at

least in part mediated by the induction of ARF, an inhibitor of the p53-specific E3-ligase MDM2⁴³⁰. In addition, c-MYC is able to stimulate cytochrome C release from mitochondria in an ARF- and p53-independent manner⁴³¹. This process is essential for Bax oligomerization and activity^{432,433}. Furthermore, c-MYC mediates cytochrome C release by inducing the BH3-only protein BIM⁴³⁴ and repression of the anti-apoptotic factors Bcl-X_L and Bcl-2^{435,436}. Apoptosis might also be provoked via induction of DNA damage: activation of c-MYC by the c-MYC-ER system was shown to provoke DNA damage in normal human fibroblasts (NHF) via generation of reactive oxygen species (ROS)¹⁷⁰. In contrast, generation of DNA double strand breaks by a tet-regulatable *c-MYC* allele in NHFs and normal murine lymphocytes was demonstrated to occur in the absence of ROS generation⁴³⁷. Interestingly, ectopic expression of c-MYC leads to elevated activity of replication origins culminating in activation of a DNA damage response¹⁶⁹. Several other oncogenes were also shown to provoke DNA damage via inducing replication stress^{172,173}.

1.3.7.5 c-MYC influences cell growth and vascularization

c-MYC is able to promote cell growth independent of cellular proliferation and this can be attributed to its ability to enhance protein biosynthesis^{438,439}. A profoundly increased synthesis of new proteins is one of the first events which occur after mitogenic stimulation. Ribosomal assembly is a tightly regulated process that requires coordinated transcription mediated by all three RNA polymerases^{440,441}. Besides regulating Pol II-mediated gene expression, c-MYC enhances the Pol I-mediated transcription of ribosomal RNAs via binding to rDNA and association with the Pol I-specific factor SL1^{372,442,443}. c-MYC also activates Pol III transcription and enhances the expression of transfer RNAs and 5S ribosomal RNA by direct association with TFIIB³⁷³ and via recruitment of the co-factors TRRAP and GCN5 which leads to acetylation of histone H3⁴⁴⁴. The gene encoding the ribosomal protein L11 is a direct transcriptional target of c-MYC and negatively regulates c-MYC function at target gene promoters and therefore L11 and c-MYC constitute a negative feedback loop⁴⁴⁵. L11 might act as a sensor of aberrant ribosomal biogenesis and presumably maintains homeostasis during ribosome assembly by regulating c-MYC activity. Finally, c-MYC induces the expression

of *PES1*, *BOPI* and *WDR12* whose protein products form a stable complex which is involved in rRNA processing⁴⁴⁶⁻⁴⁴⁸.

c-MYC is also involved in the process of vascularization⁴⁴⁹: *c-MYC* increases the mRNA-turnover of the anti-angiogenic factor Tsp-1⁴⁵⁰ and is required for the expression of vascular endothelial growth factor (VEGF)⁴⁴⁹.

Immortalization of cells is another hallmark of *c-MYC* activation^{451,452} and *c-MYC* cooperates with the *RAS* oncogene in cellular transformation⁴⁵³. Interestingly, *c-MYC* mutants still able to transactivate target genes while lacking the repressive potential due to deletion of MycBox II are unable to block cellular differentiation and do not cooperate with Ras in cellular transformation^{356,379}. A mutant *c-MYC* protein, carrying a deletion of the N-terminal MycBox I, is defective for cellular transformation despite retaining transcriptional activity³¹⁹. This observation raised the possibility that *c-MYC* contributes to oncogenic transformation via non-transcriptional pathways. Indeed, *c-MYC* interacts with components of the DNA replication machinery, as e.g. MCM2-7, Cdc6, ORC and Cdt1 proteins^{169,454}. *c-MYC* was recently shown to promote DNA replication by a non-transcriptional mechanism¹⁶⁹. Notably, activation of *c-MYC* leads to enhanced DNA replication accompanied by DNA damage^{169,455} and the resulting genomic instability, which is a feature of *c-MYC*-overexpressing cancer cells⁴⁵⁶, might contribute to tumorigenesis. However, the exact mechanism through which *c-MYC* directly enhances DNA replication is currently unknown.

1.3.8 *c-MYC* in tumor maintenance and progression

Transgenic mouse models have provided a direct link between *c-MYC* and tumorigenesis: constitutively de-regulated expression of *c-MYC* under control of the tissue specific mouse mammary tumor virus (MMTV) promoter leads to accelerated development of mammary adenocarcinoma^{457,458}. When expression of *c-MYC* is brought under control of the immunoglobulin (Ig)- μ or the Ig- κ enhancer, mice develop lymphoma early after birth^{459,460}. Further insight came from approaches using conditional *c-MYC* alleles in transgenic mice: in pancreatic β -cell oncogenesis, the oncogenic potential of *c-MYC* is counterbalanced by apoptosis³⁸². When *c-MYC*-

induced apoptosis was blocked by co-expression of Bcl-X_L, the complete *c-MYC* oncogenic program, which leads to progression into angiogenic, invasive tumors, was uncovered³⁸². Similarly, mouse model systems employing conditional *c-MYC* alleles under control of tissue specific promoters have been used to study tumor development in hematopoietic cells⁴⁶¹, mammary gland⁴⁶², liver cells⁴⁶³ and skin⁴⁶⁴.

An important conclusion, which emerged from these studies, was dependence of the tumor cells on sustained activation of an oncogenic pathway, also termed “oncogene addiction”^{465,466}. The first hint that *c-MYC*-induced tumorigenesis might be reversible came from a study focusing on hematopoietic tumor development⁴⁶¹. It is now clear that the consequences of *c-MYC* inactivation are dependent on the type of tumor. Brief inactivation of *c-MYC* is sufficient to allow sustained regression of osteogenic sarcomas accompanied by differentiation into mature osteocytes⁴⁶⁷. Others showed that inactivation of *c-MYC* causes regression of invasive hepatocellular carcinoma⁴⁶³. Interestingly, loss of *c-MYC* provoked differentiation of liver tumor cells into normal hepatic lineages and a concomitant loss of tumor marker expression⁴⁶³. However, restoration of *c-MYC* function leads to an immediate restoration of the neoplastic capacity in this system, showing that *c-MYC* inactivation causes “tumor dormancy” with cells retaining a latent potential to become cancerous⁴⁶³. In contrast, only a small number of *c-MYC*-induced mammary carcinomas undergo transient tumor regression after inactivation of *c-MYC* and a rapid tumor recurrence was observed upon re-activation of *c-MYC*⁴⁶⁸. In most cases mammary carcinomas induced by *c-MYC* rapidly progress to a state which is independent of *c-MYC* activation⁴⁶⁸. While activation of secondary oncogenic pathways, such as *KRAS2* activation, were suggested to be responsible for this escape of mammary carcinomas from *c-MYC*-dependence⁴⁶², later studies showed that this accounts only for a minor fraction of these tumors⁴⁶⁸. A mechanism potentially responsible for the escape of *c-MYC*-induced tumors from their addiction is *c-MYC*-mediated genomic instability⁴⁶⁷ which eventually causes inactivating mutations in tumor suppressor genes or activates alternative oncogenic pathways. Since the recurrence of tumors after *c-MYC* inactivation due to secondary events may represent a major problem during therapeutic oncogene inactivation⁴⁶⁹, recent efforts aim to develop strategies to override the mechanisms of tumor escape from oncogene-dependence^{470,471}.

1.4 Aim of the study

The first goal of this study was to comprehensively identify p53-interacting proteins using an improved tandem affinity purification (TAP) approach⁴⁷², called “iTAP”⁴⁷³, in combination with Multidimensional Protein Identification Technology (MudPIT)⁴⁷⁴, which is a highly accurate and sensitive mass-spectral method. Newly identified p53 interactors should then be subjected to functional analyses in order to determine their relevance for the DNA damage/p53 response.

In parallel the characterization of novel c-MYC target genes was performed. Although several genome-wide studies to identify c-MYC target genes have been reported previously, none of these was performed in human epithelial cells, which are highly relevant for cancer formation. Therefore, the first step of this study was the establishment of a conditional c-MYC expression system in breast epithelial cells. Subsequently, a global analysis of c-MYC-regulated genes was planned. Ultimately, cancer-relevant c-MYC target genes should be functionally characterized in detail.

2 Materials

2.1 Chemicals and Reagents

Compound	Supplier
1 kb DNA ladder	<i>Invitrogen GmbH, Karlsruhe</i>
10 bp DNA ladder	<i>Invitrogen GmbH, Karlsruhe</i>
100 bp DNA ladder	<i>Carl Roth GmbH & Co, Karlsruhe</i>
4-Hydroxytamoxifen (4-OHT)	<i>SIGMA-ALDRICH, St.Louis, MD, USA</i>
5-bromo-2'-deoxyuridine (BrdU)	<i>Roche Diagnostics GmbH, Mannheim</i>
AccuGel 19:1 (40% acrylamide for DNA gels)	<i>National Diagnostics, Georgia (USA)</i>
AccuGel 37.5:1 (30% acrylamide for protein gels)	<i>National Diagnostics, Georgia (USA)</i>
Adriamycin (Doxorubicin)	<i>SIGMA-ALDRICH, St.Louis, MD, USA</i>
Agarose	<i>PEQLAB Biotechnologie GmbH, Erlangen</i>
Albumin bovine serum, fatty acid free	<i>SIGMA-ALDRICH, St.Louis, MD, USA</i>
Ammonium peroxodisulfate (APS)	<i>Bio-Rad Laboratories GmbH, Munich</i>
Ampicillin	<i>Roche Diagnostics GmbH, Mannheim</i>
Bacto [®] agar	<i>Becton Dickinson GmbH, Sparks, USA</i>
Bacto [®] tryptone	<i>Becton Dickinson GmbH, Sparks, USA</i>
Bacto [®] yeast extract	<i>Becton Dickinson GmbH, Sparks, USA</i>
Bromphenol blue	<i>SIGMA-ALDRICH, St.Louis, MD, USA</i>
Calmodulin affinity resin	<i>Stratagene GmbH, Heidelberg</i>
Chloramphenicol	<i>SIGMA-ALDRICH, St.Louis, MD, USA</i>
Chloroquine diphosphate	<i>SIGMA-ALDRICH, St.Louis, MD, USA</i>
Complete mini protease inhibitor cocktail	<i>Roche Diagnostics GmbH, Mannheim</i>
Complete mini protease inhibitor cocktail, EDTA-free	<i>Roche Diagnostics GmbH, Mannheim</i>
Coomassie G250	<i>SERVA Electrophoresis GmbH, Heidelberg</i>
DABCO (1,4-Diazabicyclo[2,2,2]octane)	<i>SIGMA-ALDRICH, St.Louis, MD, USA</i>
DAPI (2-(4-Amidinophenyl)-6-indolecarb- amidine dihydrochloride)	<i>SIGMA-ALDRICH, St.Louis, MD, USA</i>
Deoxynucleotides triphosphate (dNTPs)	<i>ABgene Deutschland, Hamburg</i>
Diphtheria Toxin	<i>SIGMA-ALDRICH, St.Louis, MD, USA</i>
Dithiothreitol (DTT)	<i>SIGMA-ALDRICH, St.Louis, MD, USA</i>
DMSO	<i>SIGMA-ALDRICH, St.Louis, MD, USA</i>
Doxycycline hydrochloride	<i>SIGMA-ALDRICH, St.Louis, MD, USA</i>
Ethidium bromide	<i>Carl Roth GmbH & Co, Karlsruhe</i>
Etoposide	<i>SIGMA-ALDRICH, St.Louis, MD, USA</i>
Fetal bovine serum (FBS)	<i>Invitrogen, Carlsbad, CA (USA)</i>
Fluoromount G	<i>SouthernBiotech, Birmingham, AL, USA</i>
Freund's adjuvant incomplete	<i>SIGMA-ALDRICH, St.Louis, MD, USA</i>
FuGENE [®] 6 transfection reagent	<i>Roche Diagnostics GmbH, Mannheim</i>
Geneticin [®] (G418)	<i>Invitrogen GmbH, Karlsruhe</i>
Glycogen from mussels	<i>Roche Diagnostics GmbH, Mannheim</i>

Compound	Supplier
Herring sperm carrier DNA	<i>Promega GmbH, Mannheim</i>
HiPerFect Transfection Reagent	<i>Qiagen GmbH, Hilden, Germany</i>
Hygromycin B (HygB)	<i>Invitrogen GmbH, Karlsruhe</i>
ICI 182,780 (Fulvestrant)	<i>Tocris Biosciences, Missouri, USA</i>
IgG Sepharose™ 6 Fast Flow	<i>Amersham Biosciences, Uppsala, Sweden</i>
Imidazole (1,3-Diaza-2,4-cyclopentadiene)	<i>SIGMA-ALDRICH, St.Louis, MD, USA</i>
Kanamycin	<i>SIGMA-ALDRICH, St.Louis, MD, USA</i>
Lipofectamine™ 2000	<i>Invitrogen GmbH, Karlsruhe</i>
Liquid DAB+ (3,3'-diaminobenzidine) chromogen	<i>DakoCytomation, Carpinteria, CA, USA</i>
Mayer's hematoxylin	<i>Merck KGaA, Darmstadt</i>
MG132 (N-carbobenzoyl-Leu-Leu-leucinal)	<i>Axxora, San Diego, CA, USA</i>
N,N,N',N'-Tetramethylethylenediamine	<i>SERVA Electrophoresis GmbH, Heidelberg</i>
N-Ethylmaleimide	<i>SIGMA-ALDRICH, St.Louis, MD, USA</i>
Nickel-nitrilotriacetic acid (Ni-NTA) agarose	<i>QIAGEN GmbH, Hilden</i>
Nonidet-P40 (NP40)	<i>SIGMA-ALDRICH, St.Louis, MD, USA</i>
PageRuler™ prestained protein ladder	<i>Fermentas GmbH, St. Leon-Rot</i>
Paraformaldehyde	<i>Merck KGaA, Darmstadt</i>
Phenol /C/I for RNA extraction	<i>Promega GmbH, Mannheim</i>
Phorbol 12-myristate 13-acetate (TPA)	<i>Alexis Biochemicals, Lausen, Switzerland</i>
Phosphatase inhibitor cocktail 1	<i>SIGMA-ALDRICH, St.Louis, MD, USA</i>
Protein A-Sepharose 4B, Fast Flow, from <i>Staphylococcus aureus</i>	<i>SIGMA-ALDRICH, St.Louis, MD, USA</i>
Protein G Sepharose™ 4 Fast Flow	<i>Amersham Biosciences, Uppsala, Sweden</i>
Puromycin dihydrochloride	<i>SIGMA-ALDRICH, St.Louis, MD, USA</i>
Roti®-Phenol/chloroform/isoamylalcohol (25/24/1) for DNA extraction	<i>Carl Roth GmbH & Co, Karlsruhe</i>
Skim milk powder	<i>Fluka Chemie AG, Buchs (CH)</i>
Sodium dodecyl sulfate (SDS)	<i>Carl Roth GmbH & Co, Karlsruhe</i>
Sodium orthovanadate	<i>SIGMA-ALDRICH, St.Louis, MD, USA</i>
SulfoLink® coupling gel	<i>Pierce Biotechnology Inc., Rockford (USA)</i>
Target Retrieval Solution (TRS), pH 6.1	<i>DakoCytomation, Carpinteria, CA, USA</i>
TE-buffer for molecular biology	<i>Eurobio, Les Ulis (France)</i>
Tetracycline	<i>SIGMA-ALDRICH, St.Louis, MD, USA</i>
TiterMax® Gold Adjuvant	<i>SIGMA-ALDRICH, St.Louis, MD, USA</i>
Transforming growth factor recombinant human (rhTGF-β1)	<i>R&D Systems, Minneapolis, USA</i>
Trichloroacetic acid, 6.1 M	<i>SIGMA-ALDRICH, St.Louis, MD, USA</i>
Triton X-100	<i>Carl Roth GmbH & Co, Karlsruhe</i>
Trizma®base	<i>SIGMA-ALDRICH, St.Louis, MD, USA</i>
Tween® 20	<i>SIGMA-ALDRICH, St.Louis, MD, USA</i>
Urea	<i>Fluka Chemie AG, Buchs (CH)</i>
Water-Molecular biological grade	<i>Eurobio, Les Ulis (France)</i>

2.2 Enzymes

Enzyme	Supplier
Antarctic Phosphatase (5 U/ μ l)	<i>New England Biolabs GmbH, Frankfurt</i>
DNAse I, RNAse-free (10 U/ μ l)	<i>Roche Diagnostics GmbH, Mannheim</i>
FIREPol [®] DNA polymerase (5 U/ μ l)	<i>Solis BioDyne, Tartu, Estonia</i>
<i>Pfu</i> DNA polymerase (2-3 U/ μ l)	<i>Promega GmbH, Mannheim</i>
Platinum [®] <i>Taq</i> DNA polymerase (5 U/ μ l)	<i>Invitrogen GmbH, Karlsruhe</i>
Vent _R [®] DNA polymerase (2 U/ μ l)	<i>New England Biolabs GmbH, Frankfurt</i>
Restriction endonucleases (3-50 U/ μ l)	<i>Fermentas GmbH, St. Leon-Rot</i>
	<i>New England Biolabs GmbH, Frankfurt</i>
RNase A	<i>SIGMA-ALDRICH, St.Louis, MD, USA</i>
T4 DNA ligase (400 U/ μ l)	<i>New England Biolabs GmbH, Frankfurt</i>
T4 DNA polymerase (3 U/ μ l)	<i>New England Biolabs GmbH, Frankfurt</i>
TEV protease, recombinant (10 U/ μ l)	<i>Invitrogen GmbH, Karlsruhe</i>
Trypsin (10 \times), phenol-red free	<i>Invitrogen GmbH, Karlsruhe</i>
Trypsin-EDTA (1 \times)	<i>Invitrogen GmbH, Karlsruhe</i>

2.3 Antibodies

2.3.1 Primary antibodies

Antibody anti-	species/isotype	dilution for WB	dilution for IF (IHC) [FACS]	Supplier / Reference
AP4 (N-17)	goat polyclonal IgG	1:150	—	<i>Santa Cruz Biotechnology Inc., Santa Cruz (USA)</i>
AP4 (HPA001912)	rabbit polyclonal, monospecific IgG	—	(1:125)	<i>Atlas Antibodies AB, AlbaNova University Center, Stockholm (Sweden)</i>
p53 (C-terminus)	goat polyclonal IgG	1:1,000	1:100	<i>This work</i>
p53 (DO-1)	monoclonal mouse IgG _{2a}	1:1,000	—	<i>Santa Cruz Biotechnology Inc., Santa Cruz (USA)</i>
p53 (1801)	monoclonal mouse IgG ₁	1:1,000	—	<i>Santa Cruz Biotechnology Inc., Santa Cruz (USA)</i>
p21 ^{WAF1} (Ab-11)	monoclonal mouse IgG _{2b}	1:1,000	—	<i>NeoMarkers, Fremont, CA, USA</i>
p21 ^{WAF1} (SX118)	monoclonal mouse IgG _{1κ}	—	(1:50)	<i>DakoCytomation, Carpinteria, CA, USA</i>
p15 ^{Ink4b} (C-20)	rabbit polyclonal IgG	1:200	—	<i>Santa Cruz Biotechnology Inc., Santa Cruz (USA)</i>

Antibody anti-	species/isotype	dilution for WB	dilution for IF (IHC) [FACS]	Supplier / Reference
p-Chk2-(Thr 68)-R	polyclonal rabbit IgG	1:500	—	<i>Santa Cruz Biotechnology Inc., Santa Cruz (USA)</i>
β -actin	rabbit polyclonal IgG	1:1,000	—	<i>SIGMA-ALDRICH, St.Louis, MD, USA</i>
α -tubulin (DM 1A)	mouse monoclonal IgG ₁	1:1,000	—	<i>SIGMA-ALDRICH, St.Louis, MD, USA,</i>
c-MYC (N-term)	rabbit monoclonal IgG	1:10,000	(1:50)	<i>Epitomics, Burlingame, CA (USA)</i>
c-MYC (N-262)	rabbit polyclonal IgG	1:500	1:50	<i>Santa Cruz Biotechnology Inc., Santa Cruz (USA)</i>
BrdU, FITC-conjugated (set including isotype control)	mouse monoclonal IgG _{1k}	—	[1:10]	<i>BD Biosciences Pharmingen, San Diego, CA, USA</i>
GFP (FL)	rabbit polyclonal IgG	1:500	—	<i>Santa Cruz Biotechnology Inc., Santa Cruz (USA)</i>
Rb (G3-245)	monoclonal mouse IgG ₁	1:400	—	<i>BD Biosciences Pharmingen, San Diego, CA, USA,</i>
Ki67 (MIB1)	monoclonal mouse IgG _{1k}	—	(1:60)	<i>DakoCytomation, Carpinteria, CA, USA</i>
Cul7 (clone SA12)	mouse monoclonal IgG _{1k}	1:100	—	<i>Gift from James DeCaprio ⁴⁷⁵</i>
<i>anti-ER (H222)</i>	rat polyclonal IgG	—	<i>1:50</i>	<i>Gift from Goeffrey Greene</i>

2.3.2 Secondary antibodies

Antibody	Species (origin)	Dilution for WB	Dilution for IF	Supplier
Anti-goat IgG (H+L)-HRP conjugate	Donkey	1:10,000	—	<i>Jackson ImmunoResearch Laboratories Inc., West Grove, PA (USA)</i>
anti-mouse IgG HRP-conjugate	Goat	1:10,000	—	<i>Promega GmbH, Mannheim</i>
anti-rabbit IgG HRP-conjugate	Goat	1:20,000	—	<i>SIGMA-ALDRICH, St.Louis, MD, USA</i>
Anti-rabbit IgG Cy3-conjugate	Sheep	—	1:1,000	<i>SIGMA-ALDRICH, St.Louis, MD, USA</i>
Anti-rabbit IgG (H+L) – FITC conjugate	Donkey	—	1:100	<i>Jackson ImmunoResearch Laboratories Inc., West Grove, PA (USA)</i>

Antibody	Species (origin)	Dilution for WB	Dilution for IF	Supplier
anti-mouse IgG (H+L) - Alexa-Fluor 594 conjugate	Goat	—	1:500	<i>Invitrogen GmbH, Karlsruhe</i>
anti-rabbit IgG (H+L) - Alexa-Fluor 488 conjugate	Goat	—	1:500	<i>Invitrogen GmbH, Karlsruhe</i>

2.4 Disposables and kits

Product	Supplier
AEC substrate kit for peroxidase	<i>Vector Laboratories Inc., Burlingame, CA (USA)</i>
Assistent-coverslip (12 mm, round)	<i>Schubert&Weiss, Munich</i>
0.45 µm Millex-HA filter units	<i>Millipore GmbH, Schwalbach</i>
0.22 µm Millex-GV filter units	<i>Millipore GmbH, Schwalbach</i>
96-well white polystyrene microtiter plate	<i>Corning GmbH, Kaiserslautern</i>
3MM Whatman® filter paper	<i>Whatman GmbH, Dassel</i>
Amicon® Ultra-15 centrifugal filter devices	<i>Millipore GmbH, Schwalbach</i>
BigDye® terminator v3.1 sequencing mix	<i>Applera Deutschland GmbH, Darmstadt</i>
Costar® Spin-X tubes	<i>Corning GmbH, Kaiserslautern</i>
Dual-Luciferase® Reporter Assay System	<i>Promega GmbH, Mannheim</i>
Luciferase 1000 Assay System	<i>Promega GmbH, Mannheim</i>
Imject® Maleimide Activated mKLLH Kit	<i>Pierce Biotechnology Inc., Rockford (USA)</i>
Immobilon-P PVDF Transfer Membrane	<i>Millipore GmbH, Schwalbach</i>
LightCycler® Fast Start DNA Master SYBR Green Kit	<i>Roche Diagnostics GmbH, Mannheim</i>
LightCycler® capillaries (20 µl)	<i>Roche Diagnostics GmbH, Mannheim</i>
Pierce ECL Western blotting substrate	<i>Pierce Biotechnology Inc., Rockford (USA)</i>
Poly-Prep chromatography columns (0.8x4 cm)	<i>Bio-Rad Laboratories GmbH, Munich</i>
QIAGEN Plasmid Maxi Kit	<i>QIAGEN GmbH, Hilden</i>
QIAGEN Plasmid Maxi Kit	<i>QIAGEN GmbH, Hilden</i>
QIAquick Gel Extraction Kit	<i>QIAGEN GmbH, Hilden</i>
QIAquick PCR Purification Kit	<i>QIAGEN GmbH, Hilden</i>
QuikChange® II Site-Directed Mutagenesis Kit	<i>Stratagene, La Jolla, CA (USA)</i>
Reverse-IT™ 1 st Strand Synthesis Kit	<i>ABgene Germany, Hamburg</i>
RNAgents® total RNA isolation kit	<i>Promega GmbH, Mannheim</i>
RNeasy® Mini Kit (50)	<i>QIAGEN GmbH, Hilden</i>
QIAshredder™ (50)	<i>QIAGEN GmbH, Hilden</i>
Rotilabo® 1.5 ml cuvettes	<i>Carl Roth GmbH, Karlsruhe</i>
SafeSeal Tips® Premium (30, 100, 200, 1000 µl)	<i>Biozym Scientific GmbH, Hessisch Oldendorf</i>
Tissue culture plastic ware	<i>Corning GmbH, Kaiserslautern Nunc GmbH & Co. KG, Wiesbaden</i>

Product	Supplier
Tissue culture plastic ware	<i>Greiner bio-one, Frickenhausen BD Falcon, Franklin Lakes, New Jersey (USA)</i>
VECTASTAIN [®] Elite ABC Kit	<i>Vector Laboratories Inc., Burlingame, CA (USA)</i>
Western Lightning [®] Western Blot Chemiluminescence Reagent Plus	<i>PerkinElmer GmbH, Cologne</i>

2.5 Laboratory equipment

Device	Supplier
Axiovert 200M fluorescence microscope	<i>Carl Zeiss GmbH, Oberkochen</i>
Axioskop 40 microscope	<i>Carl Zeiss GmbH, Oberkochen</i>
Axiovert 25 microscope	<i>Carl Zeiss GmbH, Oberkochen</i>
Biofuge [®] Pico	<i>Heraeus Instruments GmbH, Osterode</i>
Biofuge [®] Primo	<i>Heraeus Instruments GmbH, Osterode</i>
BioPhotometer	<i>Eppendorf, Hamburg</i>
CoolSNAP [™] -HQ CCD camera	<i>Photometrics, Tucson (USA)</i>
DC500 camera	<i>Leica Microsystems GmbH, Wetzlar</i>
FACSCalibur [™] System	<i>BD Biosciences, California (USA)</i>
Fisherbrand FT-20E/365 transilluminator	<i>Fisher Scientific GmbH, Schwerte</i>
GeneAmp [®] PCR System 9700	<i>Applied Biosystems, Foster City (USA)</i>
Gene-Pulser [®] electroporator	<i>Bio-Rad Laboratories GmbH, Munich</i>
HyperHAD CCD camera	<i>Sony Electronics Inc., Tokyo (Japan)</i>
IDA Gel documentation system	<i>Raytest GmbH, Straubenhardt</i>
Incubator for mammalian cell culture	<i>Heraeus Sepatech GmbH, Osterode</i>
Joey [™] Gel casting system	<i>peqlab Biotechnology GmbH, Erlangen</i>
KAPPA ImageBase software	<i>KAPPA opto-electronics GmbH, Gleichen</i>
KODAK Image Station 440CF	<i>Eastman Kodak Company, Rochester (USA)</i>
KODAK Molecular Imaging Software	<i>Eastman Kodak Company, Rochester (USA)</i>
LC Carousel Centrifuge	<i>Roche Diagnostics, Mannheim</i>
LightCycler [®] System for Real-Time PCR	<i>Roche Diagnostics, Mannheim</i>
Mastercycler [®] personal system (PCR)	<i>Eppendorf, Hamburg</i>
Megafuge [®] 1.0R	<i>Heraeus Instruments GmbH, Osterode</i>
MetaMorph [®] software	<i>Universal Imaging, Downingtown (USA)</i>
MicroLumatPlus LB96V luminometer	<i>EG&G Berthold, Bad Wildbad</i>
Mini Trans-Blot [®] cell system	<i>Bio-Rad Laboratories GmbH, Munich</i>
Mini-PROTEAN [®] electrophoresis system	<i>Bio-Rad Laboratories GmbH, Munich</i>
Multiphor II Electrophoresis unit	<i>Amersham Biosciences, New Jersey (USA)</i>
ND-1000 Spectrophotometer	<i>NanoDrop Technologies, Detroit (USA)</i>
Neubauer counting chamber	<i>Carl Roth GmbH & Co, Karlsruhe</i>
Penguin [™] Water-Cooled Dual-Gel Electrophoresis System	<i>peqlab Biotechnology GmbH, Erlangen</i>
Tissue culture Lamin Air [®]	<i>Heraeus Sepatech GmbH, Osterode</i>
Vario 18 low vacuum pump	<i>Medela AG, Baar (Switzerland)</i>
Z1 [™] series Coulter counter [®]	<i>Coulter electronics, Beds (UK)</i>

2.6 Oligonucleotides

2.6.1 Oligonucleotides for cloning

Primer	Sequence (5'-3')
p53 TAPn Fwd	ATCGTCGACGGTATGGAGGAGCCGCAGTCAG
p53 TAPn Rev	GCAGGTACCGGTTTATCAGTCTGAGTCAGGCCCTT
p53 TAP Fwd	ATCGGTACCATCACCACCATGGAGGAGCCGCAGTCAG
p53 TAP Rev	ATCAGATCTCCACCACCGTCTGAGTCAGGCCCTTCT
p53 3 point	CCTCACCACGAGCTGCCC
p53 shRNA Fwd	GCGGATCCCCGTTGGCCTGCACTGGTGTATCAAGAGAA
p53 shRNA Rev	CGCTCGAGTTTCCAAAAAGTTGGCCTGACTGGTGTTC
HA×3-Fwd	CGGGATCCGGAGATCTCGGTTACCCATATGACGTTCCAGAC
HA×3-Rev	GCAGCTAGCACCTTATTATCACGAATTCGAAGCGTAGTCAGGTACATCGTA
AP4-Fwd	GGATCCGGAACCATGGAGTATTTTCATGGTGCCCA
AP4-Rev	CGTCTAGATCCGGGAAGCTCCCCGTCCCCGACG
AP4-ER-Rev	GCGGATCCGGCGGAAGCTCCCCGTCCCCGACG
Cul7 mi-Fwd	TGCTGTTGACAGTGAGCGAAACTGGAGCTGGAGTTCAGTATAGTGAAGCCACAGATG
Cul7 mi-Rev	TCCGAGGCAGTAGGCACAACCTGGAGCTGGAGTTCAGTATACATCTGTGGCTTCAC
AP4 mi-Fwd 1	TGCTGTTGACAGTGAGCGCAGCTCAGCAAGGCAGCCATTCTAGTGAAGCCACAGATG
AP4 mi-Rev 1	TCCGAGGCAGTAGGCAAAGCTCAGCAAGGCAGCCATTCTACATCTGTGGCTTCAC
AP4 mi-Fwd 2	TGCTGTTGACAGTGAGCGCAGTGATAGGAGGGCTCTGTAGTAGTGAAGCCACAGATG
AP4 mi-Rev 2	TCCGAGGCAGTAGGCAAAGTGATAGGAGGGCTCTGTAGTACATCTGTGGCTTCAC
p21 mutA3-Fwd	GAATCGGCCAGGCTGAGCTTGCTCGGCG
p21 mutA3-Rev	CGCCGAGCAAGCTCAGCCTGGCCGAGTTC
p21 mutA4-Fwd	GTCATCCTCCTGATCTTTTGAATTCCATTGGGTAAATCCTTGC
p21 mutA4-Rev	GCAAGGATTTACCCAATGGAATTCAAAAGATCAGGAGGATGAC
miR30 <i>Xho</i> I Fwd	CAGAAGGCTCGAGAAGGTATATTGCTGTTGACAGTGAGCG
miR30 <i>Eco</i> RI Rev	CTAAAGTAGCCCCTTGAATTCCGAGGCAGTAGGCA

2.6.2 Oligonucleotides used for colony-PCR and sequencing

Primer	Sequence (5'-3')
CMV-Fwd	GCTGGTTTGTAGTGAACCGTCAG
CMV-Fwd (pBI)	GCTCGTTTGTAGTGAACCGTCAG
Bgh reverse (for pcDNA3 vectors)	TAGAAGGCACAGTCGAGG
T7 promoter primer	TAATACGACTCACTATAGGG
pMT-1 promoter primer	GTCACCACGACTTCAACGTC
TMP Fwd (for miRNA containing plasmids)	CTCGACTAGGGATAACAG
TMP Rev (for miRNA containing plasmids)	CATGCTCCAGACTGCCTT
CBP-Fwd	TTCATAGCCGTCTCAGCAGC
p53 Fwd1	CCTACCAGGGCAGCTACGG

Primer	Sequence (5'-3')
p53 Fwd2	TAGTGTGGTGGTGCCCTATG
p53 Rev1	CCAGTGTGATGATGGTGAG
p53 Rev2	CTTGGCTGTCCCAGAAATGC
pUC19 Fwd	GCTGCAAGGCGATTAAGTTGG
pUC19 Rev	CATGATTACGCCAAGCTGGC
EBNA Sfi (rev)	AATCAAGGGTCCAACCTC

2.6.3 Oligonucleotides used for real-time quantitative PCR

Primer	Sequence (5'-3')	melting temp. (°C)	Reference
<i>Cul7</i> -LC-Fwd	GAACTCAACTCGGTGAATGTGA	61	This work
<i>Cul7</i> -LC-Rev	GAACCATGTAGAAGAGGCGTG	61	This work
<i>AP4</i> -LC-Fwd	GCAGGCAATCCAGCACAT	59	This work
<i>AP4</i> -LC-Rev	GGAGGCGGTGTCAGAGGT	59	This work
rat- <i>ap4</i> -Fwd	CTTCCTCCCACCACATCAAT	60	This work
rat- <i>ap4</i> -rev	TGCGGACAGACTTCACGATA	60	This work
<i>p21</i> -LC-Fwd	GGCGGCAGACCAGCATGACAGATT	60	⁴⁷⁶
<i>p21</i> -LC-Rev	GCAGGGGGCGGCCAGGGTAT	60	⁴⁷⁶
<i>DKC</i> -Fwd	CGGCTGGTTATGAAAGAC	55	Gift from Antje Menssen ⁴⁵⁵
<i>DKC</i> -Rev	TGGTTCGAGGTAGAGATG	55	Gift from Antje Menssen ⁴⁵⁵
<i>MAD2</i> -Fwd	CCTGGAAAGATGGCAGTTTG	58	Gift from Antje Menssen ⁴⁵⁵
<i>MAD2</i> -Rev	GTAAATGAACGAAGGCGGACT	58	Gift from Antje Menssen ⁴⁵⁵
<i>PHB</i> -Fwd	CAGGTGGCTCAGCAGGAAGC	58	Gift from Antje Menssen ³⁷⁰
<i>PHB</i> -Rev	TGAAGTGAATTTTACCTTTATTTCC	58	Gift from Antje Menssen ³⁷⁰
β -actin Fwd	TGACATTAAGGAGAAGCTGTGCTAC	55-61	Gift from Henrike Koerner ⁴⁷⁷
β -actin Rev	GAGTTGAAGGTAGTTTTCGTGGATG	55-61	Gift from Henrike Koerner ⁴⁷⁷
rat <i>EF1a</i> -Fwd	CACACGGCCACATAGCAT	58	Gift from Dimitri Lodyguin
rat <i>EF1a</i> -Rev	CACGAACAGCAAAACGACCA	58	Gift from Dimitri Lodyguin

2.6.4 Oligonucleotides for quantitative ChIP analyses

Primer	sequence (5'-3')	Melting temp (°C)	Position rel. to transcriptional start site (+1)
<i>AP4</i> intron 1 Fwd	GAGGTGGGCGTTCTACGG	60	+1550
<i>AP4</i> intron 1 Rev	GGTTGGGCAGGAGTGTCTAC	60	+1790
<i>AP4</i> intron 6 Fwd	TCTCAGTGGTTCGTCCCTGT	60	+14760
<i>AP4</i> intron 6 Rev	GGAGGCGGTGTCAGAGGT	60	+14861
<i>p21</i> promoter Fwd	TGTGTCCTCCTGGAGAGTGC	59	-324
<i>p21</i> promoter Rev	CAGTCCCTCGCCTGCCTTG	59	-218
<i>p21</i> intron 1 Fwd	AACAAGGGTTTGCCTTCTG	59	+2146
<i>p21</i> intron 1 Rev	TCGGGAGTTCAAGACAGGAC	59	+2310
<i>16q22</i> Fwd ⁴⁷⁷	CTACTCACTTATCCATCCAGGCTAC	58-60	---
<i>16q22</i> Rev ⁴⁷⁷	ATTTACACACTCAGACATCACAG	58-60	---

2.7 Expression plasmids

2.7.1 Standard expression vectors

Vector	Properties	Promoter	Reference / Supplier
pUC19 <i>SfiI</i>	Amp ^R , pUC19 with modified MCS flanked by <i>SfiI</i> sites	none	Gift from Georg Bornkamm ⁴⁷⁸
pSport1-AP4 IRATp970D057D	Amp ^R	T7	RZPD, Berlin
pSuper	Amp ^R	H1 (Pol III promoter)	⁴⁷⁹
pRetroSuper (pRS)	Amp ^R	H1 (Pol III promoter)	⁴⁸⁰
pRTS-1	Amp ^R , Luciferase; monomeric red fluorescent protein (mRFP)	Tet-responsive element with flanking, bidirectional CMV _{min}	Gift from Georg Bornkamm ⁴⁷⁸
pcDNA3 TM	Amp ^R	CMV	Invitrogen GmbH, Karlsruhe
pCMV-Gal	Amp ^R , β-galactosidase	CMV	Gift from Bert Vogelstein
pMK10tTA	tTA-IRES-Neo ^R , Amp ^R	<i>β-Actin</i>	Gift from Bert Vogelstein ⁴⁸¹
pCEP4	Amp ^R , Neo ^R	CMV	Gift from Bert Vogelstein ¹⁸⁰
pRL-CMV	<i>Renilla</i> luciferase, Amp ^R	CMV	Promega GmbH, Mannheim
peYFP-N1	eYFP, Kan ^R , Neo ^R	CMV	Clontech Laboratories Inc., Mountain View (USA)
pBS1539	TAPc, Amp ^R	None	Cellzome AG, Heidelberg
pBpuro <i>c-mycER</i> TM	Amp ^R	5'-long terminal repeat (LTR)	³⁸⁴
pBI	Amp ^R	Tet-responsive element with flanking, bidirectional CMV _{min}	Clontech Laboratories Inc., Mountain View (USA)
pIRES-hrGFP-2a	Amp ^R , 3×HA	CMV	Stratagene, La Jolla, CA (USA)
LMP	Amp ^R , eGFP	5'-long terminal repeat (LTR)	Gift from Gregory Hannon ⁴⁸²
pSM2c-NonS Expression Arrest TM (Cat-no. RHS1703)	Amp ^R , non silencing microRNA fragment	U6 (Pol III promoter)	Open Biosystems, Huntsville, AB, (USA)

2.7.2 Generated expression vectors

Plasmid	Properties	Cloning strategy / Reference
pMYC-HA-TAP	c-MYC-HA-TAP, Kan ^R , Neo ^R	Gift from Heike Koch, unpublished
pCEP4-p53	Amp ^R , Neo ^R , wild type p53	Gift from Bert Vogelstein ¹⁸⁰
pp53-TAP	p53-TAP, Kan ^R , Neo ^R	This work: PCR-amplified (p53-TAP Fwd and Rev) p53 (template pCEP4-p53) cut with <i>Bgl</i> III- <i>Kpn</i> I inserted into <i>Kpn</i> I- <i>Bam</i> HI cut pMYC-HA-TAP
pBI-YFP	Amp ^R	Gift from Anne Benzinger, unpublished
pBI-YFP-p53-TAP	Amp ^R , C-terminal TAP-tagged p53	This work: <i>Not</i> I- <i>Kpn</i> I (blunt) fragment of pp53-TAP inserted into <i>Eco</i> RV-cut pBI-YFP
pp53nostop	p53-ORF without stop-codon; Kan ^R , Neo ^R	This work: 3-point ligation of PCR-amplified (p53 3 point Fwd and p53-TAP rev) p53 C-terminal fragment restricted with <i>Bss</i> SI- <i>Bgl</i> III and <i>Kpn</i> I- <i>Bss</i> SI p53 N-terminal fragment (from pCEP4-p53) with <i>Kpn</i> I- <i>Bgl</i> III peYFP-N1
pp53-HA×3	p53-HA×3; Kan ^R , Neo ^R	This work: PCR-amplified (HA-Fwd and Rev) HA×3 (template pIRES-hrGFP-2a) cut with <i>Bgl</i> III- <i>Nhe</i> I inserted into <i>Bgl</i> III- <i>Nhe</i> I pp53nostop
pMT1-p53-HA×3	p53- HA×3; Amp ^R , Neo ^R	This work: <i>Kpn</i> I- <i>Nhe</i> I (blunt) fragment from pp53-HA×3 inserted into <i>Eco</i> RI- <i>Bsr</i> GI (blunt) pU265
pcDNA3-p53-HA×3	Amp ^R , p53-HA×3	This work: <i>Eco</i> RI fragment from pMT1-p53-HA×3 into <i>Eco</i> RI-restricted pcDNA3 vector
pcDNA3-VSV	VSV, Amp ^R	Gift from Ru Zhang, unpublished
pcDNA3-p53-VSV	Amp ^R , p53-VSV	This work: <i>Bgl</i> III fragment from pMT1-p53-HA×3 into <i>Bam</i> HI-restricted pcDNA3-VSV
pSUPER-p53i	Amp ^R , p53-shRNA encoding region	This work: PCR-aligned (p53 shRNA Fwd and Rev) p53sh-cDNA fragment cut with <i>Bam</i> HI- <i>Xho</i> I inserted into <i>Bgl</i> III- <i>Xho</i> I pSUPER
pRS-p53i	Amp ^R , p53-shRNA encoding region	This work: <i>Eco</i> RI- <i>Xho</i> I fragment of pSUPER-p53i inserted into <i>Eco</i> RI- <i>Xho</i> I pRetroSuper (pRS)
pCR3.1-Flag-Cul7	Amp ^R , N-terminal Flag-tagged Cul7 encoding fragment	Gift from Zhen-Qiang Pan ⁴⁸³
pCR3.1-Flag	Amp ^R , Flag-encoding region	This work: cut pCR3.1-Flag-Cul7 with <i>Bam</i> HI- <i>Not</i> I (blunt) and subsequently with <i>Sal</i> I. Re-ligation of <i>Bam</i> HI- <i>Not</i> I (blunt) fragment.
pcDNA3-Fbx29-HA	Amp ^R , Fbx29-HA encoding fragment	Gift from James DeCaprio ⁴⁸⁴
pMT107	Amp ^R , His-tagged ubiquitin	Gift from Stefan Müller ⁴⁸⁵
pUC19 <i>Sfi</i> I-FlagCul7	Amp ^R , Flag-Cul7 encoding fragment	This work: <i>Nde</i> I- <i>Not</i> I fragment from pCR3.1-Flag-Cul7 inserted into <i>Nde</i> I- <i>Not</i> I restricted pUC19 <i>Sfi</i> I
pRTS-1-Flag-Cul7	Amp ^R , Flag-Cul7	This work: <i>Sfi</i> I fragment from pUC19 <i>Sfi</i> I-FlagCul7 inserted into <i>Sfi</i> I cut pRTS-1 vector
pRTS-1empty	Amp ^R	This work: cut with <i>Sfi</i> I (blunt) and re-ligation
pU265	Amp ^R , p53-eCFP	Gift from Uri Alon ⁴⁸⁶

Plasmid	Properties	Cloning strategy / Reference
pMT1-p53-TAPc	Amp ^R , p53-TAP	This work: <i>Bam</i> HI- <i>Not</i> I (blunt) fragment from pp53-TAP inserted into <i>Eco</i> RI- <i>Bsr</i> GI (blunt) U265
LMP-Cul7miRNA	Amp ^R , Cul7miRNA encoding fragment	This work: Ligation of <i>Eco</i> RI- <i>Xho</i> I Cul7miRNA fragment (see Methods) into <i>Eco</i> RI- <i>Xho</i> I LMP vector
pUC19 <i>Sfi</i> I-Cul7miRNA	Amp ^R , Cul7miRNA encoding fragment	This work: Ligation of <i>Bgl</i> III- <i>Age</i> I fragment of LMP-Cul7miRNA into <i>Bam</i> HI- <i>Age</i> I restricted pUC19 <i>Sfi</i> I plasmid
pUC19 <i>Sfi</i> I-NonS	Amp ^R , Non-silencing microRNA encoding region	This work: Ligation of <i>Bgl</i> III- <i>Age</i> I fragment of LMP-NonS into <i>Bam</i> HI- <i>Age</i> I restricted pUC19 <i>Sfi</i> I plasmid
pEMI-Cul7miRNA	Amp ^R , Cul7miRNA encoding fragment	This work: ligation of <i>Sfi</i> I fragment from pUC19 <i>Sfi</i> I-Cul7miRNA into <i>Sfi</i> I site of pRTS-1
pEMI-1-NonS miRNA	Amp ^R , Non-silencing microRNA encoding region	This work: ligation of <i>Sfi</i> I fragment from pUC19 <i>Sfi</i> I-NonS into <i>Sfi</i> I site of pRTS-1
pcDNA3-AP4-VSV	Amp ^R ; AP4-VSV	This work: PCR amplified (AP4-Fwd and -Rev) AP4 (template: pSport1-AP4) restricted with <i>Bam</i> HI- <i>Xba</i> I inserted into <i>Bam</i> HI- <i>Xba</i> I pcDNA3-VSV
pUC19 <i>Sfi</i> I-AP4-VSV	Amp ^R ; AP4-VSV	This work: <i>Bam</i> HI- <i>Not</i> I fragment from pcDNA3-AP4-VSV into <i>Bam</i> HI- <i>Not</i> I pUC19 <i>Sfi</i> I
pRTS-1-AP4-VSV	Amp ^R ; AP4-VSV, mRFP	This work: <i>Sfi</i> I fragment from pUC19 <i>Sfi</i> I-AP4-VSV into <i>Sfi</i> I pRTS-1
pRTS-1-c-MYC	Amp ^R ; AP4-VSV, mRFP	Gift from Georg Bornkamm
pRSM	pMT1-promoter; Amp ^R	This work: pRetroSuper cut with <i>Bgl</i> III- <i>Eco</i> RI (removes H1 promoter) ligated with <i>Bam</i> HI- <i>Eco</i> RI fragment (pMT1-promoter) of U265
pRSM-AP4-VSV	pMT1-promoter; Amp ^R ; AP4-VSV	This work: Ligation of <i>Bam</i> HI- <i>Xho</i> I (blunt) fragment from pcDNA3-AP4-VSV into <i>Eco</i> RI (blunt) pRSM
pSHUMI-AP4mi1	AP4 microRNA1; miR30 flanking regions	This work: Ligation of <i>Eco</i> RI- <i>Xho</i> I AP4-miRNA1 fragment (see Methods) into <i>Eco</i> RI- <i>Xho</i> I cut pSHUMI
pSHUMI-AP4mi2	AP4 microRNA2; miR30 flanking regions	This work: Ligation of <i>Eco</i> RI- <i>Xho</i> I AP4-miRNA1 fragment (see Methods) into <i>Eco</i> RI- <i>Xho</i> I cut pSHUMI
pEMI-1-AP4mi1	Amp ^R , AP4 miRNA1 encoding fragment	This work: ligation of <i>Sfi</i> I fragment from pSHUMI-AP4mi1 into <i>Sfi</i> I site of pRTS-1
pEMI-1-AP4mi2	Amp ^R , AP4 miRNA2 encoding fragment	This work: ligation of <i>Sfi</i> I fragment from pSHUMI-AP4mi2 into <i>Sfi</i> I site of pRTS-1
pBABE-AP4-ER	AP4-ER fusion gene	This work: PCR-amplified (AP4-Fwd AP4-ER-Rev) <i>Bam</i> HI restricted AP4 cloned into <i>Bam</i> HI linearized pBpuro <i>c-mycER</i> TM

Plasmid	Properties	Cloning strategy / Reference
pAdTrack-AP4-VSV	Amp ^R , GFP, AP4-VSV	This work: Ligation of <i>KpnI-XhoI</i> fragment (from pcDNA3-AP4-VSV) with <i>KpnI-XhoI</i> -restricted pAdTrack vector
pAd1-AP4-VSV	Amp ^R , GFP, AP4-VSV	This work: <i>PmeI</i> linearized pAdTrack-AP4-VSV and Adeasy-1 plasmid: Recombination as described in Methods section XXX
pAdeasy-1-GFP	Amp ^R , GFP	Gift from Dimitri Lodyguin
p234 (pGL3)	Amp ^R , wt p21 promoter	Gift from Carme Gallego ⁴⁸⁷
p237 (pGL3)	Amp ^R , mutant p21 promoter (mA3+A4)	Gift from Carme Gallego ⁴⁸⁷
p238 (pGL3)	Amp ^R , mutant p21 promoter (mA2-A4)	This work: Site directed mutagenesis; see Methods section
p239 (pGL3)	Amp ^R , mutant p21 promoter (mA1-A4)	This work: Site directed mutagenesis; see Methods section

2.8 Bacteria strains

Strain	Genotype	Supplier
<i>E. coli</i> BJ5183 EC	<i>endA sbcBC recBC galK met thi-1 bioT hsdR (Strr)</i>	<i>Qbiogene, Heidelberg, Germany</i>
<i>E. coli</i> XL1-Blue	<i>endA1 gyrA96 hsdR17 lac-recA1 relA1 supE44 thi-1 [F' lacI^a Z ΔM15, proAB, Tn 10, Tet^R]</i>	<i>Stratagene GmbH, Heidelberg</i>
<i>E. coli</i> PirPlus™ DH10βF DOT	<i>mcrA Δ(mrr-hsdRMS-mcrBC) φ80lacZ-ΔM15 ΔlacX74 deoR recA1 endA1 araΔ139 Δ(ara,leu)7697 galU galKλ- rpsL nupG λ- tonA umuC::pir116-frtF'(lac+ pro+ ΔoriT::Tc)</i>	<i>Open Biosystems, Huntsville, AL, USA</i>

2.9 Eukaryotic cell lines

Strain	Genotype	Source / Reference
293	A human embryonic kidney cell line transformed with adenovirus type 5 (E1A/E1B)	Gift from Axel Ullrich
293T	A human embryonic kidney cell line transformed with adenovirus type 5 (E1A/E1B) and harboring the temperature sensitive gene for SV40 large T antigen	Gift from Volker-Scherhammer
911	A human embryonic retinoblast cell line transformed with adenovirus type 5 (base pairs 79-5789, E1-deleted adenovirus) ⁴⁸⁸	Gift from Bert Vogelstein ⁴⁸⁹
Phoenix A (PhoA)	An amphotropic retroviral producer cell line based on 293T cells stably selected with constructs capable of producing gag-pol and envelope proteins ⁴⁹⁰	Gift from Axel Ullrich

Strain	Genotype	Source / Reference
MCF-7	A human breast cancer cell line (estrogen-receptor positive)	Gift from Axel Ullrich
MCF-7i	MCF-7 cell line stably infected with pRetroSuper-p53shRNA based retroviruses	This work
MCF-7i-p53-TAP	MCF-7i cell line stably transfected with pMT1-p53-TAPc	This work
MCF-7-PJMMR1	MCF-7 cell line stably transfected with pRTS-1-c-MYC (+ mRFP)	This work
MCF-7-MR1	MCF-7 cell line stably transfected with pRTS-1 (+mRFP)	This work
MCF-7 EMI-Cul7 microRNA	MCF-7 cell line stably transfected with pEMI-Cul7-miRNA	This work
MCF-7 EMI non-silencing	MCF-7 cell line stably transfected with pEMI-1-NonS miRNA	This work
MCF-7 RTS-1-Cul7	MCF-7 cell line stably transfected with pRTS-1-Flag-Cul7	This work
DLD1	A human colorectal adenocarcinoma cell line with mutant p53 (S241F)	Gift from Axel Ullrich
DLD1-tTa	A DLD-1 ^{tet-off} cell line expressing the tetracycline-controlled transactivator (tTA)	Gift from Bert Vogelstein ⁴⁸¹
DLD1-tTa-p53.A2	DLD1-tTa cells harboring a tet-inducible wild-type p53 allele	Gift from Bert Vogelstein ⁴⁸¹
DLD1-tTa-p53TAP	DLD1-tTa cells stably transfected with pBI-YFP-p53-TAPc	This work
H1299	A human non-small cell lung cancer cell line deficient for p53	Gift from Dirk Eick
U-2OS	A human osteosarcoma cell line	Gift from Reinhard Fässler
U-2OS pEMI and pRTS-1 cell pools	U-2OS cell pools stably transfected with the indicated pRTS-1 or pEMI episomal expression vectors	This work
HaCaT	Human transformed keratinocytes deficient for p53 ⁴⁹¹	Gift from Axel Ullrich
HaCaT-AP4-ER	HaCaT cells stably infected with pBABE-AP4-ER based retroviruses	This work
HDF	Human primary diploid fibroblasts	<i>Clonetics Inc., San Diego (USA)</i>
HDF-c-MYC	Human primary diploid fibroblasts immortalized by ectopic <i>c-MYC</i> expression	Gift from Carla Grandori
HDF-htert	Human primary diploid fibroblasts immortalized by ectopic <i>htert</i> expression	Gift from Carla Grandori
HDF-c-MYC-ER (clone A1C1)	Human primary diploid fibroblasts stably expressing c-MYC-ER	Gift from Antje Menssen
H1299	A human non-small cell lung cancer cell line carrying a homozygous deletion of p53	Gift from Dirk Eick
U-937	A human myelo-monoblastic cell line with mutant p53	Gift from Axel Ullrich

Strain	Genotype	Source / Reference
U-937 Ctrl clone1	A human myelo-monoblastic cell line with mutant p53	Gift from Lars-Gunnar Larsson ⁴¹⁵
U-937-pRSM	U-937 cells stably infected with pRSM based retroviruses	This work
U-937-pRSM-AP4	U-937 cells stably infected with pRSM-AP4-VSV based retroviruses	This work
Rat1A-myc-ER	c-myc-deficient Rat1A (H015.19 ³⁸⁹) cells stably selected for expression of a c-myc-ER fusion construct	Gift from Dirk Eick ⁴⁹²

2.10 Stock solutions, buffers and culture media

Solution	Ingredients
ChIP SDS-buffer	50 mM Tris/HCl, pH 8.0
	100 mM NaCl
	5 mM EDTA, pH 8.0
	0.5% SDS
ChIP IP-buffer	25 mM Tris/HCl, pH 8.0
	1% (v/v) TritonX-100
	0.2% (w/v) SDS
	0.02% (w/v) NaN ₃
ChIP LiCl/detergent buffer	10 mM Tris/HCl, pH 8.0
	250 mM LiCl
	1 mM EDTA
	0.5% (v/v) NP-40
	0.5% (w/v) sodium deoxycholate
	0.02% NaN ₃
ChIP Buffer 500	50 mM HEPES, pH 7.5
	500 mM NaCl
	1 mM EDTA
	0.1% (w/v) sodium deoxycholate
	0.5% (v/v) NP-40
	0.02% (w/v) NaN ₃
ChIP Mixed Micelle Buffer	20 mM Tris/HCl, pH 8.0
	150 mM NaCl
	0.5 mM EDTA, pH 8.0
	5.2% (w/v) sucrose
	1% TritonX-100
	0.2% SDS
	0.02% NaN ₃

Materials

Solution	Ingredients
ChIP Elution buffer	50 mM Tris/HCl, pH 8.0 10 mM EDTA 1% (w/v) SDS
Coomassie blue staining solution	10% (v/v) acetic acid 50% (v/v) methanol 0.25% (v/v) Coomassie G250
Coomassie blue destaining solution	15% (v/v) acetic acid 45% (v/v) methanol
Coomassie blue drying solution	20% Ethanol 2% glycerol
DNA loading buffer (10×)	20% (v/v) Ficoll [®] 400 1 mM EDTA (pH 8.0) 0.25% (w/v) bromphenol blue or 0.15% (w/v) cresol red
IP lysis buffer	25 mM Tris/HCl (pH 8.0) 150 mM NaCl 10 mM MgCl ₂ 0.5% Nonidet P-40 (NP-40) 2 mM sodium orthovanadate 1 mM DTT 1 mM NaF 50 units /ml DNase I, RNase free complete mini protease inhibitors 0.25% (w/v) phosphatase inhibitor cocktail I
IP-washing buffer	Tris /HCl (pH 8.0) 150 mM NaCl 10 mM MgCl ₂ 0.5% NP-40
dNTP-mix	10 mM of each dATP, dCTP, dGTP, dTTP
HBS (2×)	274 mM NaCl 10 mM KCl 1.5 mM Na ₂ HPO ₄ × 2 H ₂ O 42 mM HEPES pH 7.5 0.2% (w/v) dextrose pH 6.95

Materials

Solution	Ingredients
Laemmli-buffer (2×)	100 mM Tris/HCl (pH 6.8)
	10% (w/v) SDS
	50% (v/v) glycerol
	0.05% (w/v) bromphenol blue
	10% (v/v) β-mercaptoethanol
LB-agar	1% (w/v) bacto [®] tryptone
	0.5% (w/v) bacto [®] yeast extract
	1% (w/v) NaCl
	pH 7.2
	1.2% (w/v) bacto [®] agar
LB-medium	1% (w/v) bacto [®] tryptone
	0.5% (w/v) bacto [®] yeast extract
	1% (w/v) NaCl
	pH 7.2
LB×2 low salt medium	2% (w/v) bacto [®] tryptone
	1% (w/v) bacto [®] yeast extract
	1% (w/v) NaCl
	pH 7.2
phosphate buffered saline (PBS)	13.7 mM NaCl
	2.7 mM KCl
	80.9 mM Na ₂ HPO ₄
	1.5 mM KH ₂ PO ₄ (pH 7.4)
PTS-buffer	13.7 mM NaCl
	2.7 mM KCl
	80.9 mM Na ₂ HPO ₄
	1.5 mM KH ₂ PO ₄ (pH 7.4)
	0.5 % Tween 20
	2% fetal bovine serum (FBS)
PCR-buffer (10×)	670 mM Tris/HCl (pH 8.8)
	166 mM (NH ₄) ₂ SO ₄
	67 mM MgCl ₂
	100 mM β-mercaptoethanol
RIPA lysis buffer	50 mM Tris/HCl, pH 8.0
	250 mM NaCl
	1 mM EDTA
	1% NP40
	0.1% (w/v) sodium dodecylsulfate (SDS)
	0.5% (w/v) sodium deoxycholate

Materials

Solution	Ingredients
SDS-PAGE Lower Tris (4×)	1.5 M Tris-base
	0.4% (w/v) SDS
	pH 8.8
SDS-PAGE Upper Tris (4×)	500 mM Tris-base
	0.4% (w/v) SDS
	pH 6.8
Semi-Dry Anode I buffer	0.3 M Tris at pH 10.4
Semi-Dry Anode II buffer	25 mM Tris at pH 10.4
Semi-Dry Anode III buffer	25 mM Tris at pH 9.4
	40 mM ε-aminocaproic acid
TAE-buffer (10×)	400 mM Tris-acetate
	10 mM EDTA
	pH 8.0
TAP Calmodulin binding buffer	10 mM Tris/HCl, pH 8.0
	250 mM sodium chloride
	1 mM magnesium-acetate
	1 mM imidazole
	2 mM CaCl ₂
	0.1% (v/v) NP40 or TritonX-100
	10 mM β-mercaptoethanol
TAP Calmodulin elution buffer	10 mM Tris/HCl, pH 8.0
	250 mM sodium chloride
	1 mM magnesium-acetate
	1 mM imidazole
	2 mM EGTA
	0.1% (v/v) NP40 or TritonX-100
	10 mM β-mercaptoethanol
TAP lysis buffer	25 mM Tris/HCl, pH 8.0
	150 mM NaCl
	10 mM MgCl ₂
	0.5% NP40 (v/v) or 0.1% (v/v) TritonX-100
	2 mM sodium orthovanadate
	1 mM DTT
	1 mM NaF
	50 units /ml DNaseI, RNase free (Roche)
	0.25% (v/v) phosphatase inhibitor cocktail 1
TAP IPP150 washing buffer	10 mM Tris/HCl, pH 8.0
	150 mM NaCl
	0.1% (v/v) NP40 or TritonX-100

Materials

Solution	Ingredients
TAP TEV-cleavage buffer	10 mM Tris/HCl, pH 8.0 150 mM NaCl 0.1% (v/v) NP40 or TritonX-100 0.5 mM EDTA 1 mM DTT
TBS (Tris-buffered saline) (10×)	100 mM Tris/HCl, pH 7.4 150 mM NaCl
TBS-T (1×)	10 mM Tris/HCl, pH 7.4 15 mM NaCl 0.1% (v/v) Tween20
TE-buffer (10×)	100 mM Tris/HCl, pH 8.0 10 mM EDTA
Transfer-buffer (25×)	300 mM Tris/HCl, (pH8.3) 2.4 M glycine
Tris-Glycine-SDS buffer (10×)	250 mM Tris/HCl, pH 7.5 192 mM glycine 1% (w/v) SDS
TSS-buffer	1% (w/v) bacto [®] tryptone 0.5% (w/v) bacto [®] yeast extract 100 mM NaCl 10% (v/v) PEG _{MW3000/3350} 5% (v/v) DMSO 50 mM MgCl ₂ pH 6.5

3 Methods

3.1 Bacterial cell culture

3.1.1 Propagation and storage of *Escherichia coli* (*E.coli*) strains

Bacterial *E.coli* strains used for plasmid-replication were cultured by agitation in liquid LB-Medium in case of XL1-blue and BJ5183 EC or in liquid LB×2-low salt medium for PirPlus™DH10βF`DOT strain. To isolate DNA from a single clone, bacteria were cultivated on LB-agar plates. In general, bacterial cultivation was done in a 37°C room overnight. The selection for antibiotic-resistant progeny cells was achieved by addition of 100 µg/ml ampicillin, 50 µg/ml kanamycin, or 25 µg/ml chloramphenicol dependent on the resistance cassette provided by the introduced plasmid vector. For the generation of permanent bacterial cultures for storage (“glycerol stocks”), 500 µl of bacterial liquid culture was added to an equal volume of 87% (w/v) sterile glycerol, mixed carefully and transferred to a -85°C freezer.

3.1.2 Preparation of Calcium-competent *E.coli* XL1-blue cells

Starting from a glycerol stock, a 5 ml over-night culture supplemented with 10 µg/ml tetracycline was diluted 1:50 in liquid LB-medium and grown to an OD₆₀₀ of 0.4. After cooling on ice for 15 min, cells were centrifuged at 4000×g for 15 min and resuspended in 1/10 volume of ice-cold TSS-buffer. Sterile glycerol was added to a final concentration of 20% (v/v) and 100-200 µl aliquots were shock-frozen using liquid nitrogen and stored at -80°C.

3.1.3 Transformation of competent bacteria

After thawing 100-200 µl calcium-competent bacterial aliquots on ice, 100-500 ng plasmid-DNA or 1/2 of a ligation reaction was added to the cells and mixed carefully. Hereafter, bacteria were incubated on ice for 30 min followed by a 75 sec thermo-shock at 42°C and placed on ice for another 2 min. Next, 1 ml LB-medium not containing any antibiotics was added and bacteria were placed in a rotation wheel in a 37°C room for 1 hr to allow recovery of cells and expression of the introduced resistance marker.

Finally, an appropriate amount of the transformation mixture was plated on nutrient agar containing the respective antibiotics in order to obtain separated bacterial clones.

3.2 Molecular biological standard methods

3.2.1 Purification of plasmid DNA from *E.coli*

5-250 ml liquid LB-medium containing the respective antibiotics were inoculated with bacterial clones from LB-agar plates or with a pipette-tip of a glycerol stock and cultured for 14-20 hrs overnight with agitation at 37°C. In case of small-scale preparations (5 ml bacterial culture volume), plasmid-DNA was isolated using the QIAprep Spin Miniprep Kit (Qiagen) according to the manufacturer's protocol. For transfection experiments requiring larger amounts of plasmid-DNA, the DNA was isolated from bigger culture volumes (100 ml and 250 ml for high and low copy number plasmids, respectively) with the QIAGEN Plasmid Maxi Kit according to the manufacturer's protocol. Since the small-scale purification method yields DNA of better quality leading to a higher transfection efficiency compared to the large-scale protocol, it was used preferentially.

3.2.2 Enzymatic restriction-digestion and dephosphorylation of DNA

0.3-1.0 µg of plasmid-DNA was used for analytical purposes, while 1-10 µg DNA was subjected to restriction-digestion in preparative applications. In case the DNA fragment was generated by polymerase chain reaction (PCR), the amplified products were separated from the template DNA by agarose gel electrophoresis and extracted from the gel prior to restriction-digest. In general, enzymatic digestions were performed in the reaction buffer recommended by the manufacturer and in the presence of 10 µg/ml BSA (NEB) in reaction volumes ranging from 20-100 µl. The temperature, time and amount of enzyme were adapted to the specific application. A simultaneous restriction approach with two different enzymes was performed only in case the buffer system provided optimal reaction conditions for each of them. Blunt end fragments were generated by addition of 100 µM dNTPs and 8 U T4 DNA polymerase and incubation of the reaction mixture at 12°C for 15 min.

In order to avoid self-ligation of digested vectors during ligation, DNA was 5`-dephosphorylated using 10 U antarctic phosphatase at 37°C for 2×20 min and subsequent heat-inactivation of the enzyme for 10 min at 65°C.

3.2.3 DNA ligation

Ligation of sticky ends was performed by combination of 10-20 ng linearized and de-phosphorylated vector-DNA with 30-100 ng of DNA to be inserted. This roughly equaled a molar vector to insert ratio of 1:3-1:20, dependent on the length of vector and insert DNA fragments. The ligation mixture furthermore contained 1/10 volume of 10× T4 ligase reaction buffer and 400 U T4 DNA ligase in a 10 µl total volume. The reaction time was adapted for each special application ranging from 2 hrs at RT to overnight incubation at 16°C.

In case of blunt end ligations or ligation mixtures containing the linearized episomal vectors pRTS-1⁴⁷⁸ and pEMI⁴⁹³, the reaction mixture was supplemented with 1/10 volume of 10×PEG₄₀₀₀ (NEB) and the ligation was performed in a 20 µl total volume overnight at 16°C.

3.2.4 Amplification of DNA by the polymerase chain reaction (PCR)

The standard PCR reaction was performed in a 25 µl scale and each reaction contained 2.5 µl 10x PCR-buffer (166 mM (NH₄)₂SO₄, 670 mM Tris/HCl (pH 8.8), 67 mM MgCl₂, 100 mM β-mercapto-ethanol), 1.5 µl dNTP-mix (10 mM of each dATP, dCTP, dGTP and dTTP), 1.5 µl DMSO, 5 U DNA-Polymerase, 1 ng (analytical reaction) or 100-500 ng (preparative reaction) template DNA and 20 µM oligonucleotides (“primers”). For amplification reactions requiring high-fidelity DNA synthesis, Platinum[®] *Taq* DNA polymerase was mixed 1:1 with *Pfu* DNA polymerase. All other PCR reactions were performed using the FIRE-Pol[®] DNA polymerase (Solis BioDyne). In an alternative high-fidelity PCR approach the Phusion[®]-DNA-Polymerase (NEB) was used according to the manufacturer`s instructions.

The following exemplary PCR procedure was carried out in a GeneAmp[®] PCR System 9700 cycler (Applied Biosystems) or a Mastercycler[®] personal system (Eppendorf) and

the exact settings were adapted to the specific reaction with respect to amplification-product length and melting-temperature of the oligonucleotide primers:

Initial denaturing: 96°C for 5 min
20-40 cycles: Denaturing: 96°C for 30 sec
 Annealing for 30 sec at 50-60°C (Depending on the melting temperature of the applied oligonucleotide-primers).
Extension: 45 sec per kb of product length at 72°C
Final extension step: 72°C for 2-4 min
Sample cool-down to 25°C

The PCR products were separated by agarose gel electrophoresis and purified as described in section 3.2.5.

3.2.5 Analysis and purification of DNA fragments by agarose gel electrophoresis

For preparation of agarose gels, 0.8-2.5% (w/v) agarose powder was melted in 1×TAE buffer in a microwave, cooled down to ~50°C and supplemented with 0.5 µg/ml ethidium bromide. 1/10 of 10× DNA loading buffer was added to DNA samples and horizontal electrophoresis was carried out at 50 to 110 V (dependent on the electrode distance of the used electrophoresis chamber) for 30-60 min. For preparative approaches, electrophoresis was done at 30-40 V for 1.5-2.5 hrs to reach a more efficient separation of DNA fragments. By comparison with a DNA ladder of known composition, the size and the position of DNA fragments was determined with an UV transilluminator (300-400 nm wavelength) (IDA Gel Documentation system) and recorded for documentation. When DNA fragments were separated for subsequent isolation and ligation, the bands were visualized using a Fisherbrand FT-20E/365 transilluminator. Isolation and purification of the respective DNA fragments from agarose gel pieces - excised from the gel with a sterile surgical blade - was performed with the QIAquick Gel Extraction Kit (Qiagen) according to the manufacturer`s protocol.

3.2.6 DNA sequencing

For sequencing of protein- or microRNA-encoding DNA fragments integrated into plasmid or viral vectors, 300-1000 ng DNA was supplemented with 5 pmol oligonucleotide primer, 1.5 μ l BigDye® Terminator v3.1 Sequencing Mix (Applied Biosystems) and 1 μ l 5 \times BigDye® Sequencing Buffer (Applied Biosystems) and mixed in a total volume of 10 μ l. Amplification was carried out using the following PCR parameters:

Initial denaturing: 96°C for 2 min
30 cycles: Denaturing: 96°C for 20 sec
 Annealing for 10 sec at 50°C
 Extension: 4 min at 60°C

Sample cool-down to 25°C

Processing of the reaction mixture and DNA sequencing was done by the Core-Facility of the Max-Planck Institute of Biochemistry.

3.3 Generation of microRNA-encoding DNA fragments

The DNA fragments encoding specific microRNAs were generated in a two-step PCR: 3 μ M of each mi-Fwd and mi-Rev primer were annealed and extended in an one-step-PCR reaction containing 10 μ l PCR-buffer \times 10, 10 μ l dNTPs (10 mM each) and 5 U platinum DNA polymerase in a total volume of 100 μ l using the following reaction conditions:

Initial denaturing: 96°C for 5 min
1 cycle: Denaturing: 96°C for 30 sec
 Annealing for 30 sec at 48°C
 Extension: 72°C for 4 min
Final extension step: 72°C for 2-4 min

Sample cool-down to 25°C

The reaction products were separated by vertical polyacrylamide gel electrophoresis (PAGE) using a 12% gel, the appropriate band was sliced out from the gel, reduced to small pieces, transferred into a 1.5 ml reaction tube and supplemented with 300 μ l

300 mM sodium acetate, pH 4.8. After vortexing thoroughly, elution of DNA from the gel was achieved by diffusion at 65°C for 15 min. For purification, the suspension was transferred into a SpinEx tube (Costar) and centrifuged at 16,060×g for 1 min. Next, DNA was concentrated by ethanol precipitation and 10% of the extension-reaction product was applied to the second PCR reaction which furthermore contained 1 μM of the universal miR30-*XhoI/EcoRI* primers, 10 μl 10× PCR-buffer, 2 μl dNTPs (10 mM each) and 2 U Vent-DNA-polymerase (NEB) in a total reaction volume of 100 μl. The following reaction parameters were chosen:

Initial denaturing: 96°C for 5 min
25 cycles: Denaturing: 96°C for 30 sec
 Annealing for 30 sec at 54°C°
 Extension: 75°C for 30 sec
 Final extension step: 75°C for 10 min

Sample cool-down to 25°C

The resulting amplification product was purified using the Qiagen Gel-Extraction Kit, the elution volume was chosen to 45 μl. 5 μl of this reaction was stored for analyses and the remaining PCR product was cut with *XhoI* and *EcoRI*. After purification by PAGE, elution from the gel and ethanol-precipitation (done as described for the first PCR step), the restricted miRNA-fragment was inserted into pSHUMI vector⁴⁹³ that already contained the flanking miR30 regions. *SfiI* fragments from pSHUMI containing the complete microRNA cassette were inserted into pRTS-1⁴⁷⁸ thereby creating pEMI-microRNA vectors.

3.4 Real time quantitative PCR (RT-qPCR)

Total RNA was isolated using the Total RNA Isolation System (Promega, Madison, USA). cDNA was generated from 1-1.5 μg total RNA per sample using anchored oligo-dT primers (Reverse-iT First Strand Synthesis; ABgene). RT-qPCR was performed by using the LightCycler (Roche) and the FastStart DNA Master SYBR Green 1 kit (Roche Applied Science) essentially according to the manufacturer's protocol. Primer pairs were tested using a logarithmic dilution of cDNA to generate a linear standard curve (crossing

point [CP] plotted vs. log of template concentration) and the primer pair efficiency was calculated as follows: Efficiency $E = 10^{(-1/\text{slope})}$ or the efficiency was estimated to 1.9. RT-qPCR reactions using β -actin primers served for normalization in case of cDNAs whereas genomic DNA for qChIP analyzes was normalized to 16q22 primers. For data analyzes, the second-derivative maximum method was used and induction of cDNA or enrichment of a genomic locus was calculated according to Pfaffl⁴⁹⁴ using the following equation:

$$\frac{(E_{DNAx})^{\Delta CP(\text{sample-control})}}{(E_{\beta\text{-actin}})^{\Delta CP(\text{sample-control})}} = \text{fold induction or enrichment}$$

3.5 Site directed mutagenesis

Starting from pGL3b reporter plasmids containing wild type or mutant p21 promoter (gift from Carme Gallego (Universitat de Lleida)⁴⁸⁷), CAGCTG sequences were mutated using the QuikChange II site directed mutagenesis kit (Stratagene) according to the manufacturer using specific primer pairs (see Materials section)

3.6 Mammalian cell culture

3.6.1 Cultivation of human and rodent cell lines

DLD1-tTA and HCT116 colorectal cancer cells and their derivatives were maintained in McCoy's 5A medium (Invitrogen) containing 10% fetal bovine serum (FBS). HaCaT keratinocytes, MCF-7 breast cancer cells, U-2OS osteosarcoma cells, H1299 non-small cell lung cancer cells, 911 transformed human retinoblasts and human diploid fibroblasts (HDF) and their derivatives were maintained in high glucose Dulbecco's modified Eagles medium (DMEM, Invitrogen) containing 10% fetal bovine serum (FBS). For HDF cells stably expressing a c-MYC-ER fusion protein, phenol-red free medium was applied since phenol-red in tissue culture is a weak estrogen⁴⁹⁵. HEK293 human epithelial kidney cells, HEK293T cells and the Phoenix A amphotropic packaging cell line were maintained in DMEM containing 5% FBS. *c-myc*-deficient Rat1A (H015.19³⁸⁹) cells stably selected for expression of a c-myc-ER fusion construct (Smoxyl⁴⁹²) were maintained in phenol-red free, high glucose DMEM containing 8% fetal bovine serum.

U-937 myelomonoblastic cells and their derivatives were cultured in RPMI medium (Invitrogen) supplemented with 10 FBS.

All media were further supplemented with 100 U/ml penicillin and 100 µg/ml streptomycin and cell lines were maintained at 37°C in a humidified atmosphere at 37°C. Cells were passaged every 2-4 days in order to avoid confluency of the cultures.

3.6.2 Cryo-preservation of mammalian cells

For cryo-preservation, subconfluent, exponentially growing cells were trypsinized, pelleted by centrifugation at 300×g for 5 min, and resuspended in 50% FBS, 40% growth medium and 10% (v/v) DMSO. Aliquots in cryo-vials were stored at -80°C for up to 6 months or, for long term storage, transferred into a liquid nitrogen tank. For recovery, cells were rapidly thawed in a 37 C water bath and transferred to a 15 ml tube of pre-warmed growth medium. Cells were pelleted by centrifugation to remove DMSO and resuspended in the respective growth medium for further cultivation.

3.6.3 Transient and stable transfection of eukaryotic cells

HEK293 and HEK293T cells were transfected by calcium-phosphate transfection: cells were pre-treated with 30 µl/ml FBS and 10 µl/ml of 2 mM chloroquine diphosphate for 30 min at 37°C. For transfection of one 6-well, 1-1.5 µg DNA was diluted in 110 µl 0.1× TE buffer and supplemented with 16 µl 2 M CaCl₂ and 125 µl 2×HBS. After incubation for 15 min at RT the formed precipitates were added dropwise onto cells. H1299 cells were transfected using a modified calcium-phosphate transfection protocol: for one 12-well, 0.5 µg DNA + 1 µg carrier-DNA (here: pUC19 vector) was diluted in 85 µl water and supplemented with 10 µl 10×HBS and 5 µl 2 M CaCl₂. After 15 min the formed precipitates were added to cells.

DLD1-tTa cells were transfected using Lipofectamine™ 2000 (Invitrogen) according to the manufacturer and all other cell lines were transfected with FuGENE®6 reagent (Roche) according to the manufacturer`s protocol using OptiMEM®I medium (Invitrogen). Transfection of siRNAs into MCF-7 and DLD1-tTA-c-MYC-HA cells was performed using HiPerFect reagent (Qiagen). For transfection of one 12-well, 150 ng siRNA (MCF-7) or 375 ng siRNA (DLD1-tTA) was diluted in 75 µl OptiMEM®I

medium and supplemented with 5 μ l HiPerFect[®] reagent. After brief vortexing and incubation for 10 min at RT, siRNA-containing complexes were added to cells.

Except for approaches using FuGENE[®]6 and HiPerFect[®] reagents, medium was exchanged 5-6 hrs after transfection with complete growth medium. Analyses were performed 24-48 hrs after transfection. For generation of stable cell lines, cells were split 1:5 to 1:10 one day after transfection and growth medium was supplemented with an appropriate selection marker after additional 24 hrs. Limiting dilution was used for generation of single clones.

3.6.4 Retroviral infection

The packaging cell line Phoenix A was transfected with retroviral expression vectors using a calcium-phosphate protocol and growth medium without antibiotics to enhance the production of recombinant retroviruses. For one 6 cm plate, 8 μ g retroviral vector was used. 9-12 hrs after transfection, growth medium was replaced and cells were cultured overnight in the absence of antibiotics. Next, retrovirus-containing supernatants were passed through 0.45 μ m filters (Millipore) and supplemented with 8 μ g/ml polybrene (hexadimethrin-bromide). The cationic polymer polybrene increases the efficiency of infection by shielding the negatively charged cell surface which facilitates the access of virus particles to cells⁴⁹⁶. The sterile filtered virus-containing supernatant was applied to cells and infection was repeated four times in 4 hr intervals. 24 hrs after transfection, cells were split 1:10 and selected with the appropriate selection marker for 10-14 days.

3.6.5 Generation of recombinant adenoviruses and infection of target cells

The adenoviral vector AdGFP-AP4-VSV was constructed by ligation of AP4-VSV cDNA into the plasmid pAdTrack-CMV, which is used for production of GFP-expressing viruses⁴⁸⁹, followed by electroporation together with the Adeasy-1 plasmid⁴⁸⁹ and recombination in *E. coli* (BJ5183 EC, Qbiogene) in a total volume of 25 μ l using a Bio-Rad Gene Pulser device (settings: 25 μ F; 200 Ω ; 2500 V). After recombination, 1 ml LB was added to bacteria and cells were grown at 37°C for 1 hr in antibiotic-free medium. 25 μ l and 50 μ l of the bacterial suspension were plated on kanamycin (50 μ g/ml) LB-agar plates which yielded 10-50 colonies after overnight incubation at 37°C. The smaller

colonies which should represent recombinants⁴⁸⁹ were isolated and grown in 5 ml LB-medium containing 50 µg/ml kanamycin. Clones were screened for the presence of pAdeasy-1 + insert by restriction digestion with *PacI* and *XhoI*. Plasmid DNA originating from positive clones was transformed into XL1-blue cells for amplification. Viral production and amplification was performed in 911 cells⁴⁸⁸. After calcium-phosphate based transfection of 911 cells in a 10 cm cell culture dish using *PmeI*-linearized pAdeasy-1-AP4-VSV plasmid, cells were monitored for GFP expression and collected 2 – 3 days after transfection by scraping off dishes. Supernatants and scraped cells were pelleted in 50 ml collection tubes prior to removing all but 5 ml of supernatant. Viral lysate was generated by three cycles of freezing in an ethanol/dry-ice bath and rapid thawing at 37°C. After sterile filtration (0.45 µm; Millipore), 1.5 ml viral lysate served for infection of 1×10^7 911 cells in a 10 cm dish. This process was repeated with increasing amounts of cells for high titer virus generation and finally, $4\text{-}6 \times 10^8$ packaging cells in sixteen 15 cm cell culture dishes were infected. After 3 days, cells were harvested and viruses were purified by CsCl banding. The minimal amount of virus needed to reach a more than 90% infection efficiency was determined by monitoring GFP signals with fluorescence microscopy.

24 hrs after seeding into 12-well plates, HCT116 cells were incubated with adenovirus for 12 hrs. HaCaT cells were infected in serum free medium with adenovirus for 3 hrs and an equal amount of medium containing 20% FBS was added for additional 8 hrs before infection medium was replaced by fresh medium.

3.6.6 Proliferation assay

MCF-7-PJMMR1 and –MR1 cells were seeded into 6 well plates starting with 3×10^4 cells per 6-well as determined by trypan blue staining and a cell counting chamber. 24 hrs later, cells were treated with 1 µg/ml ICI182,780 and 1 µg/ml doxycycline was added additional 30 hrs later to induce ectopic *c-MYC* expression. Cells were harvested by rinsing two times with Hanks balanced salt solution (HBSS, Invitrogen) and subsequent trypsinization. The cell number was determined with a Z1 Coulter Particle Counter (Beckmann Coulter). All experiments were performed in biological triplicates and every sample was counted at least three times.

3.6.7 Transient reporter assays based on mammalian cells

H1299 non-small cell lung cancer cells were transfected using FuGene Reagent (Roche) in 12-well plates with 15 ng Renilla luciferase control reporter plasmid pRL, 600 ng firefly luciferase reporter constructs containing either wild type or mutant p21 promoter sequences⁴⁸⁷, 20 nM pcDNA-AP4-VSV or an equimolar amount of pcDNA3 backbone. For p53-mediated p21 reporter activation, 400 ng firefly luciferase reporter constructs containing either wild type or mutant p21 promoter sequences, 250 nM pcDNA-AP4-VSV or an equimolar amount of pcDNA3 backbone and 0, 50 or 200 nM pCEP4-p53 or equimolar amounts of pCEP4 backbone were used. Firefly and Renilla luciferase activities were measured 36 hrs after transfection with the Dual-luciferase assay (Promega). Firefly activity was normalized to Renilla luciferase activity to control for transfection efficiency.

HCT116 p53^{-/-} cells in 12-wells were transiently transfected with 400 ng of BDS2-3* reporter construct¹⁸¹, 20 ng expression plasmid for renilla luciferase pRL-CMV (Promega), wild type p53 expression plasmid and pCR3.1-Flag-Cul7⁴⁸³ expression vector. Control cells were infected with an equimolar amount of pCR3.1-Flag plasmid. Cells were harvested 48 hrs after transfection and activities of firefly and renilla luciferase were measured consecutively using the Dual-Luciferase reporter assay system (Promega).

HCT116 p53^{-/-} cells in 6-wells were transiently transfected with 1000 ng of BDS2-3* reporter construct¹⁸¹, 500 ng pCMV- β -Gal, 200 ng pCEP4-p53 equimolar amounts of vector backbone. 200 ng pBI-YFP-TAPn-p53 or pBI-YFP-p53-TAP or equimolar amounts of pBI-YFP vector were transfected in combination with 200 ng pMK-tTa plasmid in order to provide the tet-responsive transactivator in trans. Cells were harvested 48 hrs after transfection and activities of firefly luciferase and β -galactosidase were measured consecutively using the β -Galactosidase Enzyme Assay System (Promega).

3.7 Protein analysis and purification

3.7.1 Generation of goat polyclonal antibodies

In the course of this study, a goat polyclonal anti-HA antibody raised against the peptide H-CYPYDVPDYASL-OH (#1452) and a goat polyclonal anti-p53 antibody raised

against the peptide H-CGQSTSRHKKLMFKTEGPDS-OH (#1467), representing the C-terminal 20 amino-acids of p53, were generated. Peptides were synthesized by the Core-Facility of the Max-Planck Institute of Biochemistry.

3.7.1.1 Conjugation of peptides to carrier protein

The peptides containing a sulfhydryl-group at their N-terminus were coupled to KLH (keyhole limpet hemocyanine) using the Imject[®] Maleimide Activated mcKLH Kit (Promega) according to the manufacturer's protocol. Here, 2 mg of peptide were coupled with 2 mg of activated KLH for 2.5 hrs prior to purification of the conjugate using D-Salt Cross-linked Dextran Gel Filtration Columns. 500 μ l fractions were collected and the absorbance at 280 nm was determined to identify the samples containing the KLH-coupled peptide. The respective fractions were combined, sterile filtered and stored in a -20°C freezer until further usage.

3.7.1.2 Immunization of goats

Goats were immunized by injection of 1 ml of a 1:1 emulsion prepared with 0.5 mg peptide-KLH conjugate (~500 μ l) and Titermax[®] Gold Adjuvant (Sigma). Prior to the first injection, 50 to 100 ml pre-immune serum were taken and stored at -80°C. 40 days later, the second injection ("boost") was done using a 1:1 emulsion of 0.5 mg protein-conjugate with Freund's Adjuvant incomplete (Sigma). 14 days after this boost, test-blood was analyzed for the presence of functional antibodies. 20 days after taking test-blood, the next boost was performed and the 3rd and 4th boosts yielded high titer antibodies. Test-blood was taken from the animals usually 11-14 days after immunization. For serum isolation, test blood was kept at 4°C over-night and centrifuged at 3000 \times g for 2 \times 20 min at 4°C. The supernatant, which represents the serum, was collected and stored at -20°C until affinity purification.

3.7.1.3 Affinity purification of polyclonal antibodies

Polyclonal anti-HA and anti-p53 antisera were affinity purified using the SulfoLink[®] Coupling Gel (Pierce). To immobilize the respective peptide (epitope) to the gel matrix, 2 mg peptide were dissolved in 2 ml de-gassed coupling buffer (50 mM Tris/HCl, pH 8.5, 5 mM EDTA) and mixed with 2 ml (bed volume) SulfoLink[®] coupling gel slurry, that

had been equilibrated with coupling buffer, in Poly-Prep® chromatography columns (Bio-Rad). After incubation for 15 min by head-over-tail rotation and additional 30 min without rotation, the columns were washed carefully with coupling buffer and subsequently incubated with 3 ml of freshly made 50 mM L-Cystein-HCl in coupling buffer for 15 min by head-over-tail rotation and additional 30 min without rotation in order to block free sulfhydryl-groups on the gel matrix. After this, the column was washed carefully with 1 M NaCl and finally with Storage Buffer (PBS + 0.05 % (w/v) NaN₃).

For affinity purification of polyclonal antibodies, 2 ml peptide-coupled SulfoLink® coupling gel slurry was incubated with 20 ml antiserum and 25 ml PBS over-night at 4°C by slow head-over-tail rotation. Next, the gel matrix was spun down by centrifugation at 200× g for 5 min at 4°C and washed twice with PBS, 500 mM NaCl before transfer into a fresh Poly-Prep® chromatography column. Further washing of the column was performed until the flow-through did not contain detectable amounts of protein as determined by Ponceau S staining of 1 µl samples spotted on nitrocellulose membrane. Antibodies bound to the gel-matrix-immobilized peptides were eluted with 0.2 M acetic acid, pH 2.7, 500 mM NaCl and collected to 500 µl fractions which were immediately neutralized by addition of 100 µl 1 M Tris, pH 8.8. Antibody-containing fractions were identified by Ponceau S staining of 1 µl samples spotted on nitrocellulose membrane, combined and the buffer was changed to PBS by repeated dilution and concentration using Amicon® Ultra-15 tubes (cut-off: 30,000 Dalton; Millipore). Subsequent to protein concentration measurement (A_{280} -detection), antibodies were mixed with 1 volume of 87% sterile glycerol and stored in 50 µl aliquots at -20°C.

3.7.2 Preparation of whole cell lysates from mammalian cells

To obtain whole cell lysates (WCL) from exponentially growing or arrested cells, cells were washed with ice-cold PBS and lysed on ice for 10-15 min using RIPA lysis buffer containing protease inhibitors. Lysates were centrifuged at 16.060×g for 20 min at 4°C to remove cellular debris. The protein concentration of the supernatant was determined using a Bradford assay reagent at OD₅₉₅ standardized to a BSA dilution series. WCL

were immediately subjected to PAGE and western blot analysis, stored at -20°C overnight or, in case of long term storage, transferred to a -80°C freezer.

3.7.3 Polyacrylamide gel electrophoresis (PAGE), Western blotting and Immunodetection of proteins

Due to the high resolution that can be achieved by discontinuous electrophoresis, the SDS-containing, discontinuous Tris/HCl-Glycin buffer system described by Laemmli⁴⁹⁷ was applied in this thesis. Dependent on the analyzed protein size window, 6% to 12% polyacrylamide separation gels were prepared and overlaid with a 4% stacking gel. 30-80 µg of protein were supplemented with an equal volume of 2× Laemmli-buffer and denatured at 95°C for 5-10 min prior to loading on the gel. To estimate the protein sizes after electrophoretic separation, a stained protein marker (PageRuler™ prestained protein ladder, Fermentas) was used. Electrophoresis was performed at 80-130 V in a vertical Mini-PROTEAN®-electrophoresis system with Tris-Glycin-SDS buffer. In order to visualize protein bands after electrophoresis as a control for equal loading, gels were stained using Coomassie blue staining solution with subsequent destaining with Coomassie blue destaining solution.

After separation, proteins were transferred onto Immobilon-P PVDF-membranes (Millipore) either by using the Trans-Blot® cell system (Bio-Rad) with a constant voltage of 100 V for 75-120 min at 4°C and transfer buffer pre-chilled to 4°C or by semi-dry blotting using the Multiphor II Electrophoresis unit (Amersham) with a constant current of 0.8 mA/cm² (~50 mM per MINI-gel) for 60-100 min at RT in a 3-buffer system (Anode I, II and cathode transfer buffer). After transfer, membranes were incubated in 10% (m/v) skim milk / TBS-T for 1-2 hrs at RT in order to block non-specific binding sites. Primary antibodies were diluted in TBS-T buffer and applied to the membranes for 1 hr at RT or over-night at 4°C. Antibodies specific for β-actin or α-tubulin served as a control for equal loading. Next, membranes were washed for 5 min with TBS, 10 min with TBS-T and another 5 min with TBS before incubation with an appropriate secondary antibody conjugated to horseradish peroxidase for 30-45 min at RT. After washing twice for 10-30 min (dependent on the primary antibody) with TBS-T buffer and once with TBS for 2-5 min, proteins were visualized using ECL Western blotting substrate (Pierce) or Western Lightning® Western Blot Chemiluminescence Reagent Plus

(PerkinElmer) as a substrate for horseradish peroxidase and signals were recorded with a CCD camera (Kodak 440CF imaging system).

3.7.4 Silver staining

Subsequent to electrophoretic separation of proteins, polyacrylamide gels were incubated for 2× 30 min in 50% (v/v) methanol/12% (v/v) acetic acid followed by 3× 20 min in 50% (v/v) ethanol. After incubation in 200 mg/l Na₂S₂O₃, gels were washed twice in H₂O and stained for 20 min in AgNO₃-solution (2g/l AgNO₃, 375 µl/l formaldehyde) at 4°C. After washing with water for 1 min, silver stains were developed for 5-10 min in Na₂CO₃-solution (60 g/l Na₂CO₃, 5 mg/l Na₂S₂O₃, 250 µl/l formaldehyde), washed briefly with H₂O followed by 10 min incubation in 5% (v/v) acetic acid. Developed gels were stored at 4°C in 1% (v/v) acetic acid or air dried.

3.7.5 Tandem affinity purification (TAP)

The TAP method takes advantage of two consecutive affinity purification steps which increases the specificity when compared to standard immuno-precipitation methods. The TAP approach used in this study is based on a special affinity tag (“TAP-tag”), which consists of calmodulin-binding protein (CBP), a TEV (tobacco etch virus) protease cleavage site and two repeats of a minimal domain of *Staphylococcus aureus* protein A (“Z domain”), which binds to IgG⁴⁷². A schematic presentation of the four experimental steps of the TAP procedure is depicted in Figure 8.

For TAP, 6× 10⁸ MCF-7i-p53-TAP cells (corresponding to 10× 500 cm² plates) were treated with 100 µM zinc chloride for 6 hrs to induce expression of the TAP-tagged p53 and for 3.5 hrs with 20 µM of the topoisomerase II inhibitor etoposide to provoke a DNA damage response and consequently the activation and stabilization of the TAP-tagged p53 protein. Hereafter, cells were washed with 100 ml ice-cold PBS (phosphate buffered saline) per 500 cm² plate and lysed in TAP lysis buffer supplemented with protease inhibitors (complete mini, EDTA-free, Roche) for 20 min rotating at 4°C. Samples were cleared by centrifugation at 13,000 rpm for 20 min in a table centrifuge at 4°C and pellets were resuspended in 300 µl fresh TAP lysis buffer and subjected to 4 freeze-thaw cycles

(liquid nitrogen, 37°C water bath), centrifuged at 13,000 rpm for 20 min at 4°C and the soluble fractions were combined.

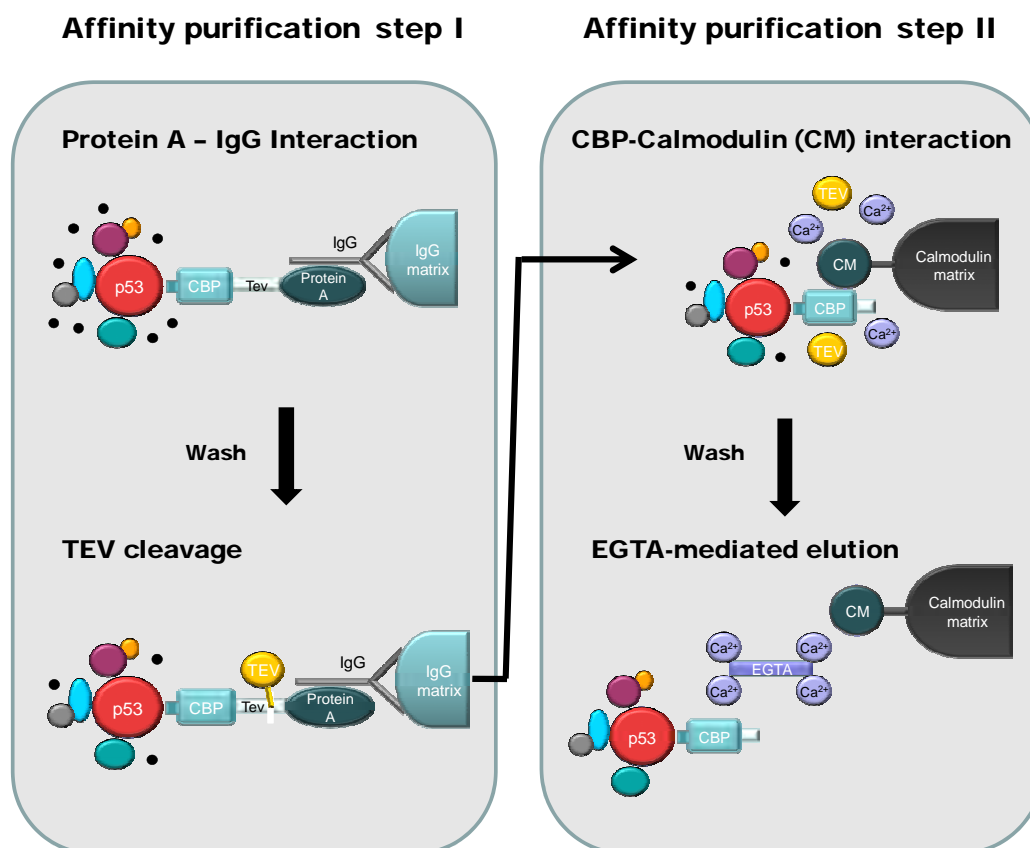


Figure 8. The tandem affinity purification (TAP) approach:

In the first step, the fusion protein (here: p53-TAP) and associated complexes are recovered from cellular extracts by selective binding to an IgG-affinity matrix. After washing, addition of TEV protease serves to release the bound protein complexes. In the second affinity step, the first eluate is incubated with calmodulin-coated beads in a calcium-containing buffer system. The second washing step removes TEV protease and contaminants which remained after the first affinity step. Finally, the tandem affinity purified material is eluted by addition of EGTA. (Adapted from Ref. 500)

Cell lysates corresponding to ~160 mg of protein were incubated with 500 µl of IgG sepharose beads (Amersham Biosciences) for 2.5 h at 4°C with head-over-tail rotation. Beads were collected using chromatography columns (Polyprep, Bio-Rad) and washed twice with 10 ml TAP IPP150 washing buffer and once with 10 ml TAP tobacco etch virus (TEV) cleavage buffer. For TEV cleavage 300 units of TEV protease (Invitrogen) in 3.0 ml TEV cleavage buffer were added to the sample and incubated for 2.5 hrs at 4°C by head-over-tail rotation. The resulting eluate was directly transferred to a fresh column

containing 400 μ l equilibrated calmodulin affinity resin (Stratagene) in 7 ml TAP calmodulin binding buffer, supplemented with CaCl_2 to 2 mM and incubated for 2.5 hrs at 4°C. After 3 times washing with 10 ml TAP calmodulin binding buffer, proteins were released by calcium chelating using 1.2 ml of TAP elution buffer. For precipitation of the eluted protein complexes, the elution fractions were supplemented with 0.015% (w/v) sodium deoxycholate and 1/5 volume of 6.1 M trichloroacetic acid (TCA), incubated for 2 hrs at -20°C and centrifuged at 13,000 rpm for 20 min at 4°C in a table centrifuge. The protein precipitates were washed twice with -20°C cold acetone and air-dried at RT for 10 min.

3.7.6 Multidimensional protein identification technology (MudPIT)

The MudPIT approach was developed for identification of proteins from complex mixtures without the necessity to separate proteins by gel electrophoresis. Two chromatography steps interfaced back to back in fused silica capillaries represent the basis of the MudPIT procedure. While a strong cation exchange column with high loading capacity is used in the first dimension, a reverse phase chromatography column is applied in the second dimension which allows for further peptide separation and removing of salt. The eluted peptides are injected into the mass spectrometer by electrospray-ionization (ESI) and fragments are analyzed to obtain protein sequence data.

MudPIT analyses were performed by Aaron Bailey in the laboratory of John Yates III. (Department of Cell Biology, The Scripps Research Institute, San Diego, USA). The precipitated p53-TAP-associated proteins underwent trypsin digestion prior to analyzes by LC/LC/MS/MS according to published protocols⁴⁹⁸. Approximately 1 μ g of protein was used for a 12-step LC/LC/MS/MS experiment on a LCQ Classic (ThermoElectron, San Jose, CA). The obtained MS/MS spectra were automatically assigned to proteins by SEQUEST 27 using a non-redundant mammalian data base (May 2003 release, NCBI). The SEQUEST outputs were further analyzed by DTASelect with the filter settings: XCorr: +1 ions, 1.8; +2 ions, 2.5; +3 ions, 3.8; Δ CN, 0.08; only half or full tryptic peptides were considered and all subset proteins were removed (the “-o” option in DTASelect). Proteins with two or more peptides that passed the DTASelect filter were considered real hits.

3.7.7 Indirect immunofluorescence labeling

Cells grown on glass slides were washed 3 times with PBS and fixed in 4% paraformaldehyde/PBS for 10 min at RT. After rinsing three times with PBS, cells were permeabilized in 0.2% (v/v) Triton X-100 for 20 min and blocked in 100% FBS for 1 hr at RT in order to block non-specific binding sites. Slides were incubated with primary antibodies in IF-buffer (PBS, 0,05% Tween20, 50% FBS) for 1 hr at RT and washed 3 times for 5 min with washing buffer (PBS, 0,05% Tween20). Subsequently, slides were incubated with secondary antibodies diluted in IF-buffer for 30 min at RT and washed two times using washing buffer. After incubation with 1 µg/ml DAPI in PBS for 2 min, slides were washed additional 3 times for 5-10 min with washing buffer and mounted in Fluoromount (Southern Biotech) solution. Images were acquired using Axiovert 200M microscope equipped with a CoolSNAP™-HQ CCD camera and the MetaVue® software package (Universal Imaging).

3.7.8 Tissue sections and immunohistochemistry

Twelve cases of sporadic colorectal carcinoma were retrieved from the archives of the Institute of Pathology (LMU Munich). All carcinomas were WHO grade 2 or 3. None of the patients had received cancer therapy prior to surgical resection of the lesions. For IHC, biopsies from diagnostic colonoscopies were used to ensure that the tumor tissue had been immediately fixed in neutral 4% buffered formalin. Colon sections of 4 µm thickness from formalin-fixed, paraffin-embedded tissue were deparaffinized for 2× 5 min in xylene followed by rehydration with solutions of decreasing ethanol concentration (100%-70%). After washing in tap water, sections were boiled for 2× 15 min in TRS solution pH 6.1 (DakoCytomation) in a microwave for antigen retrieval. After cooling down for 20 min at RT, quenching of endogenous peroxidase activity was achieved by incubation of tissue sections in 7.5% H₂O₂. The staining procedure was done using the VECTASTAIN® Elite ABC Kit (Vector) essentially according to the manufacturer's protocol. After pre-blocking for 30 min in 1% horse serum, sections were incubated with a 1:125 dilution of anti-AP4 (Atlas antibodies) antibody or, for an isotype control, polyclonal rabbit-anti-mouse IgGs (Sigma) in PBS supplemented with 10% horse serum and 0.05% Tween20 for 1 hr at room temperature.

After washing twice for 5 min with buffer (PBS, pH 7.5, 0,05% Tween 20), tissue sections were incubated with biotinylated horse-anti-rabbit antibodies (Vector) diluted 1:50 in PBS supplemented with 2% horse serum and 0,05% Tween20 for 30 min at RT. The streptavidin/peroxidase system combined with exposure to DAB+ (3,3'-diaminobenzidine) chromogen (DakoCytomation) was used for visualization according to the manufacturer`s protocol. Counterstaining was performed with Mayer`s hematoxylin (Merck) for 20 sec prior to mounting of sections in an aqueous mounting medium (Aquatex, Merck). Staining of consecutive sections with antibodies directed against p21 (DakoCytomation), Ki67 (DakoCytomation) and c-MYC (Epitomics) was performed using the LSAB2 System-HRP (DakoCytomation) detection system. The streptavidin/peroxidase system combined with exposure to AEC (β -amino-9-ethyl-carbazole) reagent (Zytomed) for 10 min was used for visualization. Images were captured on a Zeiss Axioskop 40 microscope coupled to a Leica DC500 camera.

3.7.9 Co-immunoprecipitation

For immunoprecipitation (IP) of exogenous proteins, H1299, MCF-7 and HEK293 cells were transfected by using a calcium phosphate method and processed 24 hrs after transfection. IP of exogenous and endogenous proteins was carried out starting from cells grown in 14 cm cell culture plates. Cells were lysed on ice with 400 μ l IP-lysis buffer. After sonication of whole cell lysates (WCL) (Sonifier: Bandelin HD70 Sonoplus; 5 pulses with 50% intervals, power setting: MS72D) cellular debris was removed by centrifugation at 16.060 \times g for 20 min at 4°C. 1-3 mg of pre-cleared WCL were incubated with specific antibodies or an IgG-control (serum or affinity purified IgGs) for 3 hrs at 4°C in a rotation wheel. All further centrifugation steps were performed at 2,000 rpm for 1 min at RT in a table centrifuge. For recovery of antibody-bound proteins, 25 μ l of Protein G-Sepharose beads were added for an additional 2 hrs. After washing 3 times with IP washing buffer, beads were transferred into a fresh reaction tube, washed once more and proteins were eluted from beads by addition of 30 μ l 2 \times Laemmli buffer and boiling for 10 min at 95°C. Finally, proteins were separated by SDS-PAGE and subjected to Western blot analysis.

3.7.10 Chromatin immunoprecipitation (ChIP) assay

U-2OS and MCF-7 cells and their derivatives were cultured in 14 cm plates. For cross-linking, formaldehyde was added to a final concentration of 1%. After 4 min (MCF-7) or 5 min (U-2OS) cross-linking at RT, the reaction was stopped by addition of glycine at a final concentration of 0.125 M followed by incubation for 2 min. Fixed cells were washed twice using TBS buffer and harvested in ChIP-SDS-buffer supplemented with protease inhibitors. Cells were pelleted by centrifugation at 300× g for 5 min at 4°C and resuspended in 2 ml ChIP-IP-buffer supplemented with protease inhibitors. Chromatin was sheared by sonication (Sonifier: Bandelin HD70 Sonoplus, power setting: MS72D) for 4 times (MCF-7) or 5 times (U-2OS) 20 sec to generate DNA fragments with an average size of 500-700 bp. For each immunoprecipitation, 2 ml of lysate was pre-cleared by addition of 30 µl pre-blocked (0.4 mg/ml BSA fatty acid free, Sigma; 1.5 mg/ml sheared herring-sperm DNA in PBS) protein A sepharose beads. Lysates were incubated for 20 hrs at 4°C with a polyclonal c-MYC antibody (sc-764, Santa Cruz) or rabbit anti mouse IgG (M-7023, Sigma) in case of MCF-7-PJMMR1 derived lysates or a monoclonal anti-VSV antibody (hybridoma clone P5D4) or Protein G-purified mouse IgG from mouse pre-immune serum (S-7273, Sigma) for lysates from AP4-VSV-expressing U-2OS cells. The bound protein-DNA complexes were recovered by addition of pre-blocked protein A sepharose beads (60 µl per 2 ml lysate) and incubation for 2 hrs at 4 C by head-over-tail rotation. After centrifugation at 1000× g for 1 min, samples were washed once in the following order of ChIP buffers for 1 min at RT: Mixed Micelle buffer, Buffer 500, LiCl/Detergent buffer and finally TE-buffer. Elution was carried out by addition of 100 µl freshly prepared ChIP elution buffer, careful mixing and incubation for 10 min at 65°C. After washing of bead matrix with 150 µl ChIP elution buffer the two eluate fractions were combined and incubated overnight at 65°C for crosslink-removal. Next, samples were supplemented with one volume of ChIP-proteinase K solution and incubated for 45 min (ChIP-gDNA) or 4 hrs (input gDNA) at 37°C. Purification was performed by Phenol/Chloroform/Isoamylalcohol extraction. The resulting aqueous phase was supplemented with 1/10 volume of 4 M LiCl and 20 µg glycogen and subjected to ethanol precipitation for 30 min at -20°C. After centrifugation for 15 min at 4°C in a table centrifuge, the precipitated DNA fragments were washed twice with 70% ethanol and air-

dried for 10 min at RT. The DNA pellets were reconstituted with 50 μ l ddH₂O (80 μ l for input gDNA), 0.2 mg/ml RNase was added and the samples were incubated for 30 min at 37°C. The quality and size distribution of the sheared DNA was analyzed by agarose gel electrophoresis (1.2% gel) using 10-20 μ l of the input gDNA. Prior to RT-qPCR analyses, ChIP-DNA was further purified using the PCR purification kit (Qiagen) according to the manufacturer's protocol. Purified DNA was first analyzed by amplification of a genomic fragment from chromosome 16q22 that did not contain any E-boxes up to 3 kb up- and downstream. This amplification product was used to control for equal DNA input in the RT-qPCR reactions. For analysis of c-MYC binding to the *AP4* locus equal amounts of DNA were analyzed by RT-qPCR with a primer pair flanking two E-boxes (CACGTG) in the first intron of the human *AP4* gene. A second primer pair spanning a fragment in intron 6 of *AP4* was used to control for specificity. For analysis of *AP4* binding to the proximal *p21* promoter, a primer pair flanking an E-box (CAGCTG) was used. A second primer pair spanning a fragment in intron 1 of *p21* was used to control for specificity.

3.8 DNA content analysis by FACS

5×10^4 U-2OS or 5×10^5 U-937 cells were plated into T25 cell culture flasks. 5×10^4 MCF-7 cells were plated into T25 cell culture flasks or, for analyses after siRNA transfections, MCF-7 cells were seeded into 12-well plates. Floating cells and trypsinized cells were collected by centrifugation at 1.200 rpm (300 \times g) for 7 min, fixed with ice-cold 70% ethanol and stored 2 hrs to several days on ice. After washing with PBS, cells were incubated with FACS solution (PBS, 0.1% Triton X100, 60 μ g/ml propidium iodide (PI), 0.5 mg/ml DNase free RNase), which had been passed through 0.22 μ m sterile filter units (Millipore), at room temperature for 30 min. DNA content was determined by detection of propidium iodide fluorescence by flow cytometry (FACSCalibur, Becton-Dickinson).

3.9 BrdU labeling for detection of *de novo* DNA synthesis

DNA synthesis was monitored by measuring incorporation of the artificial thymidine nucleotide analog 5-bromo-2'-deoxyuridine (BrdU)(Roche) into *de novo* synthesized DNA. After treatment of U-937 cells with TPA and zinc sulfate, 10 μ M BrdU was added

for 30 min at 37°C. Next, cells were harvested by trypsinization and centrifuged at 300×g for 5 min. After washing two times with PBS, fixation was achieved by addition of ice-cold 70% ethanol and incubation for at least 30 min at -20°C. Fixed cells were resuspended in 0.1 mg/ml pepsin in 2 M HCl and incubated for 30 min at RT. After centrifugation at 500×g, neutralization was achieved by resuspending the cells in 0.1 M Na₂B₄O₇ at RT for 5 min. Cells were washed once with each PBS and PTS buffer and subsequently resuspended in 60 µl PTS+6 µl anti-BrdU-FITC antibody (BD Pharmingen) or an appropriate isotype control IgG and incubated for 30 min at RT in the dark. Next, cells were washed twice with PTS and resuspended in 500 µl PTS + 0.5 mg/ml RNaseA (Sigma) + 50 µg/ml propidium iodide. After incubation for 30 min at RT or 2-3 hrs at 4°C cells were analyzed by flow cytometry (FACSCalibur, Becton-Dickinson).

3.10 Microscopy

Phase contrast pictures of living cells were captured using an Axiovert 25 microscope equipped with a HyperHAD CCD camera and KAPPA ImageBase software. Images of stained sections were captured with Axioskop 40 microscope connected to a Leica DC500 camera and Adobe Photoshop CS2 software. Fluorescence microscopy of living cells expressing mRFP and of fixed cells stained with antibodies was carried out by using an Axiovert 200M microscope, and pictures were taken from a CoolSNAPTM-HQ CCD camera and documented using Metamorph[®] software.

4 Results I

4.1 Proteomic identification of p53-associated proteins

Widely used approaches to study p53-associated proteins are co-immunoprecipitation of endogenous proteins and epitope-tagging. While co-immunoprecipitation suffers from cross-reactivities of the applied antibodies, classical epitope-tags (e.g. Flag-, HA-, VSV-, Myc- or Strep-tag) only allow for a single-step purification under one defined condition which leads to high background and obscures low abundant, specific interactions. This drawback of affinity-based purification methods has been overcome by utilizing two consecutive purification steps: the so-called “tandem affinity purification” (TAP) strategy (see Figure 8, Methods section) was originally developed in yeast with the intention to rapidly purify protein complexes with their composition being analyzed by mass spectrometry^{472,499,500}. For the recovery of physiological protein complexes, the TAP-tag permits purification under mild, close to native conditions⁴⁷². Therefore, the tandem-affinity-purification (TAP) approach was chosen to isolate native p53-containing protein complexes.

4.1.1 Generation of a p53-TAP fusion construct

In order to test the functionality of tagged p53 protein, a TAP-tag consisting of calmodulin-binding protein (CBP) and two copies of protein A epitopes was fused to the p53 N- or C-terminus. In transient reporter assays performed in p53-deficient HCT116 cells⁵⁰¹, expression of the C-terminal TAP-tagged p53 fusion protein (p53-TAP) increased luciferase activity, which was under control of three tandem-arranged p53 binding sites derived from the *14-3-3 σ* gene promoter (pBDS2 \times 3,¹⁸¹), almost 60-fold, while a N-terminal fusion construct only gave rise to ~25-fold reporter activation (Figure 9A). As a positive control, wild type p53 under control of a stronger, full-length CMV promoter (pCEP4-p53) was used that led to a more than 200-fold increase of luciferase activity. The C-terminal fusion protein was chosen for the following analyses. To further elucidate the functional activity of p53-TAP at promoters of endogenous target genes, an inducible DLD1 colon carcinoma cell line was generated by transfection of

DLD1-tTa cells⁴⁸¹ with a pBI-YFP-p53-TAP vector harboring a bi-directional promoter. In this cell line, expression of *p53-TAP* and *YFP* is under control of a tet-responsive element (“tet-off” system). A cell clone was isolated by limiting dilution and showed a tight regulation of p53-TAP by doxycycline (Figure 9B). DLD1 cells carry a mutant form of endogenous p53 (p53 S241F,⁵⁰²) that is unable to transactivate target genes⁵⁰³. As a consequence, expression of the p53 target gene *p21*¹⁸⁰ was hardly detectable and expression of p21 did not increase in response to DNA damage in this cell line (Figure 9B). After washing out doxycycline, expression of p53-TAP was rapidly induced and caused a strong induction of p21 demonstrating the functionality of the p53-TAP fusion protein (Figure 9B).

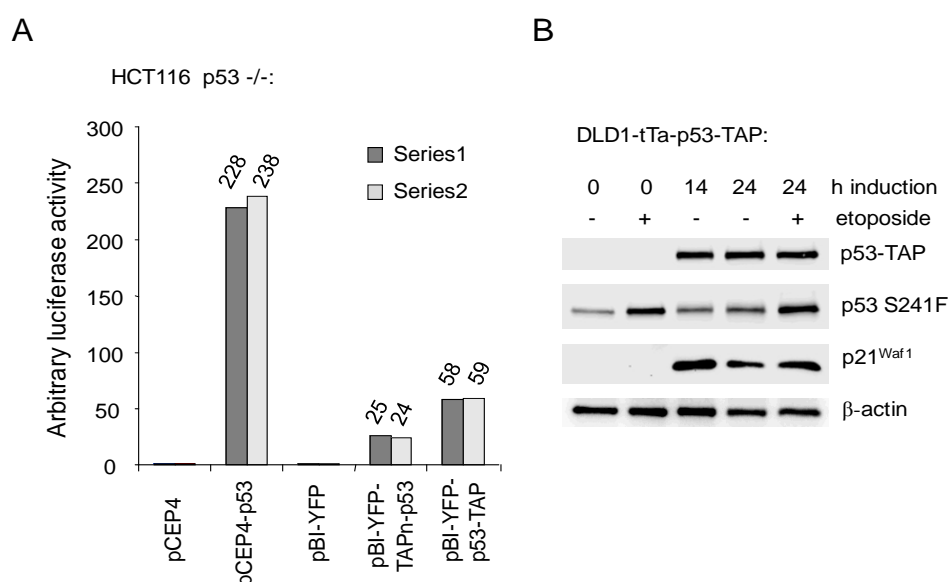


Figure 9. Functional characterization of the TAP-tagged p53 protein

A, Transient reporter assay using HCT116 p53^{-/-} cells transfected with BDS2x3 reporter plasmid harboring 3 tandem-arranged p53 binding sites derived from the *14-3-3σ* promoter and either wild-type p53 (wt, pCEP4 backbone) or plasmids expressing N- or C-terminal TAP-tagged p53 (pBI-YFP backbone), or equimolar amounts of the respective vector controls. Relative luciferase activity is depicted as the relative expression normalized to *β-galactosidase* activity. Two independent experiments (series 1 and 2) are shown.

B, DLD1-tTA-p53-TAP cells after removal of DOX (induction of p53-TAP) for the indicated periods were treated with etoposide for 8 hrs as indicated and whole cell lysates were analyzed by Western blotting and subsequent immunodetection using antibodies specific for p53, p21 and, for normalization, β-actin. p53 S241F: endogenous mutant p53 expressed in DLD1 colon cancer cells.

4.1.2 Generation of a cellular system for identification of p53 interactors

While the originally described TAP procedure - optimized for proteomic analyses in yeast - is in principle easily adaptable to studies performed in higher eukaryotes, one main obstacle needed to be overcome: in contrast to yeast, which allows substitution of the endogenous gene of interest for the gene encoding the TAP-tagged counterpart by homologous recombination, this cannot be achieved in the human system. Since the endogenous protein might be preferentially incorporated into protein complexes thereby limiting the sensitivity of the TAP approach, Forler et al. sought to mimic the situation in yeast and developed the so-called “iTAP” strategy⁴⁷³. This technique combines the TAP approach with double-stranded RNA interference (RNAi) directed against the corresponding endogenous gene. Cell lines harboring mutant, and therefore functionally inactive p53, are only suitable for the iTAP method at first sight. As an example, the endogenous mutant p53 variant in DLD1 colorectal cancer cells is not functional with respect to its transactivation potential but it still comprises wild type conformation⁵⁰³. Therefore it was likely that this p53 mutant would strongly compete with the TAP-tagged version of p53 for endogenous interactors. In addition, mutant p53 in DLD1 cells was not amenable to RNAi-mediated down-regulation (data not shown), presumably due to the increased protein half-life compared to wild-type p53⁵⁰⁴. This can be explained by the fact that mutant p53 is no longer able to maintain the regulatory feedback loops which negatively act on its stability⁵⁰⁴.

In order to meet the demands of the iTAP purification, a MCF-7 breast cancer cell line (MCF-7i) was generated by retroviral infection: the used retroviral vector (based on pRetroSuper⁴⁸⁰) encoded a short hairpin RNA (shRNA) directed against the 3'-non-translated region (3'-UTR) of p53. As a result, the levels of endogenous p53 were significantly reduced (Figure 10A). The knockdown of endogenous p53 led to a delayed increase of p53 and induction of p21 after DNA damage (Figure 10B). p53-TAP was stably expressed in this cell line under control of a truncated zinc-inducible promoter (MTΔ156⁴⁸⁶) which allowed expression of p53-TAP at a level similar to endogenous p53 (data not shown) thereby favoring the recovery of physiological p53-containing protein complexes rather than artificial complexes that might result from the strong over-expression of the bait protein. Induction of p21 after activation of *p53-TAP* and the

accumulation of the p53-TAP protein in response to DNA damage (Figure 10C) as well as the nuclear localization of the fusion protein (Figure 10D) indicated that the TAP-tag did not interfere with the physiological function and regulation of ectopic p53.

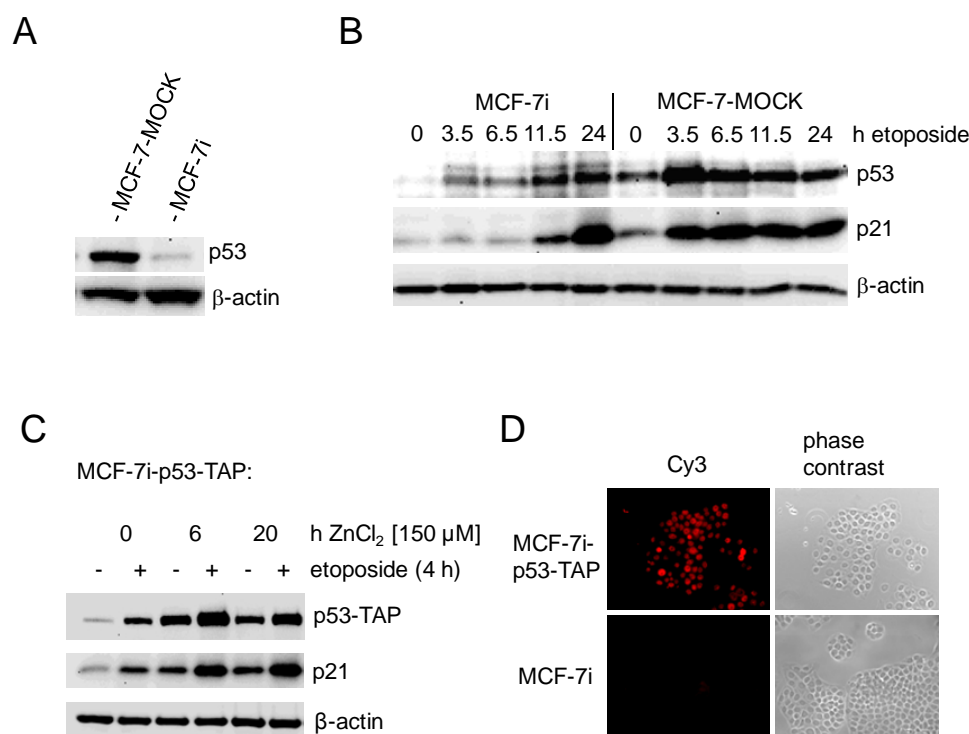


Figure 10. Establishment of a breast cancer cell line for iTAP purification

A, Detection of endogenous p53 and β -actin protein by Western blot analysis in MCF-7 cells stably expressing a p53-specific short hairpin RNA (shRNA) directed against the p53 3'-non-translated region (3'-UTR) (MCF-7i) and control infected cells (MCF-7-MOCK).

B, MCF-7i and MCF-7-MOCK cells were treated with 20 μ M etoposide for the indicated periods. Expression of p53, p21 and, for normalization, β -actin, was analyzed by Western blot analysis.

C, Detection of p53-TAP, p21 and β -actin expression by Western blot analysis in MCF-7i-p53-TAP cells. p53-TAP was induced by addition of 150 μ M ZnCl_2 for the indicated periods. Non-induced cells and cells over-expressing p53-TAP were treated with 20 μ M etoposide as indicated.

D, Indirect immunofluorescence detection of p53-TAP in MCF-7i-p53-TAP or, as a control, parental MCF-7i cells 6 hrs after addition of 150 μ M ZnCl_2 using a rabbit-anti-goat-Cy3 antibody directed against the Protein A present in p53-TAP.

4.1.3 iTAP/MudPIT analysis of p53-associated proteins

Subsequently, the optimal time-point for TAP purification of p53-associated proteins was determined (data not shown). Finally, the p53-TAP allele was induced in MCF-7i-

p53-TAP cells by addition of zinc chloride for 6 hrs and the topoisomerase II inhibitor etoposide was added 3.5 hrs prior to cell lysis and subsequent TAP purification. This duration of etoposide treatment reflects the earliest time point at which a stabilization and functional activation of p53-TAP was detectable (data not shown) and was chosen to avoid interference with the accumulation of endogenous p53 protein (see also Figure 10B). In order to yield sufficient amounts of co-purified proteins for mass-spectral analyses, each TAP purification was started using $\sim 6 \times 10^8$ cells which roughly corresponded to 160 mg total protein. 1% of the final eluate was subjected to Western blot analyses in order to detect p53-TAP (prior to purification) and p53-CBP (after purification) or gels were silver stained to control for the presence of p53-CBP and co-purified proteins (Figure 11).

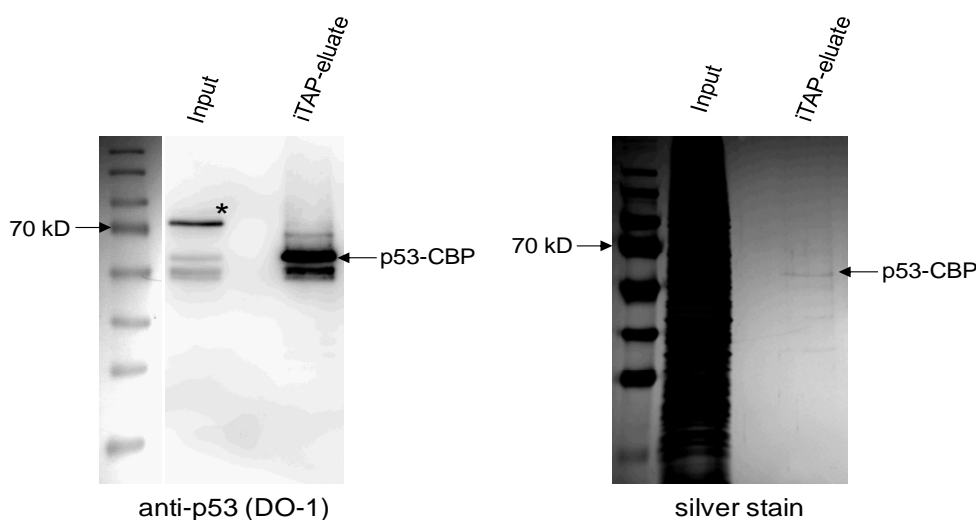


Figure 11. p53 protein in input and eluate fractions of an iTAP purification

50 μ g of input protein and 1% of the final eluate were subjected to Western blot analysis or a silver staining. In case of immunodetection, an antibody against p53 was used to detect p53-TAP (*) or p53-CBP which had undergone proteolytic cleavage by TEV protease during the iTAP procedure. In the silver stain, the strongest signal matches the molecular weight of p53-TAP with additional, weaker bands representing putative interaction partners of p53.

Multidimensional protein identification technology (MudPIT) allows the identification of peptides in highly complex mixtures of TAP-eluates without the need for gel-electrophoretic separation⁴⁷⁴. Thereby, the peptide detection sensitivity is greatly

enhanced. Precipitated eluates from the iTAP experiments were subjected to MudPIT analyses by Aaron Bailey in the laboratory of John Yates III. (Department of Cell Biology, The Scripps Research Institute, San Diego, USA). In brief, TCA-precipitated TAP-eluates were digested by trypsin, the peptide spectra were detected by MudPIT analysis and peptide sequences were determined and evaluated by SEQUEST 2.7 software using a non-redundant mammalian database.

protein identification by MudPIT	RefSeq Accession No.	TAP I	TAP II	TAP III	TAP IV	Biological function / functional domain
		sequence coverage (%)				
p53	NP_000537	37.7	12.2	32.6	53.4	Transcription factor, tumor suppressor
MDM2*	NP_002383	20.5	-----	12.7	37.6	E3 ubiquitin ligase /Ring finger domain
MDM4 / MDMX*	NP_002384	-----	-----	-----	12.9	Negative regulator of p53 activity
HSP70*	NP_005336	9.7	9.1	-----	22.3	Heat shock protein
PARC*	NP_055904	14.7	6.1	3.8	13.2	Parkin-like ubiquitin ligase /Ring finger domain
Cul7	NP_055595	16.3	4.9	4.9	10.2	component of SCF7 ubiquitin ligase

Table 1. p53-associated proteins identified in 4 iTAP/MudPIT analyses

Shown are exemplary results obtained from 4 iTAP/MudPIT analyses of p53-associated proteins. The proteins represented here are the most significant p53 interactors according to the number of identified peptides, sequence coverage and consistency in the four purifications. *known p53 interactors.

4.1.4 Putative p53 interactors identified by the iTAP/MudPIT approach

In the 4 performed TAP purifications, peptides corresponding to Cul7 were the most frequent besides those corresponding to the previously characterized p53 binding proteins MDM2⁴⁹, PARC⁷¹, HSP70⁵⁰⁵ and MDMX⁹⁸(Table 1). 11 additional putative p53 interactors were identified less frequently and/or with lower sequence coverage (data not shown). All other identified proteins were regarded as co-purified background, as they are generally detected during TAP-tag purifications^{454,506}(data not shown). For Cul7, 15 peptides were identified covering almost 20% of the amino acid sequence of the 193 kD Cul7 protein (data not shown). While one of these peptides could be assigned to both PARC and Cul7, 14 peptides exclusively matched to Cul7. Besides Cul7, only the PARC protein and p53 itself were detected in all 4 independent iTAP/MudPIT analyses. MDM2

and HSP70 were detected in 3 out of 4 TAP purifications. From this observation it can be inferred that Cul7 presumably has an exceptionally high affinity towards p53 when compared to all other p53 interacting proteins. Cul7 is highly homologous to the PARC protein, which has been previously described as a negative regulator of p53 function⁷¹. The N-terminal domain of PARC which is required for association with p53⁷¹ shows approximately 60% sequence identity with Cul7 (Figure 12).

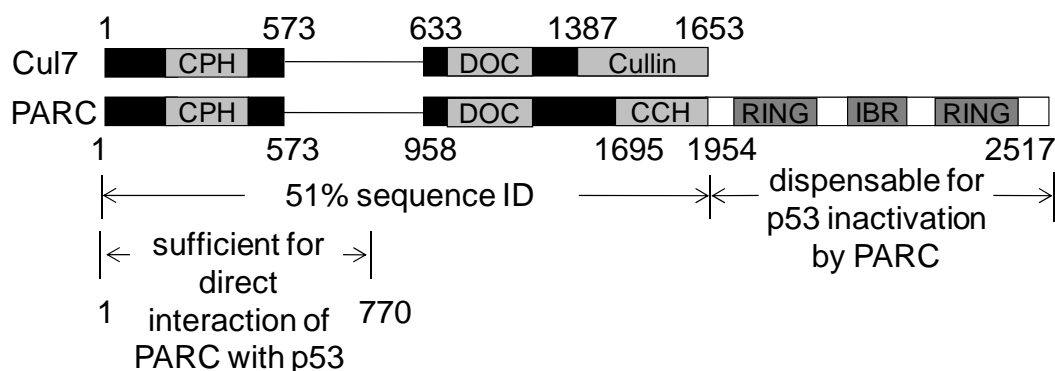


Figure 12. Schematic comparison of PARC and Cul7 protein domain structure

CPH: domain conserved in Cul7, PARC and HERC protein. DOC: DOC (DOC1/APC10) domain which shows striking similarity to APC10/DOC1, an essential subunit of the APC/C (Anaphase promoting complex/cyclosome). CCH: C-terminal Cullin homology domain; RING: RING finger domain; IBR: In Between RING Fingers domain.

4.2 Cul7: a novel inhibitor of p53 activity

4.2.1 p53 interacts with Cul7 *in vivo*

To validate the association between p53 and Cul7, both proteins were ectopically expressed in p53-deficient H1299 non-small cell lung cancer cells. In a co-immunoprecipitation approach, the precipitation of Flag-tagged Cul7 specifically co-precipitated the HA-tagged p53 protein (Figure 13A) and a specific interaction between the two putative interactors was also confirmed in an inverse co-immunoprecipitation

using HA-tagged p53 as the bait protein (Figure 13A; lower panel). The same result was obtained with HEK 293 cells using a VSV-tagged version of p53 (Figure 13B).

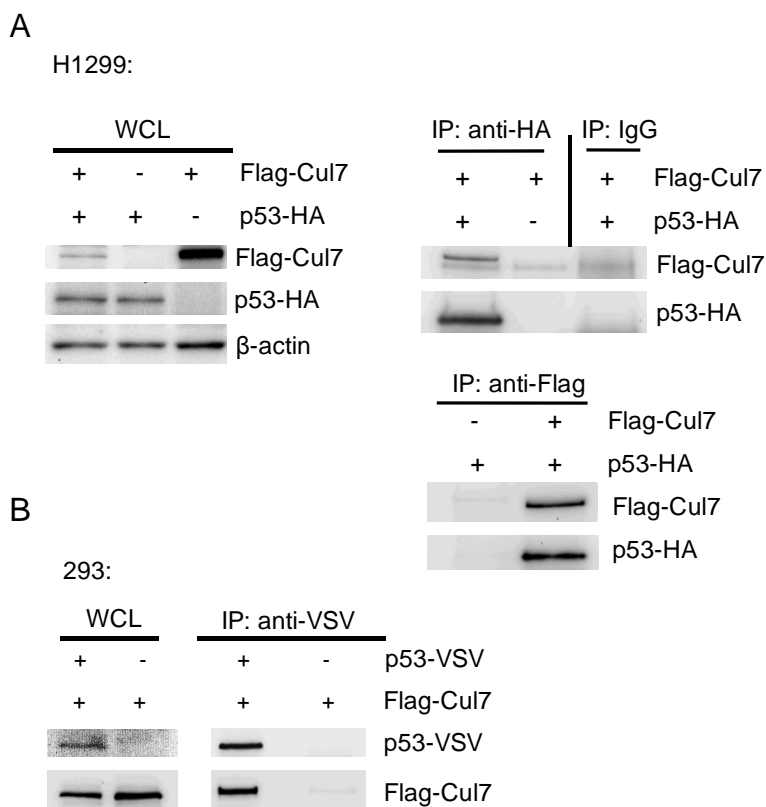


Figure 13. Interaction between ectopic Cul7 and p53 proteins cells.

A, H1299 cells were transfected with constructs encoding HA-tagged p53 and Flag-tagged Cul7. Western blot analysis of whole cell extracts (WCL) and immunoprecipitates (IP; obtained using HA-specific, Flag-specific or mouse pre-immune serum (IgG)).

B, Co-immunoprecipitation of VSV-tagged p53 and Flag-tagged Cul7 in 293 cells. Western blot analysis of whole cell extracts (WCL) and immunoprecipitates (IP; obtained by VSV-specific antibodies) using Flag- or VSV-specific monoclonal antibodies.

More important, immunoprecipitation with p53-specific antibodies identified an association with endogenous Cul7 in the breast carcinoma cell line MCF-7 which expresses wild type p53 but, as expected, not in p53-deficient H1299 cells (Figure 14). The association between endogenous p53 and Cul7 was more pronounced 4 hrs after generation of DNA damage by addition of the topoisomerase II inhibitor etoposide (Figure 14). Co-precipitation of endogenous p53 with Cul7 was also observed in the

osteosarcoma cell line U-2OS (data not shown) suggesting that Cul7 interacts with p53 in a cell type-independent manner.

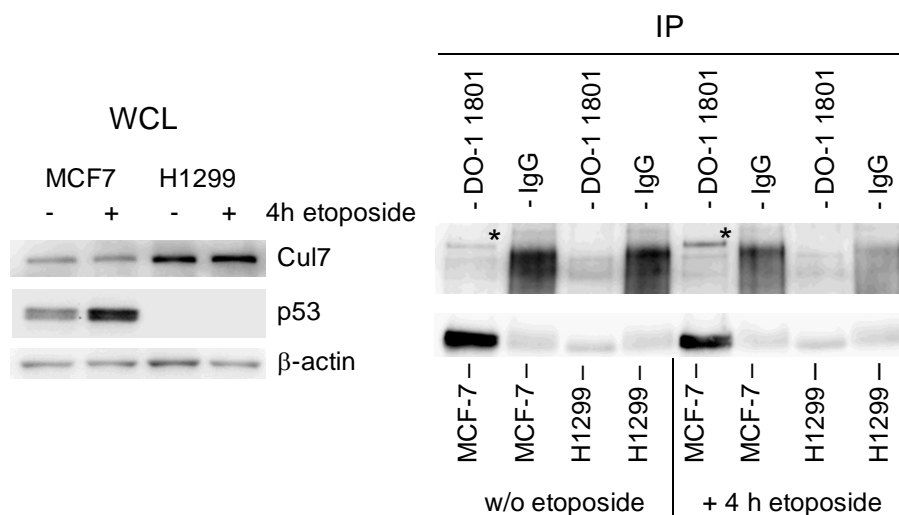


Figure 14. Interaction of endogenous p53 and Cul7 proteins in MCF-7 cells

Co-immunoprecipitation of endogenous p53 and Cul7 in MCF-7 and H1299 cells. Whole cell extracts (WCL) and immunoprecipitates (IP; obtained with p53-specific antibodies (DO-1 and 1801) or mouse pre-immune serum (IgG)) were subjected to Western blot analysis using Cul7-specific monoclonal and p53-specific polyclonal (from goat; self-made) antibodies. *specific signal for Cul7.

4.2.2 Cul7 protein and mRNA accumulate after DNA damage

Since the association between Cul7 and p53 was enhanced after treatment of cells with the genotoxic drug etoposide (Figure 14), *Cul7* mRNA and protein levels were analyzed after DNA damage. Interestingly, endogenous Cul7 protein significantly accumulated in MCF-7 cells as early as 10 hrs after treatment with etoposide and reached a maximum level after 24 hrs (Figure 15A). A similar increase of Cul7 protein was observed in the osteosarcoma cell line U-2OS and also in the p53-negative cell line H1299 (Figure 15A). Concomitant with elevated Cul7 protein level, genotoxic stress provoked an elevation of *Cul7* mRNA in MCF-7 and U-2OS cells (Figure 15B). In contrast, the p53-negative cell line H1299 showed no increase of *Cul7* mRNA 14 hrs after treatment of cells with etoposide (Figure 15B).

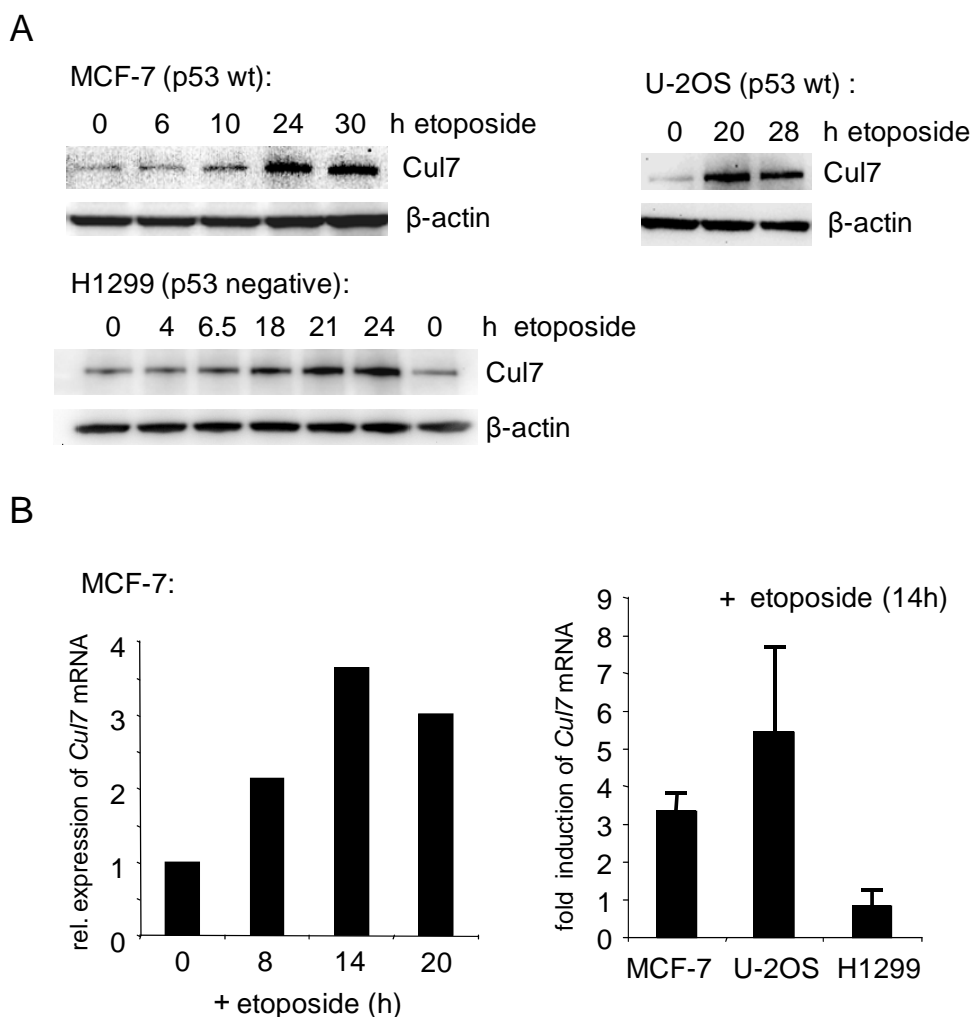


Figure 15. Increase of *Cul7* mRNA and protein in response to DNA damage.

A, Detection of *Cul7* protein levels in MCF-7, U-2OS and H1299 cancer cell lines by Western blot analysis. The respective cell lines were treated with etoposide (20 μ M) for the indicated periods.

B, Analysis of *Cul7* mRNA expression. MCF-7 cells were treated with etoposide for the indicated periods. Total RNA was isolated from the indicated cell lines and cDNA was analyzed by RT-qPCR (real-time quantitative PCR) (left panel). 14 hrs after treatment of MCF-7, U-2OS and H1299 cell lines with etoposide, RNA was isolated and analyzed by RT-qPCR (right panel). The determination was performed in biological triplicates. Error bars represent standard deviations.

This p53-dependency suggested that *CUL7* might be a p53 target gene. However, activation of a tet-regulated *p53* allele in DLD1-tTa (clone p53.A2) and H1299 cells did not affect *Cul7* mRNA expression, whereas *p21* mRNA was induced as expected (Figure 16A and data not shown). In addition, DNA damage provoked an increase of *Cul7* protein in HCT116 colon cancer cells deficient for *p53* with similar kinetics as in

cells expressing wild type p53 (Figure 16B). The *Cul7* mRNA was not significantly affected by DNA damage in these two cell lines (Figure 16C).

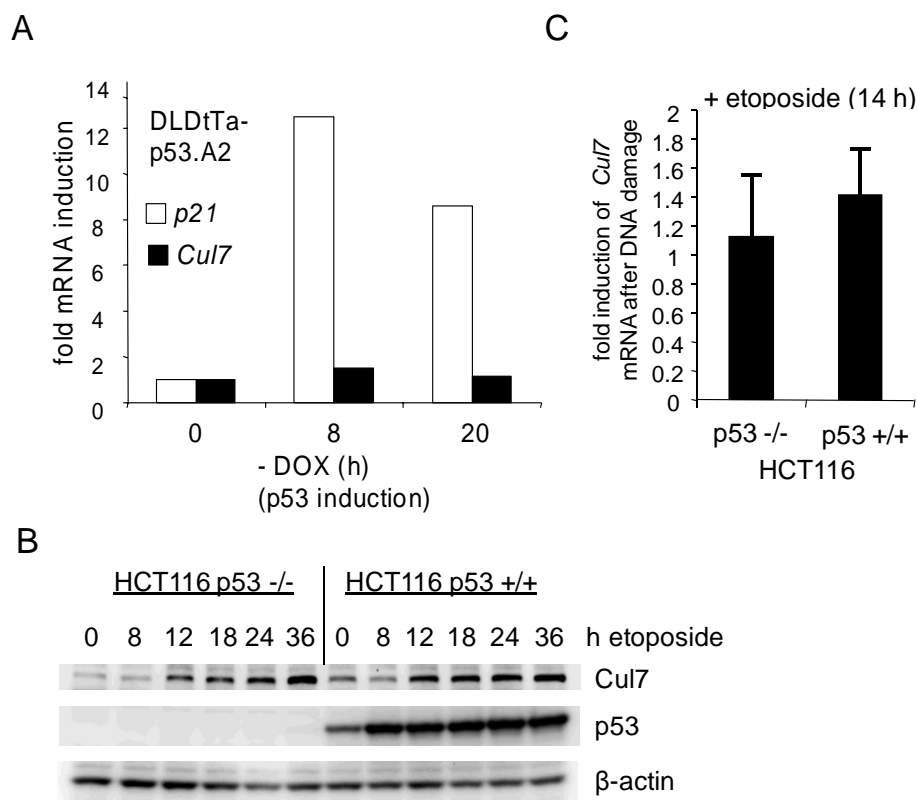


Figure 16. Induction of *Cul7* is independent of p53 activity.

A, RT-qPCR analysis of *p21* and *Cul7* mRNA levels after induction of wild-type p53 in DLD1-tTa-p53.A2 cells by removal of DOX for the indicated periods. Fold induction represents the average of two independent experiments. Expression of β -actin was detected for normalization.

B, Detection of *Cul7* protein levels in p53-deficient and wild-type HCT116 colon cancer cell lines by Western blot analysis. Cells were treated with 20 μ M etoposide for the indicated periods. Detection of β -actin was used for normalization.

C, Analysis of *Cul7* mRNA expression in wild-type and p53-deficient HCT116 colon cancer cell lines by RT-qPCR analyses. 14 hrs after treatment with etoposide total RNA was isolated from the indicated cell lines and analyzed by RT-qPCR. The determination was performed in biological triplicates. Error bars represent standard deviations.

In agreement with these data, the *Cul7* promoter region was not responsive to p53 in a transient reporter assay (data not shown), which implicates that the increase of *Cul7* mRNA observed in a subset of cell lines after DNA damage is not dependent on p53 activity and might be mediated by an unknown factor.

4.2.3 Cul7 induction upon DNA damage is caffeine-sensitive

The xanthine alkaloid compound caffeine is an inhibitor of phosphatidylinositol 3-kinase-related kinases (PIKK) such as ATM and ATR⁵⁰⁷ which represent key components of the DNA damage response network. 5 mM caffeine was added to p53-negative H1299 cells 45 min prior to etoposide treatment and this effectively blocked the accumulation of Cul7 protein (Figure 17A). Detection of threonine 68-phosphorylated CHK2 (Chk2-Thr68P), whose formation is a sign of efficient activation of CHK2 by ATM⁵⁰⁸, served to control for caffeine-mediated inhibition of ATM (Figure 17A). Similar results were obtained in the breast cancer cell line MCF-7 (Figure 17B). Here, abrogation of ATM/ATR signaling also interfered with stabilization of p53, as was expected⁵⁰⁹. In the absence of DNA damage, caffeine treatment had no significant effect on Cul7 expression level (data not shown). This excludes that other side-effects of this compound, such as the reported suppression of the proinflammatory cytokine TNF- α via the cyclic AMP/protein kinase A pathway⁵¹⁰, impinge on the expression of Cul7. Caffeine also prevented the increase of *Cul7* mRNA after DNA damage (Figure 17C). However, down-regulation of ATM and/or ATR by RNA interference using different siRNAs directed against each ATM and ATR had no obvious effect on the induction of Cul7 protein by DNA damage (data not shown). Caffeine has been demonstrated to affect other PIKK kinases besides ATM and ATR⁵⁰⁷. Therefore, other PIKK family members are presumably involved in the induction of *Cul7* mRNA and protein during the DNA damage response.

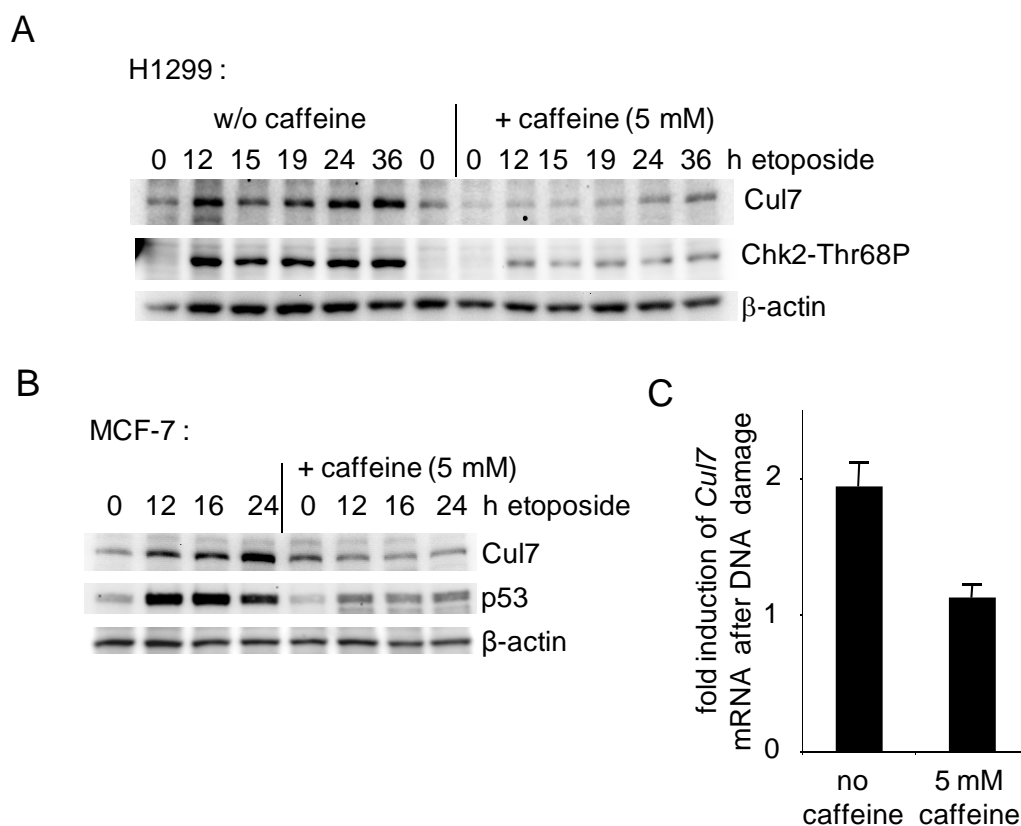


Figure 17. *Cul7* induction after DNA damage is caffeine-sensitive.

A, B Detection of *Cul7* protein in MCF-7 cells expressing wild type p53 and p53-deficient H1299 cells by Western blot analysis. Cells were treated for the indicated periods with 20 μ M etoposide alone or in combination with 5 mM caffeine. Caffeine was added 45 min prior to etoposide.

C, RT-qPCR analysis of *Cul7* mRNA levels after treatment of cells with etoposide. Cells were pre-treated with 5 mM caffeine 45 min prior to addition of 20 μ M etoposide for 14 hrs. The determination was performed in biological triplicates. Error bars represent standard deviations.

4.2.4 Increased p53 activity and G₁ arrest after knockdown of *Cul7*

In order to study the effect of *Cul7* knockdown on p53 activity, the pEMI (plasmid for Episomal MicroRNA expression) vector system⁴⁹³ for conditional microRNA expression was employed. This system was established in collaboration with my colleague Alexey Epanchintsev and allows the conditional knockdown of essential proteins. MCF-7 cell lines stably harboring pEMI constructs mediating the conditional expression of *Cul7*-specific microRNAs and mRFP from a bidirectional promoter, were generated via

limiting dilution. A cell line displaying homogenous induction of mRFP 48 hrs after addition of DOX to the medium is shown in Figure 18A. The maximum knockdown of Cul7 was detectable 3 days after induction of microRNA expression whereas a non-silencing microRNA had no effect on the level of Cul7 protein (Figure 18B).

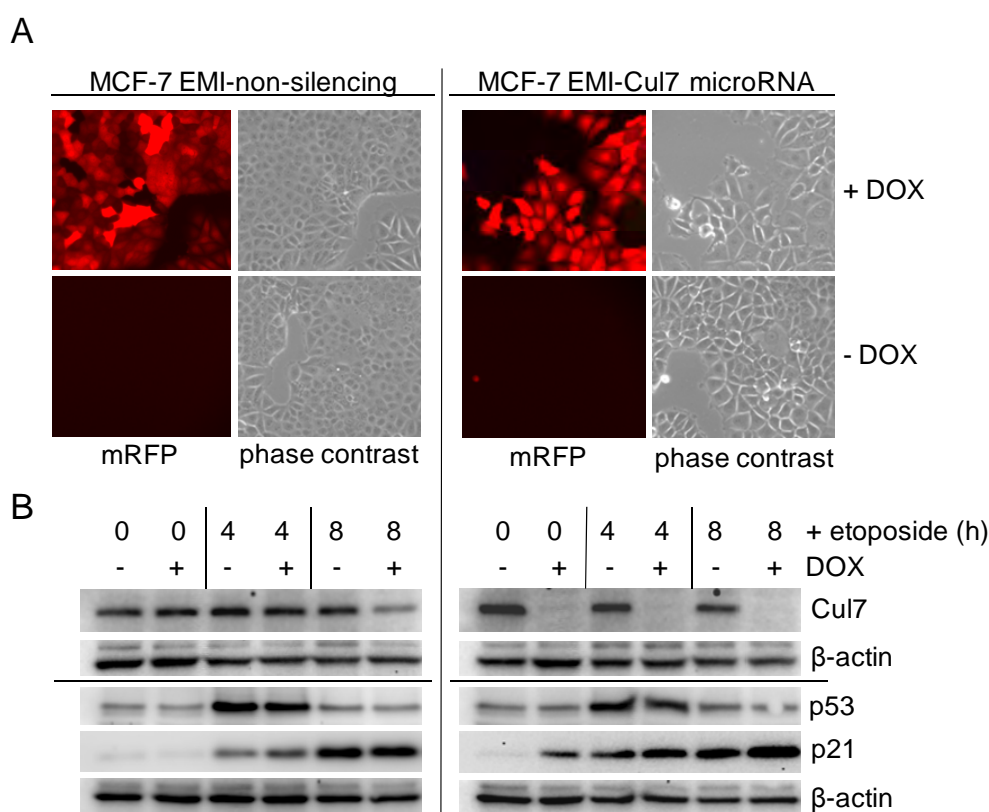


Figure 18. Effects of acute Cul7 knockdown

A, MCF-7 cell lines with inducible expression of mRFP and Cul7-microRNA (MCF-7-EMI-Cul7-microRNA) were compared to cells expressing a non-silencing microRNA (MCF-7-EMI-non-silencing). 72 hrs after addition of DOX (500 ng/ml) mRFP expression and cell morphology were analyzed by life cell microscopy (magnification 200x).

B, Down-regulation of Cul7 enhances transactivation of p21 by p53. Western blot analysis of Cul7, p53 and p21 protein levels in MCF-7 EMI-Cul7-microRNA cells and the control cell line MCF-7-EMI-non-silencing. 500 ng/ml DOX was added for 72 hrs and cells were treated with etoposide (20 μ M) for the indicated periods.

Interestingly, the p21 protein level increased as a consequence of pEMI-mediated Cul7 knockdown in untreated and in DNA damaged cells (Figure 18B). The amount of p53 protein was not significantly affected by the down-regulation of Cul7. Induction of a non-silencing microRNA in a control cell line did not affect p53 and p21 protein

expression (Figure 18B). The effect of Cul7 ablation on p21 expression was also observed with pools of U-2OS cells containing pEMI-vectors (Figure 19), thereby ruling out clonal effects.



Figure 19. Effects of conditional Cul7-knockdown in U-2OS cells

U-2OS cell pools with inducible expression of Cul7-microRNA (U-2OS EMI Cul7 miRNA) and cell pools expressing a non-silencing microRNA (U-2OS EMI Non-silencing) were treated with 100 ng/ml DOX for the indicated periods. Cul7, p21 and, for normalization, β -actin expression levels were analyzed by immunoblotting. d: days

After down-regulation of Cul7 by conditional microRNA expression, MCF-7 cells displayed an increase in size and showed an altered morphology which is indicative of a cell cycle arrest. This observation was in line with the induction of the CDK-inhibitor p21 after Cul7 ablation (Figure 18 and 19). The DNA content of these cell populations was analyzed by flow cytometry revealing that MCF-7 cells with a knockdown of Cul7 showed an increased fraction of cells in G_1 - and a decrease of cells in S-phase (Figure 20). When cells exhibiting a knockdown of Cul7 were treated with etoposide, an increase of cells arrested in the G_1 phase was obvious when compared to cells expressing a non-silencing microRNA. Cells without microRNA induction or cells expressing a non-silencing microRNA showed a more pronounced increase in the 4N DNA content after DNA damage which is indicative for a predominant G_2/M -arrest (Figure 20).

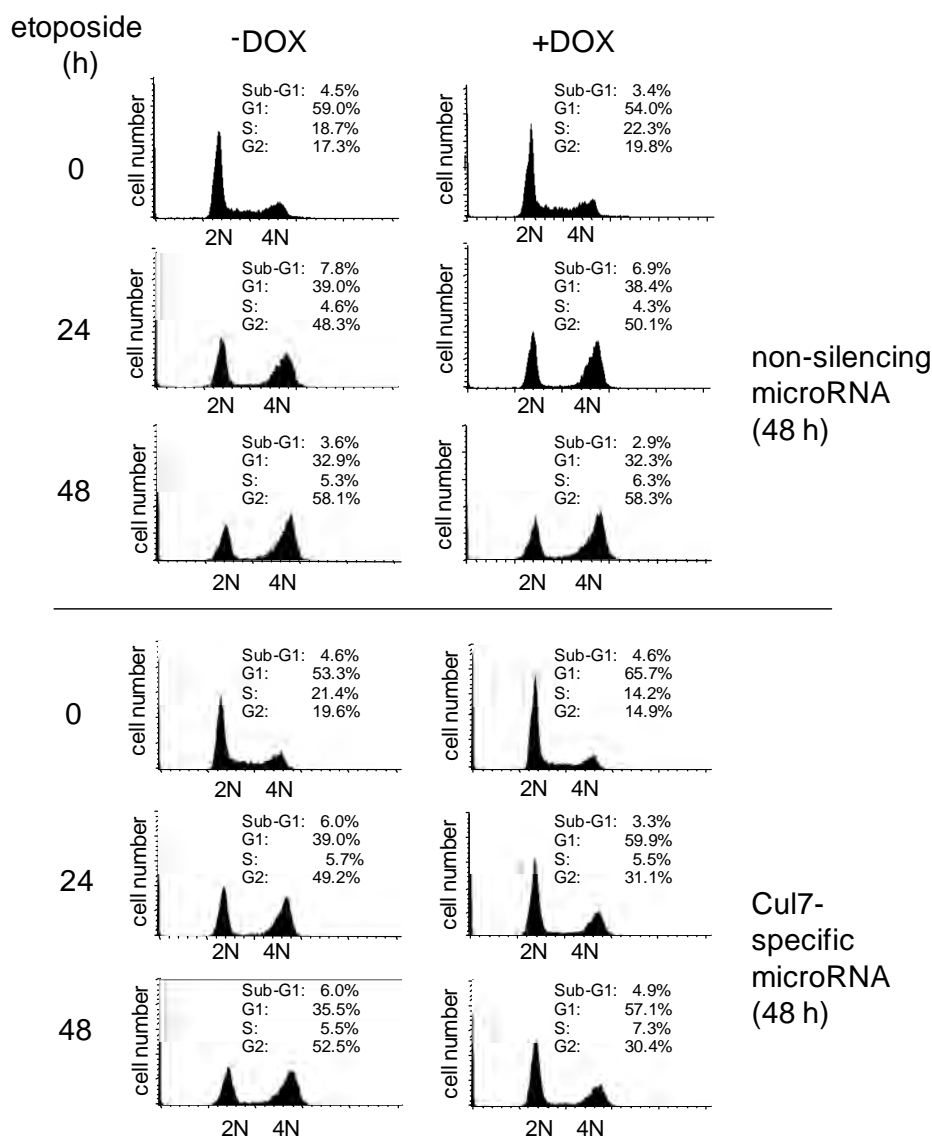


Figure 20. Cul7 ablation augments G₁ arrest in MCF-7 cells

DNA content analysis by flow cytometry after knockdown of Cul7 in MCF-7 cells. Cells were treated with 500 ng/ml DOX for 72 hrs. DNA damage was induced by addition of etoposide (20 μ M). MCF-7 cells with and without induction of Cul7-specific or a non-silencing microRNA were treated with etoposide for the indicated periods. The experiment was repeated twice and representative results are provided. The given %-cell cycle distributions are average results of two independent experiments. 2N: G₁ phase, 4N: G₂/M phase.

To test whether the effects of Cul7 down-regulation were dependent on p53 activity, MCF-7-pEMI-Cul7-microRNA cells were transfected with p53-specific or non-silencing short interfering RNAs (siRNAs) prior to induction of a Cul7-specific microRNA (Figure 21A). The down-regulation of p53, though incomplete, partially rescued the

effect of Cul7 knockdown as indicated by an increased proportion of cells that were arrested in G₂/M and a decrease of cells arrested in G₁ after DNA damage when compared to the control experiment performed with cells transfected with a non-silencing siRNA (Figure 21B). Taken together, these results show that Cul7 limits the activity of the tumor suppressor protein p53.

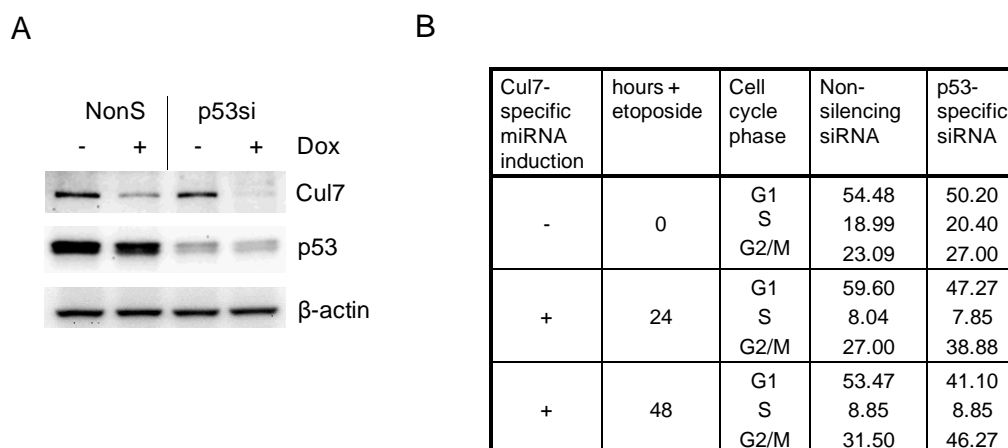


Figure 21. p53 knockdown rescues the effect of Cul7 ablation on the DNA damage response.

A, Concomitant knockdown of Cul7 and p53 in MCF-7 cells. MCF-7 EMI-Cul7-microRNA cell line was transfected with p53-specific (p53si) or non-silencing (NonS) siRNAs. 20 hrs later, Cul7 knockdown was induced by addition of DOX for 72 hrs. Cul7, p53 and, as a control for equal loading, β -actin protein levels were analyzed by Western blotting.

B, DNA content analysis by flow cytometry after Cul7 and p53 knockdown in MCF-7 cells. The MCF-7-EMI-Cul7-microRNA cell line was transfected with p53-specific or non-silencing siRNAs. 20 hrs later, Cul7 knockdown was induced by addition of 500 ng/ml DOX 48 hrs prior to etoposide treatment for the indicated periods. The %-cell cycle distributions are average results of three independent experiments.

4.2.5 Ectopic expression of Cul7 inhibits p53 function

Since the *Cul7* mRNA and protein levels increased in response to DNA damage, the consequences of ectopic Cul7 expression on endogenous p53 and p21 protein levels were studied. For this purpose, MCF-7 cells stably expressing Cul7 under control of the pRTS-1 episomal vector system were generated. Induction of ectopic Cul7 expression by addition of DOX inhibited the increase of p53 and p21 levels after etoposide treatment (Figure 22A), whereas treatment of a control cell line with DOX did not influence p53 and p21 expression (Figure 22B). In line with this observation, co-expression of Cul7 led

to a reduction in p53 transactivation activity by ~30% in a transient reporter assay performed in p53-deficient HCT116 cells (Figure 22C).

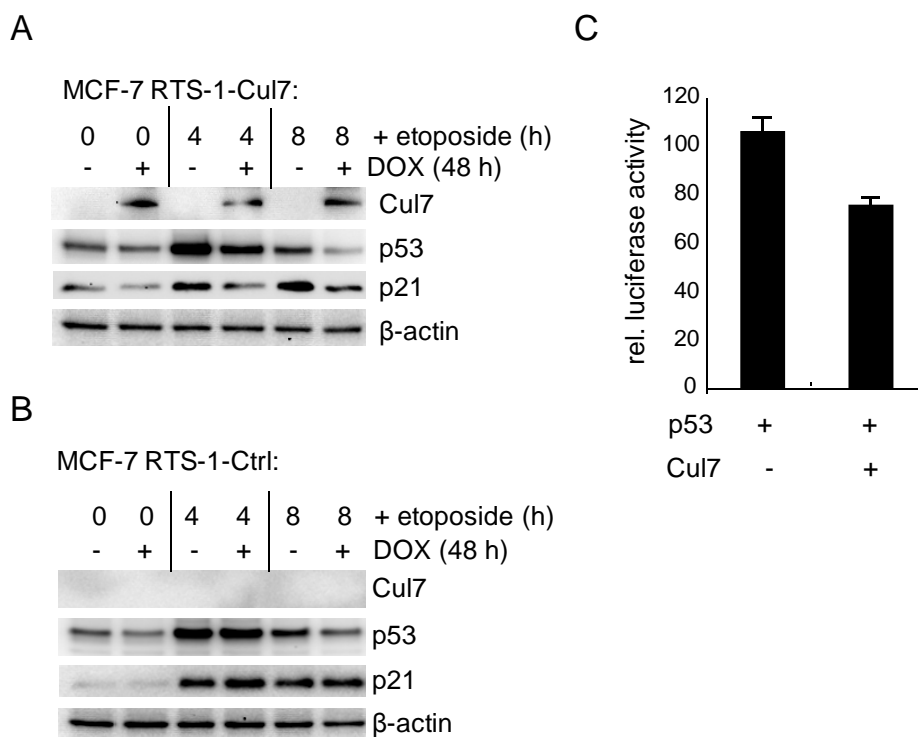


Figure 22. p53 accumulation and activity is inhibited by Cul7.

A, Western blot analysis of MCF-7 cells stably transfected with a pRTS-1 episomal expression vector encoding Flag-Cul7 or **B**, pRTS-1-Luciferase (pRTS-1-Ctrl) vector. Cul7 expression was induced by addition of 500 ng/ml DOX for 48 hrs. Cells were treated with etoposide (20 μM) for the indicated periods.

C, Transient reporter assay using HCT116 p53^{-/-} cells transfected with wild-type p53 (wt), BDS2x3 reporter plasmid with 3 tandem arranged p53 binding sites derived from the 14-3-3σ promoter and Cul7 expression plasmids or equimolar amounts of vector controls. Relative luciferase activity is depicted as the fold induction normalized to *renilla* luciferase activity.

Next, the biological consequences of the reduced p53 activity observed after ectopic expression of Cul7 was studied in cells exposed to genotoxic drugs. When MCF-7 cells ectopically expressing Cul7 were treated with the DNA damaging agent adriamycin, a topoisomerase II inhibitor, the presence of ectopic Cul7 provoked an increase in apoptosis as early as 24 hrs after addition of adriamycin (Figure 23A,B). This effect presumably resulted from an inability of cells to stably arrest due to impaired p53/p21 signaling (Figure 22A). Taken together, the presented results imply that Cul7 modulates the stabilization and function of p53 during the DNA damage response.

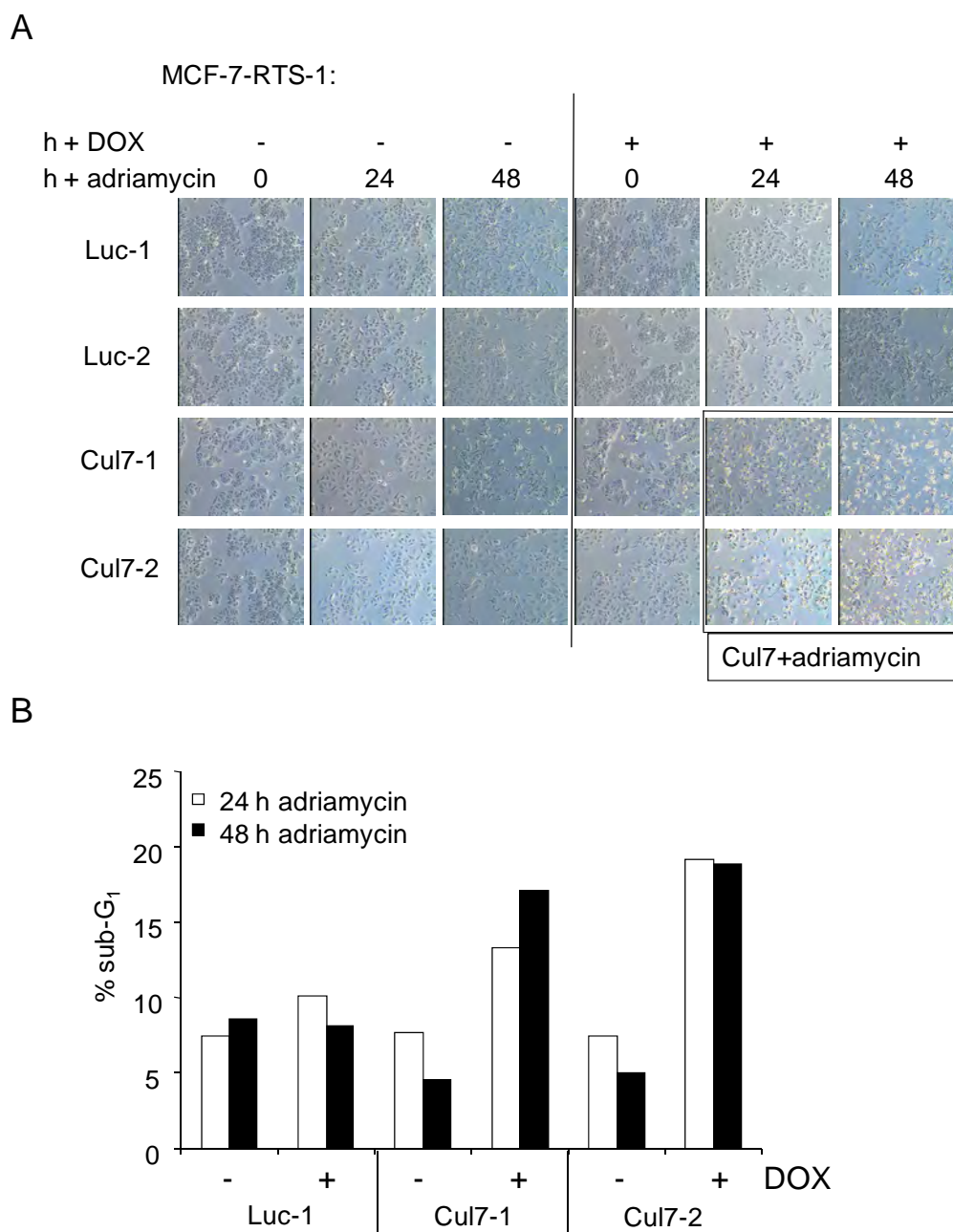


Figure 23. Cul7 sensitizes MCF-7 cells to genotoxic drugs

A, Analysis of MCF-7 cells stably transfected with pRTS-1-Flag-Cul7 (cell lines Cul7-1 and Cul7-2) or pRTS-1-Luciferase (Luc-1 and Luc-2) by microscopy. Cells were induced with 1 μ g/ml DOX for 30 hrs prior to treatment of cells with adriamycin for the indicated periods.

B, Determination of the sub-G₁ fraction (equivalent to apoptotic cell fraction) of MCF-7-RTS-1 cell lines by flow cytometry. Cells were induced with 1 μ g/ml DOX 30 hrs prior to treatment with adriamycin for the indicated periods. Luc-1: MCF-7-RTS1-Luciferase cell line. Cul7-1 and Cul7-2: MCF-7 cell lines stably transfected with pRTS-1-Flag-Cul7.

4.2.6 Cul7/Fbx29 does not exhibit E3-ligase activity towards p53

The SCF7 E3-ligase complex contains the F-box protein Fbx29⁴⁸³, which recruits the substrates for ubiquitination. For that reason it was analyzed whether Fbx29 is able to form a ternary complex with p53 and Cul7. In a co-precipitation approach with ectopically expressed proteins performed in H1299 cells, p53 associated with Fbx29 in a Cul7-dependent manner (Figure 24). Similar results were obtained for endogenous p53 in MCF-7 cells ectopically expressing Cul7 and Fbx29 (data not shown). Furthermore, ectopic Fbx29 was co-precipitated with p53 in a Cul7-dependent manner (data not shown).

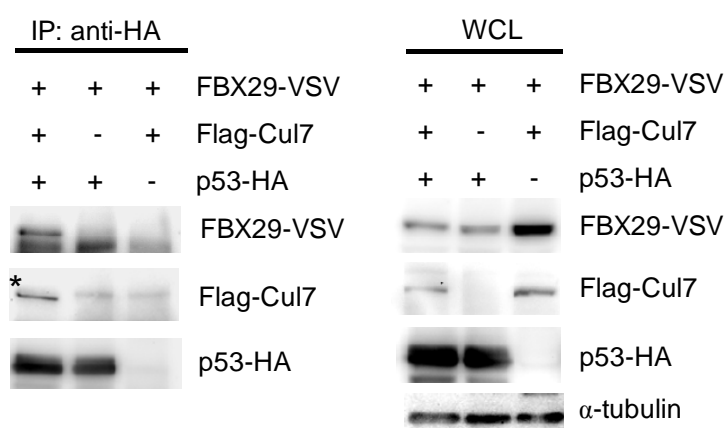


Figure 24. Cul7 recruits Fbx29 to p53

H1299 cells were transfected with plasmids encoding epitope-tagged versions of p53, Cul7, and Fbx29 as indicated. Western blot analysis of whole cell extracts (WCL) and immunoprecipitates (IP; obtained with a HA-specific antibody) using antibodies specific for Flag-, HA-, or VSV-tags. For WCL, expression of α -tubulin served as a loading control. * specific signal for Flag-tagged Cul7.

This experiment was performed by Dr. Berlinda Verdoodt.

In line with the inability of p53 to directly associate with Fbx29, p53 does not serve as a substrate for Cul7/Fbx29-mediated ubiquitination/degradation: ectopic expression of Cul7 in combination with Fbx29 did not promote ubiquitination of p53 *in vivo*

(Figure 25). The same result was obtained when MG132 was added (data not shown). This compound inhibits the proteasomal activity and enhances the sensitivity of the *in vivo* ubiquitination assay. As a positive control, the E3-ligase MDM2 was co-expressed which, as expected, led to an efficient mono- and poly-ubiquitination of p53 (Figure 25). These results suggest that other mechanisms than increased ubiquitination and subsequent proteasomal degradation are responsible for the inhibition of p53 by Cul7.

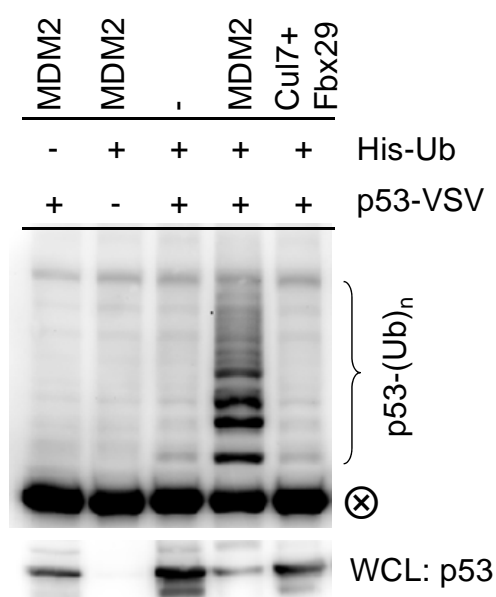


Figure 25. *In vivo* ubiquitination assay for p53 in H1299 cells.

Cells were transfected with pMT107 (His-tagged ubiquitin⁴⁸⁵), pcDNA3-p53-VSV, and plasmids expressing MDM2 or Fbx29 + Cul7, as indicated. ⊗: background signal originating from anti-VSV antibody. Bottom: Western blot analysis of whole cell lysate using p53 antibody (DO-1).

This experiment was performed by Dr. Berlinda Verdoodt essentially as described in⁵¹¹

5 Results II

5.1 AP4: a c-MYC inducible repressor of *p21*

5.1.1 Episomal, conditional expression of ectopic c-MYC in MCF-7 breast cancer cells

In order to identify genes which are regulated by c-MYC in breast epithelial cells, a MCF-7 breast carcinoma cell line stably expressing a doxycycline (DOX) -inducible c-MYC allele was generated using a recently described EBV-based vector system. The plasmid pRTS-1⁴⁷⁸ contains all elements for tetracycline-regulated gene expression and episomal propagation (Figure 26A). The Tet Repressor-KRAB fusion protein (tetR B/E-KRAB) provides tight repression in the absence of DOX⁵¹². In the presence of DOX the optimized transcriptional activator (rtTA2s-M2)⁵¹³ transactivates a bidirectional promoter which drives *mRFP* (monomeric red fluorescent protein⁵¹⁴) and c-MYC gene expression.

After transfection with a pRTS-1 vector encoding c-MYC, several MCF-7 breast cancer cell lines showing tight regulation of the *mRFP* and c-MYC alleles by DOX were obtained by limiting dilution. One of these clones showed a very rapid and almost homogeneous inducibility of ectopic c-MYC and was therefore chosen for further analysis (MCF-7-PJMMR1). As detected by Western blot analysis, an increase of ectopic c-MYC protein was detected as early as 6 hrs after addition of 1 µg/ml DOX (Figure 26B). After serum starvation (0.05% FBS), endogenous c-MYC was hardly detectable via indirect immunofluorescence (Figure 26C). Addition of DOX for 48 hrs led to a strong induction of ectopic c-MYC along with the fluorescent marker gene *mRFP*. As expected, the over-expressed c-MYC protein localized exclusively to the nucleus (Fig. 26C). The enhanced rtTA2s-M2 transactivator furthermore gives rise to a rapid and homogeneous induction of c-MYC leading to a high percentage of cells having a significant expression of ectopic c-MYC early after treatment with DOX (data not shown). This characteristic was an essential prerequisite for studying genes directly regulated by c-MYC in this cellular system.

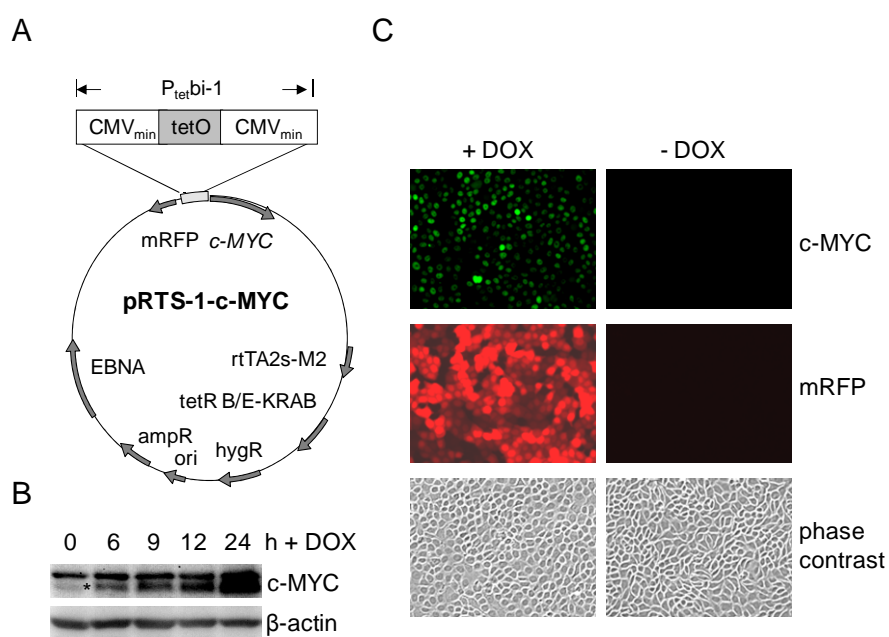


Figure 26. Conditional expression of c-MYC in MCF-7 breast cancer cells

A, Schematic representation of the c-MYC encoding plasmid pRTS-1-c-MYC. The episomal plasmid pRTS-1 allows the stringent regulation of gene expression due to the combined expression of a Tet Repressor-KRAB fusion protein (tetR B/E-KRAB) and a doxycycline-sensitive reversed tetracycline-controlled transcription activator (rtTA2s-M2). The bidirectional promoter $P_{tet,bi-1}$ drives conditional expression of a *mRFP* marker gene along with *c-MYC* expression. EBNA: Epstein Barr virus nuclear antigen 1, tetO: tetracycline responsive element, mRFP: monomeric red fluorescence protein.

B, Western blot analysis of c-MYC protein. MCF-7-PJMMR1 cells were maintained in complete medium and 1 $\mu\text{g/ml}$ doxycycline was added for different periods after pre-treatment of cells with ICI182,780/Fulvestrant (ICI) for 60 hrs. Total protein lysates were subjected to Western blot analysis and immunostained using antibodies directed against c-MYC (sc-764, Santa Cruz) and, as a loading control, β -actin. *specific signal representing c-MYC protein.

C, Indirect immunofluorescence detection of c-MYC in MCF-7-PJMMR1 cell line. Cells were treated with 1 $\mu\text{g/ml}$ doxycycline for 48 hrs subsequent to 36 hrs serum starvation (0.05% FBS). Immunostaining of c-MYC protein was done using a c-MYC antibody (sc-764, Santa Cruz) followed by anti-rabbit FITC antibody to visualize nuclear protein localization.

5.1.2 Characterization of MCF-7-PJMMR1 cell line

As a hormone-dependent cell line, MCF-7 serves as a model system for studying consequences of *c-MYC* over-expression in estrogen receptor (ER) positive breast cancer disease. For this kind of breast cancer, hormonal therapy turned out to be a very beneficial treatment. One downstream mechanism responsible for the anti-proliferative effect of the anti-estrogen ICI182,780/Fulvestrant (ICI) is a marked down-regulation of

the ER target gene *c-MYC*⁵¹⁵. Here, *c-MYC* levels also decreased upon ICI-treatment of MCF-7 cells (Figure 27A). The reduction of endogenous *c-MYC* protein due to ICI-treatment was accompanied by a cell cycle arrest in the G₁/G₀ phase (Figure 27B). Activation of ectopic *c-MYC* by addition of DOX induced re-entry into S phase in the presence of ICI (Figure 27B). The proportion of cells in S-phase increased from 9% to 25% as early as 24 hrs after induction of *c-MYC* and this was accompanied by an increase of cells in the G₂ phase. Two days after induction of ectopic *c-MYC*, the cell cycle profile resembled exponentially proliferating MCF-7 cells. Ectopic *c-MYC* was also able to promote entry into S-phase in serum-deprived MCF-7-PJMMR1 cells, though to a minor extent (data not shown).

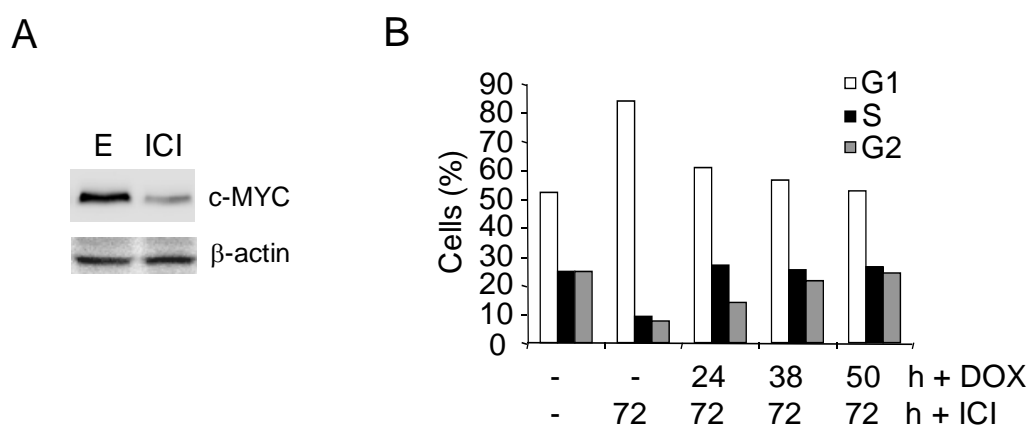


Figure 27. *c-MYC* triggers G₁/S progression in ICI-arrested MCF-7 cells.

A, *c-MYC* downregulation in response to ICI182,780 (ICI) treatment. MCF-7 cells were treated with 1 μ M ICI for 48 hrs and 72 hrs, respectively. Whole protein lysates were subjected to Western blot analyzes and immunostained with *c-MYC* and β -actin antibodies. E: exponentially proliferating cells, ICI: cells arrested by ICI treatment.

B, *c-MYC* triggers S phase re-entry in ICI-arrested MCF-7 cells. MCF-7-PJMMR1 cells grown in complete medium were treated with 1 μ g/ml ICI for 72 hrs. Untreated, exponentially proliferating cells served as a control. Ectopic expression of *c-MYC* was triggered by addition of 1 μ g/ml doxycycline for the indicated periods. DNA content of 5,000 cells was measured by flow cytometry, excluding cell doublets.

In order to determine, whether ectopic expression of *c-MYC* is able to antagonize the inhibition of proliferation by ICI (Figure 28A), ICI was added 30 hrs prior to addition of DOX. 48 hrs after treatment with DOX, the *c-MYC*-inducible MCF-7-PJMMR1 cell line showed proliferation in the presence of ICI to a similar degree as cells not arrested by addition of ICI (Figure 28A, left panel), whereas the control cell line MCF7-R1, which

only expresses mRFP after DOX treatment, did not respond with increased proliferation (Figure 28A, right panel). Furthermore, ectopic *c-MYC* reversed the increase in size and the changed morphology of ICI-arrested MCF-7 cells (Figure 28B). These results show that expression of ectopic *c-MYC* is sufficient to antagonize the anti-proliferative effects of ICI in all phases of the cell cycle.

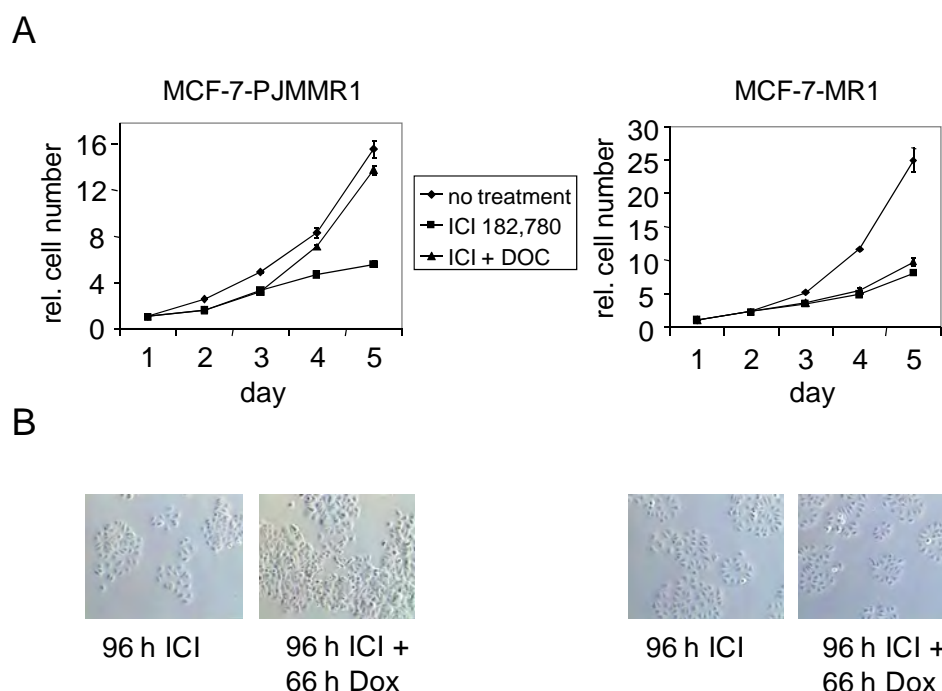


Figure 28. *c-MYC* promotes proliferation of ICI-arrested MCF-7 cells.

A, (left panel), Proliferation of MCF-7-PJMMR1 and **(right panel),** MCF-7-MR1 cells after pre-treatment with 1 μ M ICI for 30 hrs followed by induction with 1 μ g/ml DOX for the indicated periods. Cell number was determined using a cell counter (Beckmann Coulter) and the experiment was performed in biological triplicates. Error bars indicate standard deviations.

B, 96 hrs after ICI treatment, the morphology of MCF-7-PJMMR1 **(left panel)** and MCF-7-MR1 **(right panel)** cells with or without treatment with DOX for 66 hrs was analyzed by life cell microscopy (magnification: 200 \times).

5.1.3 *AP4* mRNA and protein expression is induced by *c-MYC*

In order to identify genes regulated by *c-MYC* in human epithelial cells, a triplicate microarray analysis 12 hrs after activation of an inducible *c-MYC* allele was performed in G_1 -arrested breast cancer cell line MCF-7 (data not shown). This approach revealed that *AP4* is amongst the 25 most highly induced genes upon *c-MYC* activation in a clinically

relevant scenario (data not shown) which is *c-MYC*-mediated alleviation of an ICI-mediated cell cycle arrest. Thereby, a 3.4-fold induction of *AP4* mRNA after *c-MYC* activation was observed (data not shown). The increase of *AP4* mRNA after *c-MYC* activation in this cell line was confirmed by real-time quantitative PCR (RT-qPCR) (Figure 29A) and also occurred on the protein level (Figure 29B). The magnitude of *AP4* mRNA induction 12 hrs after activation of *c-MYC* was similar to that of known *c-MYC* target genes, such as *MAD2*⁴⁵⁵, *Dyskerin (DKC)*⁵¹⁶ and *Prohibitin*³⁷⁰ (Figure 29C).

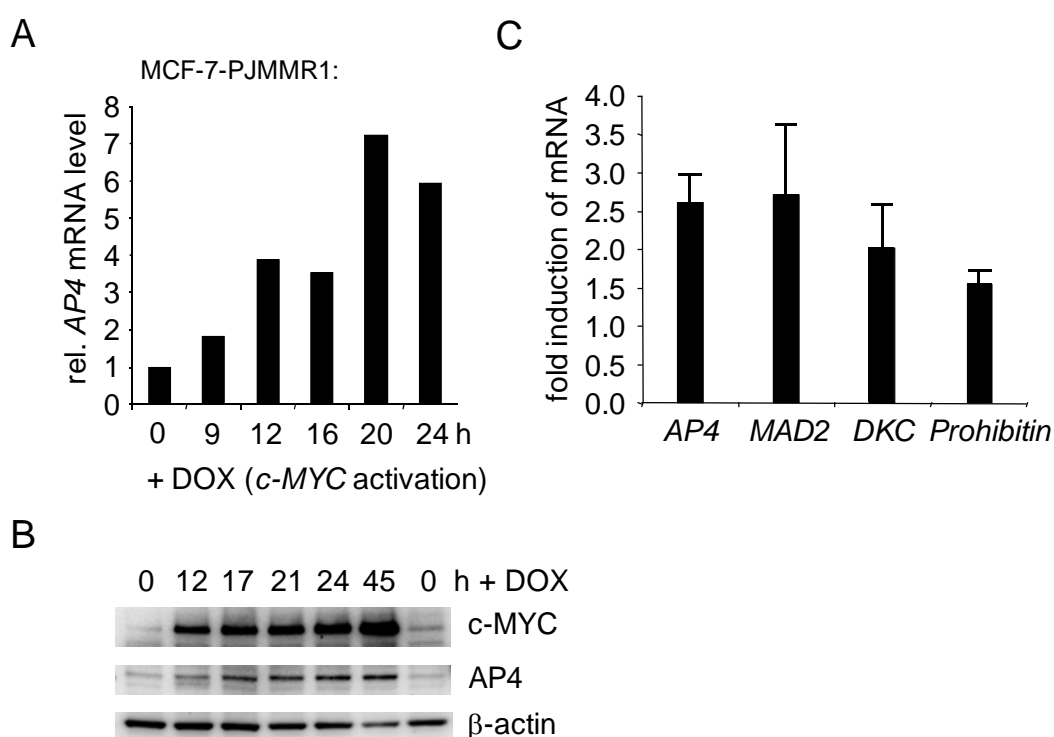


Figure 29. Induction of *AP4* mRNA and protein by *c-MYC* in MCF-7 cells

(A) Quantification of *AP4* mRNA after *c-MYC* activation. MCF-7-PJMMR1 cells were treated with ICI182,780 (ICI) for 60 hrs prior to *c-MYC* activation by addition of doxycycline (DOX) for the indicated periods and RNA was subjected to real-time quantitative PCR (RT-qPCR) analysis.

(B) *AP4* protein expression after *c-MYC* activation. Protein lysates were prepared at the indicated time-points. Expression of *c-MYC*, *AP4* and, as a control for equal loading, β -actin was detected by immunostaining.

(C) MCF-7-PJMMR1 cells were treated with ICI182,780 for 60 hrs followed by *c-MYC* induction by addition of DOX for 12 hrs. Expression of *AP4*, *MAD2*, *DKC* and *Prohibitin* was determined by RT-qPCR analysis and normalized to β -actin. Measurements were performed in triplicates. Error bars indicate standard deviations

AP4 mRNA and protein were also induced after activation of a c-MYC-ER (estrogen receptor) fusion protein³⁸⁴ in serum starved human diploid fibroblasts (HDF; Figure 30A,B). The ER domain used in this thesis has been rendered unresponsive to estrogen and responsive to 4-hydroxytamoxifen (4-OHT) by site directed mutagenesis⁵¹⁷. In the absence of 4-OHT, the c-MYC-ER fusion protein is held in a mainly cytoplasmic, latent form due to association with the chaperone HSP-90⁵¹⁸, while hormone addition leads to dissociation from this inhibitor and shuttling of c-MYC-ER to the nucleus. c-MYC-ER-mediated induction of *AP4* mRNA also occurred in the presence of the translation inhibitor cycloheximide (CHX) (Figure 30C), which was added 30 minutes prior to treatment of cells with 4-OHT for 6 hrs. In this case, cells were not serum-deprived but were grown to confluency for 48 hrs prior to 4-OHT treatment in order to down-regulate endogenous expression of c-MYC via contact inhibition⁵¹⁹. This shows that c-MYC was able to induce transcription of *AP4* in the absence of *de novo* protein biosynthesis suggesting that induction of *AP4* by c-MYC is presumably direct and not a consequence of cell cycle re-entry which occurs after activation of *c-MYC*. An increase of *AP4* expression was also observed in HDF immortalized by constitutive expression of c-MYC, but not in HDF immortalized by ectopic *htert* expression when compared to HDFs which had not been immortalized (Figure 30D).

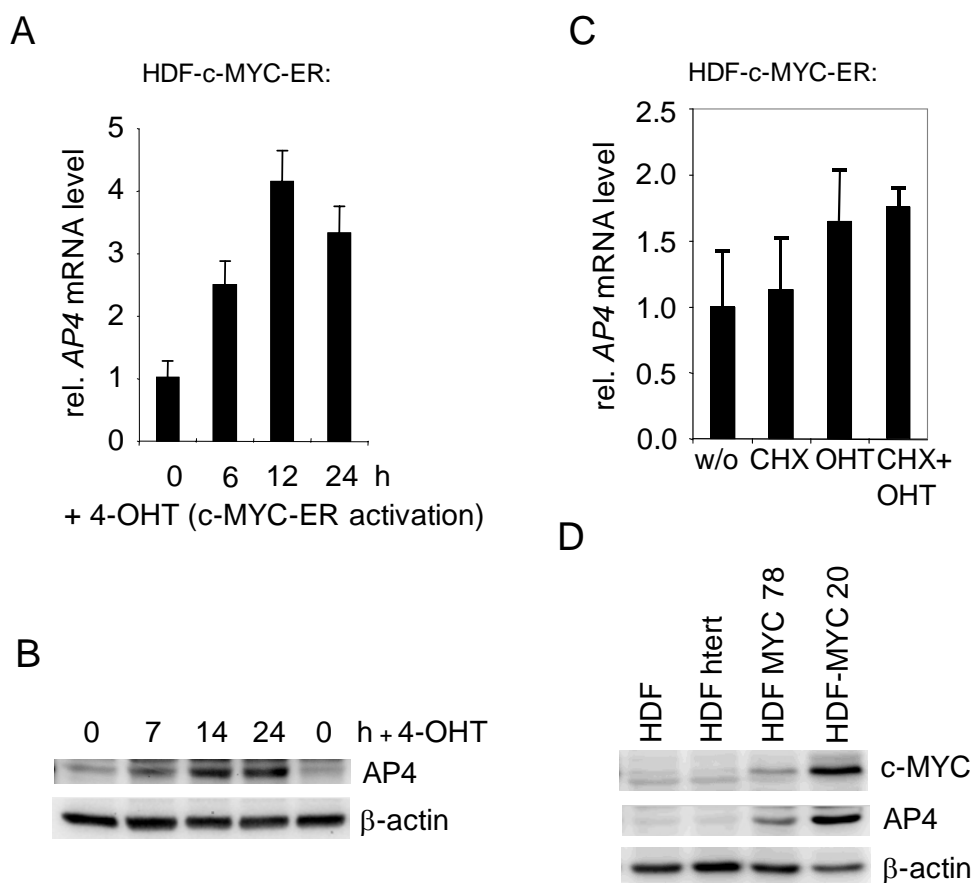


Figure 30. AP4 mRNA and protein expression is responsive to c-MYC in human diploid fibroblasts (HDF).

A, Quantification of AP4 mRNA after activation of c-MYC. HDF-c-MYC-ER cells were serum deprived for 48 hrs. After addition of 4-OHT, total RNA was isolated at the indicated time-points from biological triplicates. Expression of AP4 mRNA was determined by RT-qPCR analyses. Error bars indicate standard deviations.

B, AP4 protein expression after c-MYC activation. Protein lysates were prepared from HDF-c-MYC-ER cells at the indicated timepoints. Expression of AP4 and, as a control for equal loading, β -actin was determined by immunoblotting.

C, HDF-c-MYC-ER cells were grown to confluency and treated with either 4-OHT, cycloheximide (CHX) or CHX 30 min prior to treatment with 4-OHT for 6 hrs or left untreated (w/o). Expression of AP4 and, for normalization, β -actin mRNA was determined by RT-qPCR analysis. Measurements were performed in triplicates. Error bars indicate standard errors.

D, Expression of AP4 in human diploid fibroblasts (HDF) stably expressing an ectopic c-MYC allele (HDF c-MYC; 20, passage 20; 78, passage 78) compared to HDF (HDF) and HDF stably over-expressing htert (HDF htert). Protein lysates were prepared and expression of c-MYC, AP4 and β -actin was determined by immunoblotting.

5.1.4 *AP4* is an evolutionary conserved, direct c-MYC target gene

Next it was determined whether the induction of *AP4* mRNA and protein by c-MYC is conserved in other species. Therefore, a c-myc-ER fusion protein was activated by addition of 4-OHT in serum deprived RAT1 fibroblasts. Activation of c-myc-ER rapidly induced expression of *ap4* mRNA and protein (Figure 31A,B) indicating that *AP4* induction by c-MYC is evolutionary conserved.

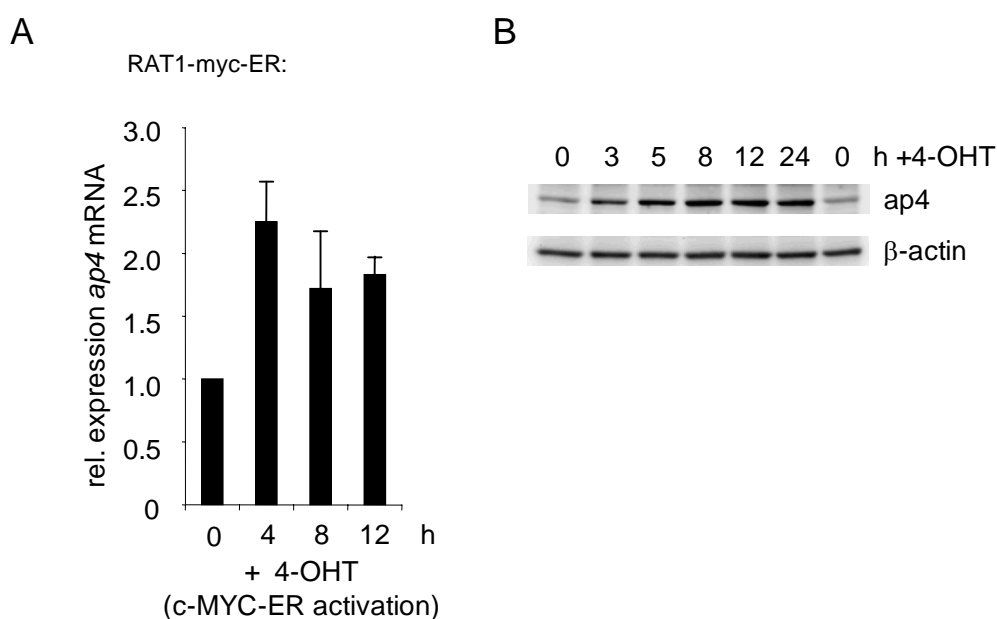


Figure 31. *AP4* is an evolutionary conserved c-MYC target gene

A, RAT1-myc-ER cells were serum deprived for 48 hrs. RNA was isolated at the indicated timepoints after treatment with 200 nM 4-OHT and analyzed for *ap4* expression by RT-qPCR analysis. *EF1 α* expression was used for normalization.

B, Analysis of *ap4* protein expression in serum deprived RAT-myc-ER cells after addition of 200 nM 4-OHT for the indicated periods by immunoblotting. β -actin expression served as a control for equal loading.

In line with these observations the first genomic intron of human *AP4* contains a cluster of four canonical c-MYC binding sites (CACGTG) two of which are conserved in the *ap4* genes of mouse and rat (Figure 32A).

Chromatin-immunoprecipitation (ChIP) allows to determine whether a given protein binds to or localizes to a specific DNA sequence. After *in vivo* cross-linking of chromatin-associated proteins to genomic DNA (gDNA), the gDNA is sheared to obtain fragments which are then isolated by immunoprecipitation using specific antibodies. Afterwards, crosslinking can be removed and the DNA can be analyzed by PCR or RT-qPCR to determine the enrichment of specific gDNA fragments.

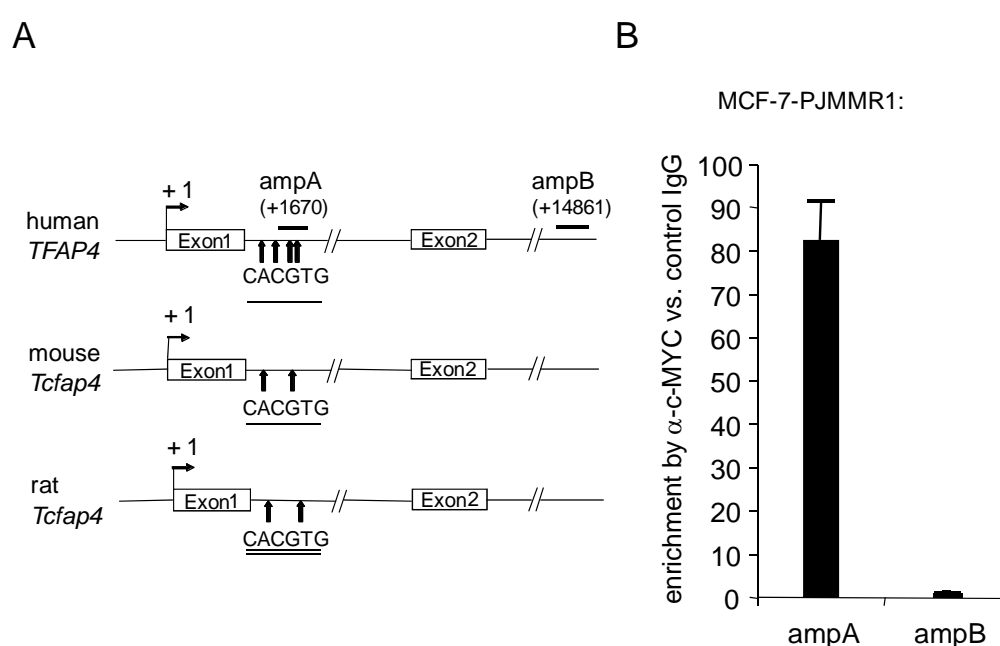


Figure 32. c-MYC binds to the first genomic intron of *AP4*

A, Comparison of the mouse, rat and human *AP4* promoter region. “+1” indicates the transcription start site. “amp” indicates PCR-amplicons used for qChIP analysis with their positions relative to the transcription start site. Arrows indicate the approximate positions of canonical c-MYC binding sites (CACGTG). The positions of these sites relative to the transcription start site (“+1”) are +660, +1262, +1645 and +1766 for human *AP4*, +560 and +1620 for the mouse *Tcfap4* and +666 and +1725 for the rat *Tcfap4*, respectively.

B, Detection of c-MYC at the *AP4* promoter. MCF-7-PJMMR1 cells were treated with doxycycline (DOX) for 12 hrs to achieve induction of ectopic c-MYC. Chromatin was cross-linked and subjected to qChIP analysis with c-MYC-specific and, as a control, rabbit IgG antibodies. RT-qPCR analysis was performed with primers flanking two of the four canonical E-boxes in the first *AP4* intron (“ampA”; see also Figure 31A) or a control primer pair (“ampB”) localized in the last intron of *AP4*. For normalization, a fragment from chromosome 16q22 not containing E-boxes was used. The experiment was performed in triplicates. Error bars indicate standard deviations.

In a quantitative chromatin immunoprecipitation (qChIP) analysis, precipitation with a c-MYC-specific antibody resulted in an enrichment of a DNA fragment (ampA) containing two of the four E-boxes in the first intron of *AP4*, whereas a DNA fragment (ampB) located ~13 kbp downstream of the transcriptional start site in intron 6 of *AP4* was not enriched (Figure 32A,B). This result demonstrates that c-MYC localizes to the first intron of *AP4*. Together with results described above, these findings provide strong evidence that c-MYC directly induces transcription of the *AP4* gene.

5.1.5 Induction of AP4 contributes to cell cycle progression

To determine whether induction of *AP4* is necessary for c-MYC-mediated S-phase entry, *AP4* expression was down-regulated by *AP4*-specific siRNAs. In cells transfected with non-silencing small interfering RNAs (siRNAs), *c-MYC* activation for 22 hrs increased the fraction of cells in S-phase from ~7% to ~16% in the presence of ICI (Figure 33A). Interestingly, siRNA-mediated down-regulation of *AP4* significantly decreased the proportion of cells re-entering the cell cycle after *c-MYC* activation (Figure 33A). Therefore, the induction of *AP4* contributes to the c-MYC-mediated cell cycle re-entry in the presence of ICI.

As the CDK inhibitor p21 is known to mediate the G₁-arrest induced by ICI⁵²⁰, it was analyzed next whether the expression of p21 can be modulated by *AP4*. Indeed, down-regulation of *AP4* by RNA interference using two siRNAs targeting different regions of the *AP4* mRNA resulted in an increased p21 protein level in MCF-7 cells (Figure 33B) when compared to cells transfected with a non-silencing control siRNA. This finding suggests that the elevated p21 level caused the negative effect of *AP4* knockdown on c-MYC-mediated cell cycle re-entry. Induction of *AP4* by c-MYC is therefore presumably necessary for c-MYC to promote efficient cell-cycle re-entry of MCF-7 cells in the presence of ICI.

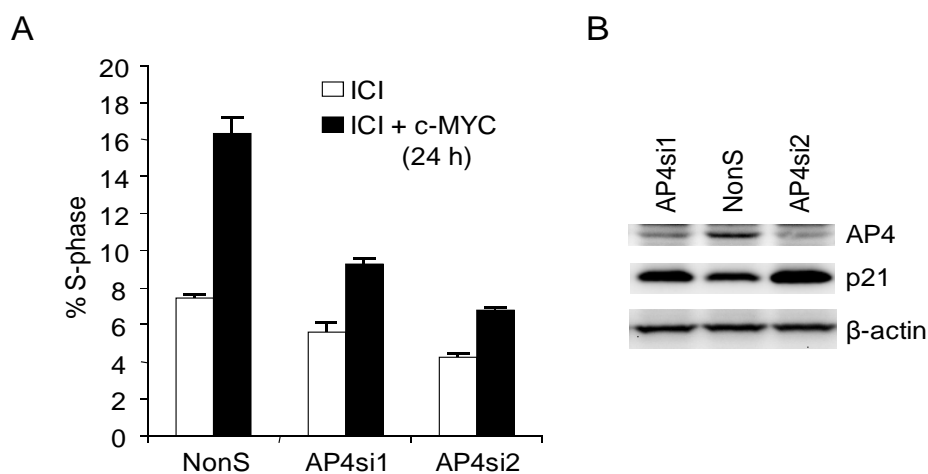


Figure 33. Requirement of AP4 induction for c-MYC-mediated cell cycle re-entry

A, Flow cytometric analysis of ICI182,780 (ICI) treated MCF-7-PJMMR cells after siRNA mediated down-regulation of *AP4*. *c-MYC* was activated by addition of DOX for 22 hrs. The depicted diagram shows the percentage of cells in S-phase after treatment with ICI alone or in combination with *c-MYC* over-expression (ICI+MYC). The experiment was performed in duplicates. The standard error is depicted.

B, MCF-7 cells were transfected with two different siRNAs targeting *AP4* or a non-silencing control siRNA (NonS). Expression of *AP4*, *p21* and, as a control for equal loading, β -actin was detected by immunoblot analysis.

Serum-restimulation of arrested (0.05 % FBS) MCF-7 cells rapidly induced the expression of endogenous *c-MYC* followed by an increase of *AP4*, whereas expression of *p21* strongly declined (Figure 34A). siRNA-mediated down-regulation of *AP4* increased *p21* levels and prevented repression of *p21* after serum addition (Figure 34B). Taken together, these results suggest, that the induction of *AP4* by *c-MYC* is required for the down-regulation of *p21* expression which occurs when MCF-7 cells re-enter the cell cycle after mitogenic stimulation.

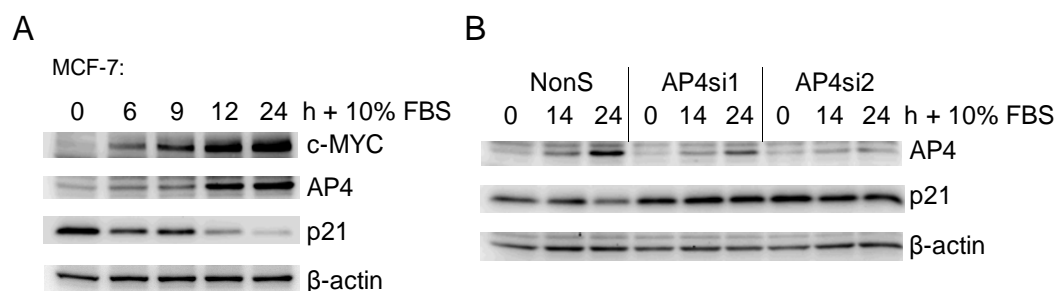


Figure 34. Requirement of AP4 induction for mitogen-mediated repression of p21

A, MCF-7 cells were serum deprived (0.05% FBS) for 48 hrs, re-stimulated with 10% serum for the indicated periods and analyzed by immunoblotting for expression of AP4, p21 and, as a control for equal loading, β-actin.

B, MCF-7 cells were transfected with siRNAs targeting AP4 (AP4si1 and AP4si2) or a non-silencing siRNA (NonS). 36 hrs later cells were serum starved for 30 hrs. After restimulation with 10% FBS-containing medium for the indicated periods, cell lysates were subjected to immunoblot analysis.

5.1.6 AP4 represses p21 mRNA and protein

The previous observations suggested that AP4 may directly regulate the expression of p21. Therefore, it was tested whether ectopic expression of AP4 is sufficient to down-regulate the expression of p21 in pools of U-2OS cells expressing *AP4* from an inducible episomal vector. Already 9 hrs after induction of ectopic *AP4* expression, p21 protein levels began to decrease and were almost undetectable by 24 hrs (Figure 35A), whereas addition of DOX did not affect expression of p21 in cells harboring an empty episomal vector (Figure 35B). Moreover, expression of *p21* mRNA decreased after activation of AP4 (Figure 35C). This indicates that the down-regulation of p21 by AP4 might be mediated through direct repression of the *p21* gene. In line with these data, conditional expression of two different microRNAs (miRNA) directed against the *AP4* mRNA using a recently described episomal vector system (pEMI⁴⁹³) led to an accumulation of p21 protein (Figure 35D). This result is in agreement with the elevation of p21 expression observed after transfection of *AP4*-specific siRNAs (Figure 33B). Induction of a non-silencing miRNA had no effect on p21 expression levels (Figure 35D).

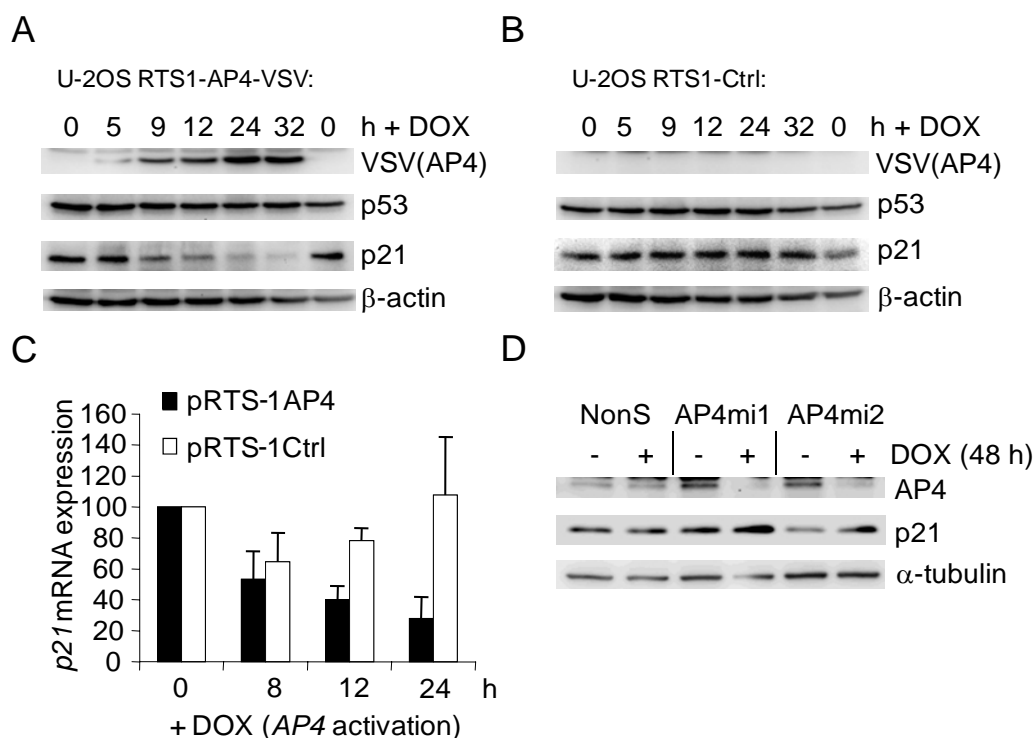


Figure 35. AP4 downregulates *p21* mRNA and protein

A, Expression levels of AP4-VSV, p53, p21 and β -actin proteins were detected by immunoblot analysis after induction of a conditional AP4 allele in U-2OS cells.

B, U-2OS cells harboring an empty pRTS-1 vector were subjected to the same analysis.

C, Quantification of *p21* mRNA after activation of AP4 in U-2OS cells by RT-qPCR analysis. Expression of *p21* was normalized to β -actin mRNA expression.

D, Expression levels of AP4, p21 and α -tubulin proteins were determined by immunoblot analysis after induction of two different microRNAs targeting AP4 mRNA (AP4mi1 and AP4mi2) or a non-silencing control miRNA (NonS) in U-2OS cells.

The expression of *p21* is regulated by p53-dependent and -independent mechanisms⁵²¹. Besides p53, other factors as e.g. IRF-1 have been shown to induce p21 after DNA damage in a p53-independent manner⁵²². Therefore, p53-deficient cells still show a minor induction of p21 after DNA damage⁵⁰¹. Infection of p53-deficient HCT116 colorectal cells with an adenovirus encoding AP4 decreased basal p21 levels and prevented the p53-independent induction of p21 following DNA damage, whereas a control virus had no significant effect on p21 (Figure 36). These results imply that the repression of *p21* expression by AP4 occurs via a p53-independent mechanism.

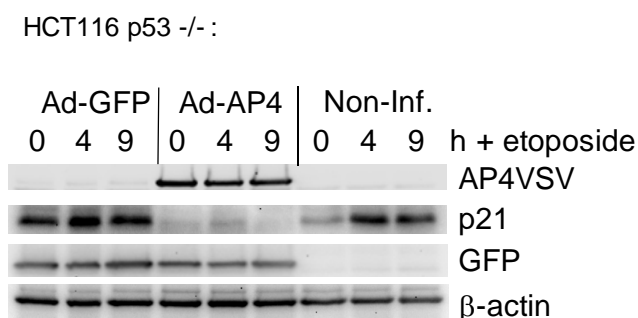


Figure 36. AP4 mediated reduction of p21 is independent of p53 activity

p53-deficient HCT116 colon cancer cells were infected with the indicated viruses or were left uninfected (Non-Inf.) for 24 hrs and etoposide was added for the specified times. Cellular extracts were subjected to immunoblot analysis with antibodies against VSV, GFP, p21 and , as a control for equal loading, β -actin.

5.1.7 AP4 occupies E-box sequences in the *p21* promoter

Interestingly, the *p21* promoter contains 4 putative AP4-binding motifs in the vicinity of its transcriptional start site (Figure 37A). By qChIP analysis it was confirmed that AP4 occupies this region of the *p21* promoter *in vivo* (Figure 37A,B): U-2OS cell pools were either treated with DOX for 16 hrs in order to induce expression of ectopic AP4-VSV or were left untreated. Upon DOX treatment, precipitation with a VSV-specific antibody resulted in an enrichment of a DNA fragment (ampC) containing one of the four E-boxes (CAGCTG) in the proximal *p21* promoter, whereas a DNA fragment (ampD) located ~2.2 kbp downstream of the transcriptional start site in intron 1 of *p21* was not enriched (Figure 37A,B). In the absence of AP4-VSV expression, no enrichment of ampC or ampD was detectable (Figure 37A,B). To determine the relevance of the CAGCTG motifs in the *p21* promoter region for AP4-mediated repression of *p21*, transient reporter assays in H1299 cells were performed using *p21* promoter constructs which harbor different combinations of wild type or mutated AP4 binding sites (Figure 38A).

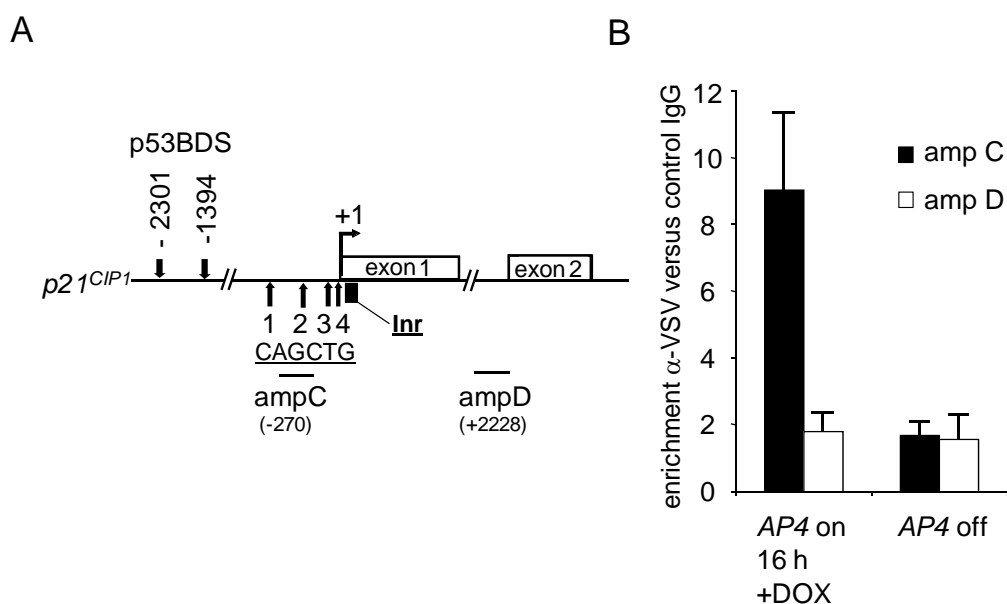


Figure 37. AP4 binds to the p21 promoter *in vivo*

A, The proximal promoter region of the human *p21* gene contains four AP4 binding sites (CAGCTG). “+1” indicates the transcription start site. “amp”: PCR-amplicons used for qChIP analysis with their position relative to the transcription start site. p53 binding sites (p53BDS) and their positions are indicated. The approximate positions of 4 putative AP4 binding sites (arrows) and the initiator (Inr) element (TCAGTTCCT) (filled square) are indicated and their precise positions relative to the transcription start site of *p21* is depicted in Figure 38A.

B, qChIP analysis of AP4 at the *p21* promoter. AP4 was induced by addition of DOX for 16 hrs in U-2OS RTS1-AP4 cells. Genomic DNA co-precipitated with anti-VSV or, as a control, mouse IgG antibody was analyzed by RT-qPCR. For normalization a fragment on chromosome 16q22 not containing E-boxes was used.

While AP4 expression dramatically reduced the activity of a wild type *p21* reporter construct, mutation of the two proximal AP4 binding sites A3 and A4 was sufficient to largely alleviate the repressive effects of AP4 (Figure 38B). Mutation of one or two additional AP4 binding sites further abolished the repressive effect of AP4. Therefore, binding of AP4 to the E-box motifs is essential for the repression of *p21* by AP4. Since removal of two motifs relieved the repression in a non-linear fashion, the 4 AP4 binding sites presumably act synergistically. Alternatively, the proximity of the sites A3 and A4 to the transcriptional start site (+1) may allow AP4 to directly block the access of the RNA-polymerase II complex to the *p21* promoter.

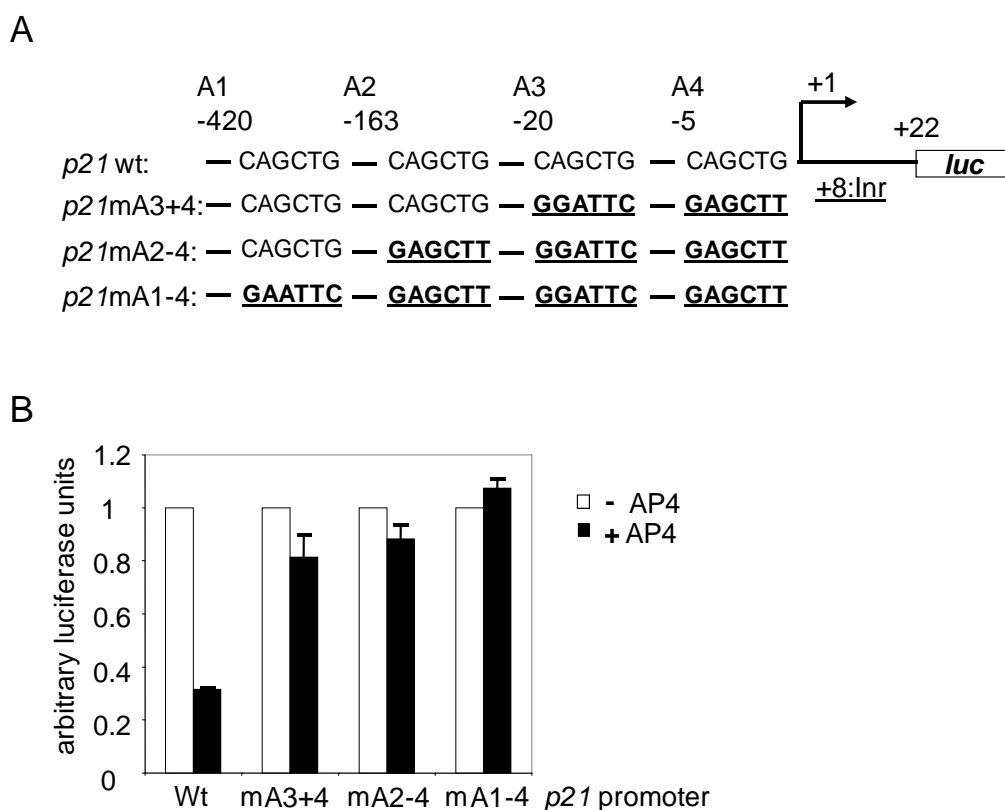


Figure 38. AP4 represses *p21* by binding to E-boxes

A, Schematic presentation of putative AP4 binding sites (A1-A4) and their precise position in the *p21* promoter region relative to the transcriptional start site (+1). Wild type and mutant *p21* promoter constructs used in transient reporter assays are depicted. Mutated AP4 binding sites are represented in bold and underlined. The Inr element (TCAGTTCCT) localizes to position +8 to +16 relative to the transcriptional start site (“+1”). *luc*: ORF encoding the firefly luciferase.

B, Determination of *p21* reporter activity in H1299 cells transfected with plasmids encoding the indicated cDNAs. Cells were transfected with 600 ng of wild type or the indicated mutant *p21* reporter plasmids, 20 ng of pcDNA3-AP4-VSV plasmid or equimolar amounts of pcDNA3-VSV backbone. Shown are the median expression values and standard errors of two independent transfection experiments. Wt, mA3+4, mA2-4 and mA1-4: reporter plasmids encoding for the *p21* promoter sequence with wild type or mutated AP4 binding sites 3+4, 2-4 or 1-4 (see also Figure 38A).

5.1.8 AP4 interferes with the DNA damage/p53/p21 pathway

Since the protein product of *p21* represents a central mediator of cell cycle regulation by the tumor suppressor protein p53, the potential involvement of AP4 in the DNA damage response was studied. Treatment of MCF-7 cells with the topoisomerase II

inhibitor etoposide reduced c-MYC and AP4 protein levels, while p53 and p21 levels were increased after DNA damage (Figure 39A). The down-regulation of AP4, which was presumably caused by the decrease in c-MYC expression, may be a prerequisite for the induction of *p21* by p53 after DNA damage.

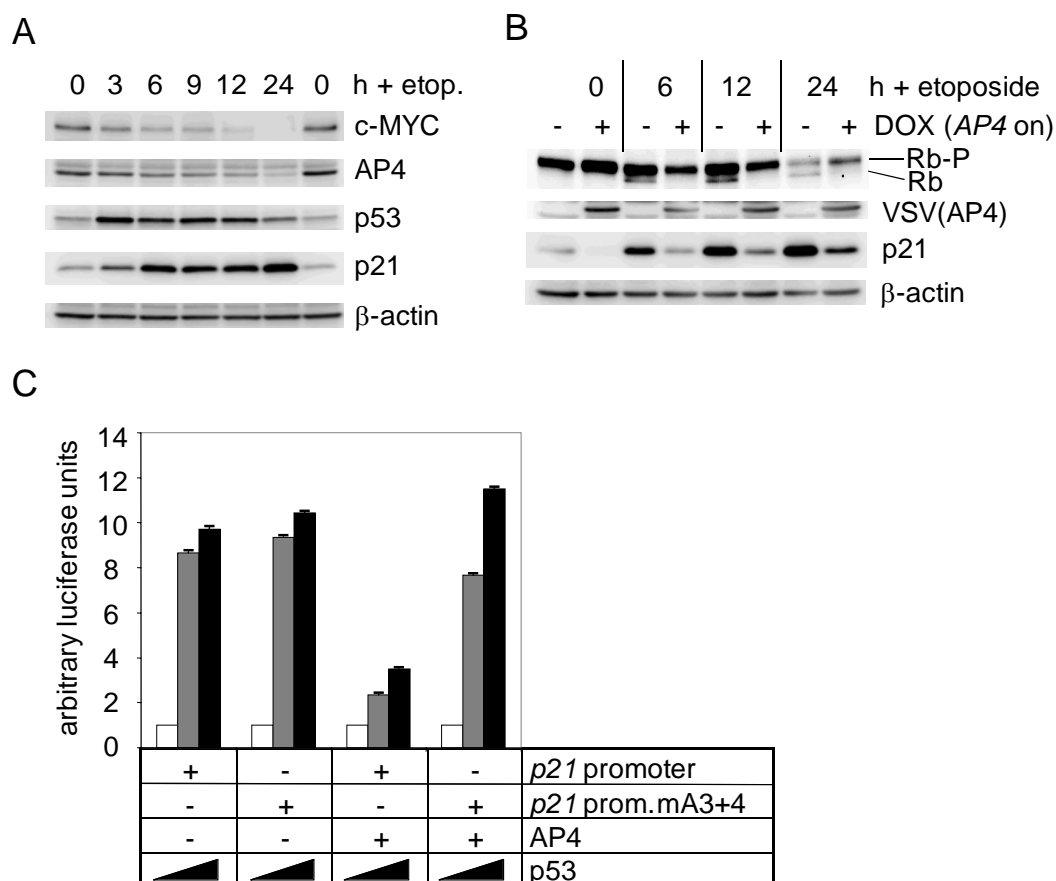


Figure 39. AP4 suppresses induction of *p21* by DNA damage/p53

A, AP4 is down-regulated by DNA damage. MCF-7 cells were treated with etoposide and cell extracts were obtained at the indicated time-points. Expression of the indicated proteins was determined by immunoblotting.

B, Ectopic AP4 was induced in U-2OS cells for 12 hrs by addition of DOX. Then etoposide was added for the indicated periods. Expression of Retinoblastoma protein (Rb), AP4-VSV, p21 or β -actin was analyzed by immunoblotting.

C, p21 reporter activity was determined in H1299 cells transfected with the indicated plasmids. Increasing expression of p53 was achieved by transfection of 0, 50 or 200 ng plasmids (indicated as ▲). Shown are the median expression values and standard errors of two independent transfection experiments. *p21* prom. mA3+4: reporter plasmid encoding *p21* promoter sequence with mutated AP4 binding sites 3+4 (see also Figure 38A).

In order to test this hypothesis, AP4 was ectopically expressed in U-2OS cell pools stably transfected using the episomal vector pRTS-1⁴⁷⁸. Due to the ectopic expression, AP4 was rendered largely resistant to down-regulation following DNA damage. Ectopic AP4 strongly interfered with p53-mediated transactivation of *p21* after DNA damage and, as a consequence of the alleviated CDK-inhibition by p21, prevented the formation of active, hypophosphorylated retinoblastoma protein (pRb) (Figure 39B). Furthermore, AP4 efficiently suppressed the p53-mediated induction of a *p21* promoter construct in a transient reporter assay (Figure 39C). This inhibitory effect of AP4 on the *p21* promoter could be circumvented by mutation of the two putative AP4 binding sites A3 and A4 in the *p21* promoter sequence. From these results it can be concluded that suppression of p53-mediated induction of *p21* by AP4 is mediated via direct binding of AP4 to CAGCTG sequences located in the *p21* proximal promoter region and not by interfering with p53 function.

On the cellular level, the simultaneous treatment of U-2OS cells with etoposide and ectopic expression of AP4 resulted in apoptosis as evidenced by the accumulation of sub-G₁ cells (cells with a DNA content smaller than 2N) as was analyzed by flow cytometry (Figure 40A,B). In this scenario, the AP4-mediated repression of *p21* might prevent the induction of cell cycle arrest after genotoxic stress and the continued cell cycle progression in the presence of DNA damage may result in apoptosis.

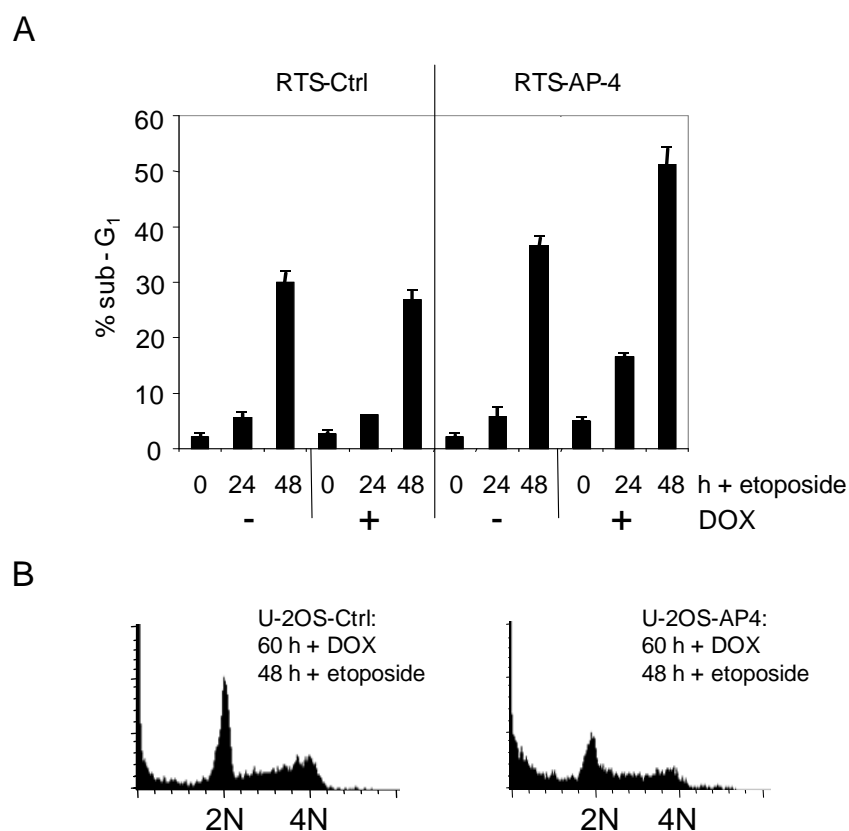


Figure 40. AP4 sensitizes cells to apoptosis

A, DOX was added to U-2OS RTS1-AP4 or U-2OS RTS1-Ctrl cells for 12 hrs. Then cells were treated with etoposide for the indicated periods and analyzed by flow cytometry. The diagram depicts the fraction of cells with sub-G₁ DNA content, which corresponds to cells undergoing apoptosis. The experiment was performed in triplicates. Standard deviations are depicted.

B, AP4 was induced by doxycycline for 12 hrs prior to treatment of cells with etoposide for 48 hrs. Then cells were analyzed by flow cytometry. Depicted are exemplary histograms representing 10,000 cells. 2N: cells in G₁, 4N: cells in G₂/M.

5.1.9 TGF- β -mediated induction of *p21* is suppressed by AP4

Constitutive expression of *c-MYC* blocks the induction of *p21* by all members of the TGF- β superfamily⁵²³. Therefore, it was determined whether AP4 is able to prevent TGF- β /Smad-mediated induction of *p21* and may represent a candidate mediator of resistance to TGF- β signaling caused by de-regulation of *c-MYC*. HaCaT cells, a human keratinocyte-derived cell line, have been reported to respond with induction of *p21* after TGF- β treatment⁵²⁴. Expression of AP4 in this cellular background was achieved by

infection using an adenovirus encoding *AP4* and *GFP*. Ectopic expression of AP4 efficiently suppressed the increase of p21 protein following exposure to TGF- β while the induction of the p15^{Ink4b} protein was not affected (Figure 41A). Infection with a control virus expressing *GFP* had no effect on the induction of p21 by TGF- β (Figure 41A and data not shown). Ectopic AP4 also reduced the TGF- β -mediated induction of *p21* mRNA when compared to cells infected with a control adenovirus (Figure 41B).

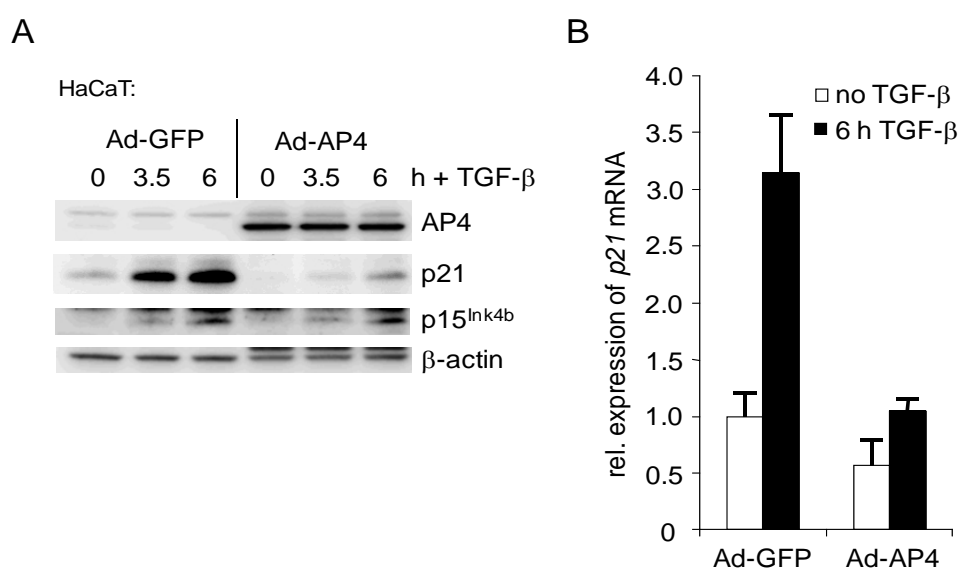


Figure 41. AP4 interferes with TGF- β -mediated induction of *p21*

A, HaCaT cells were infected with adenoviruses encoding AP4 and GFP or GFP alone. 24 hrs later cells were treated with human, recombinant TGF- β for the indicated periods. Expression of AP4-VSV, p21, p15^{Ink4b} and β -actin was determined by immunoblotting.

B, Quantification of *p21* mRNA in HaCaT cells infected with adenoviruses encoding either AP4 and GFP, or GFP alone. 24 hrs after infection, cells were treated with human recombinant TGF- β for 6 hrs. *p21* and, for normalization, *β -actin* mRNA expression was determined by RT-qPCR analyses. The experiment was performed in duplicates. Standard errors are depicted.

To validate these results and to exclude any effects potentially caused by the adenoviral infection procedure, HaCaT cells stably expressing a fusion of AP4 and the hormone binding domain of the oestrogen receptor (ER) were generated. As expected, after addition of 4-OHT the AP4-ER fusion displayed more pronounced nuclear localization (Figure 42A). Activation of AP4-ER strongly interfered with the TGF- β -mediated

induction of p21 (Figure 42B). Taken together, these data demonstrate that AP4 interferes with the TGF- β /Smad-mediated repression of the CDK inhibitor p21. However, repression of *p21* by AP4 was not able to alleviate a TGF- β -mediated cell cycle arrest in HaCaT cells (data not shown)

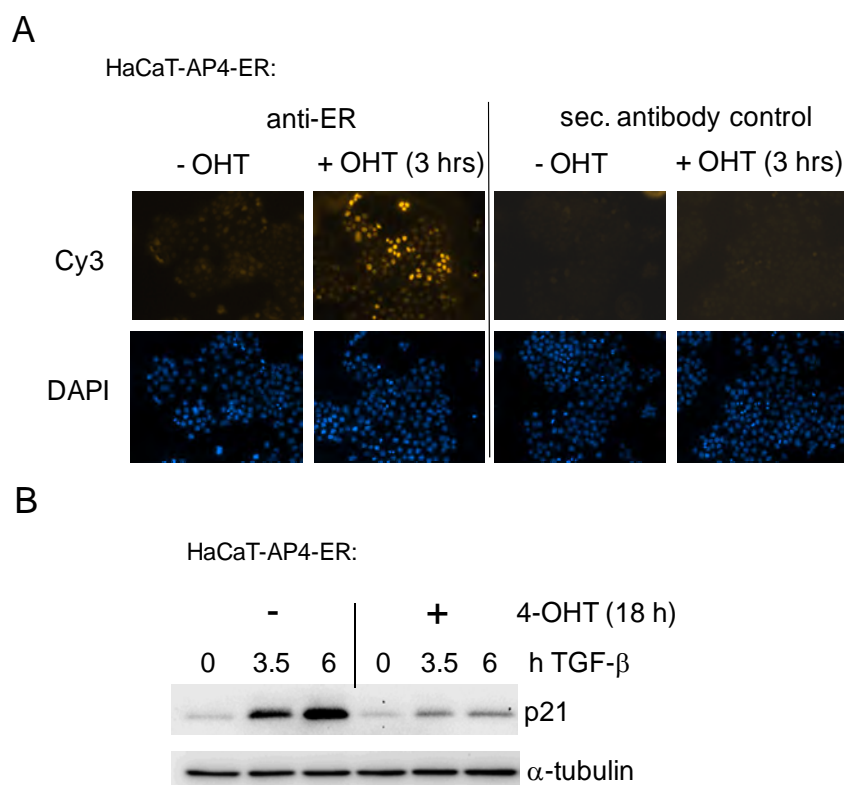


Figure 42. AP4-ER activation interferes with TGF- β -mediated induction of *p21*

A, HaCaT cells stably selected for expression of a AP4-ER fusion protein were treated with 200 nM 4-OHT for 3 hrs or left untreated. Subcellular localization of AP4-ER was detected by immunostaining using an anti-ER antibody. Indirect immunofluorescence was detected by fluorescence microscopy.

B, HaCaT cells stably infected with a retrovirus encoding AP4-ER were treated with 4-OHT for 12 hrs or left untreated before TGF- β was added for the indicated periods. Expression of p21 and β -actin was determined by Western blot analyzes.

5.1.10 AP4 interferes with cell cycle arrest during differentiation

Human U-937 myelomonoblastic cells⁵²⁵ undergo differentiation after treatment with 12-O-tetradecanoylphorbol-13-acetate (TPA)^{526,527}. Ectopic expression of *v-myc* prevents TPA-induced differentiation⁵²⁸. Interestingly, c-MYC may achieve this by interfering

with the induction of p21 expression⁴¹⁵. Treatment of U-937 cells with TPA reduces the expression level of endogenous AP4 (Figure 43A), presumably due to down-regulation of c-MYC expression (data not shown). Therefore it was determined whether expression of AP4 mimics the effect of ectopic v-myc in this scenario. To achieve a moderate expression of ectopic AP4, U-937 cells harboring an *AP4* allele under control of a truncated metallothionein-1 promoter⁵²⁹ were generated by retroviral infection. In the presence of zinc, ectopic AP4 interfered with TPA-mediated induction of p21 when compared to control-infected cells (Figure 43B).

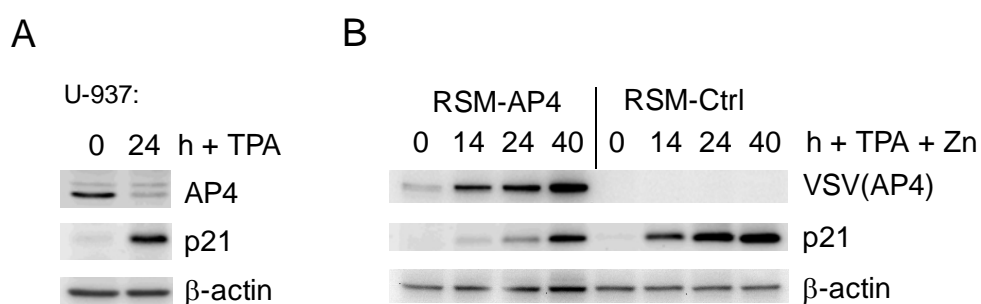


Figure 43. Effect of ectopic AP4 on p21 induction during myoblast differentiation

A, U-937 cells were treated with 10 nM 12-O-tetradecanoylphorbol-13-acetate (TPA) for 24 hrs and expression of AP4, p21 and, as a control for equal loading, β -actin was determined by immunoblotting.

B, U-937 RSM-AP4 or RSM-Ctrl cell pools were treated with 10 nM TPA and 100 μ M zinc sulfate for the indicated periods. Expression of AP4, p21 was determined by immunoblotting. Expression of β -actin was used as a control for equal loading.

In addition, cells ectopically expressing AP4 failed to stably arrest in G_1 upon TPA treatment and rather underwent apoptosis (Figure 44A). Furthermore, ectopic expression of AP4 increased the fraction of U937-cells which retained the ability to perform *de novo* DNA synthesis upon TPA treatment as exemplified by increased incorporation of the artificial thymidine nucleotide analog 5-bromo-2'-deoxyuridine (BrdU) (Figure 44B). Taken together, these data provide evidence that AP4 interferes with the cycle arrest which accompanies terminal differentiation of monoblastic cells presumably by downregulation of p21.

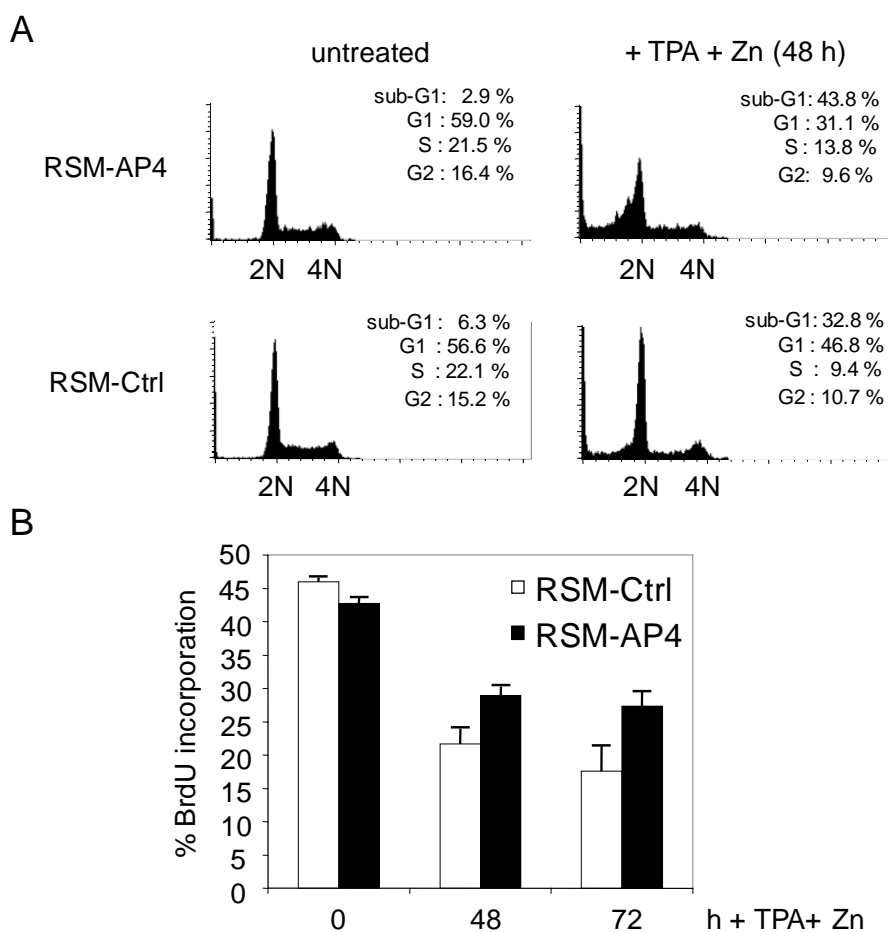


Figure 44. AP4 promotes cell cycle progression of cells undergoing differentiation

A, U-937 RSM-AP4 or RSM-Ctrl cells were treated with 10 nM TPA and 100 μ M zinc sulfate for the indicated periods and cells were analyzed by flow cytometry. The experiment was repeated twice and exemplary histograms representing 15,000 cells are provided. The % cell cycle distributions are average results of two independent experiments. 2N: cells in G₁, 4N: cells in G₂/M.

B, U-937 RSM-AP4 or RSM-Ctrl cells were treated with 10 nM TPA and 100 μ M zinc sulfate for the indicated periods and *de novo* DNA synthesis (BrdU incorporation) was determined by flow cytometry. The percentages of BrdU-incorporation represent mean values of three independent experiments. Error bars are depicted and represent standard deviations.

5.1.11 AP4 expression pattern in human colon and colorectal cancer specimen

Immunohistochemical analyses revealed that the expression of AP4 protein is restricted to the base of human colonic crypts which are populated by non-differentiated stem cells and highly proliferative progenitor cells as evidenced by the expression of the

proliferation marker Ki67 and the absence of p21 expression (Figure 45). In the differentiated upper parts of colonic crypts, expression of AP4 was not detectable (Figure 44). The expression pattern of AP4 is similar to the reported pattern of c-MYC expression in these compartments^{281,282}. As would be expected from a repressor of the *p21* gene, expression of AP4 inversely correlated with the expression of p21 which increased towards the tips of the crypts that contain terminally differentiated cells^{530,531} (Figure 45).

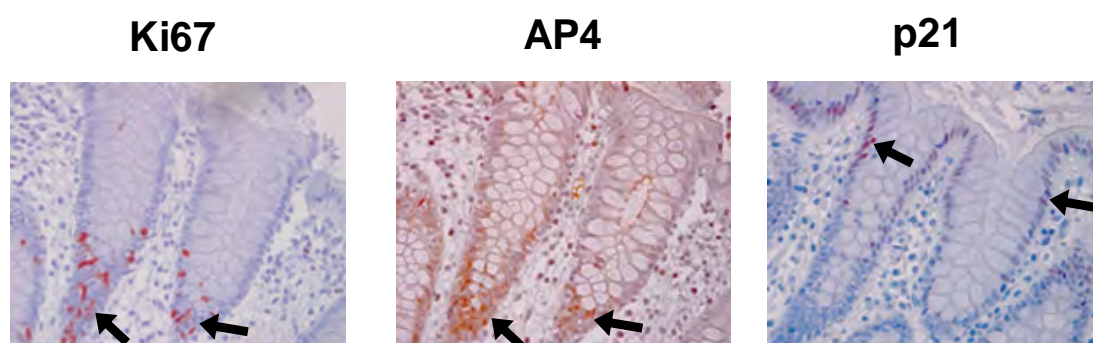


Figure 45. *In vivo* expression of AP4, Ki67 and p21 in normal human colonic crypts

A section of an endoscopic biopsy derived from normal colon area. Consecutive paraffin sections were stained with antibodies directed against Ki67, AP4 or p21. Arrows indicate positive cells. (magnification : 200×)

Staining of tissue sections for Ki67 and p21 was performed by Andrea Sendelhofert from the Institute of Pathology, LMU, Munich

Consistent with a role of *AP4* downstream of de-regulated, oncogenic c-MYC, primary colorectal carcinomas present in biopsies obtained from 12 patients showed a strong expression of AP4 which correlated with expression of c-MYC and Ki67 protein in all cases analyzed (Figure 46-48). In small adenomas, which retain a crypt-like architecture, the frequency of Ki67-positive cells was increased and extended to the surface epithelial layer (Figure 46, lower panel). Similarly, expression of c-MYC and AP4 was extended to more distal areas of the crypt (Figure 46, lower panel). Furthermore, expression of p21

was mainly limited to the surface and the compartmentalization of p21 and Ki67 expression was partially lost in this stage of crypt transformation as has been described before by Polyak et al.⁵³⁰. However, the mutual exclusion of c-MYC/AP4 and p21 expression was preserved in small adenomas. Taken together, these *in vivo* expression data suggest that AP4 may represent a mediator of the effects that activation of c-MYC has on the organismal level. The strict correlation between AP4 and c-MYC expression in human colorectal tumors further indicates that AP4 might contribute to the oncogenic effects caused by de-regulation of *c-MYC* in human cancer disease.

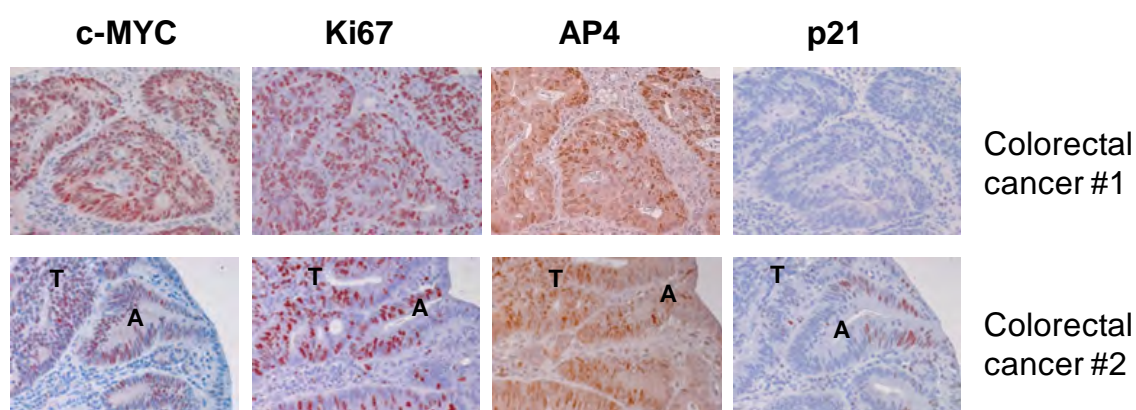


Figure 46. *In vivo* expression of AP4, c-MYC, Ki67 and p21 in colorectal cancer

Sections of endoscopic biopsies derived from primary tumors of two patients are depicted. Consecutive paraffin sections were stained with antibodies directed against c-MYC, Ki67, AP4 or p21. With colorectal carcinoma biopsies from 10 additional patients identical results were obtained (Figure 47 and 48). A, small adenoma (dysplastic), T, tumor. (magnification: 200×)

Staining of tissue sections for c-MYC, Ki67 and p21 was performed by Andrea Sendelhofert from the Institute of Pathology, LMU, Munich.

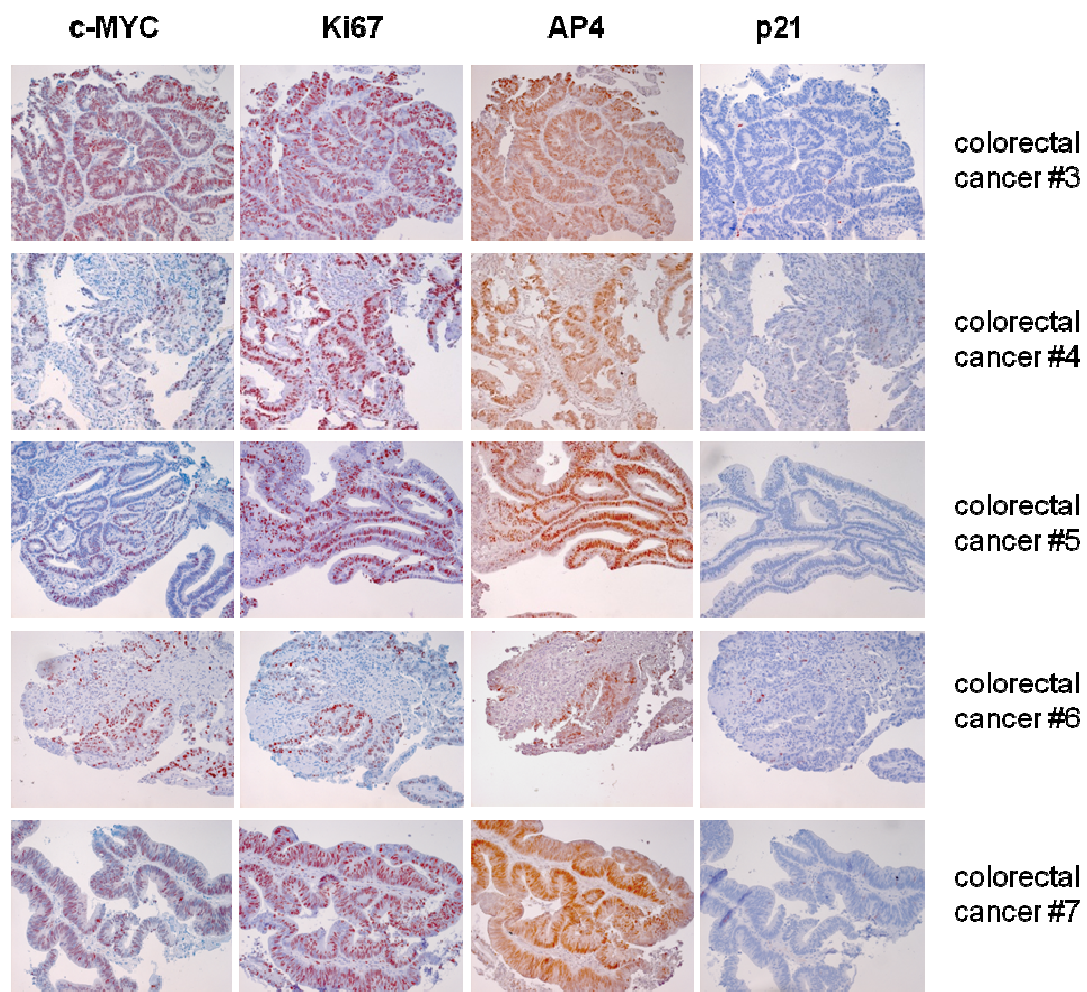


Figure 47. *In vivo* expression of AP4, c-MYC, Ki67 and p21 in colorectal cancer

Sections of endoscopic biopsies derived from primary tumors of five patients are depicted. Consecutive paraffin sections were stained with antibodies directed against c-MYC, Ki67, AP4 or p21. (magnification 200×)

Staining of tissue sections for c-MYC, Ki67 and p21 was performed by Andrea Sendelhofert from the Institute of Pathology, LMU, Munich.

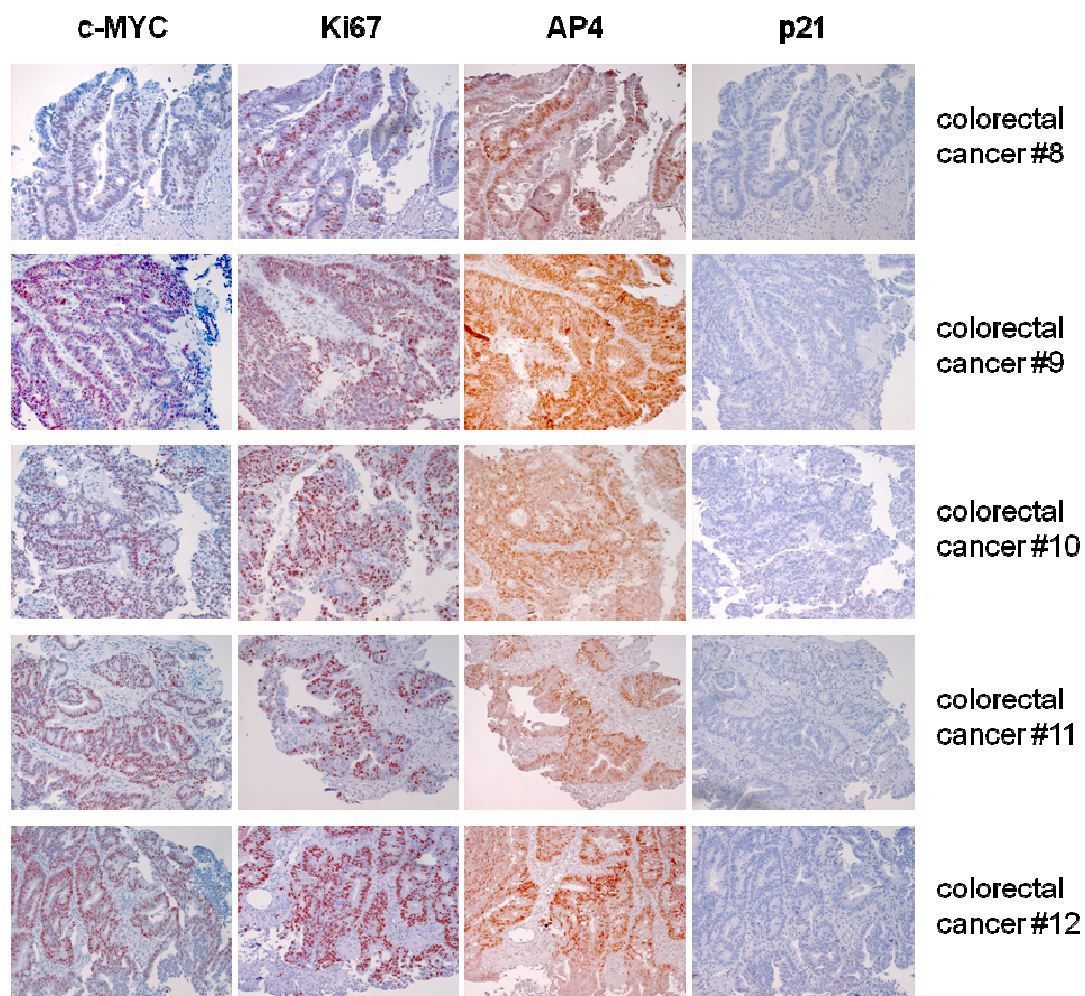


Figure 48. *In vivo* expression of AP4, c-MYC, Ki67 and p21 in colorectal cancer

Sections of endoscopic biopsies derived from primary tumors of five patients are depicted. Consecutive paraffin sections were stained with antibodies directed against c-MYC, Ki67, AP4 or p21. (magnification 200×)

Staining of tissue sections for c-MYC, Ki67 and p21 was performed by Andrea Sendelhofert from the Institute of Pathology, LMU, Munich.

6 Discussion

6.1 iTAP/MudPIT analysis of p53-associated proteins

The iTAP purification and mass-spectral analysis of p53-associated proteins described here revealed Cul7 as a putative p53 interacting protein. With respect to the number of identified peptides, sequence coverage and consistency in four independent experiments, Cul7 was considered to exhibit an outstanding binding affinity towards p53 when compared to all other co-purified proteins. Since the p53/Cul7 interaction was readily confirmed by co-immunoprecipitation of endogenous proteins, which is the current “gold standard” for describing novel protein-protein interactions, the main focus of this project was to determine its role in the regulation and/or function of p53.

6.1.1 Cul7: a component of modular E3-ligases

Several members of the superfamily of cullin-ring ligases (CRLs) are involved in ubiquitin-dependent proteolysis⁵³² thereby regulating a huge number of cellular processes, including glucose-sensing, circadian rhythms, limb patterning and DNA replication. CRLs belong to the class of multisubunit E3 ligases and were first described 11 years ago⁵³³. A main feature of these enzymes is their modular composition with the subunits being assembled on a cullin scaffold^{534,535}. The name “cullin” was derived from the ability of each family member to “cull” or sort specific substrates for ubiquitination⁵³³. Seven cullins, CUL1, 2, 3, 4A, 4B, 5 and 7, have been identified until now in human cells⁵³². In contrast to single-subunit E3-ligases, such as MDM2 and PARC, cullin-based E3-ligases lack a catalytical domain and need to associate with the Rbx1 protein which contributes a RING-domain essential for E3-ligase activity⁵³⁶⁻⁵³⁸. In the classical model describing Cul1-based SCF complexes⁵³⁹, substrate receptors, so called F-box proteins⁵³⁵, are recruited by the adaptor protein Skp1, whose C-terminus binds to the F-box motif of these substrate recognizing units.

Cullin 7 (Cul7) was originally discovered as a 185 kD protein (p185) associated with the large T antigen of simian virus 40 (SV40)⁵⁴⁰. The carboxy-terminus of Cul7 harbors a BH3 domain and ectopic expression of Cul7 was shown to promote apoptosis in NIH3T3 cells⁵⁴¹. However, this is in contrast to more recent findings showing that

inactivating Cul7 mutations negatively affect cell proliferation *in vivo*⁵⁴² and elevated expression of Cul7 increases the proliferation rate of human cancer cell lines⁵⁴³. Later, Cul7 was characterized as a central component of an SCF-ROC1 E3-ligase complex (SCF7), consisting of Skp1, Cul7, Fbx29 and Rbx1⁴⁸³. Association with this complex is required for cellular transformation by the SV40 large T antigen^{475,544}. Unlike Cul1, which is able to interact with Skp1 in the absence of Fbx29⁵⁴⁵, Cul7 associates exclusively with a preformed Skp1-Fbx29 complex⁴⁸³. Recently, Cul7 and Cul1 were shown to assemble a heterodimeric E3-ligase complex which contains two Rbx1 subunits, one bound to Cul7 and Cul1, respectively⁵⁴⁶. The formation of this complex is dependent on Fbx29, that bridges Cul7 and Cul1-Skp1, thereby presumably conferring substrate specificity to this multisubunit E3-ligase⁵⁴⁶. The work of Tsunematsu and colleagues further revealed, that the interaction of Cul7 with Fbx29 occurs independently of the F-box-domain of Fbx29 while the F-box motif is essential for association of Fbx29 with Cul1 via Skp1⁵⁴⁶. The identity of physiological substrates targeted by Cul7-containing E3-ligase complexes for proteasomal degradation remains unknown.

6.1.2 Cul7: a negative modulator of p53 activity

This thesis revealed that the E3-ligase component Cullin 7 (Cul7) is induced by genotoxic stress in a caffeine-sensitive manner and negatively regulates p53 activity presumably by direct interaction. The acute down-regulation of endogenous *Cul7* by a conditional RNA interference approach led to increased p21 protein levels in MCF-7 breast cancer cells which augmented a DNA damage-induced G₁-arrest in a p53-dependent manner. Knockdown of Cul7 had no significant influence on the p53 protein level suggesting that Cul7 acts by limiting the transcriptional activity of p53 rather than by affecting its protein turnover. A similar mode of p53 inhibition has been reported for MDMX^{101,103}, which directly interacts with p53 thereby inhibiting p53-mediated transactivation of target genes⁹⁴. Similar to the observed effect of Cul7 knockdown on p53 activity, MCF-7 cells with reduced MDMX expression due to RNA-interference display elevated expression of p21 and reduced proliferation capacity but retain unaltered levels of p53 protein⁵⁴⁷.

In agreement with the positive effect on p53 function after Cul7 ablation, accumulation and activity of p53 following DNA damage was compromised by ectopic expression of Cul7. Disruption of p53 function was previously described to sensitize human cancer cells to apoptosis induced by genotoxic drugs⁵⁴⁸. Especially the p53/p21 axis was shown to be critical for a sustained cell cycle arrest after DNA damage⁵⁰¹. In line with Cul7 acting as a negative regulator of p53 function, ectopic expression of Cul7 increased the apoptotic fraction of MCF-7 cells upon exposure to genotoxic drugs presumably by preventing the establishment of a stable, p53-mediated cell cycle arrest.

Since the substrate recognizing component of the SCF7 E3-ligase, Fbx29, did not directly interact with p53, but was recruited to p53 in a Cul7-dependent manner, it seemed unlikely that p53 represents a target for ubiquitination by the SCF7 complex. In addition, ectopic expression or acute knockdown of Cul7 did not affect the protein level of p53 in exponentially proliferating cells, suggesting that Cul7 does not target p53 for ubiquitin-dependent proteasomal degradation. Previously, a Cul7-mediated mono- and di-ubiquitination of p53 has been observed *in vitro* using immunoprecipitated complexes of Cul7 and ectopic p53 from H1299 cells⁵⁴³. However, the biochemical consequences of this p53 modification remained elusive⁵⁴³. Here, a ubiquitination of p53 by Cul7/Fbx29 *in vivo* was not detectable. Since several E3-ligases have been shown to mono- and di-ubiquitinate p53^{45,65,66,69,70}, it is possible that immunoprecipitates of Cul7/p53 complexes contain other E3-ligases responsible for the *in vitro* ubiquitination of p53 observed by Andrews et al.⁵⁴³. The lack of poly-ubiquitination activity of Cul7 towards p53 *in vivo*, which was confirmed by others⁵⁴³, makes it highly unlikely, that Cul7 represents the long-sought cytoplasmic E4-like enzyme which was postulated to poly-ubiquitinate p53 exported from the nucleus leading to its cytoplasmic degradation by the 26S proteasome⁴⁴.

During this thesis, a direct interaction between ectopic p53 and Cul7 was also reported by others^{543,549,550} which confirms findings presented. The association of Cul7 with p53 was shown to occur between the conserved CPH domain of Cul7 and the oligomerization domain of p53⁵⁵⁰ which is relevant for its activation. Kaustov et al. demonstrated that the CPH domain of Cul7 preferentially binds to an extended surface of the p53 tetramer⁵⁵⁰ and in line with these observations, genotoxic stress augmented the

interaction of endogenous p53 and Cul7 presumably by increasing the proportion of p53 tetramers. This might also explain, why ectopic Cul7 specifically interfered with activation of p53 in response to DNA damage when increased levels of p53 favor the formation of p53-tetramers. Since genotoxic stress and inhibition of nuclear export by leptomycin B did not lead to nuclear localization of Cul7 protein (data not shown), Cul7 may associate with p53 in the cytoplasm. Interestingly, the p53-targeting E3-ligases Pirh2 and COP1 localize to the nuclear and cytoplasmic compartment^{551,552} but where they act on p53 is currently unknown. In the cytoplasm, Cul7 could be involved in controlling the oligomerization status of p53. Tetrameric p53 is less efficiently imported into the nucleus than its monomeric form⁵⁵³. Andrews et al. showed that mutations targeting the p53 export signal decreased the p53/Cul7 association, whereas the p53/Cul7 interaction was augmented in case of mutations abrogating the nuclear import of p53⁵⁴³. However, according to their observations, Cul7 does not sequester p53 in the cytoplasm⁵⁴³. Thus, the exact mechanism by which Cul7 inhibits the activity of p53 remains to be determined.

6.1.3 PARC: a close relative of Cul7

Cul7 is highly homologous to PARC (PARkin-like, Cytoplasmic, p53 binding protein) which was demonstrated to negatively regulate p53 by cytoplasmic sequestration⁷¹. While ablation of PARC leads to nuclear re-localization of cytoplasmic p53 in human neuroblastoma- and osteosarcoma-derived cells, recent reports do not support this model of PARC function in mice⁵⁵⁴ and modulation of PARC does not alter p53 localization in hepatoblastoma-derived cell lines⁵⁵⁵. These findings suggest that sequestration of p53 by PARC to the cytoplasmic compartment occurs in a cell-line- and species-dependent manner. In their regions of homology, PARC and Cul7 show a sequence identity of up to 60% (see Figure 11). Cul7 and PARC contain a CPH domain which is conserved in Cul7, PARC and HERC proteins⁵⁴⁹ and the HERC domain containing protein HERC2 is proposed to serve as an E3-ligase^{483,556}. In addition, the two proteins harbor a DOC (DOC1/APC10) domain which is located in the central region of Cul7 and shows striking similarity to APC10/DOC1, an essential subunit of the APC/C (Anaphase Promoting Complex/Cyclosome)⁵⁵⁷. This domain composition together with the

presence of a CH (Cullin homology) domain suggested that PARC and Cul7 might function as E3-ubiquitin ligases and this enzymatic activity was previously confirmed for both of them ^{71,483}. As discussed before, p53 did not serve as a substrate for Cul7/Fbx29-mediated ubiquitination *in vivo* and others reported that PARC does not target p53 for ubiquitination ⁷¹. However, PARC is discussed to provide a cytoplasmic scaffold for p53 poly-ubiquitination by other cytoplasmic E4-ligases ⁷². Since Cul7 interfered with the stabilization of p53 in response to DNA damage one could speculate that Cul7, when bound to p53 after genotoxic stress, might serve as a scaffolding factor to allow other E3-ligases to ubiquitinate p53 leading to its proteasomal degradation in the cytoplasm. However, Cul7 is not able to promote MDM2-mediated poly-ubiquitination of p53 *in vivo* ⁵⁴³ suggesting other mechanisms might be responsible for the effect of Cul7 on p53 after DNA damage.

6.1.4 Role of Cul7 in normal proliferation and cell growth

PARC and Cul7 were demonstrated to form homodimers but are also able to heterodimerize with each other ⁵⁵⁴. Nevertheless, the two proteins have non-overlapping functions since knockout of *PARC* in mice has no effect on viability ⁵⁵⁴, whereas the knock-out of *Cul7* in mice is post-natal lethal and accompanied by intrauterine growth retardation, vascular abnormalities and lungs with failure in inflation and restriction of the alveolar space ⁴⁸⁴. In this scenario, Arai et al. identified FAB68/glomulin, whose inactivation can be found in patients suffering from inherited glomuvenous malformation ⁵⁵⁸, as a binding partner of the SCF7 complex but FAB68 does not serve as a substrate for SCF7-mediated ubiquitination ⁴⁸⁴. However, the reported phenotype of Cul7 knock-out mice ⁴⁸⁴ suggests that Cul7 plays a non-essential role in mammalian development, which would be consistent with a function as a checkpoint component as suggested by this thesis. The presented data further imply that deregulation of p53 activity might at least in part account for the reduced proliferation of *Cul7*-deficient mouse embryo fibroblasts derived from these knock-out mice ⁴⁸⁴. p53 may also contribute to the post-natal lethality observed after deletion of *Cul7* ⁴⁸⁴. Similar phenotypes have been observed in mice deficient for other negative regulators of p53, such as MDM2 and MDMX ^{46,47,97}. In the future it will be important to determine, to

which extent the phenotype of Cul7-deficient mice can be rescued by inactivation of p53.

In a recent study, mutations within the *Cul7* gene were identified as the cause of the 3-M syndrome, an autosomal-recessive form of dwarfism characterized by pre- and post-natal growth retardation⁵⁴². This observation is in line with a positive role of Cul7 in unperturbed cell proliferation and according to results presented here, it is possible that the increase in p53 activity, which may result from mutated, non-functional Cul7, contributes to the 3-M syndrome. However, 50% of the identified Cul7 mutations in 3-M syndrome are located within its cullin domain responsible for Rbx1-binding and two mutations, R1445X and H1464P, were demonstrated to impair the ability of Cul7 to efficiently associate with Rbx1 and compromise the ubiquitin-ligase activity of immunoprecipitated Cul7 complexes⁵⁴². For that reason, it is likely that also other, p53-independent functions, which involve ubiquitination of as yet unidentified substrates by Cul7-containing E3-ligase complexes, contribute to the 3-M syndrome phenotype.

Interestingly, Fbx29 is extremely unstable in Cul7 knock-out mice⁴⁸⁴ and undetectable in MEFs depleted of Cul7 by RNA interference⁵⁴⁶ suggesting that Cul7 acts in a chaperone-like mode and stabilizes Fbx29 by scaffolding the SCF7 complex. Since an incomplete knockdown of p53 partially rescued the effect of Cul7 ablation on a DNA damage/p53-mediated cell cycle arrest, it can be excluded, that the consequences of Cul7 ablation observed here are caused by Fbx29-specific, p53-independent effects. In addition, Fbx29 protein is specifically expressed in the placenta and, to a lower extent, in mouse embryos, whereas it is undetectable in adult tissues⁵⁴⁶. In contrast, expression of Cul7 was found in a large spectrum of adult tissues originating from mice and humans^{484,542}. In contrast to the Cul7 knock-out phenotype, Fbx29-deficient mice show abnormalities which are restricted to the placenta⁵⁴⁶ suggesting that the organismal function of Cul7 in adult tissues is not related to Fbx29-mediated substrate-recognition and -ubiquitination. The consequences of Cul7 expression and inactivation on p21 expression, cell cycle arrest and sensitization of cells towards apoptosis following DNA damage observed here are therefore presumably due to the inhibitory association of p53 and Cul7.

6.1.5 Regulation of Cul7 level by genotoxic stress

In contrast to PARC and other cullin family members, Cul7 does not serve as a substrate for neddylation^{559,560} and the regulatory mechanisms underlying Cul7 activity remained speculative. The data presented here provide the first evidence, that the level of Cul7 is positively regulated by the DNA damage response pathway. Inhibition of PIKK family members by caffeine prevented the increase of *Cul7* mRNA and protein after DNA damage. Therefore, a model can be suggested in which PIKK kinases not only activate p53 in response to genotoxic stress but also increase the level of its negative modulator Cul7. Negative feedback loops represent a common mode of p53 regulation⁴⁴. Several negative regulators of p53, e.g. MDM2, COP1 and Pirh2, are encoded by target genes of p53^{48,65,66}. However, since induction of *Cul7* mRNA and protein due to genotoxic stress does not require p53 activity, the p53/Cul7 feedback loop may involve one or several additional components. Interestingly, cullin proteins have been recently implicated in the negative regulation of the DNA damage response as ATR-mediated phosphorylation marks CHK1 for ubiquitination by SCF E3-ligase complexes which contain Cul1 and Cul4a thereby limiting the duration of ATR-CHK1 signaling after genotoxic or replicative stress⁵⁶¹. Similarly, the elevated levels of Cul7 caused by genotoxic stress may limit the activity of p53 thereby allowing cells to re-enter the cell cycle after DNA damage has been repaired.

6.1.6 Implication of the Cul7/p53 interaction for cancer therapy

In summary it was demonstrated here that p53 interacts with Cul7 *in vivo* and the induction of Cul7 after DNA damage attenuates the activation of p53 (Figure 49). Increasing efforts are being made to inhibit the association of p53 with negative regulators in order to restore its tumor-suppressive capacity in cancer cells which retain wild type p53⁵⁶²⁻⁵⁶⁴. Anti-sense oligonucleotides directed against MDM2 were demonstrated to activate p53 and consequently suppress tumor growth in xenograft models⁵⁶⁵. More recently, small molecule inhibitors of the MDM2-p53 interaction, designated as nutlins, were generated⁵⁶⁶ which exhibit p53-dependent activity in several cellular model systems^{566,567}. Moreover, reactivation of p53 in mouse tumor models was shown to provoke a dramatic response in spontaneous and experimental tumors.

Dependent on the tumor type, p53-restoration led to apoptosis (lymphoma) or cell cycle arrest with features of senescence (sarcomas) ^{568,569}.

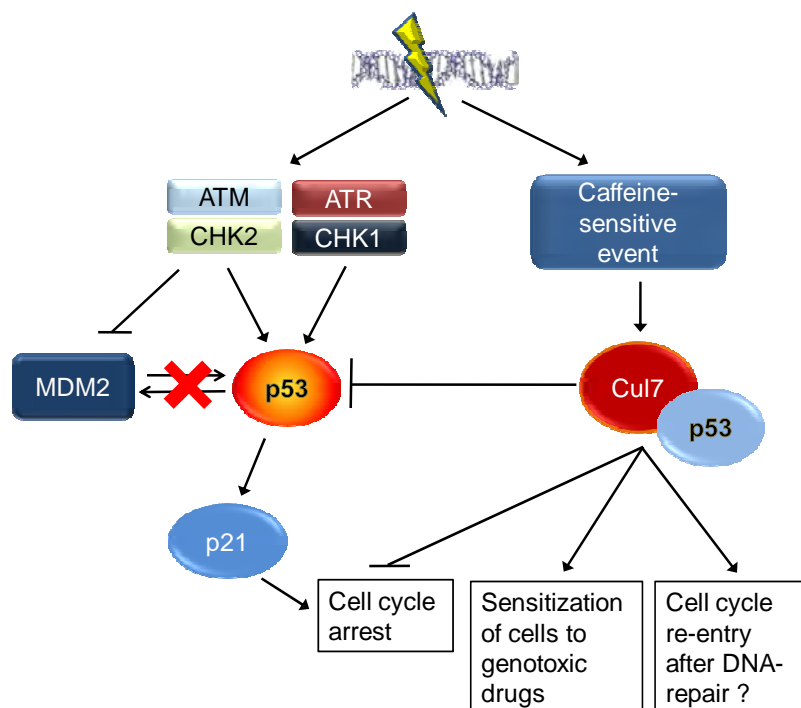


Figure 49: Cul7 is induced by DNA damage and inhibits p53 activity

In the model proposed here, genotoxic stress disrupts the well described p53/MDM2 feedback-loop (indicated by a red cross) but concomitantly increases the expression level of Cul7 via a caffeine-sensitive event. Cul7 associates preferentially with active, tetrameric p53 (red) and negatively modulates its function (blue). By disruption of the DNA damage/p53/p21 pathway, Cul7 alleviates a p21-mediated cell cycle arrest thereby sensitizing cells to p53-independent apoptosis after treatment with genotoxic drugs. It is possible that Cul7 limits p53 activity in order to allow re-entry into the cell cycle after cells have recovered from DNA damage.

The observed tumor regression by restoration of p53 legitimates the ongoing effort to treat human tumors by means of p53-based cancer therapies. In the future it will be important to determine if and to which extent Cul7 is over-expressed in tumors that retain wild type p53 and whether Cul7 contributes to inactivation of the p53 pathway in this scenario. With regard to the data presented here, it is likely that the pharmacological modulation of the Cul7/p53 interaction or of Cul7 may allow to sensitize tumor cells expressing wild-type p53 to genotoxic agents used in cancer therapy.

6.2 *AP4* is a c-MYC-responsive gene in human carcinoma

In recent years, several genome-wide studies have been performed to identify c-MYC-regulated genes by means of microarray analyses^{368,371,516,570-573}, serial analysis of gene expression (SAGE)³⁷⁰, and large scale identification of c-MYC binding sites using chromatin-immunoprecipitation (ChIP)^{369,574,575}. Except for a work performed in the laboratory of Gerard I. Evan, that analyzed c-MYC de-regulated genes in rat pancreatic β -cells⁵⁷³, none of these studies was performed in epithelial cells which are the origin of carcinomas, the most common type of human tumors. In the western world, carcinomas are responsible for more than 80% of cancer-related deaths. Since cell type-specific differences in gene regulation by c-MYC are supposed to exist³⁷⁸, it is important to determine which genes are induced by c-MYC in cells of epithelial origin.

During this thesis, microarray analyses were performed using the human breast carcinoma cell line MCF-7. This approach revealed that *AP4* is amongst the 25 most highly induced genes upon c-MYC activation in a clinically relevant scenario, which is c-MYC-mediated alleviation of an anti-estrogen mediated cell cycle arrest. Validation experiments clearly demonstrated that *AP4* meets all requirements for a direct, conserved c-MYC target gene and was therefore chosen for further analyses. The biology of *AP4* and the functional consequences of *AP4* induction by c-MYC on different cancer-relevant signaling processes will be discussed below.

6.2.1 The transcription factor *AP4*

AP4 was initially identified as a cellular protein which activates late viral gene expression from the simian virus 40 (SV40) enhancer⁵⁷⁶. The amino acid sequence of the ubiquitously expressed transcription factor *AP4* characterized it as a member of the basic helix-loop-helix leucine-zipper (bHLH-LZ) subgroup of bHLH proteins (Figure 50) which recognizes the symmetrical DNA core sequence CAGCTG⁵⁷⁷. While *AP4* belongs to the class A of bHLH proteins, c-MYC is a member of class B and binds to CA(C/T)GTG core sequences⁵⁷⁸.

Unlike other bHLH proteins, *AP4* harbors two additional protein dimerization motifs which consist of the leucine repeat elements LR1 and LR2 (Figure 50). Due to these multiple protein-protein interaction surfaces *AP4* forms homodimers but is not able to

undergo heterodimerization with other bHLH proteins⁵⁷⁷. For various genes, AP4 binding to promoter and enhancer regions has been reported⁵⁷⁹⁻⁵⁸¹. AP4 binds to the promoter of *Caspase 9* and antisense RNA-mediated downregulation of AP4 has been shown to inhibit expression and activation of *Caspase 9*⁵⁸¹. However, ectopic expression of AP4 does not influence expression of *Caspase 9*⁵⁸¹ suggesting a role of AP4 in maintaining the basal expression level of this initiator caspase. Although AP4 was shown to activate transcription of SV40⁵⁷⁶, recent studies reported AP4-mediated transcriptional repression of viral and cellular genes^{579,580,582}. A repressor complex containing AP4 has been described to downregulate expression of *PAHX-AP1* in non-neuronal cells⁵⁷⁹ and AP4 levels gradually decrease during development from the embryonic to adult brain suggesting that AP4 regulates the temporal expression of target genes during brain development⁵⁷⁹. However, upstream pathways responsible for the regulation of AP4 and a role of AP4 in cell cycle regulation and tumorigenesis has not been described before.

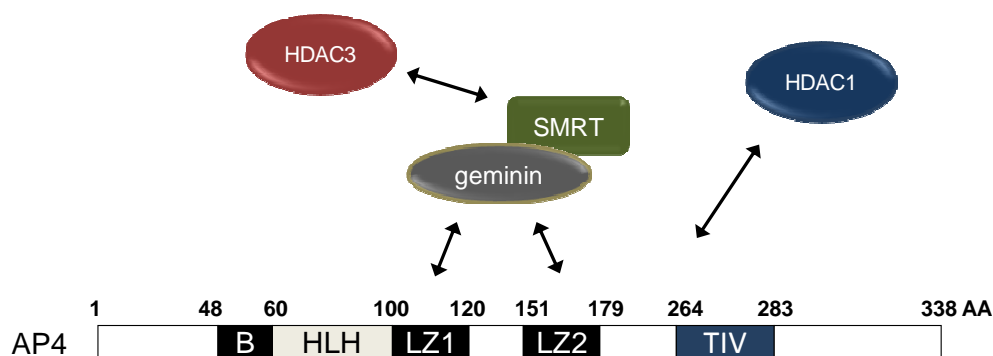


Figure 49. AP4 domain structure and known interactors

Within its N-terminal region, AP4 contains a basic region responsible for specific binding to DNA. AP4 forms homodimers via a tripartite interaction interface consisting of HLH, LZ1 and LZ2 domains. AP4 recruits HDAC3 via a geminin-SMRT complex⁵⁷⁹ and directly associates with HDAC1⁵⁸⁰ to mediate repression of target genes. A motif containing the amino acids TIV is evolutionary conserved, however, the function of this motif is unknown. B: basic region; HLH: helix-loop-helix; LZ: leucine zipper; HDAC: histone deacetylase; AA: amino acid.

6.2.2 A c-MYC / AP4 / p21 cascade represses p21

Apart from activating a number of genes involved in cell cycle progression as e.g. *CDC25A*⁴⁰¹, the cyclins A2⁵⁸³, -B1³⁷⁰, -E⁵⁸⁴, D2³²⁷ and the Cyclin-dependent kinase 4 (*CDK4*)³⁹³, c-MYC mediates trans-repression of the cell cycle and growth arrest genes *gas1*⁵⁸⁵, *p15^{Ink4b}*³⁶⁰, *p21*^{586,587} and *p27^{KIP1}*³⁵⁸. The results of this thesis establish AP4 as

a c-MYC-inducible repressor of the CDK inhibitor p21. Ectopic expression of AP4 resulted in down-regulation of *p21* mRNA and protein in several cellular systems and was mediated by binding to CAGCTG sites located in the proximal promoter region of *p21*. The down-regulation of *p21* by c-MYC plays a critical role in the development of anti-estrogen resistance during breast cancer therapy^{588,589}, β -catenin/TCF4-mediated colorectal transformation²⁸⁰⁻²⁸² and differentiation of hematopoietic cells⁴¹⁵. Several studies have been undertaken to reveal the mechanistic basis of *p21* repression by c-MYC and various mechanisms have been proposed⁵⁹⁰:

One mode of *p21* repression by c-MYC occurs via interference with the transcription factor MIZ1, which by itself acts as a transactivator of the *p21* gene⁵⁹¹. MIZ1 binds to a so-called initiator element (Inr) close to the transcriptional start site of the *p21* gene⁴¹⁵. MIZ1 is required for up-regulation of *p21* in response to UV irradiation⁵⁹¹ and also plays role in the differentiation-mediated upregulation of *p21*⁴¹⁵. However, in unperturbed cells MIZ1 may not be required for *p21* regulation since *MIZ1*-deficient mice display unaltered levels of p21 expression⁵⁹². In addition, siRNA-mediated knockdown of MIZ1 does not decrease the expression of p21 in HepG2 cells⁵⁹³. Others provided evidence that repression of *p21* by c-MYC may be mediated via interactions with Sp1/Sp3 and independently of the Inr sequence³⁶³. Furthermore, c-MYC is able to recruit the DNA methyltransferase Dnmt3a, which also functions as a corepressor, to the *p21* promoter via association of c-MYC with MIZ1³⁶⁷. Brenner et al. even suggested that DNA methylation is involved in c-MYC-mediated repression of *p21*³⁶⁷. Therefore, it is conceivable that c-MYC employs different factors and mechanisms to downregulate *p21* expression in different cell types and under divergent physiological and pathophysiological conditions. In contrast to constitutive expression of c-MYC⁴¹⁵, ectopic AP4 was only able to delay rather than completely abrogate the induction of p21 during differentiation of TPA-treated U-937 cells. In DLD1 colorectal cancer cells, partial down-regulation of AP4 by RNA interference was not sufficient to abrogate the repressive effect of conditional c-MYC activation on p21 (data not shown). Therefore, several pathways downstream of c-MYC might act synergistically or compensate for each other to fully control *p21* expression. Future efforts should aim to determine the relative contribution of these various mechanisms to c-MYC-mediated *p21* repression. In

addition it will be interesting to analyze, whether distinct modes of *p21* repression by c-MYC are preferentially used in different cell types and after certain physiological stimuli.

The AP4 transcription factor forms a complex with geminin and the co-repressor SMRT which represses the human *PAHX-AP1* gene through recruitment of histone deacetylase 3 (HDAC3)⁵⁷⁹. Furthermore, AP4 directly associates with HDAC1 to mediate transcriptional repression of HIV1⁵⁸⁰ (see Figure 50). Other studies provided evidence that AP4 may block access of the TATA-box binding protein (TBP) to the TATA box^{580,594} thereby interfering with the assembly of the RNA-Polymerase II initiation complex at target gene promoters. Treatment of U-2OS cells with the HDAC inhibitor trichostatin (TSA) increased p21 levels (data not shown), which has been demonstrated before in different cellular systems⁵⁹⁵. Interestingly, TSA treatment was not sufficient to relieve AP4-mediated repression of *p21* (data not shown) suggesting that histone deacetylase activity may not be required to maintain *p21* repression by AP4. In line with results presented here showing that AP4 contributes to the repression of *p21* after activation of *c-MYC*, c-MYC-induced repression of *p21* was demonstrated to occur independently of histone deacetylase activity⁵⁸⁶.

Since the bHLH-LZ domain and MycBox II were shown to be essential for c-MYC-mediated repression of *p21*^{CIP1}⁴¹⁵, other factors besides MIZ1, which binds the HLH domain of c-MYC³⁶¹, have been proposed to participate in c-MYC-mediated repression of *p21*⁴¹⁵. Since MycBox II is critical for transcriptional induction of many c-MYC target genes, as cyclin D2³²⁷, AP4 is a good candidate for this proposed factor. Furthermore, AP4 efficiently repressed *p21* and was critical for mitogen-mediated repression of p21. However, deletion of MycBox II affects the expression of most but not all c-MYC target genes³³⁴. Whether a mutant c-MYC protein lacking the MycBox II domain is still able to transactivate AP4 remains to be determined. The c-MYC-responsive region in the *p21* promoter was mapped between -49 and +16⁴¹⁵ which overlaps with two of the four AP4 binding sites present in the *p21* promoter. Mutation of these two sites had a strong effect on the responsiveness of the *p21* promoter to repression by AP4. Since MycBox II is required for recruitment of TRRAP and HAT activity^{324,327} it was speculated that TRRAP could also mediate trans-repression of

c-MYC target genes or that TRRAP or MycBox II might recruit different sets of transcriptional co-factors in a promoter-dependent manner⁴⁰⁴. However, the identity of these co-factors and the mechanism of their recruitment to c-MYC responsive promoters remains elusive. c-MYC-induced AP4, when bound to its cognate sequences located in the *p21* proximal promoter and therefore in the vicinity of the Inr element, might functionally cooperate with the MIZ1/c-MYC/TRRAP complex to achieve repression of *p21*. Nevertheless, the exact mechanism which AP4 uses to repress *p21* requires further investigation.

6.2.3 Role of AP4 in c-MYC-mediated anti-estrogen resistance during breast cancer therapy

The proto-oncogene c-MYC is amplified in 20-30% of breast cancer and several studies demonstrated that amplification of c-MYC is associated with a high proliferative capacity and poor prognosis in breast carcinoma^{274,596-599}. Amplification of c-MYC presumably represents an independent, powerful prognostic marker, which may even surpass the detection of *Her2/neu* amplification as a marker, which has been linked exclusively to steroid receptor-negative breast cancer disease^{271,600}.

c-MYC was shown to play a critical role in hormone-dependent and –independent breast tumor growth⁶⁰¹ and is associated with both hormone-independence and anti-estrogen resistance in breast cancer⁶⁰². ICI182,780/Fulvestrant (ICI) is a specific steroidal estrogen antagonist which was shown to be devoid of estrogen agonist activity in preclinical models⁶⁰³⁻⁶⁰⁵. Its value was also assessed clinically by administration before surgery as well as after failure of tamoxifen in patients with advanced breast cancer⁶⁰⁵⁻⁶⁰⁷. Treatment with ICI represents an additional step in the “endocrine therapy sequence” of ER-receptor positive breast carcinomas but can only delay anti-estrogen resistance in these tumors and the necessity to start chemotherapy⁶⁰⁸. However, activation of c-MYC is sufficient to overcome the antiproliferative effect of ICI⁶⁰⁹, which could be reproduced with the MCF-7-PJMMR1 cell line as part of this thesis. This effect of c-MYC activation is mediated by repression of p21^{588,589}. Under these circumstances, c-MYC efficiently induced expression of AP4. More important, induction of AP4 by c-MYC was necessary to alleviate a cell cycle arrest in ICI-treated MCF-7 cells. AP4 achieves this mitogenic effect presumably by decreasing the expression of p21 since

down-regulation of AP4 by RNA interference elevated the p21 level in this cellular background. It can be concluded that AP4 contributes to the mitogenicity of c-MYC in breast cancer cells and might represent an important mediator of anti-estrogen resistance downstream of activated *c-MYC*.

6.2.4 Effect of AP4 on TGF- β signaling

TGF- β represents an anti-mitogenic cytokine and its anti-proliferative effect plays a major role in epithelial tissue homeostasis⁶¹⁰. In agreement, TGF- β provides a tumor suppressive effect at early stages of carcinogenesis mainly via growth inhibition⁶¹⁰. However, at progressed stages in tumorigenesis, when cancer cells have acquired mutations which inactivate anti-mitogenic TGF- β signaling pathways, TGF- β shows a tumor promoting potential^{610,611}. TGF- β favors epithelial-to-mesenchymal transition (EMT) of carcinoma cells leading to increased invasion and metastasis⁶¹². Mechanistically, TGF- β -driven EMT is presumably mediated by loss of cellular adhesion molecules, activation of proteinases, immune-suppression and angiogenesis^{613,614}.

The cell cycle arrest caused by TGF- β can lead to terminal differentiation or promotes apoptosis⁶¹⁵. TGF- β signaling provokes cell cycle arrest in the G₁-phase by inhibition of *c-MYC* expression^{292,616}. In addition, TGF- β induces the CDK inhibitors *p15^{Ink4b}*⁶¹⁷ and *p21*⁶¹⁸ and downregulates the CDK-activating phosphatase *CDC25A*⁶¹⁹. Besides direct activation of *p15^{Ink4b}* and *p21* through TGF- β /Smad-responsive elements in their promoters^{360,524}, TGF- β is able to influence the repression of these CDK inhibitors by the *c-MYC* proto-oncogene^{360,620}. *c-MYC* in turn was shown to interact directly with Smad2 and Smad3 which abrogates TGF- β signaling. As a result, a large subset of TGF- β -responsive genes is influenced by this mechanism in *c-MYC*-transformed tumors⁶²¹. Here, the protein product of the *c-MYC* target gene *AP4* interfered with TGF- β -mediated induction of *p21* in HaCaT immortalized keratinocytes. This effect was achieved by *AP4*-delivery via adenoviral infection and was confirmed by 4-OHT-mediated activation of an *AP4-ER* fusion construct in order to exclude side-effects caused by the adenoviral infection procedure. However, *AP4*-mediated repression of *p21* did not prevent the TGF- β -mediated cell cycle arrest (data not shown).

Hematopoietic cell lines lacking p21 were shown to arrest after TGF- β treatment⁶²². Furthermore, cells derived from *p21* knock-out mice are still responsive to TGF- β ^{623,624} as is also the case for cell lines derived from *p15^{Ink4b}*-deficient mice⁶²⁵. Attenuation of the growth inhibitory effect of TGF- β is only possible by simultaneous ablation of several pathways downstream of TGF- β signaling as was demonstrated for over-expression of LIP, a potent inhibitor of TGF- β -mediated transcription regulation²⁹³. These data imply that suppression of the CDK-inhibitor p21 alone is not sufficient to alleviate the cell cycle arrest caused by activation of TGF- β signaling. Presumably, the concomitant regulation of other genes by TGF- β , as *p15^{Ink4b}* or *CDC25A*, is sufficient to mediate the cell cycle arrest in HaCaT keratinocytes. However, other processes downstream of TGF- β -mediated induction of *p21*, such as terminal differentiation⁶¹⁵, may be affected by elevated expression of AP4.

Abrogation of TGF- β signaling has been implicated in human colon cancer: mutations or loss of heterozygosity (LOH) which affect the TGF- β receptor mediator SMAD4 are found in familial juvenile polyposis (JPS), an autosomal dominant disease characterized by predisposition to gastrointestinal polyps and cancer^{626,627}. Since LOH (loss of heterozygosity) of SMAD4 occurs in invasive carcinomas but not in adenomas^{626,628}, inactivation of the TGF- β pathway likely happens at the transition to invasive cancer. Consistent with these earlier findings, conditional knock-out of TGF- β receptor II in mice does not give rise to spontaneous tumor formation but substantially enhances mutagen-induced carcinogenesis⁶²⁹. This implies that inactivation of tumor-suppressive TGF- β signaling is only able to promote tumorigenesis subsequently to initiation-events, which may involve activation of oncogenic pathways. SMAD4, together with SMAD2 and SMAD3 mediates the TGF- β -triggered induction of *p21* via enhancement of Sp1 affinity to the *p21* promoter^{523,630} which is blocked by ectopic expression of c-MYC⁵⁸⁶. The observed abrogation of TGF- β /Smad/p21 signaling by AP4 might contribute to TGF- β pathway inactivation in colorectal carcinomas which retain expression of wild type SMAD4 and may contribute to the morphogenetic changes observed during colon cancer formation by antagonizing the TGF- β pathway⁶³¹.

6.2.5 Role of AP4 in the DNA damage response

The decline of AP4 levels after DNA damage might be a prerequisite for efficient induction of *p21* by p53. The decrease of AP4 in this scenario is presumably caused by down-regulation of c-MYC upon treatment of cells with genotoxic drugs, as was already observed by Herbst et al.³¹⁹. Interestingly, the ubiquitin-specific protease USP28, which stabilizes c-MYC³⁰⁰, has been implicated in the DNA damage response pathway⁶³². Recently, it was found that USP28 dissociates from Fbw7 after UV irradiation and this promotes degradation c-MYC after genotoxic stress⁶³³. In addition to decreased protein stability, expression of *c-MYC* mRNA is repressed after DNA damage in a p53-dependent manner⁶³⁴.

As p21 is a potent inhibitor of cyclin dependent kinases, its repression by AP4 may contribute to the ability of c-MYC to activate CDKs⁶³⁵⁻⁶³⁷. AP4 in principle has this capability as it was able to block pRb hypophosphorylation after DNA damage. p21 plays a critical role in c-MYC-induced apoptosis⁶²⁰ and c-MYC selectively abrogates the ability of p53 to induce *p21* while p53-mediated induction of pro-apoptotic *PUMA* remains unaffected⁶²⁰ which favors an apoptotic response over cell cycle arrest. Consistent with these data, AP4 interfered with p53-mediated transactivation of *p21* and sensitized cells to apoptosis after treatment with genotoxic drugs used in cancer therapy. To which extent AP4 contributes to the accumulation of DNA damage downstream of activated c-MYC requires further investigation.

Due to its frequent inactivation in cancer and its potent anti-proliferative and proapoptotic effects, p53 is considered to be a powerful tumor suppressor⁵. While loss or mutation of p53 results in increased resistance to apoptosis provoked by various genotoxic drugs⁶³⁸, the loss of p53 function may also sensitize human cancer cells to apoptosis after DNA damage⁵⁴⁸. There is increasing evidence that tumors which lack p53 are even more sensitive to apoptosis than their wild-type p53-harboring counterparts^{639,640}. Especially the p53/p21 axis was demonstrated to be critical for sustained cell cycle arrest after DNA damage⁵⁰¹. Tumors which retain p21 were shown to undergo regrowth after IR exposure while tumor cells lacking p21 are completely erased by irradiation⁶⁴¹. Therefore, the AP4 status might predict the responsiveness of tumors which still express wild-type p53 to genotoxic drug- and irradiation-based cancer

therapy. The observation that AP4 was able to further repress the low, basal expression level of p21 in p53-negative colon cancer cells suggests that this might also hold true for p53-deficient tumors.

6.2.6 Role of AP4 in differentiation

Several studies have shown that down-regulation of c-MYC is required for terminal differentiation of many cell types^{411,467,642}. For example, ectopic expression of c-MYC blocks TPA-induced differentiation of U-937 myelomonoblasts by repressing the CDK inhibitor *p21*^{415,528}. *p21* itself plays an important role in monoblastic differentiation and supports survival of differentiated cells by maintaining a stable cell cycle arrest⁶⁴³⁻⁶⁴⁵. In agreement with these findings, ectopic expression of AP4 prevented a stable G₁ arrest and increased the apoptotic fraction of cells undergoing TPA-induced differentiation presumably by delaying the induction of *p21*. Furthermore, ectopic expression of AP4 substantially increased the fraction of cells undergoing DNA synthesis in the presence of differentiation-inducing TPA. While this effect is likely due to repression of *p21* by AP4 and, as a consequence, increased CDK activity, it cannot be excluded that other as yet unidentified transcriptional targets contribute to the cell cycle promoting capacity of AP4 in this scenario.

c-MYC is considered to play an important role in the homeostasis of hematopoietic cells^{421,646} and alterations of c-MYC expression result in hematopoietic malignancies^{257,647}. Furthermore, c-MYC is required for proliferation and expansion of the most early and late progenitor cells in hematopoietic tissue⁴²¹. *p21*-deficient mice display elevated proliferation and absolute number of hematopoietic stem cells (HSCs)⁶⁴⁸. In the future it will be interesting to reveal, which role repression of *p21* by AP4 plays during c-MYC-regulated HSC maintenance and differentiation. Elucidation of the complete transcriptional program downstream of activated *AP4* might help to clarify the importance of AP4 for proliferation and differentiation of hematopoietic cells.

6.2.7 Role of c-MYC / AP4 / p21 in colonic differentiation and colorectal carcinoma

The colonic epithelium is shaped into crypts⁶⁴⁹ with self-renewing stem cells being located at the bottom of these crypts⁶⁵⁰. The more committed progenitor cells, so called

“transit-amplifying” cells, originate from asymmetric stem cell divisions, have a limited self-renewing capacity and reside in the bottom third of the crypts⁶³¹. As these cells migrate along the vertical crypt axis, they inevitably differentiate into the mature cell lineages (enterocytes, enteroendocrine cells and goblet cells) and are finally shed by apoptosis⁶³¹. In the normal adult colonic crypt, homeostasis is maintained by morphogen gradients which determine the cellular fate dependent on the relative position of a cell within a crypt⁶³¹. Signaling by Wnt ligands is most prevalent at the base of crypts where it induces a precursor-cell phenotype of intestinal epithelial cells²⁸¹. While Wnt activity decreases when cells migrate along the crypt axis, these cells start to produce the hedgehog (Hh) family member indian Hh (IHH) which triggers their differentiation⁶⁵¹. IHH furthermore restricts Wnt target gene expression to the base of the colonic crypt while increased TCF4 levels due to activated Wnt signaling downregulate IHH expression⁶⁵¹. Additional morphogens regulating the homeostasis of colonic epithelium belong to the protein families of TGF- β , fibroblast growth factor (FGF), epithelial growth factor (EGF), keratinocyte growth factor (KGF), TGF- α and amphiregulin⁶³¹. While the underlying mechanisms as to how these molecules maintain homeostasis in the adult colonic epithelium is poorly understood, the importance of morphogenic signaling in tissue homeostasis is supported by increasing evidence that mutations affecting these pathways represent “initiators” at different stages of tumorigenesis.

The adenomatous polyposis coli tumor suppressor is encoded by the *APC* gene and germline mutations in *APC* were first associated with familial adenomatous polyposis (FAP), an inherited colorectal cancer syndrome⁶⁵². Inactivating *APC* mutations were also shown to represent a key early event in the development of sporadic colorectal cancer (CRC) disease⁶⁵³. Loss of *APC* function gives rise to constitutive activation of the β -catenin/TCF4 transcription complex⁶⁵⁴. Soon after these revelations, c-MYC was identified as a target of the Wnt/APC/ β -catenin/TCF4 pathway *in vitro*²⁸⁰ and in normal colonic crypts *in vivo*²⁸¹. In normal colonic epithelium, c-MYC is able to promote self-renewal of intestinal stem cells and is necessary for normal crypt morphogenesis⁴¹⁸. The data presented here show that AP4 expression in normal human colonic crypts is restricted to the non-differentiated, proliferative progenitor compartments. The expression pattern of AP4 correlates with the expression of c-MYC, which is

downregulated during differentiation²⁸¹ presumably due to decreasing levels of nuclear TCF4/ β -catenin⁶⁵¹. As expected, the progenitor cell compartments of colonic epithelium were devoid of p21 expression which is restricted to the distal, differentiated areas of the crypts^{281,530}. The pattern of AP4 expression in normal colonic crypts is therefore consistent with a role of AP4 as a c-MYC-inducible repressor of *p21* and the observation that AP4 interferes with up-regulation of p21 and cell cycle arrest during cellular differentiation.

Conditional *APC* knock-out mice provided the first *in vivo* evidence that inactivation of *c-MYC* represents an early event after loss of *APC*²⁸². Recently, Sansom et al. used the same transgenic model to demonstrate that parallel deletion of *c-MYC* and *APC* rescues the elevated proliferation and apoptosis displayed by *APC*-deficient crypts⁶⁵⁵. Even more interesting, concomitant loss of *c-MYC* rescues abnormal cell migration and differentiation of *APC*-deficient colonic crypts and restores a normal crypt architecture⁶⁵⁵. Biopsies from primary CRCs derived from 12 patients displayed a high expression of AP4 in compartments positive for *c-MYC* and Ki-67 expression. These regions were devoid of detectable expression of p21 which only occurred sporadically and in non-proliferative areas of the analyzed tumors. Down-regulation of *p21* is a known phenomenon during colorectal carcinogenesis which is presumably caused by oncogenic activation of *c-MYC*^{281,282,530}.

The data obtained from immunohistochemistry suggest that AP4 contributes to the high proliferative capacity of activated *c-MYC* in tumor cells and AP4 might support a non-differentiated state in normal and malignant tissues. However, the *in vivo* contribution of AP4 to tumor formation and progression requires further investigation. A possible approach would be to use conditional gene knock-out or RNA interference-based techniques to ask whether AP4-inactivation results in regression of *c-MYC*-driven tumors in mouse models.

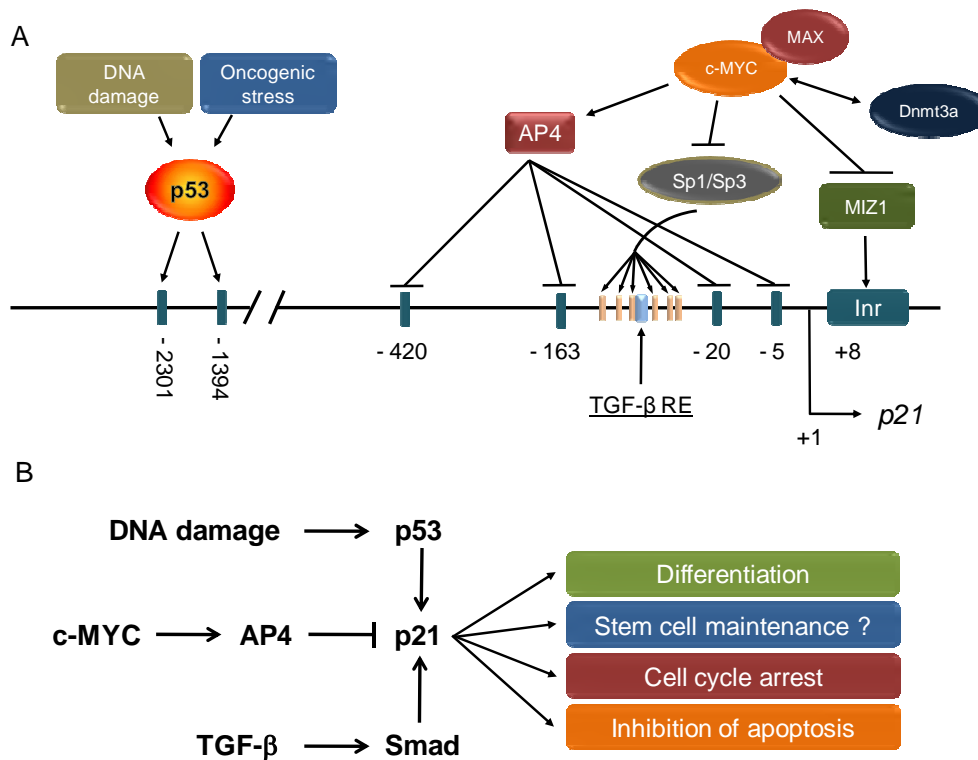


Figure 51: AP4 represents a novel mediator of c-MYC-induced repression of *p21* and interferes with a stable cell cycle arrest during genotoxic stress and differentiation.

A, In this model, c-MYC, besides repressing *p21* via inhibitory association with transcription factors MIZ1 and Sp1/Sp3 or recruitment of the co-repressor Dnmt3a, directly induces expression of AP4 whose protein product represents a transcriptional repressor. AP4 binds to CAGCTG sites located within the *p21* proximal promoter region and acts as a repressor of *p21*. The tumor suppressor p53 and the cytostatic cytokine TGF- β (via Smad) induce *p21* through the indicated response elements.

B, AP4 blocks the induction of *p21* by the DNA damage/p53 and TGF- β /Smad pathways. The c-MYC/AP4/*p21* cascade interferes with cell cycle arrest, blocks differentiation and sensitizes cells to genotoxic drug-mediated apoptosis. AP4 presumably plays a role in stem cell maintenance and –differentiation. TGF- β RE: TGF- β -responsive element.

Taken together, this study revealed that AP4 is a critical new component of the c-MYC target gene network and for the first time provides evidence that c-MYC directly regulates the expression of a transcriptional repressor, AP4, to repress the CDK inhibitor *p21*. It is likely that AP4 coordinates a wider-ranging transcriptional program downstream of activated c-MYC. Future genome-wide studies will reveal the spectrum of AP4-deregulated genes and help to uncover which functional aspects of oncogenic c-MYC might be mediated by AP4.

7 Summary

In this study, Cul7 was identified as a new p53-interactor by an iTAP/MudPIT analysis. *Cul7* mRNA and protein levels increased after DNA damage in several cell lines in a p53-independent and caffeine-sensitive manner, suggesting that members of the PIKK kinase family are responsible for Cul7-induction. Acute ablation of Cul7 by specific microRNAs augmented p53 activity culminating in elevated expression of p21 and cell cycle arrest in the G₁ phase. Ectopic Cul7 prevented the establishment of a stable, p53/p21-mediated cell cycle arrest which ultimately resulted in an apoptotic response. Cul7 recruited the SCF7 E3-ligase subunit Fbx29 to p53. However, Cul7/Fbx29 did not target p53 for mono- or poly-ubiquitination *in vivo*. These results reveal a new aspect of p53 regulation: after DNA damage, the negative regulator Cul7 is induced concomitantly with p53 and limits p53 activity by direct association.

In the second part of this work, AP4 was established as a c-MYC-inducible repressor of *p21*. *AP4* is a direct, evolutionary conserved c-MYC target gene. Downregulation of AP4 by RNA interference led to accumulation of p21. AP4 itself mediates repression of *p21* via binding to CAGCTG motifs located in the *p21* promoter. Induction of *AP4* was required for c-MYC to overcome a p21-dependent cell cycle arrest and for downregulation of p21 after mitogen-stimulation of cells. AP4 interfered with induction of *p21* via the DNA damage/p53 and TGF- β /Smad pathways and also during differentiation. DNA damage and differentiation-promoting stimuli provoked a decline in AP4 levels and the ectopic expression of AP4 counteracted cell cycle arrest in these scenarios resulting in cell cycle progression, apoptosis or presumably block of differentiation. In colonic epithelium, expression of AP4 occurred in progenitor cell compartments, overlapped with expression of c-MYC and inversely correlated with expression of p21. AP4 and c-MYC were highly expressed in proliferative compartments of colorectal cancer. In conclusion, AP4 presumably represents an important mediator of the mitogenic and oncogenic functions of c-MYC.

8 References

1. Weinberg, R. A. *The biology of cancer* (Garland Science, 2007).
2. Vogelstein, B. & Kinzler, K. W. The multistep nature of cancer. *Trends Genet* **9**, 138-41 (1993).
3. Weinberg, R. A. How cancer arises. *Sci Am* **275**, 62-70 (1996).
4. Bishop, J. M. Cancer: the rise of the genetic paradigm. *Genes Dev* **9**, 1309-15 (1995).
5. Vogelstein, B., Lane, D. & Levine, A. J. Surfing the p53 network. *Nature* **408**, 307-10 (2000).
6. Vousden, K. H. & Lane, D. P. p53 in health and disease. *Nat Rev Mol Cell Biol* **8**, 275-83 (2007).
7. Kress, M., May, E., Cassingena, R. & May, P. Simian virus 40-transformed cells express new species of proteins precipitable by anti-simian virus 40 tumor serum. *J Virol* **31**, 472-83 (1979).
8. Linzer, D. I. & Levine, A. J. Characterization of a 54K dalton cellular SV40 tumor antigen present in SV40-transformed cells and uninfected embryonal carcinoma cells. *Cell* **17**, 43-52 (1979).
9. Braithwaite, A. W. et al. Mouse p53 inhibits SV40 origin-dependent DNA replication. *Nature* **329**, 458-60 (1987).
10. Finlay, C. A., Hinds, P. W. & Levine, A. J. The p53 proto-oncogene can act as a suppressor of transformation. *Cell* **57**, 1083-93 (1989).
11. Eliyahu, D., Michalovitz, D., Eliyahu, S., Pinhasi-Kimhi, O. & Oren, M. Wild-type p53 can inhibit oncogene-mediated focus formation. *Proc Natl Acad Sci U S A* **86**, 8763-7 (1989).
12. Wang, E. H., Friedman, P. N. & Prives, C. The murine p53 protein blocks replication of SV40 DNA in vitro by inhibiting the initiation functions of SV40 large T antigen. *Cell* **57**, 379-92 (1989).
13. Hollstein, M., Sidransky, D., Vogelstein, B. & Harris, C. C. p53 mutations in human cancers. *Science* **253**, 49-53 (1991).
14. Baker, S. J. et al. Chromosome 17 deletions and p53 gene mutations in colorectal carcinomas. *Science* **244**, 217-21 (1989).
15. Baker, S. J., Markowitz, S., Fearon, E. R., Willson, J. K. & Vogelstein, B. Suppression of human colorectal carcinoma cell growth by wild-type p53. *Science* **249**, 912-5 (1990).
16. Hinds, P., Finlay, C. & Levine, A. J. Mutation is required to activate the p53 gene for cooperation with the ras oncogene and transformation. *J Virol* **63**, 739-46 (1989).
17. Bykov, V. J. & Wiman, K. G. Novel cancer therapy by reactivation of the p53 apoptosis pathway. *Ann Med* **35**, 458-65 (2003).
18. Chang, J., Kim, D. H., Lee, S. W., Choi, K. Y. & Sung, Y. C. Transactivation ability of p53 transcriptional activation domain is directly related to the binding affinity to TATA-binding protein. *J Biol Chem* **270**, 25014-9 (1995).
19. Romer, L., Klein, C., Dehner, A., Kessler, H. & Buchner, J. p53--a natural cancer killer: structural insights and therapeutic concepts. *Angew Chem Int Ed Engl* **45**, 6440-60 (2006).
20. Dawson, R. et al. The N-terminal domain of p53 is natively unfolded. *J Mol Biol* **332**, 1131-41 (2003).
21. Lee, H. et al. Local structural elements in the mostly unstructured transcriptional activation domain of human p53. *J Biol Chem* **275**, 29426-32 (2000).
22. Sigler, P. B. Transcriptional activation. Acid blobs and negative noodles. *Nature* **333**, 210-2 (1988).
23. Hahn, S. Transcription. Efficiency in activation. *Nature* **363**, 672-3 (1993).
24. Kussie, P. H. et al. Structure of the MDM2 oncoprotein bound to the p53 tumor suppressor transactivation domain. *Science* **274**, 948-53 (1996).
25. Uesugi, M. & Verdine, G. L. The alpha-helical FXXPhiPhi motif in p53: TAF interaction and discrimination by MDM2. *Proc Natl Acad Sci U S A* **96**, 14801-6 (1999).
26. Zhang, Y. & Xiong, Y. A p53 amino-terminal nuclear export signal inhibited by DNA damage-induced phosphorylation. *Science* **292**, 1910-5 (2001).
27. el-Deiry, W. S., Kern, S. E., Pietenpol, J. A., Kinzler, K. W. & Vogelstein, B. Definition of a consensus binding site for p53. *Nat Genet* **1**, 45-9 (1992).
28. Balagurumorthy, P. et al. Four p53 DNA-binding domain peptides bind natural p53-response elements and bend the DNA. *Proc Natl Acad Sci U S A* **92**, 8591-5 (1995).

References

29. Beroud, C. & Soussi, T. The UMD-p53 database: new mutations and analysis tools. *Hum Mutat* **21**, 176-81 (2003).
30. Petitjean, A. et al. Impact of mutant p53 functional properties on TP53 mutation patterns and tumor phenotype: lessons from recent developments in the IARC TP53 database. *Hum Mutat* **28**, 622-9 (2007).
31. Jeffrey, P. D., Gorina, S. & Pavletich, N. P. Crystal structure of the tetramerization domain of the p53 tumor suppressor at 1.7 angstroms. *Science* **267**, 1498-502 (1995).
32. Clore, G. M. et al. Refined solution structure of the oligomerization domain of the tumour suppressor p53. *Nat Struct Biol* **2**, 321-33 (1995).
33. Lee, W. et al. Solution structure of the tetrameric minimum transforming domain of p53. *Nat Struct Biol* **1**, 877-90 (1994).
34. Chene, P. The role of tetramerization in p53 function. *Oncogene* **20**, 2611-7 (2001).
35. Stommel, J. M. et al. A leucine-rich nuclear export signal in the p53 tetramerization domain: regulation of subcellular localization and p53 activity by NES masking. *Embo J* **18**, 1660-72 (1999).
36. Liang, S. H. & Clarke, M. F. A bipartite nuclear localization signal is required for p53 nuclear import regulated by a carboxyl-terminal domain. *J Biol Chem* **274**, 32699-703 (1999).
37. Hupp, T. R., Meek, D. W., Midgley, C. A. & Lane, D. P. Regulation of the specific DNA binding function of p53. *Cell* **71**, 875-86 (1992).
38. Ahn, J. & Prives, C. The C-terminus of p53: the more you learn the less you know. *Nat Struct Biol* **8**, 730-2 (2001).
39. Klein, C. et al. NMR spectroscopy reveals the solution dimerization interface of p53 core domains bound to their consensus DNA. *J Biol Chem* **276**, 49020-7 (2001).
40. Hupp, T. R. & Lane, D. P. Allosteric activation of latent p53 tetramers. *Curr Biol* **4**, 865-75 (1994).
41. Wang, Y. et al. p53 domains: identification and characterization of two autonomous DNA-binding regions. *Genes Dev* **7**, 2575-86 (1993).
42. Anderson, M. E., Woelker, B., Reed, M., Wang, P. & Tegtmeyer, P. Reciprocal interference between the sequence-specific core and nonspecific C-terminal DNA binding domains of p53: implications for regulation. *Mol Cell Biol* **17**, 6255-64 (1997).
43. Maltzman, W. & Czyzyk, L. UV irradiation stimulates levels of p53 cellular tumor antigen in nontransformed mouse cells. *Mol Cell Biol* **4**, 1689-94 (1984).
44. Brooks, C. L. & Gu, W. p53 ubiquitination: Mdm2 and beyond. *Mol Cell* **21**, 307-15 (2006).
45. Fang, S., Jensen, J. P., Ludwig, R. L., Vousden, K. H. & Weissman, A. M. Mdm2 is a RING finger-dependent ubiquitin protein ligase for itself and p53. *J Biol Chem* **275**, 8945-51 (2000).
46. Jones, S. N., Roe, A. E., Donehower, L. A. & Bradley, A. Rescue of embryonic lethality in Mdm2-deficient mice by absence of p53. *Nature* **378**, 206-8 (1995).
47. Montes de Oca Luna, R., Wagner, D. S. & Lozano, G. Rescue of early embryonic lethality in mdm2-deficient mice by deletion of p53. *Nature* **378**, 203-6 (1995).
48. Barak, Y., Juven, T., Haffner, R. & Oren, M. mdm2 expression is induced by wild type p53 activity. *Embo J* **12**, 461-8 (1993).
49. Wu, X., Bayle, J. H., Olson, D. & Levine, A. J. The p53-mdm-2 autoregulatory feedback loop. *Genes Dev* **7**, 1126-32 (1993).
50. Oliner, J. D., Kinzler, K. W., Meltzer, P. S., George, D. L. & Vogelstein, B. Amplification of a gene encoding a p53-associated protein in human sarcomas. *Nature* **358**, 80-3 (1992).
51. Momand, J., Jung, D., Wilczynski, S. & Niland, J. The MDM2 gene amplification database. *Nucleic Acids Res* **26**, 3453-9 (1998).
52. Bond, G. L. et al. A single nucleotide polymorphism in the MDM2 promoter attenuates the p53 tumor suppressor pathway and accelerates tumor formation in humans. *Cell* **119**, 591-602 (2004).
53. Rodriguez, M. S., Desterro, J. M., Lain, S., Lane, D. P. & Hay, R. T. Multiple C-terminal lysine residues target p53 for ubiquitin-proteasome-mediated degradation. *Mol Cell Biol* **20**, 8458-67 (2000).
54. Lai, Z. et al. Human mdm2 mediates multiple mono-ubiquitination of p53 by a mechanism requiring enzyme isomerization. *J Biol Chem* **276**, 31357-67 (2001).
55. Li, M. et al. Mono- versus polyubiquitination: differential control of p53 fate by Mdm2. *Science* **302**, 1972-5 (2003).

References

56. Grossman, S. R. et al. Polyubiquitination of p53 by a ubiquitin ligase activity of p300. *Science* **300**, 342-4 (2003).
57. Grossman, S. R. p300/CBP/p53 interaction and regulation of the p53 response. *Eur J Biochem* **268**, 2773-8 (2001).
58. Gronroos, E., Terentiev, A. A., Punga, T. & Ericsson, J. YY1 inhibits the activation of the p53 tumor suppressor in response to genotoxic stress. *Proc Natl Acad Sci U S A* **101**, 12165-70 (2004).
59. Sui, G. et al. Yin Yang 1 is a negative regulator of p53. *Cell* **117**, 859-72 (2004).
60. Li, L. et al. PACT is a negative regulator of p53 and essential for cell growth and embryonic development. *Proc Natl Acad Sci U S A* **104**, 7951-6 (2007).
61. Higashitsuji, H. et al. The oncoprotein gankyrin binds to MDM2/HDM2, enhancing ubiquitylation and degradation of p53. *Cancer Cell* **8**, 75-87 (2005).
62. Dawson, S. et al. Gankyrin is an ankyrin-repeat oncoprotein that interacts with CDK4 kinase and the S6 ATPase of the 26 S proteasome. *J Biol Chem* **277**, 10893-902 (2002).
63. Feng, L., Lin, T., Uranishi, H., Gu, W. & Xu, Y. Functional analysis of the roles of posttranslational modifications at the p53 C terminus in regulating p53 stability and activity. *Mol Cell Biol* **25**, 5389-95 (2005).
64. Krummel, K. A., Lee, C. J., Toledo, F. & Wahl, G. M. The C-terminal lysines fine-tune P53 stress responses in a mouse model but are not required for stability control or transactivation. *Proc Natl Acad Sci U S A* **102**, 10188-93 (2005).
65. Leng, R. P. et al. Pirh2, a p53-induced ubiquitin-protein ligase, promotes p53 degradation. *Cell* **112**, 779-91 (2003).
66. Dornan, D. et al. COP1, the negative regulator of p53, is overexpressed in breast and ovarian adenocarcinomas. *Cancer Res* **64**, 7226-30 (2004).
67. Chen, D. et al. ARF-BP1/Mule is a critical mediator of the ARF tumor suppressor. *Cell* **121**, 1071-83 (2005).
68. Scheffner, M., Huibregtse, J. M., Vierstra, R. D. & Howley, P. M. The HPV-16 E6 and E6-AP complex functions as a ubiquitin-protein ligase in the ubiquitination of p53. *Cell* **75**, 495-505 (1993).
69. Esser, C., Scheffner, M. & Hohfeld, J. The chaperone-associated ubiquitin ligase CHIP is able to target p53 for proteasomal degradation. *J Biol Chem* **280**, 27443-8 (2005).
70. Yamasaki, S. et al. Cytoplasmic destruction of p53 by the endoplasmic reticulum-resident ubiquitin ligase 'Synoviolin'. *Embo J* **26**, 113-22 (2007).
71. Nikolaev, A. Y., Li, M., Puskas, N., Qin, J. & Gu, W. Parc: a cytoplasmic anchor for p53. *Cell* **112**, 29-40 (2003).
72. Nikolaev, A. Y. & Gu, W. PARC: a potential target for cancer therapy. *Cell Cycle* **2**, 169-71 (2003).
73. Imai, Y. et al. CHIP is associated with Parkin, a gene responsible for familial Parkinson's disease, and enhances its ubiquitin ligase activity. *Mol Cell* **10**, 55-67 (2002).
74. Le Cam, L. et al. E4F1 is an atypical ubiquitin ligase that modulates p53 effector functions independently of degradation. *Cell* **127**, 775-88 (2006).
75. Cummins, J. M. et al. Tumour suppression: disruption of HAUSP gene stabilizes p53. *Nature* **428**, 1 p following 486 (2004).
76. Li, M., Brooks, C. L., Kon, N. & Gu, W. A dynamic role of HAUSP in the p53-Mdm2 pathway. *Mol Cell* **13**, 879-86 (2004).
77. Tang, J. et al. Critical role for Daxx in regulating Mdm2. *Nat Cell Biol* **8**, 855-62 (2006).
78. Meulmeester, E. et al. Loss of HAUSP-mediated deubiquitination contributes to DNA damage-induced destabilization of Hdmx and Hdm2. *Mol Cell* **18**, 565-76 (2005).
79. Li, M. et al. Deubiquitination of p53 by HAUSP is an important pathway for p53 stabilization. *Nature* **416**, 648-53 (2002).
80. Stevenson, L. F. et al. The deubiquitinating enzyme USP2a regulates the p53 pathway by targeting Mdm2. *Embo J* **26**, 976-86 (2007).
81. Xirodimas, D. P., Saville, M. K., Bourdon, J. C., Hay, R. T. & Lane, D. P. Mdm2-mediated NEDD8 conjugation of p53 inhibits its transcriptional activity. *Cell* **118**, 83-97 (2004).
82. Abida, W. M., Nikolaev, A., Zhao, W., Zhang, W. & Gu, W. FBXO11 promotes the Neddylaton of p53 and inhibits its transcriptional activity. *J Biol Chem* **282**, 1797-804 (2007).

References

83. Gostissa, M. et al. Activation of p53 by conjugation to the ubiquitin-like protein SUMO-1. *Embo J* **18**, 6462-71 (1999).
84. Rodriguez, M. S. et al. SUMO-1 modification activates the transcriptional response of p53. *Embo J* **18**, 6455-61 (1999).
85. Kahyo, T., Nishida, T. & Yasuda, H. Involvement of PIAS1 in the sumoylation of tumor suppressor p53. *Mol Cell* **8**, 713-8 (2001).
86. Nelson, V., Davis, G. E. & Maxwell, S. A. A putative protein inhibitor of activated STAT (PIASy) interacts with p53 and inhibits p53-mediated transactivation but not apoptosis. *Apoptosis* **6**, 221-34 (2001).
87. Megidish, T., Xu, J. H. & Xu, C. W. Activation of p53 by protein inhibitor of activated Stat1 (PIAS1). *J Biol Chem* **277**, 8255-9 (2002).
88. Schmidt, D. & Muller, S. Members of the PIAS family act as SUMO ligases for c-Jun and p53 and repress p53 activity. *Proc Natl Acad Sci U S A* **99**, 2872-7 (2002).
89. Watson, I. R. & Irwin, M. S. Ubiquitin and ubiquitin-like modifications of the p53 family. *Neoplasia* **8**, 655-66 (2006).
90. Melchior, F. & Hengst, L. SUMO-1 and p53. *Cell Cycle* **1**, 245-9 (2002).
91. Li, T. et al. Expression of SUMO-2/3 induced senescence through p53- and pRB-mediated pathways. *J Biol Chem* **281**, 36221-7 (2006).
92. Bischof, O. et al. The E3 SUMO ligase PIASy is a regulator of cellular senescence and apoptosis. *Mol Cell* **22**, 783-94 (2006).
93. Lee, M. H. et al. SUMO-specific protease SUSP4 positively regulates p53 by promoting Mdm2 self-ubiquitination. *Nat Cell Biol* **8**, 1424-31 (2006).
94. Marine, J. C., Dyer, M. A. & Jochemsen, A. G. MDMX: from bench to bedside. *J Cell Sci* **120**, 371-8 (2007).
95. Finch, R. A. et al. mdmx is a negative regulator of p53 activity in vivo. *Cancer Res* **62**, 3221-5 (2002).
96. Migliorini, D. et al. Mdm4 (Mdmx) regulates p53-induced growth arrest and neuronal cell death during early embryonic mouse development. *Mol Cell Biol* **22**, 5527-38 (2002).
97. Parant, J. et al. Rescue of embryonic lethality in Mdm4-null mice by loss of Trp53 suggests a nonoverlapping pathway with MDM2 to regulate p53. *Nat Genet* **29**, 92-5 (2001).
98. Shvarts, A. et al. MDMX: a novel p53-binding protein with some functional properties of MDM2. *Embo J* **15**, 5349-57 (1996).
99. Jackson, M. W. & Berberich, S. J. MdmX protects p53 from Mdm2-mediated degradation. *Mol Cell Biol* **20**, 1001-7 (2000).
100. Stad, R. et al. Mdmx stabilizes p53 and Mdm2 via two distinct mechanisms. *EMBO Rep* **2**, 1029-34 (2001).
101. Francoz, S. et al. Mdm4 and Mdm2 cooperate to inhibit p53 activity in proliferating and quiescent cells in vivo. *Proc Natl Acad Sci U S A* **103**, 3232-7 (2006).
102. Xiong, S., Van Pelt, C. S., Elizondo-Fraire, A. C., Liu, G. & Lozano, G. Synergistic roles of Mdm2 and Mdm4 for p53 inhibition in central nervous system development. *Proc Natl Acad Sci U S A* **103**, 3226-31 (2006).
103. Toledo, F. et al. A mouse p53 mutant lacking the proline-rich domain rescues Mdm4 deficiency and provides insight into the Mdm2-Mdm4-p53 regulatory network. *Cancer Cell* **9**, 273-85 (2006).
104. Poyurovsky, M. V. et al. The Mdm2 RING domain C-terminus is required for supramolecular assembly and ubiquitin ligase activity. *Embo J* **26**, 90-101 (2007).
105. Uldrijan, S., Pannekoek, W. J. & Vousden, K. H. An essential function of the extreme C-terminus of MDM2 can be provided by MDMX. *Embo J* **26**, 102-12 (2007).
106. Lane, D. P. Cancer. p53, guardian of the genome. *Nature* **358**, 15-6 (1992).
107. Horn, H. F. & Vousden, K. H. Coping with stress: multiple ways to activate p53. *Oncogene* **26**, 1306-16 (2007).
108. Shiloh, Y. ATM and ATR: networking cellular responses to DNA damage. *Curr Opin Genet Dev* **11**, 71-7 (2001).
109. Shiloh, Y. ATM and related protein kinases: safeguarding genome integrity. *Nat Rev Cancer* **3**, 155-68 (2003).

References

110. Bartek, J., Lukas, C. & Lukas, J. Checking on DNA damage in S phase. *Nat Rev Mol Cell Biol* **5**, 792-804 (2004).
111. Barzilai, A. & Yamamoto, K. DNA damage responses to oxidative stress. *DNA Repair (Amst)* **3**, 1109-15 (2004).
112. Liu, Q. et al. Chk1 is an essential kinase that is regulated by Atr and required for the G(2)/M DNA damage checkpoint. *Genes Dev* **14**, 1448-59 (2000).
113. Appella, E. & Anderson, C. W. Post-translational modifications and activation of p53 by genotoxic stresses. *Eur J Biochem* **268**, 2764-72 (2001).
114. Jazayeri, A. et al. ATM- and cell cycle-dependent regulation of ATR in response to DNA double-strand breaks. *Nat Cell Biol* **8**, 37-45 (2006).
115. Myers, J. S. & Cortez, D. Rapid activation of ATR by ionizing radiation requires ATM and Mre11. *J Biol Chem* **281**, 9346-50 (2006).
116. Saito, S. et al. ATM mediates phosphorylation at multiple p53 sites, including Ser(46), in response to ionizing radiation. *J Biol Chem* **277**, 12491-4 (2002).
117. Tibbetts, R. S. et al. A role for ATR in the DNA damage-induced phosphorylation of p53. *Genes Dev* **13**, 152-7 (1999).
118. Shieh, S. Y., Ikeda, M., Taya, Y. & Prives, C. DNA damage-induced phosphorylation of p53 alleviates inhibition by MDM2. *Cell* **91**, 325-34 (1997).
119. Unger, T. et al. Critical role for Ser20 of human p53 in the negative regulation of p53 by Mdm2. *Embo J* **18**, 1805-14 (1999).
120. Maya, R. et al. ATM-dependent phosphorylation of Mdm2 on serine 395: role in p53 activation by DNA damage. *Genes Dev* **15**, 1067-77 (2001).
121. Meulmeester, E., Pereg, Y., Shiloh, Y. & Jochemsen, A. G. ATM-mediated phosphorylations inhibit Mdmx/Mdm2 stabilization by HAUSP in favor of p53 activation. *Cell Cycle* **4**, 1166-70 (2005).
122. Dornan, D. et al. ATM engages autodegradation of the E3 ubiquitin ligase COP1 after DNA damage. *Science* **313**, 1122-6 (2006).
123. Duan, S. et al. Phosphorylation of Pirh2 by Calmodulin-dependent kinase II impairs its ability to ubiquitinate p53. *Embo J* **26**, 3062-74 (2007).
124. Bode, A. M. & Dong, Z. Post-translational modification of p53 in tumorigenesis. *Nat Rev Cancer* **4**, 793-805 (2004).
125. Saito, S. et al. Phosphorylation site interdependence of human p53 post-translational modifications in response to stress. *J Biol Chem* **278**, 37536-44 (2003).
126. Sakaguchi, K. et al. Damage-mediated phosphorylation of human p53 threonine 18 through a cascade mediated by a casein 1-like kinase. Effect on Mdm2 binding. *J Biol Chem* **275**, 9278-83 (2000).
127. Higashimoto, Y. et al. Human p53 is phosphorylated on serines 6 and 9 in response to DNA damage-inducing agents. *J Biol Chem* **275**, 23199-203 (2000).
128. Stommel, J. M. & Wahl, G. M. Accelerated MDM2 auto-degradation induced by DNA-damage kinases is required for p53 activation. *Embo J* **23**, 1547-56 (2004).
129. Avantaggiati, M. L. et al. Recruitment of p300/CBP in p53-dependent signal pathways. *Cell* **89**, 1175-84 (1997).
130. Gu, W. & Roeder, R. G. Activation of p53 sequence-specific DNA binding by acetylation of the p53 C-terminal domain. *Cell* **90**, 595-606 (1997).
131. Sakaguchi, K. et al. DNA damage activates p53 through a phosphorylation-acetylation cascade. *Genes Dev* **12**, 2831-41 (1998).
132. Liu, L. et al. p53 sites acetylated in vitro by PCAF and p300 are acetylated in vivo in response to DNA damage. *Mol Cell Biol* **19**, 1202-9 (1999).
133. Ito, A. et al. p300/CBP-mediated p53 acetylation is commonly induced by p53-activating agents and inhibited by MDM2. *Embo J* **20**, 1331-40 (2001).
134. Sabbatini, P. & McCormick, F. MDMX inhibits the p300/CBP-mediated acetylation of p53. *DNA Cell Biol* **21**, 519-25 (2002).
135. Lambert, P. F., Kashanchi, F., Radonovich, M. F., Shiekhattar, R. & Brady, J. N. Phosphorylation of p53 serine 15 increases interaction with CBP. *J Biol Chem* **273**, 33048-53 (1998).
136. Juan, L. J. et al. Histone deacetylases specifically down-regulate p53-dependent gene activation. *J Biol Chem* **275**, 20436-43 (2000).

References

137. Luo, J., Su, F., Chen, D., Shiloh, A. & Gu, W. Deacetylation of p53 modulates its effect on cell growth and apoptosis. *Nature* **408**, 377-81 (2000).
138. Vaziri, H. et al. hSIR2(SIRT1) functions as an NAD-dependent p53 deacetylase. *Cell* **107**, 149-59 (2001).
139. Langley, E. et al. Human SIR2 deacetylates p53 and antagonizes PML/p53-induced cellular senescence. *Embo J* **21**, 2383-96 (2002).
140. Solomon, J. M. et al. Inhibition of SIRT1 catalytic activity increases p53 acetylation but does not alter cell survival following DNA damage. *Mol Cell Biol* **26**, 28-38 (2006).
141. Huang, J. et al. Repression of p53 activity by Smyd2-mediated methylation. *Nature* **444**, 629-32 (2006).
142. Yang, W. H. et al. Modification of p53 with O-linked N-acetylglucosamine regulates p53 activity and stability. *Nat Cell Biol* **8**, 1074-83 (2006).
143. Chuikov, S. et al. Regulation of p53 activity through lysine methylation. *Nature* **432**, 353-60 (2004).
144. Shi, X. et al. Modulation of p53 function by SET8-mediated methylation at lysine 382. *Mol Cell* **27**, 636-46 (2007).
145. Toledo, F. & Wahl, G. M. Regulating the p53 pathway: in vitro hypotheses, in vivo veritas. *Nat Rev Cancer* **6**, 909-23 (2006).
146. Dornan, D. et al. The ubiquitin ligase COP1 is a critical negative regulator of p53. *Nature* **429**, 86-92 (2004).
147. Hermeking, H. & Eick, D. Mediation of c-Myc-induced apoptosis by p53. *Science* **265**, 2091-3 (1994).
148. Wagner, A. J., Kokontis, J. M. & Hay, N. Myc-mediated apoptosis requires wild-type p53 in a manner independent of cell cycle arrest and the ability of p53 to induce p21/waf1/cip1. *Genes Dev* **8**, 2817-30 (1994).
149. Palmero, I., Pantoja, C. & Serrano, M. p19ARF links the tumour suppressor p53 to Ras. *Nature* **395**, 125-6 (1998).
150. Bates, S. et al. p14ARF links the tumour suppressors RB and p53. *Nature* **395**, 124-5 (1998).
151. Lowe, S. W. & Ruley, H. E. Stabilization of the p53 tumor suppressor is induced by adenovirus 5 E1A and accompanies apoptosis. *Genes Dev* **7**, 535-45 (1993).
152. Cong, F., Zou, X., Hinrichs, K., Calame, K. & Goff, S. P. Inhibition of v-Abl transformation by p53 and p19ARF. *Oncogene* **18**, 7731-9 (1999).
153. Damalas, A., Kahan, S., Shtutman, M., Ben-Ze'ev, A. & Oren, M. Deregulated beta-catenin induces a p53- and ARF-dependent growth arrest and cooperates with Ras in transformation. *Embo J* **20**, 4912-22 (2001).
154. Gil, J. & Peters, G. Regulation of the INK4b-ARF-INK4a tumour suppressor locus: all for one or one for all. *Nat Rev Mol Cell Biol* **7**, 667-77 (2006).
155. Sherr, C. J. Divorcing ARF and p53: an unsettled case. *Nat Rev Cancer* **6**, 663-73 (2006).
156. Pomerantz, J. et al. The Ink4a tumor suppressor gene product, p19Arf, interacts with MDM2 and neutralizes MDM2's inhibition of p53. *Cell* **92**, 713-23 (1998).
157. Kamijo, T. et al. Functional and physical interactions of the ARF tumor suppressor with p53 and Mdm2. *Proc Natl Acad Sci U S A* **95**, 8292-7 (1998).
158. Stott, F. J. et al. The alternative product from the human CDKN2A locus, p14(ARF), participates in a regulatory feedback loop with p53 and MDM2. *Embo J* **17**, 5001-14 (1998).
159. Lohrum, M. A., Ludwig, R. L., Kubbutat, M. H., Hanlon, M. & Vousden, K. H. Regulation of HDM2 activity by the ribosomal protein L11. *Cancer Cell* **3**, 577-87 (2003).
160. Kamijo, T., Bodner, S., van de Kamp, E., Randle, D. H. & Sherr, C. J. Tumor spectrum in ARF-deficient mice. *Cancer Res* **59**, 2217-22 (1999).
161. Kamijo, T. et al. Tumor suppression at the mouse INK4a locus mediated by the alternative reading frame product p19ARF. *Cell* **91**, 649-59 (1997).
162. Kamijo, T. et al. Loss of the ARF tumor suppressor reverses premature replicative arrest but not radiation hypersensitivity arising from disabled atm function. *Cancer Res* **59**, 2464-9 (1999).
163. Donehower, L. A. et al. Mice deficient for p53 are developmentally normal but susceptible to spontaneous tumours. *Nature* **356**, 215-21 (1992).
164. Jacks, T. et al. Tumor spectrum analysis in p53-mutant mice. *Curr Biol* **4**, 1-7 (1994).

References

165. Lindstrom, M. S. & Wiman, K. G. Myc and E2F1 induce p53 through p14ARF-independent mechanisms in human fibroblasts. *Oncogene* **22**, 4993-5005 (2003).
166. Voorhoeve, P. M. & Agami, R. The tumor-suppressive functions of the human INK4A locus. *Cancer Cell* **4**, 311-9 (2003).
167. Olsen, C. L., Gardie, B., Yaswen, P. & Stampfer, M. R. Raf-1-induced growth arrest in human mammary epithelial cells is p16-independent and is overcome in immortal cells during conversion. *Oncogene* **21**, 6328-39 (2002).
168. Takaoka, M. et al. Ha-Ras(G12V) induces senescence in primary and immortalized human esophageal keratinocytes with p53 dysfunction. *Oncogene* **23**, 6760-8 (2004).
169. Dominguez-Sola, D. et al. Non-transcriptional control of DNA replication by c-Myc. *Nature* (2007).
170. Vafa, O. et al. c-Myc can induce DNA damage, increase reactive oxygen species, and mitigate p53 function: a mechanism for oncogene-induced genetic instability. *Mol Cell* **9**, 1031-44 (2002).
171. Mallette, F. A., Gaumont-Leclerc, M. F. & Ferbeyre, G. The DNA damage signaling pathway is a critical mediator of oncogene-induced senescence. *Genes Dev* **21**, 43-8 (2007).
172. Bartkova, J. et al. Oncogene-induced senescence is part of the tumorigenesis barrier imposed by DNA damage checkpoints. *Nature* **444**, 633-7 (2006).
173. Di Micco, R. et al. Oncogene-induced senescence is a DNA damage response triggered by DNA hyper-replication. *Nature* **444**, 638-42 (2006).
174. Lee, A. C. et al. Ras proteins induce senescence by altering the intracellular levels of reactive oxygen species. *J Biol Chem* **274**, 7936-40 (1999).
175. DiTullio, R. A., Jr. et al. 53BP1 functions in an ATM-dependent checkpoint pathway that is constitutively activated in human cancer. *Nat Cell Biol* **4**, 998-1002 (2002).
176. Bartkova, J. et al. DNA damage response as a candidate anti-cancer barrier in early human tumorigenesis. *Nature* **434**, 864-70 (2005).
177. Gorgoulis, V. G. et al. Activation of the DNA damage checkpoint and genomic instability in human precancerous lesions. *Nature* **434**, 907-13 (2005).
178. Efeyan, A., Garcia-Cao, I., Herranz, D., Velasco-Miguel, S. & Serrano, M. Tumour biology: Policing of oncogene activity by p53. *Nature* **443**, 159 (2006).
179. Christophorou, M. A., Ringshausen, I., Finch, A. J., Swigart, L. B. & Evan, G. I. The pathological response to DNA damage does not contribute to p53-mediated tumour suppression. *Nature* **443**, 214-7 (2006).
180. el-Deiry, W. S. et al. WAF1, a potential mediator of p53 tumor suppression. *Cell* **75**, 817-25 (1993).
181. Hermeking, H. et al. 14-3-3 sigma is a p53-regulated inhibitor of G2/M progression. *Mol Cell* **1**, 3-11 (1997).
182. Kastan, M. B. et al. A mammalian cell cycle checkpoint pathway utilizing p53 and GADD45 is defective in ataxia-telangiectasia. *Cell* **71**, 587-97 (1992).
183. Ohki, R. et al. Reprimo, a new candidate mediator of the p53-mediated cell cycle arrest at the G2 phase. *J Biol Chem* **275**, 22627-30 (2000).
184. Ben-Porath, I. & Weinberg, R. A. The signals and pathways activating cellular senescence. *Int J Biochem Cell Biol* **37**, 961-76 (2005).
185. Levine, A. J., Hu, W. & Feng, Z. The P53 pathway: what questions remain to be explored? *Cell Death Differ* **13**, 1027-36 (2006).
186. Brown, J. P., Wei, W. & Sedivy, J. M. Bypass of senescence after disruption of p21CIP1/WAF1 gene in normal diploid human fibroblasts. *Science* **277**, 831-4 (1997).
187. Pantoja, C. & Serrano, M. Murine fibroblasts lacking p21 undergo senescence and are resistant to transformation by oncogenic Ras. *Oncogene* **18**, 4974-82 (1999).
188. Smogorzewska, A. & de Lange, T. Different telomere damage signaling pathways in human and mouse cells. *Embo J* **21**, 4338-48 (2002).
189. Haupt, S., Berger, M., Goldberg, Z. & Haupt, Y. Apoptosis - the p53 network. *J Cell Sci* **116**, 4077-85 (2003).
190. Miyashita, T. & Reed, J. C. Tumor suppressor p53 is a direct transcriptional activator of the human bax gene. *Cell* **80**, 293-9 (1995).
191. Oda, E. et al. Noxa, a BH3-only member of the Bcl-2 family and candidate mediator of p53-induced apoptosis. *Science* **288**, 1053-8 (2000).

References

192. Yu, J., Wang, Z., Kinzler, K. W., Vogelstein, B. & Zhang, L. PUMA mediates the apoptotic response to p53 in colorectal cancer cells. *Proc Natl Acad Sci U S A* **100**, 1931-6 (2003).
193. Oda, K. et al. p53AIP1, a potential mediator of p53-dependent apoptosis, and its regulation by Ser-46-phosphorylated p53. *Cell* **102**, 849-62 (2000).
194. Attardi, L. D. et al. PERP, an apoptosis-associated target of p53, is a novel member of the PMP-22/gas3 family. *Genes Dev* **14**, 704-18 (2000).
195. Ihrie, R. A. et al. Perp is a mediator of p53-dependent apoptosis in diverse cell types. *Curr Biol* **13**, 1985-90 (2003).
196. Bourdon, J. C., Renzing, J., Robertson, P. L., Fernandes, K. N. & Lane, D. P. Scotin, a novel p53-inducible proapoptotic protein located in the ER and the nuclear membrane. *J Cell Biol* **158**, 235-46 (2002).
197. Owen-Schaub, L. B. et al. Wild-type human p53 and a temperature-sensitive mutant induce Fas/APO-1 expression. *Mol Cell Biol* **15**, 3032-40 (1995).
198. Wu, G. S. et al. KILLER/DR5 is a DNA damage-inducible p53-regulated death receptor gene. *Nat Genet* **17**, 141-3 (1997).
199. Lin, Y., Ma, W. & Benchimol, S. Pidd, a new death-domain-containing protein, is induced by p53 and promotes apoptosis. *Nat Genet* **26**, 122-7 (2000).
200. Moroni, M. C. et al. Apaf-1 is a transcriptional target for E2F and p53. *Nat Cell Biol* **3**, 552-8 (2001).
201. Liebermann, D. A., Hoffman, B. & Vesely, D. p53 induced growth arrest versus apoptosis and its modulation by survival cytokines. *Cell Cycle* **6**, 166-70 (2007).
202. Chen, X., Ko, L. J., Jayaraman, L. & Prives, C. p53 levels, functional domains, and DNA damage determine the extent of the apoptotic response of tumor cells. *Genes Dev* **10**, 2438-51 (1996).
203. Kaeser, M. D. & Iggo, R. D. Chromatin immunoprecipitation analysis fails to support the latency model for regulation of p53 DNA binding activity in vivo. *Proc Natl Acad Sci U S A* **99**, 95-100 (2002).
204. Espinosa, J. M., Verdun, R. E. & Emerson, B. M. p53 functions through stress- and promoter-specific recruitment of transcription initiation components before and after DNA damage. *Mol Cell* **12**, 1015-27 (2003).
205. Maheswaran, S., Englert, C., Bennett, P., Heinrich, G. & Haber, D. A. The WT1 gene product stabilizes p53 and inhibits p53-mediated apoptosis. *Genes Dev* **9**, 2143-56 (1995).
206. MacLachlan, T. K., Takimoto, R. & El-Deiry, W. S. BRCA1 directs a selective p53-dependent transcriptional response towards growth arrest and DNA repair targets. *Mol Cell Biol* **22**, 4280-92 (2002).
207. Samuels-Lev, Y. et al. ASPP proteins specifically stimulate the apoptotic function of p53. *Mol Cell* **8**, 781-94 (2001).
208. Bergamaschi, D. et al. iASPP oncoprotein is a key inhibitor of p53 conserved from worm to human. *Nat Genet* **33**, 162-7 (2003).
209. Shikama, N. et al. A novel cofactor for p300 that regulates the p53 response. *Mol Cell* **4**, 365-76 (1999).
210. Townsend, P. A. et al. STAT-1 interacts with p53 to enhance DNA damage-induced apoptosis. *J Biol Chem* **279**, 5811-20 (2004).
211. Jack, M. T. et al. Chk2 is dispensable for p53-mediated G1 arrest but is required for a latent p53-mediated apoptotic response. *Proc Natl Acad Sci U S A* **99**, 9825-9 (2002).
212. Wahl, G. M., Linke, S. P., Paulson, T. G. & Huang, L. C. Maintaining genetic stability through TP53 mediated checkpoint control. *Cancer Surv* **29**, 183-219 (1997).
213. Sengupta, S. & Harris, C. C. p53: traffic cop at the crossroads of DNA repair and recombination. *Nat Rev Mol Cell Biol* **6**, 44-55 (2005).
214. Hwang, B. J., Ford, J. M., Hanawalt, P. C. & Chu, G. Expression of the p48 xeroderma pigmentosum gene is p53-dependent and is involved in global genomic repair. *Proc Natl Acad Sci U S A* **96**, 424-8 (1999).
215. Adimoolam, S. & Ford, J. M. p53 and DNA damage-inducible expression of the xeroderma pigmentosum group C gene. *Proc Natl Acad Sci U S A* **99**, 12985-90 (2002).
216. Tanaka, H. et al. A ribonucleotide reductase gene involved in a p53-dependent cell-cycle checkpoint for DNA damage. *Nature* **404**, 42-9 (2000).

References

217. Offer, H. et al. Direct involvement of p53 in the base excision repair pathway of the DNA repair machinery. *FEBS Lett* **450**, 197-204 (1999).
218. Zurer, I. et al. The role of p53 in base excision repair following genotoxic stress. *Carcinogenesis* **25**, 11-9 (2004).
219. Achanta, G. & Huang, P. Role of p53 in sensing oxidative DNA damage in response to reactive oxygen species-generating agents. *Cancer Res* **64**, 6233-9 (2004).
220. Teodoro, J. G., Evans, S. K. & Green, M. R. Inhibition of tumor angiogenesis by p53: a new role for the guardian of the genome. *J Mol Med* (2007).
221. Dameron, K. M., Volpert, O. V., Tainsky, M. A. & Bouck, N. Control of angiogenesis in fibroblasts by p53 regulation of thrombospondin-1. *Science* **265**, 1582-4 (1994).
222. Lawler, J. Thrombospondin-1 as an endogenous inhibitor of angiogenesis and tumor growth. *J Cell Mol Med* **6**, 1-12 (2002).
223. Nishimori, H. et al. A novel brain-specific p53-target gene, BAI1, containing thrombospondin type 1 repeats inhibits experimental angiogenesis. *Oncogene* **15**, 2145-50 (1997).
224. Dohn, M., Jiang, J. & Chen, X. Receptor tyrosine kinase EphA2 is regulated by p53-family proteins and induces apoptosis. *Oncogene* **20**, 6503-15 (2001).
225. Brantley, D. M. et al. Soluble Eph A receptors inhibit tumor angiogenesis and progression in vivo. *Oncogene* **21**, 7011-26 (2002).
226. Pal, S., Datta, K. & Mukhopadhyay, D. Central role of p53 on regulation of vascular permeability factor/vascular endothelial growth factor (VPF/VEGF) expression in mammary carcinoma. *Cancer Res* **61**, 6952-7 (2001).
227. Ueba, T. et al. Transcriptional regulation of basic fibroblast growth factor gene by p53 in human glioblastoma and hepatocellular carcinoma cells. *Proc Natl Acad Sci U S A* **91**, 9009-13 (1994).
228. Subbaramaiah, K. et al. Inhibition of cyclooxygenase-2 gene expression by p53. *J Biol Chem* **274**, 10911-5 (1999).
229. Ravi, R. et al. Regulation of tumor angiogenesis by p53-induced degradation of hypoxia-inducible factor 1alpha. *Genes Dev* **14**, 34-44 (2000).
230. Feng, Z., Zhang, H., Levine, A. J. & Jin, S. The coordinate regulation of the p53 and mTOR pathways in cells. *Proc Natl Acad Sci U S A* **102**, 8204-9 (2005).
231. Crighton, D. et al. DRAM, a p53-induced modulator of autophagy, is critical for apoptosis. *Cell* **126**, 121-34 (2006).
232. Tarasov, V. et al. Differential regulation of microRNAs by p53 revealed by massively parallel sequencing: miR-34a is a p53 target that induces apoptosis and G1-arrest. *Cell Cycle* **6**, 1586-93 (2007).
233. Chang, T. C. et al. Transactivation of miR-34a by p53 broadly influences gene expression and promotes apoptosis. *Mol Cell* **26**, 745-52 (2007).
234. Raver-Shapira, N. et al. Transcriptional activation of miR-34a contributes to p53-mediated apoptosis. *Mol Cell* **26**, 731-43 (2007).
235. He, L. et al. A microRNA component of the p53 tumour suppressor network. *Nature* **447**, 1130-4 (2007).
236. Bommer, G. T. et al. p53-mediated activation of miRNA34 candidate tumor-suppressor genes. *Curr Biol* **17**, 1298-307 (2007).
237. Corney, D. C., Flesken-Nikitin, A., Godwin, A. K., Wang, W. & Nikitin, A. Y. MicroRNA-34b and MicroRNA-34c Are Targets of p53 and Cooperate in Control of Cell Proliferation and Adhesion-Independent Growth. *Cancer Res* **67**, 8433-8 (2007).
238. Jones, R. G. et al. AMP-activated protein kinase induces a p53-dependent metabolic checkpoint. *Mol Cell* **18**, 283-93 (2005).
239. Matoba, S. et al. p53 regulates mitochondrial respiration. *Science* **312**, 1650-3 (2006).
240. Warburg, O. On respiratory impairment in cancer cells. *Science* **124**, 269-70 (1956).
241. Bensaad, K. et al. TIGAR, a p53-inducible regulator of glycolysis and apoptosis. *Cell* **126**, 107-20 (2006).
242. Budanov, A. V., Sablina, A. A., Feinstein, E., Koonin, E. V. & Chumakov, P. M. Regeneration of peroxiredoxins by p53-regulated sestrins, homologs of bacterial AhpD. *Science* **304**, 596-600 (2004).
243. Yoon, K. A., Nakamura, Y. & Arakawa, H. Identification of ALDH4 as a p53-inducible gene and its protective role in cellular stresses. *J Hum Genet* **49**, 134-40 (2004).

References

244. Millington, G. W. Proopiomelanocortin (POMC): the cutaneous roles of its melanocortin products and receptors. *Clin Exp Dermatol* **31**, 407-12 (2006).
245. Cui, R. et al. Central role of p53 in the suntan response and pathologic hyperpigmentation. *Cell* **128**, 853-64 (2007).
246. Brash, D. E. Roles of the transcription factor p53 in keratinocyte carcinomas. *Br J Dermatol* **154 Suppl 1**, 8-10 (2006).
247. Tyner, S. D. et al. p53 mutant mice that display early ageing-associated phenotypes. *Nature* **415**, 45-53 (2002).
248. Garcia-Cao, I. et al. "Super p53" mice exhibit enhanced DNA damage response, are tumor resistant and age normally. *Embo J* **21**, 6225-35 (2002).
249. Mendrysa, S. M. et al. Tumor suppression and normal aging in mice with constitutively high p53 activity. *Genes Dev* **20**, 16-21 (2006).
250. Matheu, A. et al. Increased gene dosage of Ink4a/Arf results in cancer resistance and normal aging. *Genes Dev* **18**, 2736-46 (2004).
251. Matheu, A. et al. Delayed ageing through damage protection by the Arf/p53 pathway. *Nature* **448**, 375-9 (2007).
252. Bensaad, K. & Vousden, K. H. Savior and slayer: the two faces of p53. *Nat Med* **11**, 1278-9 (2005).
253. Sheiness, D. & Bishop, J. M. DNA and RNA from uninfected vertebrate cells contain nucleotide sequences related to the putative transforming gene of avian myelocytomatosis virus. *J Virol* **31**, 514-21 (1979).
254. Dalla-Favera, R. et al. Human c-myc onc gene is located on the region of chromosome 8 that is translocated in Burkitt lymphoma cells. *Proc Natl Acad Sci U S A* **79**, 7824-7 (1982).
255. Taub, R. et al. Translocation of the c-myc gene into the immunoglobulin heavy chain locus in human Burkitt lymphoma and murine plasmacytoma cells. *Proc Natl Acad Sci U S A* **79**, 7837-41 (1982).
256. Dang, C. V. et al. The c-Myc target gene network. *Semin Cancer Biol* **16**, 253-64 (2006).
257. Boxer, L. M. & Dang, C. V. Translocations involving c-myc and c-myc function. *Oncogene* **20**, 5595-610 (2001).
258. Miranda Peralta, E. I. et al. [MYC protein and proteins antigenically related with MYC in acute lymphoblastic leukemia]. *Rev Invest Clin* **43**, 139-45 (1991).
259. Avet-Loiseau, H. et al. Rearrangements of the c-myc oncogene are present in 15% of primary human multiple myeloma tumors. *Blood* **98**, 3082-6 (2001).
260. Sumegi, J. et al. Amplification of the c-myc oncogene in human plasma-cell leukemia. *Int J Cancer* **36**, 367-71 (1985).
261. Eick, D. et al. Aberrant c-myc RNAs of Burkitt's lymphoma cells have longer half-lives. *Embo J* **4**, 3717-25 (1985).
262. Rabbitts, P. H., Forster, A., Stinson, M. A. & Rabbitts, T. H. Truncation of exon 1 from the c-myc gene results in prolonged c-myc mRNA stability. *Embo J* **4**, 3727-33 (1985).
263. Chappell, S. A. et al. A mutation in the c-myc-IRES leads to enhanced internal ribosome entry in multiple myeloma: a novel mechanism of oncogene de-regulation. *Oncogene* **19**, 4437-40 (2000).
264. Henriksson, M., Bakardjiev, A., Klein, G. & Luscher, B. Phosphorylation sites mapping in the N-terminal domain of c-myc modulate its transforming potential. *Oncogene* **8**, 3199-209 (1993).
265. Albert, T., Urbauer, B., Kohlhuber, F., Hammersen, B. & Eick, D. Ongoing mutations in the N-terminal domain of c-Myc affect transactivation in Burkitt's lymphoma cell lines. *Oncogene* **9**, 759-63 (1994).
266. Salghetti, S. E., Kim, S. Y. & Tansey, W. P. Destruction of Myc by ubiquitin-mediated proteolysis: cancer-associated and transforming mutations stabilize Myc. *Embo J* **18**, 717-26 (1999).
267. Grignani, F. et al. Negative autoregulation of c-myc gene expression is inactivated in transformed cells. *Embo J* **9**, 3913-22 (1990).
268. Penn, L. J. et al. Domains of human c-myc protein required for autosuppression and cooperation with ras oncogenes are overlapping. *Mol Cell Biol* **10**, 4961-6 (1990).
269. Collins, S. & Groudine, M. Amplification of endogenous myc-related DNA sequences in a human myeloid leukaemia cell line. *Nature* **298**, 679-81 (1982).

References

270. Dalla-Favera, R. et al. Cloning and characterization of different human sequences related to the onc gene (v-myc) of avian myelocytomatosis virus (MC29). *Proc Natl Acad Sci U S A* **79**, 6497-501 (1982).
271. Berns, E. M. et al. c-myc amplification is a better prognostic factor than HER2/neu amplification in primary breast cancer. *Cancer Res* **52**, 1107-13 (1992).
272. Berns, E. M. et al. Prevalence of amplification of the oncogenes c-myc, HER2/neu, and int-2 in one thousand human breast tumours: correlation with steroid receptors. *Eur J Cancer* **28**, 697-700 (1992).
273. Escot, C. et al. Genetic alteration of the c-myc protooncogene (MYC) in human primary breast carcinomas. *Proc Natl Acad Sci U S A* **83**, 4834-8 (1986).
274. Schlotter, C. M., Vogt, U., Bosse, U., Mersch, B. & Wassmann, K. C-myc, not HER-2/neu, can predict recurrence and mortality of patients with node-negative breast cancer. *Breast Cancer Res* **5**, R30-6 (2003).
275. Hayward, W. S., Neel, B. G. & Astrin, S. M. Activation of a cellular onc gene by promoter insertion in ALV-induced lymphoid leukemia. *Nature* **290**, 475-80 (1981).
276. Clarke, I. D. & Dirks, P. B. A human brain tumor-derived PDGFR-alpha deletion mutant is transforming. *Oncogene* **22**, 722-33 (2003).
277. Golub, T. R., Barker, G. F., Lovett, M. & Gilliland, D. G. Fusion of PDGF receptor beta to a novel ets-like gene, tel, in chronic myelomonocytic leukemia with t(5;12) chromosomal translocation. *Cell* **77**, 307-16 (1994).
278. Weng, A. P. et al. Activating mutations of NOTCH1 in human T cell acute lymphoblastic leukemia. *Science* **306**, 269-71 (2004).
279. Palomero, T. et al. NOTCH1 directly regulates c-MYC and activates a feed-forward-loop transcriptional network promoting leukemic cell growth. *Proc Natl Acad Sci U S A* **103**, 18261-6 (2006).
280. He, T. C. et al. Identification of c-MYC as a target of the APC pathway. *Science* **281**, 1509-12 (1998).
281. van de Wetering, M. et al. The beta-catenin/TCF-4 complex imposes a crypt progenitor phenotype on colorectal cancer cells. *Cell* **111**, 241-50 (2002).
282. Sansom, O. J. et al. Loss of Apc in vivo immediately perturbs Wnt signaling, differentiation, and migration. *Genes Dev* **18**, 1385-90 (2004).
283. Kelly, K., Cochran, B. H., Stiles, C. D. & Leder, P. Cell-specific regulation of the c-myc gene by lymphocyte mitogens and platelet-derived growth factor. *Cell* **35**, 603-10 (1983).
284. Armelin, H. A. et al. Functional role for c-myc in mitogenic response to platelet-derived growth factor. *Nature* **310**, 655-60 (1984).
285. Waters, C. M., Littlewood, T. D., Hancock, D. C., Moore, J. P. & Evan, G. I. c-myc protein expression in untransformed fibroblasts. *Oncogene* **6**, 797-805 (1991).
286. Campisi, J., Gray, H. E., Pardee, A. B., Dean, M. & Sonenshein, G. E. Cell-cycle control of c-myc but not c-ras expression is lost following chemical transformation. *Cell* **36**, 241-7 (1984).
287. Thompson, C. B., Challoner, P. B., Neiman, P. E. & Groudine, M. Levels of c-myc oncogene mRNA are invariant throughout the cell cycle. *Nature* **314**, 363-6 (1985).
288. Hann, S. R., Thompson, C. B. & Eisenman, R. N. c-myc oncogene protein synthesis is independent of the cell cycle in human and avian cells. *Nature* **314**, 366-9 (1985).
289. Barone, M. V. & Courtneidge, S. A. Myc but not Fos rescue of PDGF signalling block caused by kinase-inactive Src. *Nature* **378**, 509-12 (1995).
290. Chiariello, M., Marinissen, M. J. & Gutkind, J. S. Regulation of c-myc expression by PDGF through Rho GTPases. *Nat Cell Biol* **3**, 580-6 (2001).
291. Chen, C. R., Kang, Y. & Massague, J. Defective repression of c-myc in breast cancer cells: A loss at the core of the transforming growth factor beta growth arrest program. *Proc Natl Acad Sci U S A* **98**, 992-9 (2001).
292. Chen, C. R., Kang, Y., Siegel, P. M. & Massague, J. E2F4/5 and p107 as Smad cofactors linking the TGFbeta receptor to c-myc repression. *Cell* **110**, 19-32 (2002).
293. Gomis, R. R., Alarcon, C., Nadal, C., Van Poznak, C. & Massague, J. C/EBPbeta at the core of the TGFbeta cytostatic response and its evasion in metastatic breast cancer cells. *Cancer Cell* **10**, 203-14 (2006).

References

294. Luscher, B. & Eisenman, R. N. c-myc and c-myb protein degradation: effect of metabolic inhibitors and heat shock. *Mol Cell Biol* **8**, 2504-12 (1988).
295. Ramsay, G., Evan, G. I. & Bishop, J. M. The protein encoded by the human proto-oncogene c-myc. *Proc Natl Acad Sci U S A* **81**, 7742-6 (1984).
296. Ciechanover, A. et al. Degradation of nuclear oncoproteins by the ubiquitin system in vitro. *Proc Natl Acad Sci U S A* **88**, 139-43 (1991).
297. von der Lehr, N. et al. The F-box protein Skp2 participates in c-Myc proteosomal degradation and acts as a cofactor for c-Myc-regulated transcription. *Mol Cell* **11**, 1189-200 (2003).
298. Welcker, M. et al. The Fbw7 tumor suppressor regulates glycogen synthase kinase 3 phosphorylation-dependent c-Myc protein degradation. *Proc Natl Acad Sci U S A* **101**, 9085-90 (2004).
299. Yada, M. et al. Phosphorylation-dependent degradation of c-Myc is mediated by the F-box protein Fbw7. *Embo J* **23**, 2116-25 (2004).
300. Popov, N. et al. The ubiquitin-specific protease USP28 is required for MYC stability. *Nat Cell Biol* **9**, 765-74 (2007).
301. Sears, R., Leone, G., DeGregori, J. & Nevins, J. R. Ras enhances Myc protein stability. *Mol Cell* **3**, 169-79 (1999).
302. Sears, R. et al. Multiple Ras-dependent phosphorylation pathways regulate Myc protein stability. *Genes Dev* **14**, 2501-14 (2000).
303. Cross, D. A., Alessi, D. R., Cohen, P., Andjelkovich, M. & Hemmings, B. A. Inhibition of glycogen synthase kinase-3 by insulin mediated by protein kinase B. *Nature* **378**, 785-9 (1995).
304. Yeh, E. et al. A signalling pathway controlling c-Myc degradation that impacts oncogenic transformation of human cells. *Nat Cell Biol* **6**, 308-18 (2004).
305. Vervoorts, J. et al. Stimulation of c-MYC transcriptional activity and acetylation by recruitment of the cofactor CBP. *EMBO Rep* **4**, 484-90 (2003).
306. Battey, J. et al. The human c-myc oncogene: structural consequences of translocation into the IgH locus in Burkitt lymphoma. *Cell* **34**, 779-87 (1983).
307. Hann, S. R., Sloan-Brown, K. & Spotts, G. D. Translational activation of the non-AUG-initiated c-myc 1 protein at high cell densities due to methionine deprivation. *Genes Dev* **6**, 1229-40 (1992).
308. Spotts, G. D., Patel, S. V., Xiao, Q. & Hann, S. R. Identification of downstream-initiated c-Myc proteins which are dominant-negative inhibitors of transactivation by full-length c-Myc proteins. *Mol Cell Biol* **17**, 1459-68 (1997).
309. Murre, C., McCaw, P. S. & Baltimore, D. A new DNA binding and dimerization motif in immunoglobulin enhancer binding, daughterless, MyoD, and myc proteins. *Cell* **56**, 777-83 (1989).
310. Landschulz, W. H., Johnson, P. F. & McKnight, S. L. The leucine zipper: a hypothetical structure common to a new class of DNA binding proteins. *Science* **240**, 1759-64 (1988).
311. Blackwood, E. M., Luscher, B. & Eisenman, R. N. Myc and Max associate in vivo. *Genes Dev* **6**, 71-80 (1992).
312. Blackwood, E. M. & Eisenman, R. N. Max: a helix-loop-helix zipper protein that forms a sequence-specific DNA-binding complex with Myc. *Science* **251**, 1211-7 (1991).
313. Blackwell, T. K. et al. Binding of myc proteins to canonical and noncanonical DNA sequences. *Mol Cell Biol* **13**, 5216-24 (1993).
314. Blackwell, T. K., Kretzner, L., Blackwood, E. M., Eisenman, R. N. & Weintraub, H. Sequence-specific DNA binding by the c-Myc protein. *Science* **250**, 1149-51 (1990).
315. Kato, G. J., Barrett, J., Villa-Garcia, M. & Dang, C. V. An amino-terminal c-myc domain required for neoplastic transformation activates transcription. *Mol Cell Biol* **10**, 5914-20 (1990).
316. Stone, J. et al. Definition of regions in human c-myc that are involved in transformation and nuclear localization. *Mol Cell Biol* **7**, 1697-709 (1987).
317. Evan, G. I. et al. Induction of apoptosis in fibroblasts by c-myc protein. *Cell* **69**, 119-28 (1992).
318. Freytag, S. O., Dang, C. V. & Lee, W. M. Definition of the activities and properties of c-myc required to inhibit cell differentiation. *Cell Growth Differ* **1**, 339-43 (1990).
319. Herbst, A. et al. A conserved element in Myc that negatively regulates its proapoptotic activity. *EMBO Rep* **6**, 177-83 (2005).

References

320. Cowling, V. H., Chandriani, S., Whitfield, M. L. & Cole, M. D. A conserved Myc protein domain, MBIV, regulates DNA binding, apoptosis, transformation, and G2 arrest. *Mol Cell Biol* **26**, 4226-39 (2006).
321. Oster, S. K., Mao, D. Y., Kennedy, J. & Penn, L. Z. Functional analysis of the N-terminal domain of the Myc oncoprotein. *Oncogene* **22**, 1998-2010 (2003).
322. Cowling, V. H. & Cole, M. D. Mechanism of transcriptional activation by the Myc oncoproteins. *Semin Cancer Biol* **16**, 242-52 (2006).
323. Adhikary, S. & Eilers, M. Transcriptional regulation and transformation by Myc proteins. *Nat Rev Mol Cell Biol* **6**, 635-45 (2005).
324. McMahon, S. B., Van Buskirk, H. A., Dugan, K. A., Copeland, T. D. & Cole, M. D. The novel ATM-related protein TRRAP is an essential cofactor for the c-Myc and E2F oncoproteins. *Cell* **94**, 363-74 (1998).
325. Park, J., Kunjibettu, S., McMahon, S. B. & Cole, M. D. The ATM-related domain of TRRAP is required for histone acetyltransferase recruitment and Myc-dependent oncogenesis. *Genes Dev* **15**, 1619-24 (2001).
326. Brown, C. E. et al. Recruitment of HAT complexes by direct activator interactions with the ATM-related Tra1 subunit. *Science* **292**, 2333-7 (2001).
327. Bouchard, C. et al. Regulation of cyclin D2 gene expression by the Myc/Max/Mad network: Myc-dependent TRRAP recruitment and histone acetylation at the cyclin D2 promoter. *Genes Dev* **15**, 2042-7 (2001).
328. Frank, S. R., Schroeder, M., Fernandez, P., Taubert, S. & Amati, B. Binding of c-Myc to chromatin mediates mitogen-induced acetylation of histone H4 and gene activation. *Genes Dev* **15**, 2069-82 (2001).
329. Grant, P. A., Schieltz, D., Pray-Grant, M. G., Yates, J. R., 3rd & Workman, J. L. The ATM-related cofactor Tra1 is a component of the purified SAGA complex. *Mol Cell* **2**, 863-7 (1998).
330. Martinez, E. et al. Human STAGA complex is a chromatin-acetylating transcription coactivator that interacts with pre-mRNA splicing and DNA damage-binding factors in vivo. *Mol Cell Biol* **21**, 6782-95 (2001).
331. Ikura, T. et al. Involvement of the TIP60 histone acetylase complex in DNA repair and apoptosis. *Cell* **102**, 463-73 (2000).
332. Cheng, S. W. et al. c-MYC interacts with INI1/hSNF5 and requires the SWI/SNF complex for transactivation function. *Nat Genet* **22**, 102-5 (1999).
333. Kingston, R. E., Bunker, C. A. & Imbalzano, A. N. Repression and activation by multiprotein complexes that alter chromatin structure. *Genes Dev* **10**, 905-20 (1996).
334. Nikiforov, M. A. et al. TRRAP-dependent and TRRAP-independent transcriptional activation by Myc family oncoproteins. *Mol Cell Biol* **22**, 5054-63 (2002).
335. Kingston, R. E. & Narlikar, G. J. ATP-dependent remodeling and acetylation as regulators of chromatin fluidity. *Genes Dev* **13**, 2339-52 (1999).
336. Strahl, B. D. & Allis, C. D. The language of covalent histone modifications. *Nature* **403**, 41-5 (2000).
337. Eberhardy, S. R. & Farnham, P. J. c-Myc mediates activation of the cad promoter via a post-RNA polymerase II recruitment mechanism. *J Biol Chem* **276**, 48562-71 (2001).
338. Eberhardy, S. R. & Farnham, P. J. Myc recruits P-TEFb to mediate the final step in the transcriptional activation of the cad promoter. *J Biol Chem* **277**, 40156-62 (2002).
339. Gargano, B., Amente, S., Majello, B. & Lania, L. P-TEFb is a Crucial Co-Factor for Myc Transactivation. *Cell Cycle* **6** (2007).
340. Zippo, A., De Robertis, A., Serafini, R. & Oliviero, S. PIM1-dependent phosphorylation of histone H3 at serine 10 is required for MYC-dependent transcriptional activation and oncogenic transformation. *Nat Cell Biol* **9**, 932-44 (2007).
341. Salghetti, S. E., Caudy, A. A., Chenoweth, J. G. & Tansey, W. P. Regulation of transcriptional activation domain function by ubiquitin. *Science* **293**, 1651-3 (2001).
342. Kim, S. Y., Herbst, A., Tworkowski, K. A., Salghetti, S. E. & Tansey, W. P. Skp2 regulates Myc protein stability and activity. *Mol Cell* **11**, 1177-88 (2003).
343. Adhikary, S. et al. The ubiquitin ligase HectH9 regulates transcriptional activation by Myc and is essential for tumor cell proliferation. *Cell* **123**, 409-21 (2005).

References

344. Kato, G. J., Lee, W. M., Chen, L. L. & Dang, C. V. Max: functional domains and interaction with c-Myc. *Genes Dev* **6**, 81-92 (1992).
345. Ayer, D. E., Kretzner, L. & Eisenman, R. N. Mad: a heterodimeric partner for Max that antagonizes Myc transcriptional activity. *Cell* **72**, 211-22 (1993).
346. Zervos, A. S., Gyuris, J. & Brent, R. Mxi1, a protein that specifically interacts with Max to bind Myc-Max recognition sites. *Cell* **72**, 223-32 (1993).
347. Hurlin, P. J. et al. Mad3 and Mad4: novel Max-interacting transcriptional repressors that suppress c-myc dependent transformation and are expressed during neural and epidermal differentiation. *Embo J* **14**, 5646-59 (1995).
348. Hurlin, P. J., Queva, C. & Eisenman, R. N. Mnt, a novel Max-interacting protein is coexpressed with Myc in proliferating cells and mediates repression at Myc binding sites. *Genes Dev* **11**, 44-58 (1997).
349. Hurlin, P. J., Steingrimsson, E., Copeland, N. G., Jenkins, N. A. & Eisenman, R. N. Mga, a dual-specificity transcription factor that interacts with Max and contains a T-domain DNA-binding motif. *Embo J* **18**, 7019-28 (1999).
350. Ayer, D. E., Lawrence, Q. A. & Eisenman, R. N. Mad-Max transcriptional repression is mediated by ternary complex formation with mammalian homologs of yeast repressor Sin3. *Cell* **80**, 767-76 (1995).
351. Alland, L. et al. Role for N-CoR and histone deacetylase in Sin3-mediated transcriptional repression. *Nature* **387**, 49-55 (1997).
352. Knoepfler, P. S. & Eisenman, R. N. Sin meets NuRD and other tails of repression. *Cell* **99**, 447-50 (1999).
353. Ayer, D. E. & Eisenman, R. N. A switch from Myc:Max to Mad:Max heterocomplexes accompanies monocyte/macrophage differentiation. *Genes Dev* **7**, 2110-9 (1993).
354. Xu, D. et al. Switch from Myc/Max to Mad1/Max binding and decrease in histone acetylation at the telomerase reverse transcriptase promoter during differentiation of HL60 cells. *Proc Natl Acad Sci U S A* **98**, 3826-31 (2001).
355. Roy, A. L., Meisterernst, M., Pognonec, P. & Roeder, R. G. Cooperative interaction of an initiator-binding transcription initiation factor and the helix-loop-helix activator USF. *Nature* **354**, 245-8 (1991).
356. Li, L. H., Nerlov, C., Prendergast, G., MacGregor, D. & Ziff, E. B. c-Myc represses transcription in vivo by a novel mechanism dependent on the initiator element and Myc box II. *Embo J* **13**, 4070-9 (1994).
357. Smale, S. T. & Baltimore, D. The "initiator" as a transcription control element. *Cell* **57**, 103-13 (1989).
358. Yang, W. et al. Repression of transcription of the p27(Kip1) cyclin-dependent kinase inhibitor gene by c-Myc. *Oncogene* **20**, 1688-702 (2001).
359. Staller, P. et al. Repression of p15INK4b expression by Myc through association with Miz-1. *Nat Cell Biol* **3**, 392-9 (2001).
360. Seoane, J. et al. TGFbeta influences Myc, Miz-1 and Smad to control the CDK inhibitor p15INK4b. *Nat Cell Biol* **3**, 400-8 (2001).
361. Peukert, K. et al. An alternative pathway for gene regulation by Myc. *Embo J* **16**, 5672-86 (1997).
362. Shrivastava, A. et al. Inhibition of transcriptional regulator Yin-Yang-1 by association with c-Myc. *Science* **262**, 1889-92 (1993).
363. Gartel, A. L. et al. Myc represses the p21(WAF1/CIP1) promoter and interacts with Sp1/Sp3. *Proc Natl Acad Sci U S A* **98**, 4510-5 (2001).
364. Izumi, H. et al. Mechanism for the transcriptional repression by c-Myc on PDGF beta-receptor. *J Cell Sci* **114**, 1533-44 (2001).
365. Etard, C., Gradl, D., Kunz, M., Eilers, M. & Wedlich, D. Pontin and Reptin regulate cell proliferation in early Xenopus embryos in collaboration with c-Myc and Miz-1. *Mech Dev* **122**, 545-56 (2005).
366. Okano, M., Bell, D. W., Haber, D. A. & Li, E. DNA methyltransferases Dnmt3a and Dnmt3b are essential for de novo methylation and mammalian development. *Cell* **99**, 247-57 (1999).
367. Brenner, C. et al. Myc represses transcription through recruitment of DNA methyltransferase corepressor. *Embo J* **24**, 336-46 (2005).

References

368. Coller, H. A. et al. Expression analysis with oligonucleotide microarrays reveals that MYC regulates genes involved in growth, cell cycle, signaling, and adhesion. *Proc Natl Acad Sci U S A* **97**, 3260-5 (2000).
369. Fernandez, P. C. et al. Genomic targets of the human c-Myc protein. *Genes Dev* **17**, 1115-29 (2003).
370. Menssen, A. & Hermeking, H. Characterization of the c-MYC-regulated transcriptome by SAGE: identification and analysis of c-MYC target genes. *Proc Natl Acad Sci U S A* **99**, 6274-9 (2002).
371. Schuhmacher, M. et al. The transcriptional program of a human B cell line in response to Myc. *Nucleic Acids Res* **29**, 397-406 (2001).
372. Grandori, C. et al. c-Myc binds to human ribosomal DNA and stimulates transcription of rRNA genes by RNA polymerase I. *Nat Cell Biol* **7**, 311-8 (2005).
373. Gomez-Roman, N., Grandori, C., Eisenman, R. N. & White, R. J. Direct activation of RNA polymerase III transcription by c-Myc. *Nature* **421**, 290-4 (2003).
374. O'Donnell, K. A., Wentzel, E. A., Zeller, K. I., Dang, C. V. & Mendell, J. T. c-Myc-regulated microRNAs modulate E2F1 expression. *Nature* **435**, 839-43 (2005).
375. He, L. et al. A microRNA polycistron as a potential human oncogene. *Nature* **435**, 828-33 (2005).
376. Dewes, M. et al. Augmentation of tumor angiogenesis by a Myc-activated microRNA cluster. *Nat Genet* **38**, 1060-5 (2006).
377. Lu, Y., Thomson, J. M., Wang, H. Y., Hammond, S. M. & Hogan, B. L. Transgenic over-expression of the microRNA miR-17-92 cluster promotes proliferation and inhibits differentiation of lung epithelial progenitor cells. *Dev Biol* (2007).
378. Zeller, K. I., Jegga, A. G., Aronow, B. J., O'Donnell, K. A. & Dang, C. V. An integrated database of genes responsive to the Myc oncogenic transcription factor: identification of direct genomic targets. *Genome Biol* **4**, R69 (2003).
379. Cole, M. D. & McMahon, S. B. The Myc oncoprotein: a critical evaluation of transactivation and target gene regulation. *Oncogene* **18**, 2916-24 (1999).
380. Berns, K., Hijmans, E. M., Koh, E., Daley, G. Q. & Bernards, R. A genetic screen to identify genes that rescue the slow growth phenotype of c-myc null fibroblasts. *Oncogene* **19**, 3330-4 (2000).
381. Hanahan, D. & Weinberg, R. A. The hallmarks of cancer. *Cell* **100**, 57-70 (2000).
382. Pelengaris, S., Khan, M. & Evan, G. I. Suppression of Myc-induced apoptosis in beta cells exposes multiple oncogenic properties of Myc and triggers carcinogenic progression. *Cell* **109**, 321-34 (2002).
383. Eilers, M., Schirm, S. & Bishop, J. M. The MYC protein activates transcription of the alpha-prothymosin gene. *Embo J* **10**, 133-41 (1991).
384. Littlewood, T. D., Hancock, D. C., Danielian, P. S., Parker, M. G. & Evan, G. I. A modified oestrogen receptor ligand-binding domain as an improved switch for the regulation of heterologous proteins. *Nucleic Acids Res* **23**, 1686-90 (1995).
385. Davis, A. C., Wims, M., Spotts, G. D., Hann, S. R. & Bradley, A. A null c-myc mutation causes lethality before 10.5 days of gestation in homozygotes and reduced fertility in heterozygous female mice. *Genes Dev* **7**, 671-82 (1993).
386. Hirning, U., Schmid, P., Schulz, W. A., Kozak, L. P. & Hameister, H. In developing brown adipose tissue c-myc protooncogene expression is restricted to early differentiation stages. *Cell Differ Dev* **27**, 243-8 (1989).
387. Schmid, P., Schulz, W. A. & Hameister, H. Dynamic expression pattern of the myc protooncogene in midgestation mouse embryos. *Science* **243**, 226-9 (1989).
388. Hirvonen, H. et al. Expression of the myc proto-oncogenes in developing human fetal brain. *Oncogene* **5**, 1787-97 (1990).
389. Mateyak, M. K., Obaya, A. J., Adachi, S. & Sedivy, J. M. Phenotypes of c-Myc-deficient rat fibroblasts isolated by targeted homologous recombination. *Cell Growth Differ* **8**, 1039-48 (1997).
390. Pardee, A. B. G1 events and regulation of cell proliferation. *Science* **246**, 603-8 (1989).
391. Blagosklonny, M. V. & Pardee, A. B. The restriction point of the cell cycle. *Cell Cycle* **1**, 103-10 (2002).
392. Bouchard, C. et al. Direct induction of cyclin D2 by Myc contributes to cell cycle progression and sequestration of p27. *Embo J* **18**, 5321-33 (1999).

References

393. Hermeking, H. et al. Identification of CDK4 as a target of c-MYC. *Proc Natl Acad Sci U S A* **97**, 2229-34 (2000).
394. Perez-Roger, I., Kim, S. H., Griffiths, B., Sewing, A. & Land, H. Cyclins D1 and D2 mediate myc-induced proliferation via sequestration of p27(Kip1) and p21(Cip1). *Embo J* **18**, 5310-20 (1999).
395. Muller, D. et al. Cdk2-dependent phosphorylation of p27 facilitates its Myc-induced release from cyclin E/cdk2 complexes. *Oncogene* **15**, 2561-76 (1997).
396. Montagnoli, A. et al. Ubiquitination of p27 is regulated by Cdk-dependent phosphorylation and trimeric complex formation. *Genes Dev* **13**, 1181-9 (1999).
397. Ungermannova, D., Gao, Y. & Liu, X. Ubiquitination of p27Kip1 requires physical interaction with cyclin E and probable phosphate recognition by SKP2. *J Biol Chem* **280**, 30301-9 (2005).
398. O'Hagan, R. C. et al. Myc-enhanced expression of Cul1 promotes ubiquitin-dependent proteolysis and cell cycle progression. *Genes Dev* **14**, 2185-91 (2000).
399. Rank, K. B., Evans, D. B. & Sharma, S. K. The N-terminal domains of cyclin-dependent kinase inhibitory proteins block the phosphorylation of cdk2/Cyclin E by the CDK-activating kinase. *Biochem Biophys Res Commun* **271**, 469-73 (2000).
400. Cowling, V. H. & Cole, M. D. The Myc transactivation domain promotes global phosphorylation of the RNA polymerase II carboxy-terminal domain independently of direct DNA binding. *Mol Cell Biol* **27**, 2059-73 (2007).
401. Galaktionov, K., Chen, X. & Beach, D. Cdc25 cell-cycle phosphatase as a target of c-myc. *Nature* **382**, 511-7 (1996).
402. Vigo, E. et al. CDC25A phosphatase is a target of E2F and is required for efficient E2F-induced S phase. *Mol Cell Biol* **19**, 6379-95 (1999).
403. Sherr, C. J. & Roberts, J. M. Inhibitors of mammalian G1 cyclin-dependent kinases. *Genes Dev* **9**, 1149-63 (1995).
404. Wanzel, M., Herold, S. & Eilers, M. Transcriptional repression by Myc. *Trends Cell Biol* **13**, 146-50 (2003).
405. Weinberg, R. A. The retinoblastoma protein and cell cycle control. *Cell* **81**, 323-30 (1995).
406. Beijersbergen, R. L. & Bernards, R. Cell cycle regulation by the retinoblastoma family of growth inhibitory proteins. *Biochim Biophys Acta* **1287**, 103-20 (1996).
407. Lasorella, A., Nosedà, M., Beyna, M., Yokota, Y. & Iavarone, A. Id2 is a retinoblastoma protein target and mediates signalling by Myc oncoproteins. *Nature* **407**, 592-8 (2000).
408. Sears, R., Ohtani, K. & Nevins, J. R. Identification of positively and negatively acting elements regulating expression of the E2F2 gene in response to cell growth signals. *Mol Cell Biol* **17**, 5227-35 (1997).
409. Adams, M. R., Sears, R., Nuckolls, F., Leone, G. & Nevins, J. R. Complex transcriptional regulatory mechanisms control expression of the E2F3 locus. *Mol Cell Biol* **20**, 3633-9 (2000).
410. Santoni-Rugiu, E., Falck, J., Mailand, N., Bartek, J. & Lukas, J. Involvement of Myc activity in a G(1)/S-promoting mechanism parallel to the pRb/E2F pathway. *Mol Cell Biol* **20**, 3497-509 (2000).
411. Freytag, S. O. Enforced expression of the c-myc oncogene inhibits cell differentiation by precluding entry into a distinct predifferentiation state in G0/G1. *Mol Cell Biol* **8**, 1614-24 (1988).
412. Miner, J. H. & Wold, B. J. c-myc inhibition of MyoD and myogenin-initiated myogenic differentiation. *Mol Cell Biol* **11**, 2842-51 (1991).
413. Nagl, N. G., Jr., Zweitzig, D. R., Thimmapaya, B., Beck, G. R., Jr. & Moran, E. The c-myc gene is a direct target of mammalian SWI/SNF-related complexes during differentiation-associated cell cycle arrest. *Cancer Res* **66**, 1289-93 (2006).
414. Johansen, L. M. et al. c-Myc is a critical target for c/EBPalpha in granulopoiesis. *Mol Cell Biol* **21**, 3789-806 (2001).
415. Wu, S. et al. Myc represses differentiation-induced p21CIP1 expression via Miz-1-dependent interaction with the p21 core promoter. *Oncogene* **22**, 351-60 (2003).
416. Freytag, S. O. & Geddes, T. J. Reciprocal regulation of adipogenesis by Myc and C/EBP alpha. *Science* **256**, 379-82 (1992).
417. Wu, K. J., Polack, A. & Dalla-Favera, R. Coordinated regulation of iron-controlling genes, H-ferritin and IRP2, by c-MYC. *Science* **283**, 676-9 (1999).

References

418. Bettess, M. D. et al. c-Myc is required for the formation of intestinal crypts but dispensable for homeostasis of the adult intestinal epithelium. *Mol Cell Biol* **25**, 7868-78 (2005).
419. Gandarillas, A. & Watt, F. M. c-Myc promotes differentiation of human epidermal stem cells. *Genes Dev* **11**, 2869-82 (1997).
420. Frye, M., Gardner, C., Li, E. R., Arnold, I. & Watt, F. M. Evidence that Myc activation depletes the epidermal stem cell compartment by modulating adhesive interactions with the local microenvironment. *Development* **130**, 2793-808 (2003).
421. Wilson, A. et al. c-Myc controls the balance between hematopoietic stem cell self-renewal and differentiation. *Genes Dev* **18**, 2747-63 (2004).
422. Cowling, V. H. & Cole, M. D. E-cadherin repression contributes to c-Myc-induced epithelial cell transformation. *Oncogene* **26**, 3582-6 (2007).
423. Liotta, L. A. Tumor invasion and metastases: role of the basement membrane. Warner-Lambert Parke-Davis Award lecture. *Am J Pathol* **117**, 339-48 (1984).
424. Askew, D. S., Ashmun, R. A., Simmons, B. C. & Cleveland, J. L. Constitutive c-myc expression in an IL-3-dependent myeloid cell line suppresses cell cycle arrest and accelerates apoptosis. *Oncogene* **6**, 1915-22 (1991).
425. Harrington, E. A., Bennett, M. R., Fanidi, A. & Evan, G. I. c-Myc-induced apoptosis in fibroblasts is inhibited by specific cytokines. *Embo J* **13**, 3286-95 (1994).
426. Janicke, R. U., Lee, F. H. & Porter, A. G. Nuclear c-Myc plays an important role in the cytotoxicity of tumor necrosis factor alpha in tumor cells. *Mol Cell Biol* **14**, 5661-70 (1994).
427. Klefstrom, J. et al. c-Myc induces cellular susceptibility to the cytotoxic action of TNF-alpha. *Embo J* **13**, 5442-50 (1994).
428. Hueber, A. O. et al. Requirement for the CD95 receptor-ligand pathway in c-Myc-induced apoptosis. *Science* **278**, 1305-9 (1997).
429. Prendergast, G. C. Mechanisms of apoptosis by c-Myc. *Oncogene* **18**, 2967-87 (1999).
430. Zindy, F. et al. Myc signaling via the ARF tumor suppressor regulates p53-dependent apoptosis and immortalization. *Genes Dev* **12**, 2424-33 (1998).
431. Juin, P., Hueber, A. O., Littlewood, T. & Evan, G. c-Myc-induced sensitization to apoptosis is mediated through cytochrome c release. *Genes Dev* **13**, 1367-81 (1999).
432. Soucie, E. L. et al. Myc potentiates apoptosis by stimulating Bax activity at the mitochondria. *Mol Cell Biol* **21**, 4725-36 (2001).
433. Mitchell, K. O. et al. Bax is a transcriptional target and mediator of c-myc-induced apoptosis. *Cancer Res* **60**, 6318-25 (2000).
434. Egle, A., Harris, A. W., Bouillet, P. & Cory, S. Bim is a suppressor of Myc-induced mouse B cell leukemia. *Proc Natl Acad Sci U S A* **101**, 6164-9 (2004).
435. Eischen, C. M. et al. Bcl-2 is an apoptotic target suppressed by both c-Myc and E2F-1. *Oncogene* **20**, 6983-93 (2001).
436. Eischen, C. M., Woo, D., Roussel, M. F. & Cleveland, J. L. Apoptosis triggered by Myc-induced suppression of Bcl-X(L) or Bcl-2 is bypassed during lymphomagenesis. *Mol Cell Biol* **21**, 5063-70 (2001).
437. Ray, S. et al. MYC can induce DNA breaks in vivo and in vitro independent of reactive oxygen species. *Cancer Res* **66**, 6598-605 (2006).
438. Iritani, B. M. & Eisenman, R. N. c-Myc enhances protein synthesis and cell size during B lymphocyte development. *Proc Natl Acad Sci U S A* **96**, 13180-5 (1999).
439. Johnston, L. A., Prober, D. A., Edgar, B. A., Eisenman, R. N. & Gallant, P. Drosophila myc regulates cellular growth during development. *Cell* **98**, 779-90 (1999).
440. White, R. J. RNA polymerases I and III, growth control and cancer. *Nat Rev Mol Cell Biol* **6**, 69-78 (2005).
441. Ruggero, D. & Pandolfi, P. P. Does the ribosome translate cancer? *Nat Rev Cancer* **3**, 179-92 (2003).
442. Arabi, A. et al. c-Myc associates with ribosomal DNA and activates RNA polymerase I transcription. *Nat Cell Biol* **7**, 303-10 (2005).
443. Grewal, S. S., Li, L., Orian, A., Eisenman, R. N. & Edgar, B. A. Myc-dependent regulation of ribosomal RNA synthesis during Drosophila development. *Nat Cell Biol* **7**, 295-302 (2005).
444. Kenneth, N. S. et al. TRRAP and GCN5 are used by c-Myc to activate RNA polymerase III transcription. *Proc Natl Acad Sci U S A* (2007).

445. Dai, M. S., Arnold, H., Sun, X. X., Sears, R. & Lu, H. Inhibition of c-Myc activity by ribosomal protein L11. *Embo J* **26**, 3332-45 (2007).
446. Strezoska, Z., Pestov, D. G. & Lau, L. F. Functional inactivation of the mouse nucleolar protein Bop1 inhibits multiple steps in pre-rRNA processing and blocks cell cycle progression. *J Biol Chem* **277**, 29617-25 (2002).
447. Lapik, Y. R., Fernandes, C. J., Lau, L. F. & Pestov, D. G. Physical and functional interaction between Pes1 and Bop1 in mammalian ribosome biogenesis. *Mol Cell* **15**, 17-29 (2004).
448. Holzel, M. et al. Mammalian WDR12 is a novel member of the Pes1-Bop1 complex and is required for ribosome biogenesis and cell proliferation. *J Cell Biol* **170**, 367-78 (2005).
449. Baudino, T. A. et al. c-Myc is essential for vasculogenesis and angiogenesis during development and tumor progression. *Genes Dev* **16**, 2530-43 (2002).
450. Janz, A., Seignani, C., Kenyon, K., Ngo, C. V. & Thomas-Tikhonenko, A. Activation of the myc oncoprotein leads to increased turnover of thrombospondin-1 mRNA. *Nucleic Acids Res* **28**, 2268-75 (2000).
451. Wang, J., Xie, L. Y., Allan, S., Beach, D. & Hannon, G. J. Myc activates telomerase. *Genes Dev* **12**, 1769-74 (1998).
452. Greenberg, R. A. et al. Telomerase reverse transcriptase gene is a direct target of c-Myc but is not functionally equivalent in cellular transformation. *Oncogene* **18**, 1219-26 (1999).
453. Land, H., Parada, L. F. & Weinberg, R. A. Tumorigenic conversion of primary embryo fibroblasts requires at least two cooperating oncogenes. *Nature* **304**, 596-602 (1983).
454. Koch, H. B. et al. Large-scale identification of c-MYC-associated proteins using a combined TAP/MudPIT approach. *Cell Cycle* **6**, 205-17 (2007).
455. Messen, A. et al. c-MYC Delays Prometaphase by Direct Transactivation of MAD2 and BubR1: Identification of Mechanisms Underlying c-MYC-Induced DNA Damage and Chromosomal Instability. *Cell Cycle* **6**, 339-352 (2007).
456. Felsher, D. W. & Bishop, J. M. Transient excess of MYC activity can elicit genomic instability and tumorigenesis. *Proc Natl Acad Sci U S A* **96**, 3940-4 (1999).
457. Schoenenberger, C. A. et al. Targeted c-myc gene expression in mammary glands of transgenic mice induces mammary tumours with constitutive milk protein gene transcription. *Embo J* **7**, 169-75 (1988).
458. Stewart, T. A., Pattengale, P. K. & Leder, P. Spontaneous mammary adenocarcinomas in transgenic mice that carry and express MTV/myc fusion genes. *Cell* **38**, 627-37 (1984).
459. Adams, J. M. et al. The c-myc oncogene driven by immunoglobulin enhancers induces lymphoid malignancy in transgenic mice. *Nature* **318**, 533-8 (1985).
460. Park, S. S. et al. Insertion of c-Myc into Igh induces B-cell and plasma-cell neoplasms in mice. *Cancer Res* **65**, 1306-15 (2005).
461. Felsher, D. W. & Bishop, J. M. Reversible tumorigenesis by MYC in hematopoietic lineages. *Mol Cell* **4**, 199-207 (1999).
462. D'Cruz, C. M. et al. c-MYC induces mammary tumorigenesis by means of a preferred pathway involving spontaneous Kras2 mutations. *Nat Med* **7**, 235-9 (2001).
463. Shachaf, C. M. et al. MYC inactivation uncovers pluripotent differentiation and tumour dormancy in hepatocellular cancer. *Nature* **431**, 1112-7 (2004).
464. Arnold, I. & Watt, F. M. c-Myc activation in transgenic mouse epidermis results in mobilization of stem cells and differentiation of their progeny. *Curr Biol* **11**, 558-68 (2001).
465. Weinstein, I. B. Cancer. Addiction to oncogenes--the Achilles heal of cancer. *Science* **297**, 63-4 (2002).
466. Jonkers, J. & Berns, A. Oncogene addiction: sometimes a temporary slavery. *Cancer Cell* **6**, 535-8 (2004).
467. Jain, M. et al. Sustained loss of a neoplastic phenotype by brief inactivation of MYC. *Science* **297**, 102-4 (2002).
468. Boxer, R. B., Jang, J. W., Sintasath, L. & Chodosh, L. A. Lack of sustained regression of c-MYC-induced mammary adenocarcinomas following brief or prolonged MYC inactivation. *Cancer Cell* **6**, 577-86 (2004).
469. Vita, M. & Henriksson, M. The Myc oncoprotein as a therapeutic target for human cancer. *Semin Cancer Biol* **16**, 318-30 (2006).

References

470. Giuriato, S. et al. Sustained regression of tumors upon MYC inactivation requires p53 or thrombospondin-1 to reverse the angiogenic switch. *Proc Natl Acad Sci U S A* **103**, 16266-71 (2006).
471. Wu, C. H. et al. Cellular senescence is an important mechanism of tumor regression upon c-Myc inactivation. *Proc Natl Acad Sci U S A* **104**, 13028-33 (2007).
472. Rigaut, G. et al. A generic protein purification method for protein complex characterization and proteome exploration. *Nat Biotechnol* **17**, 1030-2 (1999).
473. Forler, D. et al. An efficient protein complex purification method for functional proteomics in higher eukaryotes. *Nat Biotechnol* **21**, 89-92 (2003).
474. Washburn, M. P., Wolters, D. & Yates, J. R., 3rd. Large-scale analysis of the yeast proteome by multidimensional protein identification technology. *Nat Biotechnol* **19**, 242-7 (2001).
475. Ali, S. H., Kasper, J. S., Arai, T. & DeCaprio, J. A. Cul7/p185/p193 binding to simian virus 40 large T antigen has a role in cellular transformation. *J Virol* **78**, 2749-57 (2004).
476. Untergasser, G., Koch, H. B., Menssen, A. & Hermeking, H. Characterization of epithelial senescence by serial analysis of gene expression: identification of genes potentially involved in prostate cancer. *Cancer Res* **62**, 6255-62 (2002).
477. Korner, H. et al. Digital karyotyping reveals frequent inactivation of the dystrophin/DMD gene in malignant melanoma. *Cell Cycle* **6**, 189-98 (2007).
478. Bornkamm, G. W. et al. Stringent doxycycline-dependent control of gene activities using an episomal one-vector system. *Nucleic Acids Res* **33**, e137 (2005).
479. Brummelkamp, T. R., Bernards, R. & Agami, R. A system for stable expression of short interfering RNAs in mammalian cells. *Science* **296**, 550-3 (2002).
480. Brummelkamp, T. R., Bernards, R. & Agami, R. Stable suppression of tumorigenicity by virus-mediated RNA interference. *Cancer Cell* **2**, 243-7 (2002).
481. Yu, J. et al. Identification and classification of p53-regulated genes. *Proc Natl Acad Sci U S A* **96**, 14517-22 (1999).
482. Dickins, R. A. et al. Probing tumor phenotypes using stable and regulated synthetic microRNA precursors. *Nat Genet* **37**, 1289-95 (2005).
483. Dias, D. C., Dolios, G., Wang, R. & Pan, Z. Q. CUL7: A DOC domain-containing cullin selectively binds Skp1.Fbx29 to form an SCF-like complex. *Proc Natl Acad Sci U S A* **99**, 16601-6 (2002).
484. Arai, T. et al. Targeted disruption of p185/Cul7 gene results in abnormal vascular morphogenesis. *Proc Natl Acad Sci U S A* **100**, 9855-60 (2003).
485. Treier, M., Staszewski, L. M. & Bohmann, D. Ubiquitin-dependent c-Jun degradation in vivo is mediated by the delta domain. *Cell* **78**, 787-98 (1994).
486. Lahav, G. et al. Dynamics of the p53-Mdm2 feedback loop in individual cells. *Nat Genet* **36**, 147-50 (2004).
487. Liu, Y., Encinas, M., Comella, J. X., Aldea, M. & Gallego, C. Basic helix-loop-helix proteins bind to TrkB and p21(Cip1) promoters linking differentiation and cell cycle arrest in neuroblastoma cells. *Mol Cell Biol* **24**, 2662-72 (2004).
488. Fallaux, F. J. et al. Characterization of 911: a new helper cell line for the titration and propagation of early region 1-deleted adenoviral vectors. *Hum Gene Ther* **7**, 215-22 (1996).
489. He, T. C. et al. A simplified system for generating recombinant adenoviruses. *Proc Natl Acad Sci U S A* **95**, 2509-14 (1998).
490. Kinsella, T. M. & Nolan, G. P. Episomal vectors rapidly and stably produce high-titer recombinant retrovirus. *Hum Gene Ther* **7**, 1405-13 (1996).
491. Boukamp, P. et al. Normal keratinization in a spontaneously immortalized aneuploid human keratinocyte cell line. *J Cell Biol* **106**, 761-71 (1988).
492. Holz, M. et al. Myc/Max/Mad regulate the frequency but not the duration of productive cell cycles. *EMBO Rep* **2**, 1125-32 (2001).
493. Epanchintsev, A., Jung, P., Menssen, A. & Hermeking, H. Inducible microRNA expression by an all-in-one episomal vector system. *Nucleic Acids Res* **34**, e119 (2006).
494. Pfaffl, M. W., Horgan, G. W. & Dempfle, L. Relative expression software tool (REST) for group-wise comparison and statistical analysis of relative expression results in real-time PCR. *Nucleic Acids Res* **30**, e36 (2002).

References

495. Berthois, Y., Katzenellenbogen, J. A. & Katzenellenbogen, B. S. Phenol red in tissue culture media is a weak estrogen: implications concerning the study of estrogen-responsive cells in culture. *Proc Natl Acad Sci U S A* **83**, 2496-500 (1986).
496. Davis, H. E., Morgan, J. R. & Yarmush, M. L. Polybrene increases retrovirus gene transfer efficiency by enhancing receptor-independent virus adsorption on target cell membranes. *Biophys Chem* **97**, 159-72 (2002).
497. Laemmli, U. K., Beguin, F. & Gujer-Kellenberger, G. A factor preventing the major head protein of bacteriophage T4 from random aggregation. *J Mol Biol* **47**, 69-85 (1970).
498. Link, A. J. et al. Direct analysis of protein complexes using mass spectrometry. *Nat Biotechnol* **17**, 676-82 (1999).
499. Puig, O. et al. The tandem affinity purification (TAP) method: a general procedure of protein complex purification. *Methods* **24**, 218-29 (2001).
500. Bauer, A. & Kuster, B. Affinity purification-mass spectrometry. Powerful tools for the characterization of protein complexes. *Eur J Biochem* **270**, 570-8 (2003).
501. Bunz, F. et al. Requirement for p53 and p21 to sustain G2 arrest after DNA damage. *Science* **282**, 1497-501 (1998).
502. De Vries, E. M. et al. Database of mutations in the p53 and APC tumor suppressor genes designed to facilitate molecular epidemiological analyses. *Hum Mutat* **7**, 202-13 (1996).
503. Joerger, A. C. & Fersht, A. R. Structure-function-rescue: the diverse nature of common p53 cancer mutants. *Oncogene* **26**, 2226-42 (2007).
504. Blagosklonny, M. V. p53 from complexity to simplicity: mutant p53 stabilization, gain-of-function, and dominant-negative effect. *Faseb J* **14**, 1901-7 (2000).
505. Clarke, C. F. et al. Purification of complexes of nuclear oncogene p53 with rat and Escherichia coli heat shock proteins: in vitro dissociation of hsc70 and dnaK from murine p53 by ATP. *Mol Cell Biol* **8**, 1206-15 (1988).
506. Benzinger, A., Muster, N., Koch, H. B., Yates, J. R., 3rd & Hermeking, H. Targeted proteomic analysis of 14-3-3 sigma, a p53 effector commonly silenced in cancer. *Mol Cell Proteomics* **4**, 785-95 (2005).
507. Sarkaria, J. N. et al. Inhibition of ATM and ATR kinase activities by the radiosensitizing agent, caffeine. *Cancer Res* **59**, 4375-82 (1999).
508. Ahn, J. Y., Schwarz, J. K., Piwnica-Worms, H. & Canman, C. E. Threonine 68 phosphorylation by ataxia telangiectasia mutated is required for efficient activation of Chk2 in response to ionizing radiation. *Cancer Res* **60**, 5934-6 (2000).
509. Kastan, M. B., Onyekwere, O., Sidransky, D., Vogelstein, B. & Craig, R. W. Participation of p53 protein in the cellular response to DNA damage. *Cancer Res* **51**, 6304-11 (1991).
510. Horrigan, L. A., Kelly, J. P. & Connor, T. J. Caffeine suppresses TNF-alpha production via activation of the cyclic AMP/protein kinase A pathway. *Int Immunopharmacol* **4**, 1409-17 (2004).
511. Jung, P. et al. Induction of cullin 7 by DNA damage attenuates p53 function. *Proc Natl Acad Sci U S A* **104**, 11388-93 (2007).
512. Forster, K. et al. Tetracycline-inducible expression systems with reduced basal activity in mammalian cells. *Nucleic Acids Res* **27**, 708-10 (1999).
513. Urlinger, S. et al. Exploring the sequence space for tetracycline-dependent transcriptional activators: novel mutations yield expanded range and sensitivity. *Proc Natl Acad Sci U S A* **97**, 7963-8 (2000).
514. Campbell, R. E. et al. A monomeric red fluorescent protein. *Proc Natl Acad Sci U S A* **99**, 7877-82 (2002).
515. Dubik, D. & Shiu, R. P. Mechanism of estrogen activation of c-myc oncogene expression. *Oncogene* **7**, 1587-94 (1992).
516. O'Connell, B. C. et al. A large scale genetic analysis of c-Myc-regulated gene expression patterns. *J Biol Chem* **278**, 12563-73 (2003).
517. Danielian, P. S., White, R., Hoare, S. A., Fawell, S. E. & Parker, M. G. Identification of residues in the estrogen receptor that confer differential sensitivity to estrogen and hydroxytamoxifen. *Mol Endocrinol* **7**, 232-40 (1993).
518. Eilers, M., Picard, D., Yamamoto, K. R. & Bishop, J. M. Chimaeras of myc oncoprotein and steroid receptors cause hormone-dependent transformation of cells. *Nature* **340**, 66-8 (1989).

References

519. Dean, M. et al. Regulation of c-myc transcription and mRNA abundance by serum growth factors and cell contact. *J Biol Chem* **261**, 9161-6 (1986).
520. Varshochi, R. et al. ICI182,780 induces p21Waf1 gene transcription through releasing histone deacetylase 1 and estrogen receptor alpha from Sp1 sites to induce cell cycle arrest in MCF-7 breast cancer cell line. *J Biol Chem* **280**, 3185-96 (2005).
521. Gartel, A. L. & Tyner, A. L. Transcriptional regulation of the p21((WAF1/CIP1)) gene. *Exp Cell Res* **246**, 280-9 (1999).
522. Tanaka, N. et al. Cooperation of the tumour suppressors IRF-1 and p53 in response to DNA damage. *Nature* **382**, 816-8 (1996).
523. Pardali, K., Kowanzet, M., Heldin, C. H. & Moustakas, A. Smad pathway-specific transcriptional regulation of the cell cycle inhibitor p21(WAF1/Cip1). *J Cell Physiol* **204**, 260-72 (2005).
524. Datto, M. B., Yu, Y. & Wang, X. F. Functional analysis of the transforming growth factor beta responsive elements in the WAF1/Cip1/p21 promoter. *J Biol Chem* **270**, 28623-8 (1995).
525. Sundstrom, C. & Nilsson, K. Establishment and characterization of a human histiocytic lymphoma cell line (U-937). *Int J Cancer* **17**, 565-77 (1976).
526. Chorvath, B., Duraj, J. & Stockbauer, P. Differentiation of human myeloid leukemia cell lines induced by tumor-promoting phorbol ester (TPA). II. Electrophoretic patterns of metabolically- and cell surface radiolabeled proteins and glycoproteins. *Neoplasma* **30**, 273-80 (1983).
527. Stockbauer, P., Malaskova, V., Soucek, J. & Chudomel, V. Differentiation of human myeloid leukemia cell lines induced by tumor-promoting phorbol ester (TPA). I. Changes of the morphology, cytochemistry and the surface differentiation antigens analyzed with monoclonal antibodies. *Neoplasma* **30**, 257-72 (1983).
528. Larsson, L. G. et al. Phorbol ester-induced terminal differentiation is inhibited in human U-937 monoblastic cells expressing a v-myc oncogene. *Proc Natl Acad Sci U S A* **85**, 2638-42 (1988).
529. Andersen, R. D. et al. Metal-dependent binding of a factor in vivo to the metal-responsive elements of the metallothionein 1 gene promoter. *Mol Cell Biol* **7**, 3574-81 (1987).
530. Polyak, K., Hamilton, S. R., Vogelstein, B. & Kinzler, K. W. Early alteration of cell-cycle-regulated gene expression in colorectal neoplasia. *Am J Pathol* **149**, 381-7 (1996).
531. Doglioni, C. et al. p21/WAF1/CIP1 expression in normal mucosa and in adenomas and adenocarcinomas of the colon: its relationship with differentiation. *J Pathol* **179**, 248-53 (1996).
532. Petroski, M. D. & Deshaies, R. J. Function and regulation of cullin-RING ubiquitin ligases. *Nat Rev Mol Cell Biol* **6**, 9-20 (2005).
533. Kipreos, E. T., Lander, L. E., Wing, J. P., He, W. W. & Hedgecock, E. M. cul-1 is required for cell cycle exit in *C. elegans* and identifies a novel gene family. *Cell* **85**, 829-39 (1996).
534. Feldman, R. M., Correll, C. C., Kaplan, K. B. & Deshaies, R. J. A complex of Cdc4p, Skp1p, and Cdc53p/cullin catalyzes ubiquitination of the phosphorylated CDK inhibitor Sic1p. *Cell* **91**, 221-30 (1997).
535. Skowyra, D., Craig, K. L., Tyers, M., Elledge, S. J. & Harper, J. W. F-box proteins are receptors that recruit phosphorylated substrates to the SCF ubiquitin-ligase complex. *Cell* **91**, 209-19 (1997).
536. Kamura, T. et al. Rbx1, a component of the VHL tumor suppressor complex and SCF ubiquitin ligase. *Science* **284**, 657-61 (1999).
537. Ohta, T., Michel, J. J., Schottelius, A. J. & Xiong, Y. ROC1, a homolog of APC11, represents a family of cullin partners with an associated ubiquitin ligase activity. *Mol Cell* **3**, 535-41 (1999).
538. Tan, P. et al. Recruitment of a ROC1-CUL1 ubiquitin ligase by Skp1 and HOS to catalyze the ubiquitination of I kappa B alpha. *Mol Cell* **3**, 527-33 (1999).
539. Cardozo, T. & Pagano, M. The SCF ubiquitin ligase: insights into a molecular machine. *Nat Rev Mol Cell Biol* **5**, 739-51 (2004).
540. Kohrman, D. C. & Imperiale, M. J. Simian virus 40 large T antigen stably complexes with a 185-kilodalton host protein. *J Virol* **66**, 1752-60 (1992).
541. Tsai, S. C. et al. Simian virus 40 large T antigen binds a novel Bcl-2 homology domain 3-containing proapoptosis protein in the cytoplasm. *J Biol Chem* **275**, 3239-46 (2000).
542. Huber, C. et al. Identification of mutations in CUL7 in 3-M syndrome. *Nat Genet* **37**, 1119-24 (2005).
543. Andrews, P., He, Y. J. & Xiong, Y. Cytoplasmic localized ubiquitin ligase cullin 7 binds to p53 and promotes cell growth by antagonizing p53 function. *Oncogene* (2006).

References

544. Kasper, J. S., Kuwabara, H., Arai, T., Ali, S. H. & DeCaprio, J. A. Simian virus 40 large T antigen's association with the CUL7 SCF complex contributes to cellular transformation. *J Virol* **79**, 11685-92 (2005).
545. Michel, J. J. & Xiong, Y. Human CUL-1, but not other cullin family members, selectively interacts with SKP1 to form a complex with SKP2 and cyclin A. *Cell Growth Differ* **9**, 435-49 (1998).
546. Tsunematsu, R. et al. Fbxw8 is essential for Cul1-Cul7 complex formation and for placental development. *Mol Cell Biol* **26**, 6157-69 (2006).
547. Danovi, D. et al. Amplification of Mdmx (or Mdm4) directly contributes to tumor formation by inhibiting p53 tumor suppressor activity. *Mol Cell Biol* **24**, 5835-43 (2004).
548. Bunz, F. et al. Disruption of p53 in human cancer cells alters the responses to therapeutic agents. *J Clin Invest* **104**, 263-9 (1999).
549. Kasper, J. S., Arai, T. & Decaprio, J. A. A novel p53-binding domain in CUL7. *Biochem Biophys Res Commun* **348**, 132-8 (2006).
550. Kaustov, L. et al. The Conserved CPH Domains of Cul7 and PARC Are Protein-Protein Interaction Modules That Bind the Tetramerization Domain of p53. *J Biol Chem* **282**, 11300-7 (2007).
551. Logan, I. R., Sapountzi, V., Gaughan, L., Neal, D. E. & Robson, C. N. Control of human PIRH2 protein stability: involvement of TIP60 and the proteasome. *J Biol Chem* **279**, 11696-704 (2004).
552. Yi, C., Wang, H., Wei, N. & Deng, X. W. An initial biochemical and cell biological characterization of the mammalian homologue of a central plant developmental switch, COP1. *BMC Cell Biol* **3**, 30 (2002).
553. Liang, S. H. & Clarke, M. F. Regulation of p53 localization. *Eur J Biochem* **268**, 2779-83 (2001).
554. Skaar, J. R., Arai, T. & Decaprio, J. A. Dimerization of CUL7 and PARC Is Not Required for All CUL7 Functions and Mouse Development. *Mol Cell Biol* **25**, 5579-89 (2005).
555. Yamamoto, H. et al. Oxidative stress induces p53-dependent apoptosis in hepatoblastoma cell through its nuclear translocation. *Genes Cells* **12**, 461-71 (2007).
556. Hochrainer, K. et al. The human HERC family of ubiquitin ligases: novel members, genomic organization, expression profiling, and evolutionary aspects. *Genomics* **85**, 153-64 (2005).
557. Kominami, K., Seth-Smith, H. & Toda, T. Apc10 and Ste9/Srw1, two regulators of the APC-cyclosome, as well as the CDK inhibitor Rum1 are required for G1 cell-cycle arrest in fission yeast. *Embo J* **17**, 5388-99 (1998).
558. Brouillard, P. et al. Mutations in a novel factor, glomulin, are responsible for glomuvenous malformations ("glomangiomas"). *Am J Hum Genet* **70**, 866-74 (2002).
559. Hori, T. et al. Covalent modification of all members of human cullin family proteins by NEDD8. *Oncogene* **18**, 6829-34 (1999).
560. Skaar, J. R. et al. PARC and CUL7 form atypical cullin RING ligase complexes. *Cancer Res* **67**, 2006-14 (2007).
561. Zhang, Y. W. et al. Genotoxic stress targets human Chk1 for degradation by the ubiquitin-proteasome pathway. *Mol Cell* **19**, 607-18 (2005).
562. Wiman, K. G. Strategies for therapeutic targeting of the p53 pathway in cancer. *Cell Death Differ* **13**, 921-6 (2006).
563. Vassilev, L. T. MDM2 inhibitors for cancer therapy. *Trends Mol Med* **13**, 23-31 (2007).
564. Stuhmer, T. & Bargou, R. C. Selective pharmacologic activation of the p53-dependent pathway as a therapeutic strategy for hematologic malignancies. *Cell Cycle* **5**, 39-42 (2006).
565. Zhang, Z., Li, M., Wang, H., Agrawal, S. & Zhang, R. Antisense therapy targeting MDM2 oncogene in prostate cancer: Effects on proliferation, apoptosis, multiple gene expression, and chemotherapy. *Proc Natl Acad Sci U S A* **100**, 11636-41 (2003).
566. Vassilev, L. T. et al. In vivo activation of the p53 pathway by small-molecule antagonists of MDM2. *Science* **303**, 844-8 (2004).
567. Efeyan, A. et al. Induction of p53-Dependent Senescence by the MDM2 Antagonist Nutlin-3a in Mouse Cells of Fibroblast Origin. *Cancer Res* **67**, 7350-7 (2007).
568. Ventura, A. et al. Restoration of p53 function leads to tumour regression in vivo. *Nature* **445**, 661-5 (2007).
569. Xue, W. et al. Senescence and tumour clearance is triggered by p53 restoration in murine liver carcinomas. *Nature* **445**, 656-60 (2007).

References

570. Guo, Q. M. et al. Identification of c-myc responsive genes using rat cDNA microarray. *Cancer Res* **60**, 5922-8 (2000).
571. Schlosser, I. et al. Dissection of transcriptional programmes in response to serum and c-Myc in a human B-cell line. *Oncogene* **24**, 520-4 (2005).
572. Watson, J. D., Oster, S. K., Shago, M., Khosravi, F. & Penn, L. Z. Identifying genes regulated in a Myc-dependent manner. *J Biol Chem* **277**, 36921-30 (2002).
573. Lawlor, E. R. et al. Reversible kinetic analysis of Myc targets in vivo provides novel insights into Myc-mediated tumorigenesis. *Cancer Res* **66**, 4591-601 (2006).
574. Li, Z. et al. A global transcriptional regulatory role for c-Myc in Burkitt's lymphoma cells. *Proc Natl Acad Sci U S A* **100**, 8164-9 (2003).
575. Zeller, K. I. et al. Global mapping of c-Myc binding sites and target gene networks in human B cells. *Proc Natl Acad Sci U S A* **103**, 17834-9 (2006).
576. Mermod, N., Williams, T. J. & Tjian, R. Enhancer binding factors AP-4 and AP-1 act in concert to activate SV40 late transcription in vitro. *Nature* **332**, 557-61 (1988).
577. Hu, Y. F., Luscher, B., Admon, A., Mermod, N. & Tjian, R. Transcription factor AP-4 contains multiple dimerization domains that regulate dimer specificity. *Genes Dev* **4**, 1741-52 (1990).
578. Atchley, W. R. & Fitch, W. M. A natural classification of the basic helix-loop-helix class of transcription factors. *Proc Natl Acad Sci U S A* **94**, 5172-6 (1997).
579. Kim, M. Y. et al. A repressor complex, AP4 transcription factor and geminin, negatively regulates expression of target genes in nonneuronal cells. *Proc Natl Acad Sci U S A* **103**, 13074-9 (2006).
580. Imai, K. & Okamoto, T. Transcriptional repression of human immunodeficiency virus type 1 by AP-4. *J Biol Chem* **281**, 12495-505 (2006).
581. Tsujimoto, K. et al. Regulation of the expression of caspase-9 by the transcription factor activator protein-4 in glucocorticoid-induced apoptosis. *J Biol Chem* **280**, 27638-44 (2005).
582. Cui, Y., Narayanan, C. S., Zhou, J. & Kumar, A. Exon-I is involved in positive as well as negative regulation of human angiotensinogen gene expression. *Gene* **224**, 97-107 (1998).
583. Jansen-Durr, P. et al. Differential modulation of cyclin gene expression by MYC. *Proc Natl Acad Sci U S A* **90**, 3685-9 (1993).
584. Perez-Roger, I., Solomon, D. L., Sewing, A. & Land, H. Myc activation of cyclin E/Cdk2 kinase involves induction of cyclin E gene transcription and inhibition of p27(Kip1) binding to newly formed complexes. *Oncogene* **14**, 2373-81 (1997).
585. Lee, T. C., Li, L., Philipson, L. & Ziff, E. B. Myc represses transcription of the growth arrest gene *gas1*. *Proc Natl Acad Sci U S A* **94**, 12886-91 (1997).
586. Claassen, G. F. & Hann, S. R. A role for transcriptional repression of p21CIP1 by c-Myc in overcoming transforming growth factor beta -induced cell-cycle arrest. *Proc Natl Acad Sci U S A* **97**, 9498-503 (2000).
587. Mitchell, K. O. & El-Deiry, W. S. Overexpression of c-Myc inhibits p21WAF1/CIP1 expression and induces S-phase entry in 12-O-tetradecanoylphorbol-13-acetate (TPA)-sensitive human cancer cells. *Cell Growth Differ* **10**, 223-30 (1999).
588. Carroll, J. S., Swarbrick, A., Musgrove, E. A. & Sutherland, R. L. Mechanisms of growth arrest by c-myc antisense oligonucleotides in MCF-7 breast cancer cells: implications for the antiproliferative effects of antiestrogens. *Cancer Res* **62**, 3126-31 (2002).
589. Mukherjee, S. & Conrad, S. E. c-Myc suppresses p21WAF1/CIP1 expression during estrogen signaling and antiestrogen resistance in human breast cancer cells. *J Biol Chem* **280**, 17617-25 (2005).
590. Gartel, A. L. & Radhakrishnan, S. K. Lost in transcription: p21 repression, mechanisms, and consequences. *Cancer Res* **65**, 3980-5 (2005).
591. Herold, S. et al. Negative regulation of the mammalian UV response by Myc through association with Miz-1. *Mol Cell* **10**, 509-21 (2002).
592. Adhikary, S. et al. Miz1 is required for early embryonic development during gastrulation. *Mol Cell Biol* **23**, 7648-57 (2003).
593. Ziegelbauer, J., Wei, J. & Tjian, R. Myc-interacting protein 1 target gene profile: a link to microtubules, extracellular signal-regulated kinase, and cell growth. *Proc Natl Acad Sci U S A* **101**, 458-63 (2004).
594. Ou, S. H., Garcia-Martinez, L. F., Paulssen, E. J. & Gaynor, R. B. Role of flanking E box motifs in human immunodeficiency virus type 1 TATA element function. *J Virol* **68**, 7188-99 (1994).

595. Sowa, Y. et al. Histone deacetylase inhibitor activates the WAF1/Cip1 gene promoter through the Sp1 sites. *Biochem Biophys Res Commun* **241**, 142-50 (1997).
596. Liao, D. J. & Dickson, R. B. c-Myc in breast cancer. *Endocr Relat Cancer* **7**, 143-64 (2000).
597. Deming, S. L., Nass, S. J., Dickson, R. B. & Trock, B. J. C-myc amplification in breast cancer: a meta-analysis of its occurrence and prognostic relevance. *Br J Cancer* **83**, 1688-95 (2000).
598. Bieche, I. et al. Quantitation of MYC gene expression in sporadic breast tumors with a real-time reverse transcription-PCR assay. *Cancer Res* **59**, 2759-65 (1999).
599. Berns, E. M. et al. Prognostic factors in human primary breast cancer: comparison of c-myc and HER2/neu amplification. *J Steroid Biochem Mol Biol* **43**, 13-9 (1992).
600. Kreipe, H. et al. Amplification of c-myc but not of c-erbB-2 is associated with high proliferative capacity in breast cancer. *Cancer Res* **53**, 1956-61 (1993).
601. Dubik, D., Dembinski, T. C. & Shiu, R. P. Stimulation of c-myc oncogene expression associated with estrogen-induced proliferation of human breast cancer cells. *Cancer Res* **47**, 6517-21 (1987).
602. Shiu, R. P., Watson, P. H. & Dubik, D. c-myc oncogene expression in estrogen-dependent and -independent breast cancer. *Clin Chem* **39**, 353-5 (1993).
603. Howell, A. Faslodex (ICI 182780). an oestrogen receptor downregulator. *Eur J Cancer* **36 Suppl 4**, S87-8 (2000).
604. Howell, A. & Robertson, J. Response to a specific antioestrogen (ICI 182780) in tamoxifen-resistant breast cancer. *Lancet* **345**, 989-90 (1995).
605. Dowsett, M., Nicholson, R. I. & Pietras, R. J. Biological characteristics of the pure antiestrogen fulvestrant: overcoming endocrine resistance. *Breast Cancer Res Treat* **93 Suppl 1**, S11-8 (2005).
606. Howell, A. et al. Pharmacokinetics, pharmacological and anti-tumour effects of the specific anti-oestrogen ICI 182780 in women with advanced breast cancer. *Br J Cancer* **74**, 300-8 (1996).
607. Cheung, K. L. & Robertson, J. F. Fulvestrant. *Expert Opin Investig Drugs* **11**, 303-8 (2002).
608. Perey, L. et al. Clinical benefit of fulvestrant in postmenopausal women with advanced breast cancer and primary or acquired resistance to aromatase inhibitors: final results of phase II Swiss Group for Clinical Cancer Research Trial (SAKK 21/00). *Ann Oncol* **18**, 64-9 (2007).
609. Venditti, M., Iwasiow, B., Orr, F. W. & Shiu, R. P. C-myc gene expression alone is sufficient to confer resistance to antiestrogen in human breast cancer cells. *Int J Cancer* **99**, 35-42 (2002).
610. Bierie, B. & Moses, H. L. TGF-beta and cancer. *Cytokine Growth Factor Rev* **17**, 29-40 (2006).
611. Siegel, P. M. & Massague, J. Cytostatic and apoptotic actions of TGF-beta in homeostasis and cancer. *Nat Rev Cancer* **3**, 807-21 (2003).
612. Han, G. et al. Distinct mechanisms of TGF-beta1-mediated epithelial-to-mesenchymal transition and metastasis during skin carcinogenesis. *J Clin Invest* **115**, 1714-23 (2005).
613. Weeks, B. H., He, W., Olson, K. L. & Wang, X. J. Inducible expression of transforming growth factor beta1 in papillomas causes rapid metastasis. *Cancer Res* **61**, 7435-43 (2001).
614. Roberts, A. B. & Wakefield, L. M. The two faces of transforming growth factor beta in carcinogenesis. *Proc Natl Acad Sci U S A* **100**, 8621-3 (2003).
615. Massague, J., Blain, S. W. & Lo, R. S. TGFbeta signaling in growth control, cancer, and heritable disorders. *Cell* **103**, 295-309 (2000).
616. Coffey, R. J., Jr. et al. Selective inhibition of growth-related gene expression in murine keratinocytes by transforming growth factor beta. *Mol Cell Biol* **8**, 3088-93 (1988).
617. Hannon, G. J. & Beach, D. p15INK4B is a potential effector of TGF-beta-induced cell cycle arrest. *Nature* **371**, 257-61 (1994).
618. Datto, M. B. et al. Transforming growth factor beta induces the cyclin-dependent kinase inhibitor p21 through a p53-independent mechanism. *Proc Natl Acad Sci U S A* **92**, 5545-9 (1995).
619. Iavarone, A. & Massague, J. Repression of the CDK activator Cdc25A and cell-cycle arrest by cytokine TGF-beta in cells lacking the CDK inhibitor p15. *Nature* **387**, 417-22 (1997).
620. Seoane, J., Le, H. V. & Massague, J. Myc suppression of the p21(Cip1) Cdk inhibitor influences the outcome of the p53 response to DNA damage. *Nature* **419**, 729-34 (2002).
621. Feng, X. H., Liang, Y. Y., Liang, M., Zhai, W. & Lin, X. Direct interaction of c-Myc with Smad2 and Smad3 to inhibit TGF-beta-mediated induction of the CDK inhibitor p15(Ink4B). *Mol Cell* **9**, 133-43 (2002).
622. Cheng, T., Shen, H., Rodrigues, N., Stier, S. & Scadden, D. T. Transforming growth factor beta 1 mediates cell-cycle arrest of primitive hematopoietic cells independent of p21(Cip1/Waf1) or p27(Kip1). *Blood* **98**, 3643-9 (2001).

References

623. Deng, C., Zhang, P., Harper, J. W., Elledge, S. J. & Leder, P. Mice lacking p21CIP1/WAF1 undergo normal development, but are defective in G1 checkpoint control. *Cell* **82**, 675-84 (1995).
624. Martin-Caballero, J., Flores, J. M., Garcia-Palencia, P. & Serrano, M. Tumor susceptibility of p21(Waf1/Cip1)-deficient mice. *Cancer Res* **61**, 6234-8 (2001).
625. Latres, E. et al. Limited overlapping roles of P15(INK4b) and P18(INK4c) cell cycle inhibitors in proliferation and tumorigenesis. *Embo J* **19**, 3496-506 (2000).
626. Miyaki, M. et al. Genetic changes and histopathological types in colorectal tumors from patients with familial adenomatous polyposis. *Cancer Res* **50**, 7166-73 (1990).
627. Howe, J. R. et al. Mutations in the SMAD4/DPC4 gene in juvenile polyposis. *Science* **280**, 1086-8 (1998).
628. Maitra, A., Molberg, K., Albores-Saavedra, J. & Lindberg, G. Loss of Dpc4 expression in colonic adenocarcinomas correlates with the presence of metastatic disease. *Am J Pathol* **157**, 1105-11 (2000).
629. Biswas, S. et al. Transforming growth factor beta receptor type II inactivation promotes the establishment and progression of colon cancer. *Cancer Res* **64**, 4687-92 (2004).
630. Pardali, K. et al. Role of Smad proteins and transcription factor Sp1 in p21(Waf1/Cip1) regulation by transforming growth factor-beta. *J Biol Chem* **275**, 29244-56 (2000).
631. van den Brink, G. R. & Offerhaus, G. J. The morphogenetic code and colon cancer development. *Cancer Cell* **11**, 109-17 (2007).
632. Zhang, D., Zaugg, K., Mak, T. W. & Elledge, S. J. A role for the deubiquitinating enzyme USP28 in control of the DNA-damage response. *Cell* **126**, 529-42 (2006).
633. Popov, N., Herold, S., Llamazares, M., Schulein, C. & Eilers, M. Fbw7 and Usp28 Regulate Myc Protein Stability in Response to DNA Damage. *Cell Cycle* **6** (2007).
634. Ho, J. S., Ma, W., Mao, D. Y. & Benchimol, S. p53-Dependent transcriptional repression of c-myc is required for G1 cell cycle arrest. *Mol Cell Biol* **25**, 7423-31 (2005).
635. Steiner, P. et al. Identification of a Myc-dependent step during the formation of active G1 cyclin-cdk complexes. *Embo J* **14**, 4814-26 (1995).
636. Hermeking, H., Funk, J. O., Reichert, M., Ellwart, J. W. & Eick, D. Abrogation of p53-induced cell cycle arrest by c-Myc: evidence for an inhibitor of p21WAF1/CIP1/SDI1. *Oncogene* **11**, 1409-15 (1995).
637. Vlach, J., Hennecke, S., Alevizopoulos, K., Conti, D. & Amati, B. Growth arrest by the cyclin-dependent kinase inhibitor p27Kip1 is abrogated by c-Myc. *Embo J* **15**, 6595-604 (1996).
638. Vousden, K. H. & Lu, X. Live or let die: the cell's response to p53. *Nat Rev Cancer* **2**, 594-604 (2002).
639. Blagosklonny, M. V., Robey, R., Bates, S. & Fojo, T. Pretreatment with DNA-damaging agents permits selective killing of checkpoint-deficient cells by microtubule-active drugs. *J Clin Invest* **105**, 533-9 (2000).
640. Lo, P. K., Huang, S. Z., Chen, H. C. & Wang, F. F. The prosurvival activity of p53 protects cells from UV-induced apoptosis by inhibiting c-Jun NH2-terminal kinase activity and mitochondrial death signaling. *Cancer Res* **64**, 8736-45 (2004).
641. Waldman, T. et al. Cell-cycle arrest versus cell death in cancer therapy. *Nat Med* **3**, 1034-6 (1997).
642. Bellmeyer, A., Krase, J., Lindgren, J. & LaBonne, C. The protooncogene c-myc is an essential regulator of neural crest formation in xenopus. *Dev Cell* **4**, 827-39 (2003).
643. Asada, M., Yamada, T., Fukumuro, K. & Mizutani, S. p21Cip1/WAF1 is important for differentiation and survival of U937 cells. *Leukemia* **12**, 1944-50 (1998).
644. Asada, M. et al. Apoptosis inhibitory activity of cytoplasmic p21(Cip1/WAF1) in monocytic differentiation. *Embo J* **18**, 1223-34 (1999).
645. Steinman, R. A. Cell cycle regulators and hematopoiesis. *Oncogene* **21**, 3403-13 (2002).
646. Hoffman, B., Amanullah, A., Shafarenko, M. & Liebermann, D. A. The proto-oncogene c-myc in hematopoietic development and leukemogenesis. *Oncogene* **21**, 3414-21 (2002).
647. Nesbit, C. E., Tersak, J. M. & Prochownik, E. V. MYC oncogenes and human neoplastic disease. *Oncogene* **18**, 3004-16 (1999).
648. Cheng, T. et al. Hematopoietic stem cell quiescence maintained by p21cip1/waf1. *Science* **287**, 1804-8 (2000).
649. Heath, J. P. Epithelial cell migration in the intestine. *Cell Biol Int* **20**, 139-46 (1996).

References

650. Marshman, E., Booth, C. & Potten, C. S. The intestinal epithelial stem cell. *Bioessays* **24**, 91-8 (2002).
651. van den Brink, G. R. et al. Indian Hedgehog is an antagonist of Wnt signaling in colonic epithelial cell differentiation. *Nat Genet* **36**, 277-82 (2004).
652. Kinzler, K. W. et al. Identification of FAP locus genes from chromosome 5q21. *Science* **253**, 661-5 (1991).
653. Miyoshi, Y. et al. Somatic mutations of the APC gene in colorectal tumors: mutation cluster region in the APC gene. *Hum Mol Genet* **1**, 229-33 (1992).
654. Korinek, V. et al. Constitutive transcriptional activation by a beta-catenin-Tcf complex in APC^{-/-} colon carcinoma. *Science* **275**, 1784-7 (1997).
655. Sansom, O. J. et al. Myc deletion rescues Apc deficiency in the small intestine. *Nature* **446**, 676-9 (2007).

9 Abbreviations

53BP1	p53 binding protein 1
ALDH4	Aldehyde dehydrogenase 4
AMPK	AMP-activated protein kinase
AP4	Activating enhancer-binding protein 4
ap4	Murine AP4 homolog (also known as Tcfap4)
APAF-1	Apoptotic protease activating factor 1
APC	Anaphase promoting complex
APS	Adenosine-5` phosphosulfate
(i)ASPP	(inhibitor of) Apoptosis-stimulating protein of p53
ATM	Ataxia telangiectasia mutated
ATP	Adenosin-5`-triphosphat
ARF	Alternative reading frame (of <i>p16</i> locus)
ATR	ATM and Rad3-related
b	Basic region
BAX	BCL2-associated protein
bFGF	Basic fibroblast growth factor
bp	Base pair
Bcl-2	B-cell lymphoma 2
Bcl-X _L	B-cell leukemia-x long
BL	Burkitt`s lymphoma
BOP1	Block of Proliferation 1
BRCA1	Breast cancer susceptibility gene 1
BSA	Bovine serum albumin
C/EBP α	CCAAT/enhancer binding protein alpha
c-MYC	v-MYC avian myelocytomatosis viral oncogene homologue
CAK	Cyclin-activating kinase
CBP	CREB-binding protein
CDK	Cycline-dependent kinase
cDNA	Complementary DNA
(q)ChIP	(quantitative) Chromatin immunoprecipitation
CHIP	Carboxy terminus of HSP70p-interacting protein
CHK	Checkpoint kinase
CMV	Cytomegalovirus
COP1	Constitutive photomorphogenic protein 1
COX2	Cytochrome C oxidase 2
CREB	cAMP-responsive element binding protein
CTD	Carboxy-terminal domain
CUL	Cullin
Cy3	Cyanine 3
DAPI	2-(4-Amidinophenyl)-6-indolecarbamide-dihydrochloride
DAXX	Death associated protein 6
DBD	DNA binding domain
DMEM	Dulbecco`s modified eagle medium
DMSO	Dimethylsulfoxide
dNTPs	2`-deoxynucleotide-5` triphosphate
DR5	Death receptor 5
DSB	DNA double strand break
DTT	Dithiotreitol
E6-AP	E6 protein (from HPV virus)-associated protein
E-box	Enhancer box
EBNA	Epstein-Barr virus nuclear antigen

Abbreviations

EBV	Epstein Barr virus
<i>E.coli</i>	<i>Escherichia coli</i>
EDTA	Ethylenediamine-tetraacetic acid
EGTA	Ethylene glycol-tetraacetic acid
eGFP	Enhanced green fluorescent protein
EMT	Epithelial to mesenchymal transition
ER	Estrogen receptor
ERK	Extracellular signal-regulated kinase
Fas	F7-associated surface protein
FBS	Fetal bovine serum
FBX29	F-box and WD-40 domain protein 8
FITC	Fluorescein isothiocyanate
GADD45	Growth arrest and DNA damage-inducible 45
gDNA	genomic DNA
GFP	Green fluorescent protein
GTP	Guanosine-5`-triphosphate
GSK3 β	Glycogen synthase kinase 3 beta
HA	Hemagglutinin
HAT	Histone acetyltransferase
HAUSP	Herpesvirus-associated ubiquitin-specific protease
HBSS	Hanks` balanced salt solution
HDAC	Histone deacetylase
HectH9	HECT, UBA and WWE domain containing 1
HIF-1 α	Hypoxia inducible factor 1 alpha
HIS	Histidine
HLH	Helix-loop-helix
HPV	Human papillomavirus
HRP	Horseradish peroxidase
HSC	Hematopoietic stem cell
HygB	Hygromycin B
IBR	In between RING finger domain
ID2	Inhibitor of DNA binding 2
IHC	Immunohistochemistry
IHh	Indian Hedgehog
INI1	Integrase interactor 1
Inr	Initiator
IRES	Internal ribosome entry site
kbp	Kilo base pair
kD	Kilo Dalton
KLH	Keyhole limpet hemocyanin
LB	Luria Bertani
LIP	Liver enriched protein
LOH	Loss of heterozygosity
LTR	Long terminal repeat
LZ	Leucine zipper
MAD	MAX dimerization protein
MAPK	Mitogen-activated protein kinase
MAX	MYC-associated factor X
MCM	Minichromosome maintenance deficient
MEK	Mitogen and extracellular signal regulated kinase
mir-17	MicroRNA precursor mir-17
MIZ1	MYC-interacting zinc finger protein 1
MNT	Maintenance of lysogeny (MAX interacting protein)
mRNA	Messenger RNA
mTOR	Mammalian target of rapamycin
MudPIT	Multidimensional protein identification technology

Abbreviations

MDM2	mouse double minute 2 homolog
MDMX	mouse double minute X homolog
MXI	MAX interactor 1
NF-Y	Nuclear transcription factor Y
NLS	Nuclear localization signal
NP40	Nonidet-P40
NES	Nuclear export signal
NLS	Nuclear localization signal
NOXA	Stands for “damage”
NTD	Amino-terminal domain
OD	Optical density
p53AIP1	p53-regulated apoptosis-inducing protein 1
PAGE	Polyacrylamide gel electrophoresis
PARC	p53-associated, parkin-like cytoplasmic protein
PCAF	p300/CBP-associated factor
p-TEFb	Positive transcription elongation factor
p107	Retinoblastoma-like 1
p130	Retinoblastoma-like 2
p21	CDK inhibitor p21
PBS	Phosphate buffered saline
PCR	Polymerase chain reaction
PDGF	Platelet-derived growth factor
PES1	Pescadillo homolog 1
PERP	p53 apoptosis effector related to Pmp22
PI3K	Phosphoinositide-3-kinase
PIAS	Protein inhibitors of activated STAT
PIDD	p53-induced protein with a death domain
PIKK	Phosphatidylinositol-3 kinase-like family of kinases
Pirh2	p53-induced protein with a RING-H2 domain
PP2A	Protein-phosphatase 2A
POMC	Proopiomelanocortin
pRB	Retinoblastoma protein
Pu	Purine containing nucleotide
PUMA	p53 upregulated mediator of apoptosis
PVDF	Polyvinylidene difluoride
Py	Pyrimidine containing nucleotide
RAF	v-Raf-1 murine leukemia viral oncogene homologue 1
RAS	Rat sarcoma viral oncogene homologue
Rbx1	Ring box protein 1 (also known as Roc1)
RD	Regulatory domain
REPRIMO	Stands for “stop/repress”
RING	Really interesting new gene
RNAi	RNA interference
ROS	Reactive oxygen species
rpm	Rotations per minute
rRNA	Ribosomal RNA
RT	Room temperature
RT-qPCR	Real-time quantitative PCR
RZPD	German resource center for genome research
SAGE	Serial analysis of gene expression
SCF	SKP-Cullin-F-box
SCO2	Synthesis of cytochrome C oxidase
SDS	Sodium dodecyl sulfate
SIN3	Switch insensitive 3
SIRT1	Silent mating type information regulation 2 homolog 1
SKP	S-phase kinase associated protein

Abbreviations

SMAD4	Mothers against decapentaplegic homolog 4
SP1/3	Specificity protein 1/3
STAT	Signal transducers and activators of transcription
SUMO	Small ubiquitin-related modifier
SV40	Simian virus 40
SWI/SNF	Switch/sucrose non-fermenting
T	Temperature
T7	Enterobacteria phage T7
TAD	Transactivation domain
TAP	tandem affinity purification
TBP	TATA binding protein
TCA	Trichloroacetic acid
TCF4	Transcription factor 4
TD	Transactivation domain
TEMED	Tetramethylethylenediamine
htert	Human telomerase reverse transcriptase
Tet	Tetracycline
TEV	Tobacco etch virus
TF	Transcription factor
TGF β	Transforming growth factor beta
TIGAR	Tp53-induced glycolysis and apoptosis regulator
TNF α	Tumor necrosis factor alpha
TPA	12-O-tetradecanoylphorbol-13-acetate
TP53	Tumor protein 53
tRNA	Transfer RNA
TRRAP	Transformation/transcription domain associated protein
tTa	Tetracycline-controlled transactivator
U	Units
v/v	Volume per volume
VEGF	Vascular endothelial growth factor
VSV	Vesicular stomatitis virus
w/v	Weight per volume
WB	Western blot
WDR12	WD repeat domain 12
XPC	Xeroderma pigmentosum protein C
YY1	Yin-Yang 1

10 Acknowledgments

I am sincerely grateful to PD. Dr. Heiko Hermeking who not only served as my supervisor but also encouraged and challenged me throughout my academic program. I also want to thank him for valuable discussions and ideas for my project and for organizing the successful collaborations with Prof. Dr. John Yates 3rd and Dr. Doris Mayr.

I would like to express my gratitude to Dr. Antje Menssen, who guided me through the dissertation process, never accepting less than my best efforts. I would like to thank her for sharing her scientific expertise, many helpful discussions and for contributing important material to this work.

I am grateful to the people who provided data and materials to this work especially to Prof. John Yates 3rd and Aaron Bailey for the mass-spectral analysis of purified protein complexes and also for the valuable discussions on the data. I am also grateful to Dr. Doris Mayr and Andrea Sendelhofert for contributing important biological data and for sharing their expertise in immunohistochemistry.

I also want to thank Dr. Berlinda Verdoodt for providing important data to the biology of Cul7, for helpful comments on my work and for critical reading of this thesis.

I would like to express my gratitude to Alex Epanchintsev for his collaboration in generating the microRNA expression system and also for his sense of humor.

I am grateful to Dr. Dimitri Lodyguin for providing materials and sharing his scientific expertise and also for his help during the generation of adenoviruses.

I want to thank all my lab colleagues for their daily help and communication in matters of scientific research and beyond, especially Dr. Berlinda Verdoodt, Dr. Antje Menssen, Dr. Valery Tarasov, Henrike Koerner, Dr. Dimitri Lodyguin, Alex Epanchintsev, James Scrivens, Dr. Chang-Dong Zhang and Dr. Nils Hartmann. I'm also grateful to Dr. Anne Benzinger and Dr. Heike Koch for helpful advices concerning the tandem affinity purification procedure. Many thanks go to Dr. Ru Zhang for her helpfulness, her optimism and vitality and also for valuable discussions concerning research and the art of chinese cooking.

I am deeply grateful to my family for their patience and support during the past years. I am especially thankful to my parents and grand-parents for their love and support even in the hardest times and for always having an open ear for my concerns.

11 Curriculum vitae

Personal facts

Family name: Jung
 First name: Peter
 Date/place of birth: March 18th, 1978 (Lich, Germany)
 Citizenship: German
 Marital status: single

School education

1984 – 1988: Elementary school “Limesschule”, Pohlheim
 1988 – 1991: Comprehensive school, Pohlheim
 1991 – 1997: High school “Liebigshule”, Gießen

Community service:

1997-1998: Clinical center of the Justus-Liebig-University
 in Gießen, Department of Anesthesia and Intensive Care

University Education:

11/1998 – 10/2002: Studies of biochemistry at the University of Bayreuth
 10/2002 – 4/2003: Diploma thesis at the University of Bayreuth, Department
 of Biochemistry (Supervisor: Prof. Dr. Mathias Sprinzl)
 19.05.2003: Diploma in Biochemistry

Doctoral thesis:

since 07/2003: SNWG Molecular Oncology
 Max-Planck Institute of Biochemistry, Martinsried,
 Germany (Supervisor: PD. Dr. Heiko Hermeking)
 Title: “Analysis of p53 and c-MYC, two key transcription
 factors involved in tumorigenesis“